Complexes of flexible ditopic catechol phosphines: synthesis, metal assisted self-assembly and catalytic application

Von der Fakultät Chemie der Universität Stuttgart

Zur Erlangung der Würde eines

Doktors der Naturwissenschaften (Dr. rer. Nat.)

genehmigte Abhandlung

vorgelegt von

Samir H. Chikkali

aus Solapur (Indien)

Hauptberichter:	Prof. Dr. D. Gudat
Mitberichter:	Prof. Dr. W. Kaim
Tag der mündlichen Prüfung:	12.09.2007

Institut für Anorganische Chemie der Universität Stuttgart

2007

To My Grandmother

“The most beautiful experience we can have is the mysterious….the fundamental emotion which stands at the cradle of true art and true science”-

---Albert Einstein

“ I do not agree with the view that the universe is a mystery”-

---Stephen Hawking

Acknowledgements

My deepest appreciation goes to my Ph. D. mentor Prof. Dr. Dietrich Gudat for the brainstorming discussions on basic as well as applied scientific issues related to the present work. He taught me very basic to very complicated inorganic chemistry, showed different ways to approach a research problem and the need to be persistent to accomplish any goal.

I would like to thank Prof. Dr. W. Kaim for his efforts to correct the present work.

I also thank Prof. Dr. H. Bertagnolli for being the chairperson of this dissertation.

Further I am thankful to Prof. Dr. G. Becker and Prof. Dr. T. Schleid for providing the institute facilities, without which this work would not have completed.

I am obliged to Priv.-Doz. Dr. M. Niemeyer, Dr. M. Nieger, Dr. F. Lissner, Dr. I. Hartenbach for measuring the single crystals, sometime really small crystals. Let me also say “thank you” to the following people at University of Stuttgart: Herr P. Bergk, Frau K. Toroek for the NMR measurements and Frau. B. Foertsch for her accurate CHN analysis as well as NMR measurements. I am thankful to Herr Naegelein, Herr Wesch and Herr Lenz for their anytime help, Herr Zahl, Herr Heim who helped me to build the Schlenk line and gave a good start, Herr Achstetter, Herr Jergler for blowing special glass apparatus required.

I am thankful to Herr Dr. J. Opitz, Herr J. Trinkner and Frau K. Wohlbold for the Mass Spectrometric measurements, which changed the course of my research during the final days.

A special thanks goes to my lab mates Sebastian, Zoltan, Andrea, Laura, Imre, Samith, Dirk, Gernot, Nicholas, Anke and Daniela for the lively lab atmosphere and endless discussions. Thanks to Paula, Tushar and Christian, for their help in the preparation of this manuscript.

I am grateful to my research students for their contribution to this dissertation, specially for their outstanding research work. Also many thanks to my Indian friends Amar, Venkat, Mahendra and the Busnau group who made my life at Stuttgart easy.

I am also greatly indebted to many teachers in the past: Dr. Sivaram, Dr. Wadgaonkar, Dr. Saxena, Dr. Mohandas, Dr. Guruswamy, Dr. Lele and Dr. Premnath at National Chemical Laboratory, Pune, India, for the motivation and for getting me interested in research and coming to Germany. Prof. Maldar and Prof. Lonikar who taught me basics of polymer Chemistry with its importance in day to day life. Dr. Manikshetti and Mr. Battin for introducing me to chemistry. My school teacher Handge sir who gave me the vision to see things differently. Thanks to working group Sivaram, Wadgaonkar and CFPE for making my stay comfortable at NCL.

I feel myself very lucky to have a company of genuine, jolly and spiritful friends. Mohan, Wasif, Amit, Suleman, Chandrashekhar, Ankush and Jabeen deserve special mention for their out of the way help during my dissertation. I am thankful to my competitive exam group “Mahatma Gandhi Mitramandal”. I should mention Kiran and my graduate friends who were always there to hear my complaints and frustration and made me comfortable during those difficult times.

Last, but not least, I thank my family: my Abba and Ammi, for educating me with aspects from both social and personal life, for unconditional support to pursue my interests and for believing in me. My brothers, Amin, Sharif and sisters, Mohaseena, Madeena, for sharing their happy moments in life. My Dada, Bade-abba, Shabeer-chacha and Papa-chacha, for the care and love during my childhood days. My fiancée Nasreen, for believing in me, for her support and love.

Symbols and Abbreviations

B3LYP = Becke-3-Lee-Yang-Parr

br = Broad

CN = Coordination number

COD = 1,5 cyclooctadiene

CP/MAS = Cross polarization/ Magic angle spinning

conc. = Concentrated

d = Doublet

δ = Chemical Shift

D = Donor

D = Diffusion coefficient

DABCO = 1,4-Diazabicyclo [2.2.2] octane

DCM = Dichloromethane

DFT = Density functional theory

DMAP = Dimethyl aminopyridine

DME = 1,2-dimethoxyethane

DMF = Dimethylformamide

DOSY = Diffusion ordered spectroscopy

E = Element

E_{rel} = relative energy

EI-MS = Electron Ionization-Mass Spectroscopy

Et = Ethyl

EXSY = Exchange spectroscopy

F = Functional group

FAB = fast atom bombardment

Fig. = Figure

HSAB = Hard/ Soft/ Acid/ Base

HMQC = Heteronuclear multiple-quantum coherence

HOMO = Highest Occupied Molecular Orbital

I = isotop

KJ/mol. = Kilo joule/mol

LUMO = Lowest Unoccupied Molecular Orbital

M = Metal

m = multiplets

m/e = Mass to charge ratio

MAS = Magic angle spinning

Me = Methyl

Mes = Mesityl, 2,4,6-Trimethyl phenyl

NLO = Non linear-optical

NMR = Nuclear Magnetic Resonance

NOESY = Nuclear overhauser enhancement and exchange spectroscopy

OTf = Triflate

PGSE = Pulsed Graadient Spin Echo

Ph = Phenyl

ppm = parts per million

PTSA = p-toluenesulfonic acid

r_H = Hydrodynamic radii

s = singlet

Sec. = Secondary

sect. = section

THF = tetrahydrofuran

Tol = Toluene

Table of Contents

1. Introduction.....15

1.1. Self-assembly, ligand designing and catalysis:.....15

1.2. Setting the Goals: 19

2. Syntheses of diphenyl-phosphinomethyl substituted phenols and catechols and mechanistic details on their formation.....23

2.1. Introduction:.....23

2.2. Results and discussion:.....25

2.2.1. Syntheses and mechanistic insights on the formation of methyl phosphinoyl phenols and catechols:.....25

2.2.2. Synthesis and characterization of chiral mesityl phenyl phosphinoyl methyl catechols:.....30

2.3. Reduction of the phosphine oxides to ditopic phosphines:.....31

2.4. Syntheses and characterization of transition metal complexes of diphenyl-phosphanyl methyl phenols and catechols:.....34

2.5. Synthesis and characterization of a palladium complex of 3-[(Mesitylphenyl phosphanyl)-methyl]-benzene-1,2-diol:.....41

2.6. Conclusions:.....41

3. Phosphine functionalized catechol borates and their Lewis-acid/base behavior.....43

3.1. Introduction.....43

3.2. Results and discussion:.....46

3.2.1. Detailed investigations on the synthesis and Lewis acid/base behavior of Diphenyl-(2-phenyl-benzo[1,3,2]-dioxaborol-4-ylmethyl) phosphine:.....46

3.2.2. Syntheses and characterization of Silver (I) bis {diphenyl- (benzo- [1,3]-dioxo-4-ylmethyl)-phosphane} 2-borate:.....52

3.2.3. Synthesis and characterization of a Silver (I) bis {diphenyl- (benzo-[1,3]-dioxo-5-ylmethyl)-phosphane} 2-borate macrocycle:..... 58
3.3. Attempted synthesis of Triethyl ammonium [Dichloro palladium bis {diphenyl-(benzo- [1,3]-dioxo-4-ylmethyl)-phosphane}] 2-borate:..... 63
3.4. Conclusions: 64
4. Transition metal complexes of templated symmetric bisphosphane ligands and potential application in catalysis 65
4.1. Introduction: 65
4.2. Results and discussion:..... 67
4.2.1. Synthesis and characterization of self-assembled palladium-bis {diphenyl-(benzo- [1, 3]-μ-oxo-k-oxo-4-ylmethyl) phosphane)}-gallium chloride (25): 67
4.2.2. Syntheses and characterization of self-assembled palladium–bis {diphenyl-(benzo-[1, 3]-μ-oxo-k-oxo-4-ylmethyl) phosphane)}-tin complexes:..... 72
4.2.3. Synthesis and characterization of a platinum -bis{diphenyl-(benzo-[1, 3]-μ-oxo-k-oxo-4-ylmethyl) phosphane)}-tin complex (28): 81
4.2.4. Synthesis and characterization of a palladium- bis{diphenyl-(benzo-[1, 3]-μ-oxo-k-oxo-4-ylmethyl) phosphane)}-bismuth complex (29a):..... 84
4.2.5. Zirconium assisted synthesis of a trinuclear di-palladium zirconium complex of 3-[(Diphenylphosphanyl) methyl] benzene-1, 2-diol (30): 87
4.2.6. Stoichiometry controlled syntheses of tri- and octanuclear palladium-yttrium complexes of 3-[(Diphenylphosphanyl) methyl] benzene-1, 2-diol (31):..... 91
4.3. Investigations on the catalytic behavior of selected metal complexes: 99
4.4. Conclusions: 101
5. Some considerations on stereochemical aspects in octahedral tin templated bisphosphine complexes 104
5.1. Introduction: 104
5.1.1. Stereochemistry in bis-chelating octahedral complexes: 105
5.2. Results and discussion:..... 108
5.2.1. Chiral tin templated assemblies of 3-[(Diphenylphosphanyl)-methyl]-benzene-1, 2-diol (33):..... 108
5.2.2. Tin templated chiral assemblies of 3-{[Phenyl- (2,4,6-trimethyl-phenyl)-phosphanyl]-methyl}-benzene-1, 2-diol (34):..... 112
5.3. Conclusions: 117

6. Experimental details.....119
6.1. General remarks: 119
6.2. General procedure for the syntheses of phenol functionalized phosphane oxides (5a-e and 9f):.....121
6.2.1. 2-[(Diphenyl phosphinoyl) methyl] phenol (5a): 121
6.2.2. 3-[(Diphenyl phosphinoyl) methyl] benzene-1, 2-diol (5b):.....122
6.2.3. 4-[(Diphenyl phosphinoyl) methyl] phenol (5c): 122
6.2.4. 4-[(Diphenyl phosphinoyl) methyl] benzene-1, 2-diol (5d):.....123
6.2.5. 3-[(Diphenyl phosphinoyl) methyl] phenol (5e): 124
6.2.6. 3-[(Mesitylphenylphosphinoyl) methyl] benzene-1, 2-diol (10):.....124
6.2.7. 2-[(Diphenylphosphanyl)hydroxymethyl]phenol Hydrochloride (6a): 125
6.2.8. 4-[(Diphenylphosphanyl) hydroxymethyl] phenol (4c):.....125
6.2.9. Bis [hydroxy (3-hydroxyphenyl) methyl] diphenyl phosphonium Toluenesulfonate (7e/7e_): 126
6.3. General procedure for the synthesis of phenol-functionalized phosphanes 9a-d and 101: 127
6.3.1. 2-[(Diphenylphosphanyl) methyl] phenol (9a): 127
6.3.2. 3-[(Diphenylphosphanyl) methyl] benzene-1, 2-diol (9b):.....127
6.3.3. 4-[(Diphenylphosphanyl) methyl] benzene-1, 2-diol (9d):.....128
6.3.4. 3-[(Mesitylphenyl phosphanyl)-methyl]-benzene-1, 2-diol (9g): 129
6.4. General procedure for the syntheses of transition metal complexes of 9b-d:....129
6.4.1. Bis {3-[(Diphenylphosphanyl)-methyl]-benzene-1, 2-diol} Palladium dichloride, 13b: 130
6.4.2. Bis {4-[(Diphenylphosphanyl)-methyl]-benzene-1, 2-diol} Palladium dichloride, 13d: 130
6.4.3. Silver- bis {3-[(Diphenylphosphanyl)-methyl]-benzene-1, 2-diol}, 14b: .131
6.4.4. Silver- bis {4-[(Diphenylphosphanyl)-methyl]-benzene-1, 2-diol}, 14d: .131
6.4.5. Bis {4-[(Diphenylphosphanyl)-methyl]-benzene-1, 2-diol} platinum dichloride, 15: 132
6.4.6. Bis{3-[(Mesitylphenyl phosphanyl)-methyl]-benzene-1, 2-diol} palladium(II), 101: 133
6.5. General procedure for the syntheses of boranes: 134

6.5.1. (a) Diphenyl- (2-phenyl-benzo [1,3,2]-dioxaborol-4-ylmethyl)-phosphane 16a:……..... 134
6.5.1 (b) Diphenyl- (2-pentaflurophenyl-benzo [1,3,2]-dioxaborol-4-ylmethyl)-phosphane 16b:..... 134
6.5.2. (a) Synthesis of Diphenyl- (2-phenyl-benzo [1,3,2]-dioxaborol-4-ylmethyl)-phosphane-3- (Dimethyl amino pyridine) 17a: 135
6.5.2 (b) Synthesis of Diphenyl- (2-pentaflurophenyl-benzo [1,3,2]-dioxaborol-4-ylmethyl)-phosphane-3- (Dimethyl amino pyridine) 17b:..... 136
6.5.3. Synthesis of Dichloro bis {Diphenyl- (2-phenyl-benzo [1,3,2]-dioxaborol-4-ylmethyl)-phosphane}-palladium, 18: 136
6.5.4. Synthesis of Dichloro palladium bis {Diphenyl- (2-phenyl-benzo [1,3,2]-dioxaborol-4-ylmethyl)-phosphane-3- (Dimethyl amino pyridine)}, 19:..... 137
6.5.5. General procedure for the syntheses of borates 20 and 22:..... 137
6.5.6. Synthesis of the silver complex [Ag (20)], 21:..... 139
6.5.7. Synthesis of the Ag-B macrocycle $Ag_2(22)_2$, 23:..... 140
6.6. Transition metal complexes of templated symmetric bisphosphane ligands and their potential application in catalysis 142
6.6.1. Synthesis of palladium-bis {diphenyl- (benzo- [1, 3]-μ-oxo-k-oxo-4-ylmethyl) phosphane)}- gallium chloride (25):..... 142
6.6.2. Synthesis of palladium-bis {diphenyl- (benzo- [1, 3]-μ-oxo- k-oxo-4-ylmethyl)-phosphane)}-tin dichloride (26a): 143
6.6.3. Synthesis of palladium-bis {diphenyl- (benzo- [1, 3]-μ-oxo- k-oxo-4-ylmethyl)-phosphane)}-dimethyl tin (26b):..... 144
6.6.4. Synthesis of platinum -bis {diphenyl- (benzo- [1, 3]-μ-oxo-k-oxo-4-ylmethyl) phosphane)}-dimethyl tin (28): 145
6.6.5. Syntheses of palladium- bis {diphenyl- (benzo- [1, 3]-μ-oxo-k-oxo-4-ylmethyl) phosphane)}-bismuth chloride (29):..... 146
6.6.6. (a) Synthesis of bis {palladium- bis {diphenyl- (benzo- [1, 3]-μ-oxo-k-oxo-4-ylmethyl) phosphane)}- zirconium (30):..... 147
6.6.6 (b) Synthesis of dicyclopentadienyl {palladium- bis {diphenyl- (benzo- [1, 3]-μ-oxo-k-oxo-4-ylmethyl) phosphane)}- zirconium (30A): 148
6.6.7. Synthesis of tetrakis {palladium- bis {diphenyl- (benzo- [1, 3]-μ-oxo-k-oxo-4-ylmethyl) phosphane)- yttrium} μ_4-hydroxy tri-chloride (31):..... 148

6.6.8. Synthesis of bis {palladium- 3-[(Diphenyl phosphanyl)-methyl]-2-{4-[(diphenyl phosphanyl)-methyl]-benzo[1,3,3'] μ-oxo- μ'-oxo k-oxo -2-yloxy}-phenol]}- yttrium chloride (32): 149
6.6.9. Investigations on the catalytic behavior of selected metal complexes: Sonogashira C-C coupling reaction: 150
6.7. Transition metal complexes of templated bisphosphane ligands with diastereotopic donor sites: 151
6.7.1. Synthesis of palladium -bis {phenyl, 2,4,6-trimethyl-phenyl (benzo- [1, 3]-μ-oxo-k-oxo-4-ylmethyl) phosphane)}-dimethyl tin (33a/b): 151
6.7.2. Synthesis of palladium -bis {biphenyl- (benzo- [1, 3]-μ-oxo-k-oxo-4-ylmethyl) phosphane)}-methyl tin chloride (34): 152
6.8. Results of computational studies on complex 26a/27a: 153
7. Summary and outlook 155
7.1. Summary: 155
7.2. Outlook: 159
7.2.1. Prospective ligands: 159
7.2.2. Extending the self-assemblies: 161
7.2.3. Applications: 161
7.3 Zusammenfassung: 163
8. Crystallographic Appendix 168
9. References: 190
10. Curriculum vitae 200

1. Introduction

1.1. Self-assembly, ligand designing and catalysis:

Among many theories put forward in the creation of earth, physics played an important role. In the later stage came the chemistry followed by biology. After the big bang, particles united to form atoms,[1] atoms to molecules, molecules to supermolecules and supermolecules to supramolecules. This higher ordering some time later resulted in to the creation of first living being "Ameba". Chemistry is the science of atoms and molecules, which are the simplest building blocks of variety of materials and are unavoidable ingredients of many processes. Chemistry helps us in understanding the properties of matter and there by resulting in the creation of new materials. It is a bridge between basic and applied, simple and complex, between living and non-living.

Chemistry is a toolbox, which has the power to produce new molecules and materials that never existed before they were created by chemists. Self-assembling based on the range of noncovalent inter or intra molecular interactions[2] is another tool in the kit of chemistry and nature provides range of examples of this kind, such as, a few amino acids in human body assemble in different ways to carry out thousands of processes. An important factor in the process of assembling are the complementary binding motifs on the components and these components could be simple organic molecules to metals to complex amino acids. A precautious engineering of the process components can provide the desired architecture. Shortening the width of the broad spectrum of self-assemblies to the relatively smaller

[1] P. J. E. Peebles, D. N. Schramm, E. L. Turner, R. G. Kron, *Nature*, **1991**, 352, 769-776; S. W. Hawking, G. F. R. Ellis, 1968, *The Astrophysical Journal*, **1968**, 152, 25; G. L. Schroeder, *"Genesis and the big bang" Bantam Books, New York,* **1990**.
[2] H.J. Schneider, A. K. Yatsimirsky, *Principles and Methods in Supramolecular Chemistry*, Wiley-VCH, New York, **2000**.

class of inorganic self-assemblies will probably provide better insight into these architectures.

Inorganic self-assembly involves spontaneous organization of organic ligands around the metal center. The metal center acts both as cement to hold the ligands and as center to orient the ligands in a particular direction. The importance lies in designing ligands and the choice of the metal to obtain a desired architecture from the mixture of subunits. Metal ions have their own stake in this process, a) they prefer particular geometries of ligands, b) they have varying strength in terms of acidity or basicity, c) in addition to this they can be redox or photochemically active providing further interesting properties. A range of architectures can be obtained by fine-tuning the ligand or metal or both ligand and metal. These assemblies show a range of excellent properties. For example a triangle[3] or square assembly[4] can be utilized as a host for trapping a guest molecule. Star[5] or rectangular box[6] like assemblies bound to the substrate molecules[7] may enable to perform chemical transformations on the substrate molecule. Supramolecular capsules[8] can act as catalysts in unimolecular rearrangements.[9] A triple helix obtained by self-assembly provides insights into the double helix interactions.[10] Supramolecular self-recognition may provide details of amino acid sequencing in proteins.[11] A great diversity of polynuclear metal clusters have been obtained by self-assembly where in the number of metals atoms range from few to over hundred which shows a metallic behavior[12] or catalytic activity.[13]

One of the important components of an assembling process is the ligand. A crucial ligand design may circumvent laborious syntheses. The properties of an assembly or complex can be very easily fine-tuned by varying the ligand, though it's teamwork. In order to assist the ligand design on rational basis there is a need of a general concept. In an effort, Tolman introduced the concept of "cone angle (Θ)".[14] According to Tolman's definition, cone

[3] G. Suess-Fink, J. L. Wolfender, F. Neumann, H. Stoeckli-Evans, *Angew. Chem. Int. Ed.* **1990**, 29, 429.
[4] G. Newton, I. Haiduc, R. B. King, C. Silvestru, *J. Am. Chem. Soc*. **1993**, 115, 1229.
[5] S. Gambarotta, C. Floriani, A. Chiesi-Villa, C. Guastini, *J. Am. Chem. Soc.* **1983**, 105, 1156.
[6] S. K. Mandal, L. K. Thompson, M. J. Newlands, E. J. Gabe, F. L. Lee, *J. Chem. Soc. Chem. Commun.* **1989**, 744.
[7] A. W. Maverick, M. L. Ivie, J. H. Waggenspack, F. R. Fronczek, *Inorg. Chem*. **1990**, 29, 2403.
[8] A. W. Kleij, J. N. H. Reek, *Chem. Eur. J*. **2006**, 12, 4218.
[9] D. Fiedler, H. van Halbeek, R. G. Bergman, K. N. Raymond, *J. Am. Chem. Soc*. **2006**, 128, 10240.
[10] J. M. Lehn, *Supramolecular Chemistry: Concepts and Perspectives*, VCH, Weinheim **1995**.
[11] D. L. Caulder, K. N. Raymond, *Angew. Chem. Int. Ed.* **1997**, 36, 1440.
[12] F. M. Mulder, T. A. Stegink, R. C. Thiel, L. J. de Jongh, G. Schmid, *Nature*, **1994**, 367, 716.
[13] M. N. Vargaftik, I. I. Moiseev, D. I. Kochubey, K. I. Zamaraev, *Faraday Discuss*. **1991**, 92, 13.
[14] C. A. Tolman, *Chem. Rev*. **1977**, 77, 313.

angle is a mean of describing the steric properties of a monodentate ligand. He was the first to quantify the electronic properties of some of the ligands and went on to introduce a term X to describe them.[15] Much later the importance of the geometry of the bidentate ligand was recognized and was termed as "Natural bite angle" by Leeuwen and coworkers.[16] The natural bite angle can be defined as the angle at which the two donor atoms of a chelating ligand bite at the metal center. A very close term to the bite angle is the "flexibility range" which is defined as the accessible range of bite angles within less than 12.6 kJ/mol excess strain energy from the calculated bite angle.[17] Though the above factors are quantified, there are other factors, which equally influence the ligand design. The nature of donating atoms in a ligand is very important in order to achieve coordination with a particular metal center. The availability of range of soft to very hard donors allows chemists to select donors of their choice.

Substituents, more precisely steric bulk on the donors, as well influence the coordination. Bulky substituents may shield the donor subsequently, decreasing the donating ability, and vice versa. Electronic factors are of equal importance; hence while designing ligands, electronic factors should also be considered. Electron withdrawing substitutents may decrease the donating ability and electron accepting substituents may increase the donating ability. Tolman's method provides a rough quantification of steric and electronic factors, but a precise determination of these factors is still missing, although good sophisticated guesses can be made with the help of modern computational methods. Depending on the number of donor sites, ligands can be classified as mono-, bi-, tri- or polydentate. Monodentate ligands can be easily synthesized but have limited applications. On the other hand bidentate ligands can induce rigidity in a complex and thus increase the regio or stereo selectivity. But syntheses of bidentate ligands are generally multistep, time consuming and laborious. In order to circumvent the tedious syntheses there is a need of a new synthetic strategy.[18]

Having designed the ligand and selected a metal, a step forward could be utilizing them to demonstrate the true power of chemistry in catalysis. Catalysis can be defined as an action between two or more substrates, initiated by an agent called catalyst that itself remains

[15] C. A. Tolman. *J. Am. Chem. Soc.* **1970**, 92, 2953.
[16] P. W. N. M. van Leeuwen, P. C. J. Kamer, J. N. H. Reek, P. Dierkes, *Chem. Rev.* **2000**, 100, 2741; P. W. N. M. van Leeuwen, P. C. J. Kamer, J. N. H. Reek, *Pure Appl. Chem*. **1999**, 71, 1443.
[17] A. J. Sandee, J. N. H. Reek, *J. Chem. Soc. Dalton. Trans.* **2006**, 3385.
[18] J. M. Tackas, D. S. Reddy, S. A. Moteki, D. Wu, H. Palencia, *J. Am. Chem. Soc*. **2004**, 126, 14, 4494.

unaffected by the action and accelerates the rate of action. Assembling ligands around a metal to obtain a catalyst of interest is a challenge in chemistry. Traditional synthetic pathways to develop a catalyst are multi-step and time consuming; this is specially inconvenient where a large ligand library has to be screened in order to find out the most suitable candidate for a suitable application. New synthetic strategies are therefore necessary. Major break throughs have been achieved in recent years and a few interesting strategies have been emerged.

Breit and coworkers (see **Fig. 1**) came up with the idea of utilizing hydrogen bonding between two monodentate ligands and assembling them on a metal center, which then mimics a bidentate ligand.[19] The key role is played by the ligand-ligand interactions. Depending on the ligand-ligand interaction a continuum can be drawn beginning with the weakest and ending in the strongest ligand-ligand interaction. Thus with a small number of monodentate ligands a large library of metal complexes can be easily synthesized.[20]

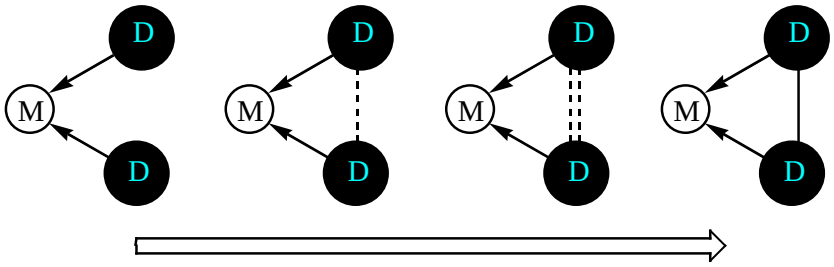

Fig. 1: Monodentate ligands that mimic bidentate ligand.

Another strategy is to assemble the ligands on a preformed template. Takacs et. al. used Zinc bis-oxazoline complexes (see **Fig. 2**) as template and attached a long organic tether with a functional group at the end of the tether, which offer donating sites for further coordination and assembly.[18] In a similar fashion Reek and coworkers used

[19] B. Breit. *Angew. Chem. Int. Ed.* **2005**, 44, 6816.
[20] B. Breit, W. Seiche, *Angew. Chem. Int. Ed.* **2005**, 44, 1640.

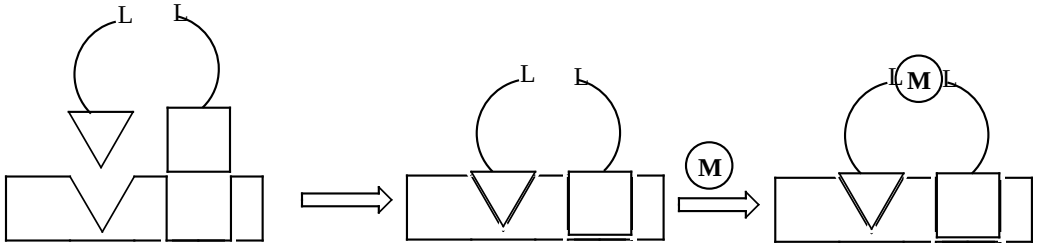

Fig. 2: Template controlled complex designing

zinc porphyrin as template and assembled ligands on this template which are capable of coordinating further metals.[21] They demonstrated that the assembly of heteroleptic complexes was preferred over homoleptic ones. Complexes generated using self-assembling approaches were shown to be highly active and selective in hydration of terminal alkynes,[22] asymmetric hydroformylation[23] and in many other catalytic reactions.[24] Recently Love[25] and Reek[26] independently introduced a similar concept called "anion sequestering" in that one end of the ligand is anchored on an anion and the other end is coordinated to a metal. The development of these and related strategies has already been summarized in a number of recent reviews.[19, 27]

1.2. Setting the Goals:

Recent years have witnessed a few break-throughs in the field of catalyst designing via self-assembly, but there is immense need of new approaches. The chemistry of self-assembly relies on non-covalent interactions such as hydrogen bonding, van der Waals interactions, cation-π interactions, electrostatic interactions, charge transfer interactions, π stacking interactions and coordinative interactions.[2] The present study is aimed at utilizing the coordinating behavior of a phosphine at one end of a bifunctional molecule, whereas the other end is templated on an element (E) (refer to **Fig. 4**). The template E is expected to assemble two or more catechol phosphines to generate bi- or multifunctional ligands. The template E is anticipated to play a crucial role in controlling the bite angle and coordination behavior of the phosphine donors and can be any hard acid from in the sense

[21] V. F. Slagt, M. Roeder, P. C. J. Kamer, P. W. N. M. van Leeuwen, J. N. H. Reek, *J. Am. Chem. Soc.* **2004**, 126, 4056.
[22] F. Chevallier, B. Breit, *Angew. Chem. Int. Ed.* **2006**, 45, 1599.
[23] M. Kuil, P. E. Goudriaan, P. W. N. M. van Leeuwen, J. N. H. Reek, *J. Chem. Soc. Chem. Commun.* **2006**, 4679.
[24] B. Breit, W. Seiche, *J. Am. Chem. Soc.* **2003**, 125, 6608.
[25] P. A. Duckmanton, A. J. Blake, J. B. Love, *Inorg. Chem*. **2005**, 44, 7708.
[26] L. K. Knight, Z. Freixa, P. W. N. M. van Leeuwen, J. N. H. Reek, *Organometallics*, **2006**, 25, 954.
[27] M. J. Wilkinson, P. W. N. M. van Leeuwen, J. N. H. Reek, *Org. Bio. Chem.* **2005**, 3, 2371.

of the hard/soft/acid/base concept[28] main group elements to transition metals, providing an array of diversity. Phosphines are well known in catalysis due to their easily accessible lone pair (**Fig. 3**). Phosphines are known to be soft donors and according to hard/soft acid/ base theory[28] these may selectively coordinate to soft acceptors. Thus, coordination of a metal with bi- or multidentate E produces the final "Assembly" i. e. E, M-chelate complex (see **Fig. 4**). Changing the substituents on phosphorus may allow to fine-tune the steric and electronic properties of the ligand.

Thus the first aim of this work is to rationally design phosphine functionalized monodentate ligands and to develop a short synthetic methodology for the syntheses of these ligands, which may suite to a self-assembling approach to generate bidentate donors.

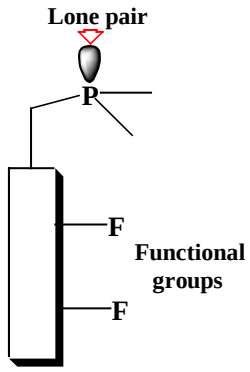

Fig. 3: Functional phosphine with lone pair

An attempt will be made to demonstrate the feasibility of the template formation by exploring a stepwise "Aufbau" of a supramolecular bidentate ligand, followed by introduction of a transition metal across the soft phosphine donors. Thus the template with the ligand now mimics a bidentate ligand that can be self-assembled on a metal. Another area of interest is to explore the Lewis acid base chemistry of the functional phosphine ligands. The coordination of hard acids at the hard donor sites generating acidic center will be utilized to synthesize multimetallic complexes, which have attracted great interest in recent years.

The main goal of this study is to employ the new classes of functionalized phosphines in the process of supramolecular self-assembly, which may produce the templated metal complexes in a single step (**Fig. 4** demonstrating the goals). Such an assembling methodology may offer greater opportunities over the traditional synthetic protocols

[28] R. G. Pearson, *J. Chem. Ed.* **1987**, 64, 561-567.

established in the syntheses of metal complexes. In that, varying the size and coordination geometry of the template center (E) shall control the preorganization of the phosphines.

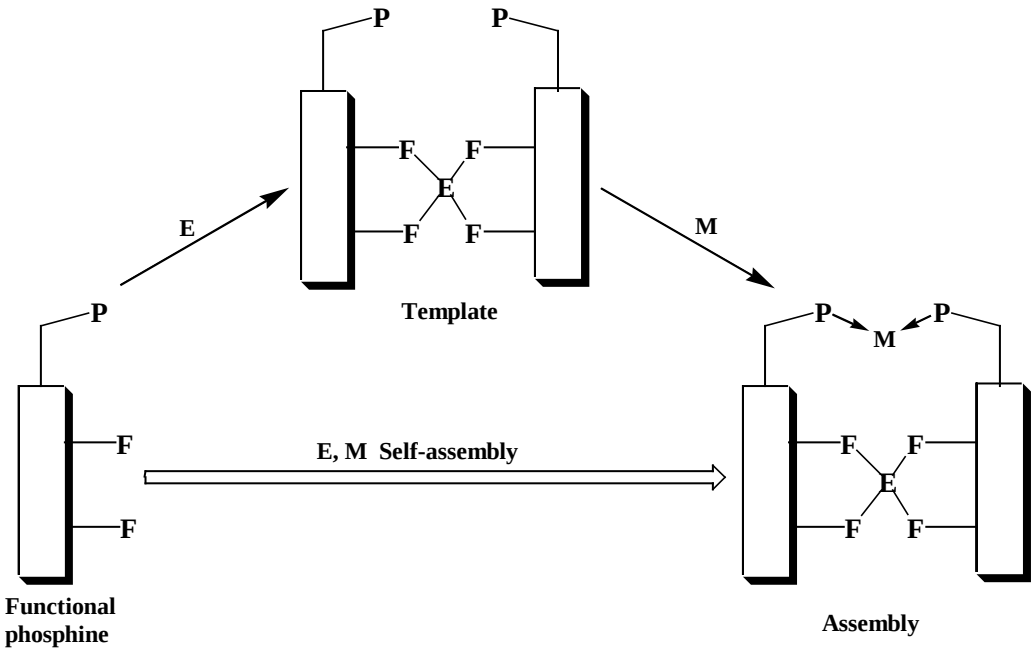

Fig. 4: Schematic representation of Aufbau and self-assembling approaches.

Variation in the template center may allow to study the bite angle properties of the final assembly. A closer look at the complexes obtained by the self-assembling approach revealed that the composition of these complexes resembles to those used in C-C coupling reactions. The catalytic potential of selected complexes in the Sonogashira coupling of phenyl acetylene with p-iodo-nitrobenzene will be explored.

Nature provides an immense number of examples of chiral entities, but rational syntheses of such chiral entities presents an active challenge to synthetic chemists around the world. In this view, a further point of interest in this work is to synthesize chiral complexes by a self-assembling approach. This goal can be achieved either by introducing chirality at the template center or at the phosphine moiety.

In short, the goal of the present study is a) to synthesize bidentate phosphine functionalized ligands in possibly the least number of synthetic steps, which may suite for a self-assembling approach, b) to generate a template which mimics a bidentate ligand and can self-assemble to produce a metal complex, c) to develop a new strategy based on supramolecular self-assembly wherein hard donors reacts with hard acids and soft donors to soft acid in a single step to produce the desired architectures, d) to study changes in bite

angle and cone angle of a complex by varying the geometry of the template center, e) to demonstrate the catalytic potential of the self-assembled complexes and f) to synthesize chiral complexes by the self-assembling approach.

2. Syntheses of diphenyl-phosphinomethyl substituted phenols and catechols and mechanistic details on their formation

2.1. Introduction:

Phosphines are one of the most commonly used class of ligands in modern day catalysis. They are routinely employed in C-C coupling reactions,[29] in hydrogenation,[22] allylic alkylation,[21] etc. As the complexity of their applications increases, synthesis of the phosphine also becomes complex. The last few decades have been dominated by an increasing use of bidentate phosphines (bis-phosphines) rather than their monodentate counterparts.[30] The bidentate ligands offer diverse characteristics like variable coordination sites, controlled (regio and stereo) selectivity, and structural rigidity. But many times the synthesis of such bidentate ligands is multistep and time consuming. Multistep synthesis is practically inconvenient where a large ligand library is needed in order to find out the most suitable ligand for a particular application. To avoid this, there is an immense need of new strategies that will provide easy synthetic pathways towards the syntheses of bidentate ligands.

In this chapter the focus will be on providing an easy synthetic pathway to functional phosphines that can be used to build bidentate ligands. Phosphines functionalized with hard donor groups appear to be interesting candidates in applications such as self-assembly. As rigidity is one of the most important criteria in self-assembly, it was envisioned that phosphines with functional groups on a rigid framework would further

[29] J. Tsuji, *Palladium Reagents and Catalysts*, Wiley, **2000.**
[30] I. V. Komarov, A. Borner, *Angew. Chem. Int. Ed.* **2001**, *40*, 1197; T. Hayashi, *Acc. Chem. Res.* **2000,** *33*, 354.

benefit the purpose. In this view, functionalzing the phosphines with catechol or phenol substituents was thought to be a good starting point.

The addition of a P–H bond to a carbonyl group is a synthetically useful and fundamental reaction mode of phosphorus-hydrogen substituted phosphines. In particular, the reaction between an aldehyde/ketone and secondary phosphine is an important pathway to prepare organophosphorus compounds and was reported as early as in 1962 by Buckler et al.[31] These transformations proceed normally strictly regioselective via P–C bond formation to give α-phosphanyl-carbinols (**Scheme 1, a**) and have found application in the synthesis of functional tertiary phosphines.[32] Recently it has been found that *N*-heterocyclic phosphines **1** deviate from the common behavior as they react with aldehydes and ketones via reduction rather than alkylation of the carbonyl moiety (**Scheme 1, b**).[33] The unusual reversed regioselectivity ("Umpolung") has been related to the unique hydride-like polarization of the P–H bond in **1** which owes to the special bonding situation in the heterocyclic ring .[33]

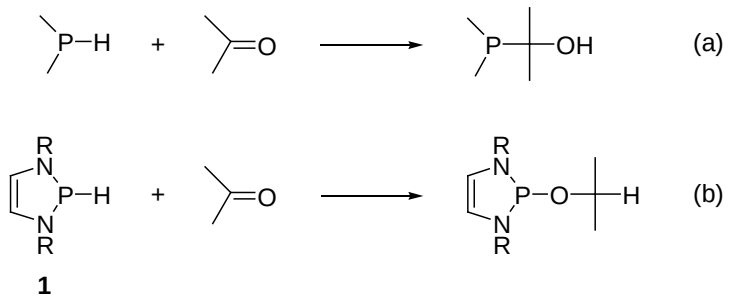

1

Scheme 1: Possible reaction modes of phosphanes with carbonyl groups

During a literature survey on hydrophosphanation of carbonyl compounds it was found that the reaction of diphenyl phosphine with salicylic aldehyde proceeds directly to give a benzyl phosphine oxide (**Scheme 2**).[34] Similar reactions had been observed earlier and were explained by a two-step sequence involving a "normal" hydrophosphanation followed by isomerization of the transient α-phosphanyl-carbinol (pathway (i), **Scheme 2**).[35] In the context of present studies on controlling the regioselectivity of hydrophosphanations[33] it was of interest to elucidate the mechanistic aspects of this reaction in more detail. Of

[31] M. Epstein and S. A. Buckler, *Tetrahedron*, **1962**, 18, 11, 1231.
[32] K.V. Katti, H. Gali, C. J. Smith, D.E. Berning, *Acc. Chem. Res*. **1999**, *32*, 9.
[33] D. Gudat, A. Haghverdi, M. Nieger, *Angew. Chem.* **2000**, *112*, 3211-3214; S. Burck, D. Gudat, M. Nieger, W.W. Du Mont, *J. Am. Chem. Soc*. **2006**, *128*, 12, 3946.
[34] V. I. Evreinov, V. E. Baulin, Z. N. Vostroknutova, N. A. Bondarenko, T. Kh. Syundyukova, E. N. Tsvetkov, *Izv. Akad. Nauk SSSR, Ser. Khim*. **1989**, 1990.
[35] S. Trippett, *J. Chem. Soc*. **1961**, 1813.

particular interest was to exclude the possibility that the product was formed via "inverse" addition of the P–H bond of the phosphine and subsequent Michaelis-Arbuzov rearrangement of a transient phosphinite (pathway (ii) in **Scheme 2**) which might, in view of the reactivity of **1** and earlier observations of Michaelis-Arbuzov rearrangements under conditions similar to the ones applied here,[36] provide a conceivable alternative to the standard mechanism.

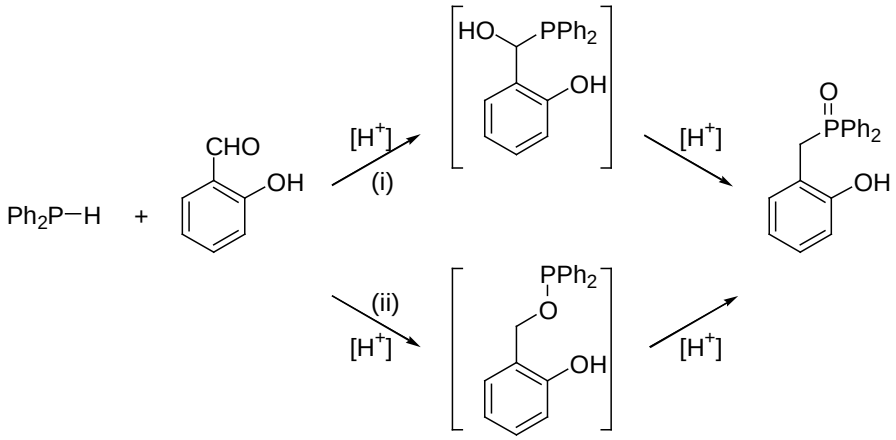

Scheme 2: addition of P-H bond to an aldehyde and rearrangement modes

Herewith the results of studies of the transformations of diphenyl phosphine and phenolic aldehydes into phenol-functionalized phosphine oxides are presented, and it is demonstrated that these species can be easily converted into phosphines. The products thus accessible belong to a class of multifunctional ligands and may find interesting applications in host-guest chemistry[37] or catalysis.[38]

2.2. Results and discussion:

2.2.1. Syntheses and mechanistic insights on the formation of methyl phosphinoyl phenols and catechols:

The reaction of equimolar amounts of diphenyl phosphine **2** and salicylic aldehyde **3a** in methanol or ethers (Et_2O, DME) in the presence of catalytic amounts of hydrochloric or p-toluenesulfonic acid affords directly the phosphine oxide **5a,**[34] which has been isolated in

[36] P. Y. Renard, P. Vayron, C. Mioskowski, *Organic Lett*. **2003**, *5*, 1661; A. N. Bovin, A. N. Yarkevich, A. N. Kharitonov, E. N. Tsvetkov, *Chem. Commun*. **1994**, 973.
[37] X. Sun, D. W. Johnson, D. L. Caulder, K. N. Raymond, E. H. Wong, *J. Am. Chem. Soc*. **2001**, *123*, 2752.
[38] N. T. Lucas, J. M. Hook, A. M. McDonagh, S. B. Colbran, *Eur. J. Inorg. Chem*. **2005**, 496; N. T. Lucas, A. M. McDonagh, I. G. Dance, S. B. Colbran, D. C. Craig, *Dalton Trans*. **2006**, 680.

good yield after work-up (**Scheme 3**). Monitoring the progress of the reaction by ^{31}P NMR spectroscopy revealed that **5a** remained the only spectroscopically detectable species beside unreacted **2** (which disappeared when the reaction took progress) and minor side products. Even though the latter were not further characterized, the observed chemical shifts precluded a structural assignment as an α-phosphanyl-carbinol. In order to elucidate mechanistic details it was attempted to find reaction conditions that facilitated the detection of a precursor to **5a**. In these studies it was established that treatment of an ethereal solution of **2** and **3a** with excess conc. hydrochloric acid led to immediate precipitation of a colorless solid, which was isolated by filtration. A solid-state ^{31}P CP/MAS NMR spectrum disclosed an isotropic shift $\delta^{31}P_{iso}$ = -0.8 which differs clearly from that of **5a**

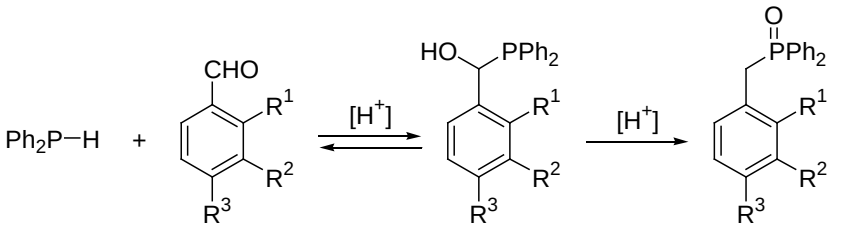

2 **3a-e** **4a-e** **5a-d**

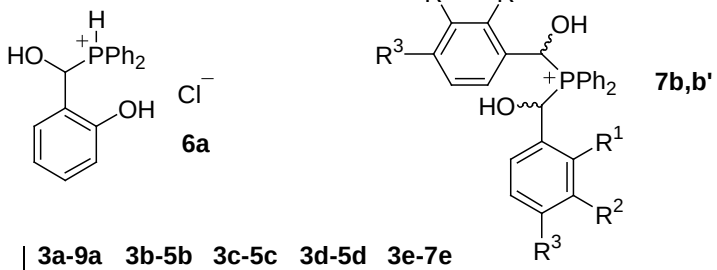

6a **7b,b'**

	3a-9a	**3b-5b**	**3c-5c**	**3d-5d**	**3e-7e**
R^1	OH	OH	H	H	H
R^2	H	OH	H	OH	OH
R^3	H	H	OH	OH	H

Scheme 3: Designing and syntheses of catechol phosphine oxides

($\delta^{31}P_{iso}$ = 39.3) but resembles that of the α-phosphanyl-carbinol obtained from the reaction of **2** and benzaldehyde. As a spectrum recorded under conditions that allow to detect scalar couplings to protons revealed a doublet splitting attributable to a one-bond *J*-coupling (**Fig. 1**, J_{PH} = 501 Hz), the product was assigned as the α-phosphanyl-carbinol hydrochloride **6a** which is deemed to represent the initial product formed by attack of the nucleophilic phosphine on the protonated aldehyde. The structural assignment was further corroborated by satisfactory analytical data. **6a** was isolated as white solid melting at

104ºC in 90% yield. Attempts to characterize **6a** by solution NMR spectroscopy revealed that the product decayed upon dissolution in methanol to give a mixture of the starting materials and the phosphine oxide **5a**, and emphasized thus its nature as a reaction intermediate. The results presented above allow to conclude that the reaction of **2** with salicylic aldehyde involves a "normal" hydrophosphanation as the key step.

Reaction of **3b** was carried out under similar conditions as that of the **3a**. The same regioselectivity was observed in the acid-catalyzed reaction of **2** with 2,3-dihydroxybenzaldehyde **3b** as that of **3a**. NMR studies allowed in this case the direct detection of a small amount of the α-phosphanyl- carbinol **4b** and two further intermediates. The constitution of the latter was assigned as diastereomeric phosphonium

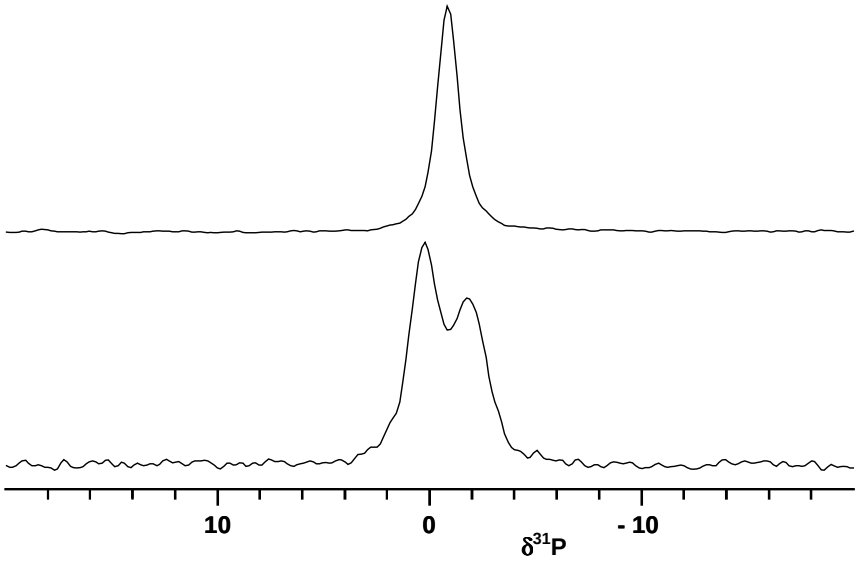

Figure 1: Isotropic line of the solid state CP/MAS ^{31}P NMR spectrum of 6a at a spinning speed of 13.2 kHz recorded with high power proton decoupling (top trace) and frequency-shifted Lee-Goldburg decoupling (bottom trace) for the suppression of homonuclear dipolar coupling between protons. As the decoupling sequence scales heteronuclear couplings by a factor of 0.577, the observed splitting of 289 Hz corresponds to a value of $^{1}J_{PH}$ = 501 Hz.

salts **7b, 7'b** by two-dimensional NMR studies, and dynamic exchange between all four species was established by a 2D ^{31}P EXSY NMR spectrum. Similar species as **7b, 7'b** have previously been obtained by reaction of diphenyl phosphine with formaldehyde and strong acids.[32,39] All products were eventually converted into the phosphine oxides **5a-d.** The

[39] J. Fawcett, John; P. A. T. Hoye, R. D.W. Kemmitt, D. J. Law, D. R. Russell, *J. Chem. Soc. Dalton Trans*. **1993**, 2563.

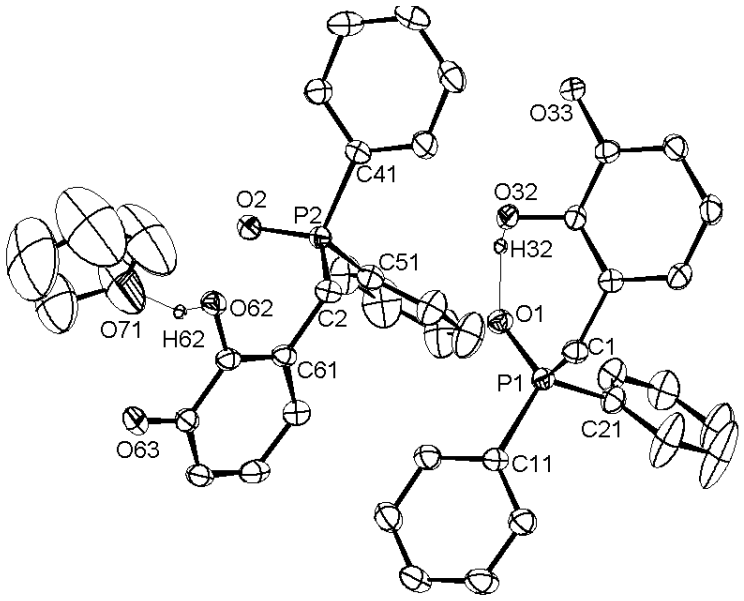

Bond lengths [Å]	Bond lengths[Å]	Bond angles [°]	Bond angles [°]
P2-O2 1.500(1)	P1-O1 1.510(3)	C41-P2-C51 106.06(1)	O1-P1-C11 110.75(1)
P1-C21 1.797(2)	P1-C1 1.817(1)	O2-P2-C51 110.98(1)	O1-P1-C21 111.3(1)
P2-C2 1.812(1)	H32-O1 1.786(1)	O2-P2-C41 110.3(1)	C1-P1-C21 108.1(1)
P2-C41 1.806(1)	H62-O2 4.606(2)	O2-P2-C2 114.1(1)	C1-P1-C11 107.2(1)

Fig. 2.2: Molecular structure of 5b; H-atoms except H32 and H62 are omitted for clarity (50% probability thermal ellipsoids), important bond lengths and bond angles are given in the table.

phosphine oxide **5b** was isolated after work-up as white solid in 85% yield and melts at 194°C. The ^{31}P NMR spectrum of the white solid displayed a single resonance at 40.4 ppm. EI-Mass spectroscopy showed a molecular ion peak at m/e = 324, which corresponds to the expected molar mass of **5b**. As a representative of all phosphine oxides, the molecular structure of **5b** was determined by a single crystal X-ray diffraction study. Suitable single crystals were obtained by crystallization from a concentrated DME solution at room temperature. The phosphine oxide **5b** crystallizes in a triclinic unit cell in the space group P1(bar) (**Fig. 2.2**). The asymmetric unit contains two crystallographically independent molecules of **5b**, which are disposed in head to tail fashion (see **fig. 2.2**) and a solvent molecule (THF). The P2 centered molecule shows a weak hydrogen bonding (H62-O71: 1.99 Å) interaction with the solvent (THF) molecule, whereas the P1 centered

molecule does not show any intermolecular interaction. On the other hand the P1 centered ligand display intramolecular hydrogen bonding, where H32 is weakly bonded to O1 (1.78 Å). As a consequence, the O1-O32 (2.60 Å) distance is shorter than the O2-O62 (3.89 Å) distance. Further noticeable is the P-O distance (1.51 Å), which confirms the P-O double bond as is expected.[40] The phosphorus atoms display tetrahedral geometry with minor deviation of all the angles from the standard tetrahedral angle of 109.4º (see **Table 1**). The remaining bond distances and angles show no peculiarities.

The reaction of **2** with 4-hydroxybenzaldehyde **3c** afforded as primary product the α-phosphanyl-carbinol **4c**, which was isolated in 90% yield as colorless powder with melting point of 168ºC by precipitation from methanol and characterized by ^{31}P CP/MAS NMR. Key to the structural assignment was the observation of a single resonance [$\delta(^{31}P) = -7.2$] which appeared at somewhat higher field than that of **6a** and showed no splitting due to $^{1}J_{PH}$ coupling. In contrast to the elusive 2-hydroxy-substituted carbinol **4a**, the signal of **4c** was also observable in solution ^{31}P NMR spectra [$\delta(^{31}P) = -2.3$] although in these solutions, even in the absence of additional acid, partial decomposition into **2** and **3c** occurred (obviously the acidity of the phenolic OH-moiety is sufficient to promote an auto-catalytic reaction). Acid catalysts promoted complete conversion of the mixture into the phosphine oxide **5c.** The ^{31}P NMR spectrum showed a single resonance at 32 ppm confirming the complete conversion. The phosphine oxide **5c** was isolated as white solid, melting at 223ºC in 60%. The same behavior was observed as well in the reaction of **2** with 3,4-dihydroxybenzaldehyde **3d** which afforded the phosphine oxide **5d** as final product. A single ^{31}P resonance at 40.4 ppm supports the complete conversion to the phosphine oxide **5d** which was isolated as white powder in 90% yield with a melting point of 192°C.

Finally, acid-catalyzed reaction of **2** with 3-hydroxybenzaldehyde **3e** gave a mixture of products which were assigned as the phosphanyl-carbinol **4e** and phosphonium ions **7e/7e'** on the basis of a comparison of the observed ^{31}P chemical shifts with those of the products of the previously described reactions. Although after some hours a weak signal of a new

[40] P. Perez-Lourido, J. A. Gracia-Vazquez, J. Romero, A. Sousa, *Inorg. Chem*. **1999**, 38, 538.

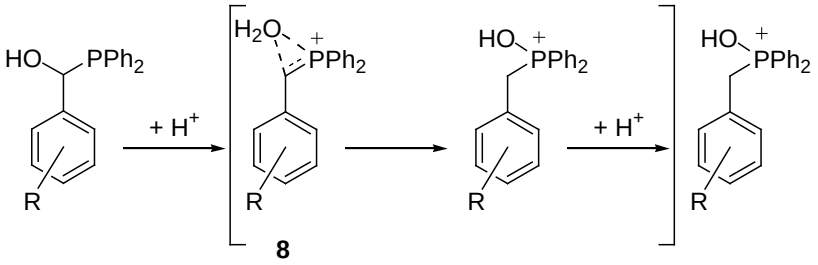

Scheme 4: Presumed mechanism of the phosphanyl-carbinol – phosphine oxide isomerization

product with a chemical shift compatible with a phosphine oxide structure was observable, the conversion remained incomplete even after prolonged reaction time. As isolation and identification of individual products proved unfeasible, the reaction was not pursued further.

In summary, it can be stated that all reactions of the phosphine **2** with hydroxyl-benzaldehydes **3a-e** proceed via hydrophosphanation to yield α-phosphanyl-carbinols **4a-e** as initial products. The reactions of aldehydes **3a-d** featuring at least one OH-substituent in 2- or 4-position are distinguished by the fact that the equilibrium between the starting materials and the addition product is shifted to side of the former, and that the α-phosphanyl-carbinols rearrange easily to the isomeric phosphine oxides. The reduced stability of these adducts with respect to the starting materials can be understood as a consequence of the electron releasing nature of the additional hydroxyl-substituents which should render the aldehydes weaker electrophiles and the attack by the nucleophilic phosphine energetically less favorable. Aldehydes with 2-hydroxy-substituents such as **3a,b** may further benefit from additional stabilization by strong intramolecular hydrogen bonding. As a consequence of these effects, the concentration of α-phosphanyl-carbinols in these reactions may be very low (**4b**) or not detectable at all (**4a**). Considering that the conversion of **4a-d** to the phosphine oxides **5a-d** proceeds presumably via an electrophilic methylenephosphonium type intermediate **8** (Scheme 4), the same substituent effects can be considered to facilitate the isomerization into the phosphine oxides.

2.2.2. Synthesis and characterization of chiral mesityl phenyl phosphinoyl methyl catechols:

The successful syntheses of the above mentioned mono/di-hydroxy ligands enhanced the confidence level and it was decided to design more challenging ligands. As chirality is one

of the important aspects in catalysis, attention was turned towards the syntheses of chiral catechol phosphines. Mesityl phenyl phosphine was synthesized according to the reported literature.[41] Addition of a racemate of the chiral phosphine to 2,3 dihydroxy benzaldehyde along with a catalytic amount of p-toluene sulfonic acid, followed by stirring for 24 hours at room temperature gave a white powder. The ^{31}P NMR spectrum of the white powder displayed a single resonance at 46.4 ppm indicating the formation of the expected phosphine oxide **4f**. Filtration followed by washing (thrice) with DME and drying gave a clean product. The white powder with the melting point of 220°C was isolated in 85% yield. The Mass spectrum showed a molecular ion peak at m/e = 366[M], further confirming the formation of a phosphine oxide.

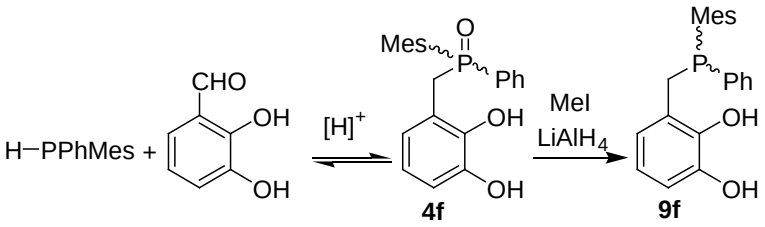

Scheme 5: Synthesis of 3-[(Mesitylphenylphosphinoyl) methyl] benzene-1, 2-diol

2.3. Reduction of the phosphine oxides to ditopic phosphines:

Deoxygenation of the phosphine oxides **5a-d** was readily achieved by adaptation of an established procedure involving quaternization of the phosphine oxide moiety with methyl

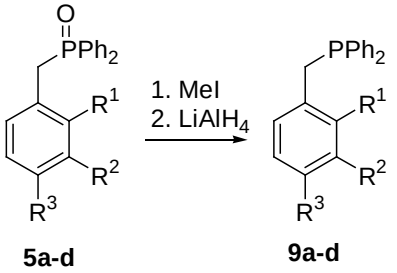

	5, 9a	5, 9b	5, 9c	5, 9d
R^1	OH	OH	H	H
R^2	H	OH	H	OH
R^3	H	H	OH	OH

Scheme 6: Reduction of phosphane oxides to phosphanes.

iodide and subsequent reduction with $LiAlH_4$ (**Scheme 6**).[42] No special protection of the phenol groups was necessary, however, the use of a sufficient excess of the hydride to achieve complete deprotonation of the acidic OH-groups was mandatory to obtain reasonable yields of products. The reaction was monitored by TLC and complete

[41] I. Kovacik, D. K. Wicht, N. S. Grewal, D. S. Glueck, C. D. Incarvito, I. A. Guzei, A. L. Rheingold, *Organometallics*, **2000,** *19,6,* 950.
[42] T. Imamoto, S.-I. Kikuchi, T. Miura, Y. Wada, *Org. Lett.* **2001,** 3, 1, 87.

conversion was achieved in 4-6 hours. Aqueous work-up of the reaction mixture and purification of the crude products by column chromatography afforded the phosphines **9a-d** as moderately oxygen sensitive materials. Compounds **9a-d** were isolated as colorless oils (**9a**) or white solids (**9b-d**) in yields of 60-70%.

As a representative of all other phosphines (**9a-d**), 3-[(Diphenylphosphanyl) methyl] benzene-1, 2-diol (**9b**) is discussed in detail herein. The white solid of **9b** melts at 82°C and was isolated in 60% yield. A single ^{31}P resonance was detected at –13.1 ppm as can be expected for such a phosphine.[43] The proton NMR displayed a multiplet between 7.5-7.3 ppm, accounting for 10 protons which is assigned to the phenyl groups. A doublet (AX spin system) at 6.78 ppm was observed which can be assigned to a catechol proton next to the hydroxy group. A triplet at 6.64 ppm is assigned to a central proton on the catechol ring and another doublet at 6.43 ppm is assigned to the catechol proton

Bond lengths [Å]	Bond angles [°]
P1-C14 1.840(1)	C8-P1-C14 101.66(1)
P1-C7 1.867(1)	C7-P1-C14 100.37(1)
P1-C8 1.839(0)	C7-P1-C8 101.78(1)
O2-H1 2.170(2)	

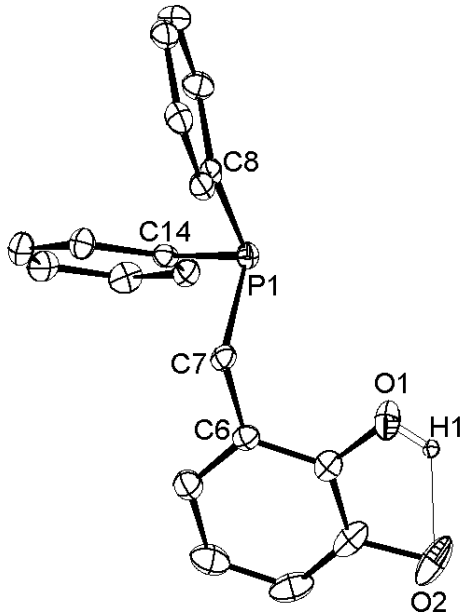

Fig. 2.3: Molecular structure of 9b; (H-atoms omitted for clarity, thermal ellipsoids with 50% probability) important bond angles and bond lengths are given in the table.

[43] K. Kellner, S. Rothe, E. M. Steyer, A. Tzschach, *Phosphorus, Sulfur, Relat. Elem.* **1980**, 9, 269.

next to the CH_2PPh_2 substituent. The methylene protons appear as a doublet at 3.52 ppm with a small two bond phosphorus proton coupling of 1.7 Hz. The Mass spectrum showed an ion peak at m/e = 308.1[M^+] and further fragments at 186.1 [Ph_2PH^+], 185.1 [Ph_2P^+], 183.0 [$Ph_2P^+–H_2$], 123.1[$M^+–PPh_2$], confirming the formation of **9b**.

The phosphine **9b** was crystallized from Ethyl acetate: hexane (3:7) at room temperature. The compound crystallizes in a monoclinic unit cell in the space group $P2_{1/c}$ (see **fig. 2.3**). The crystals contain discrete molecules of **9b** with specific intramolecular hydrogen bonding (H1-O2 2.17Å) interactions. The coordination sphere around phosphorus is a regular trigonal pyramid. The sum of the three bond angles (303º) is much less than 360º and is comparable with triphenyl phosphine (308º)[44] or tri-o-tolyl phosphine (308º).[45] The P-C7 (1.87 Å) bond distance was found to be longer than the other two P-C14/8 (1.83 Å) bonds and the P-C distances in triphenyl phosphine.[44] The hydroxy groups on the catechol ring are on the same side of the phosphorus lone pair. This particular arrangement of hydroxy groups and lone pair indicate that compound **9b** may prefer concave coordination.

The chiral phosphine oxide **4f** was reduced to the phosphine **9f** under similar reaction conditions as mentioned for **9b**. The white solid of **9f** obtained after column chromatography melts at 93°C and was isolated in good yields (70%). A single ^{31}P NMR resonance at –27.6 ppm was detected, the observed up field shift compared to the achiral phosphine (**9b/d**) is attributed to increased shielding of the phosphorus atom by the sterically bulky mesityl group. This observation is in accordance with the literature reported[46] fact that trimesityl phosphine (-35.8 ppm) is much more upfield shifted compared to the less bulky triphenyl phosphine (-5.6 ppm). The proton NMR of **9f** displayed a multiplet at 7.35-7.20 ppm accounting for five protons that are assigned to the phenyl group. A doublet at 6.9 ppm with a four-bond phosphorus proton coupling of 1.9 Hz was attributed to the two m-mesityl protons. The aliphatic protons show at the AB part an ABX spin pattern due to coupling with each other and the phosphorus atom(X) and appear at 3.7 and 3.5 ppm. The three methyl groups appeared as multiplet at 2.30-2.28 ppm, accounting for nine protons. The remaining NMR signals were similar to that of **9b**. ESI-MS positive mode spectrum of this phosphine showed pseudo-molecular ion peaks at m/e = 351.15 $[M+H]^+$ and m/e = 373.13 $[M+Na]^+$.

[44] J. J. Daly, *J. Chem. Soc.* **1964**, 3799.
[45] T. S. Cameron, B. Dahlen, *J. Chem. Soc. Perkin Trans. 2*, **1975**, 1737.
[46] E. C. Alyea, J. Malto, *Phosphorus, Sulfur and silicon*, **1989**, 46, 175.

2.4. Syntheses and characterization of transition metal complexes of diphenyl-phosphanyl methyl phenols and catechols:

There is a long standing interest in metal complexes with catechol phosphines, where the P-only, O-only or P-O coordination mode can be observed. The latter is particularly interesting with respect to the well studied coordination chemistry of phosphino phenols such as **11**, which may give complexes (see **Scheme 7**) of type **12**[43] with different metals like Pd,[47] W,[48] Ni, Co, Pt[49] and Rh[50] with variable substituents on the metal. These complexes have been studied because of their potential use as catalysts for olefin polymerization or hydrogenation.

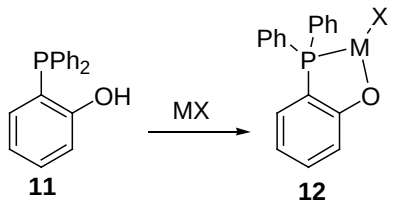

11 **12**

Scheme 7: Transition metal complexes of rigid catechol phosphine.

Having synthesized the above mentioned catechol phosphines **9b-d**, it was decided to study their coordination behavior, with particular emphasis on the generation of complexes with a P-only coordination mode. Selection of the metal center is another important issue in metal complex chemistry. According to the HSAB theory[28], soft metals like palladium and silver prefer soft phosphine donors and have low affinity towards hard donors like oxygen. Inspection of mechanical molecular models suggested that it might be difficult to form a chelating complex with a similar coordination mode as **12** with soft metals and hence Pd and Ag were selected in order to achieve the P-only coordination complexes.

To perform the reaction, two equivalents of **9b** were dissolved in dry THF and one equivalent of $(COD)PdCl_2$ was added to it under constant stirring. The reaction progress was monitored by ^{31}P NMR and showed completion of the reaction in 2 hours. THF was

[47] J. Heinicke, M. Koehler, N. Peulecke, M. K. Kindermann, W. Keim, M. Kockerling, *Organometallics*, **2005**, 24, 344.
[48] L. Dahlenburg, K. Herbst, G. Liehr, *Zeitschrift fuer Kristallographie - New Crystal Structures* **1998**, 213 (1), 209.
[49] H. D. Impsall, B. L. Shaw and B. L. Turtle, *J. C. S. Dalton. Trans.* **1976**, 1500.
[50] S. Priya, M. S. Balakrishna and J. T. Mague, *J. Organomet. Chem.* **2004,** 689, 3335.

evaporated to half the total volume and the Schlenk tube was kept at +4ºC overnight. Decanting the supernatant solution, followed by 3 hours drying of the precipitated solid in vacuum gave the neutral complex **13b** as shining yellow crystalline compound (See **scheme 8**). The yellow powder of **13b** melts at 176ºC and was isolated in 95% yield. The ^{31}P NMR spectrum of **13b** at ambient temperature in $CDCl_3$ displayed a sharp singlet at 19.1 ppm that can be attributed to a P-only coordinated trans complex of **9b**. The observed ^{1}H and ^{13}C NMR resonance data are similar to those of the free ligand.

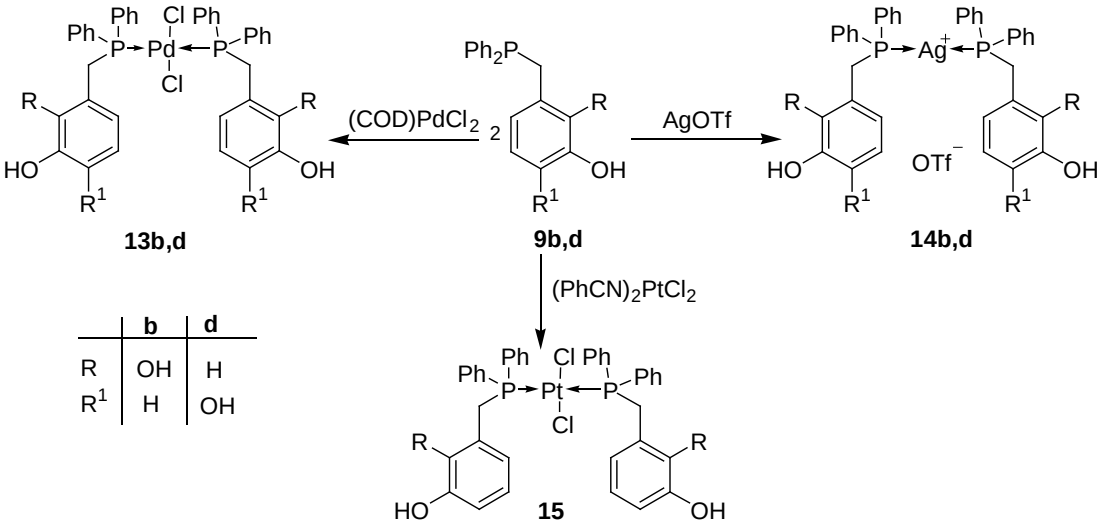

Scheme 8: Syntheses of transition metal complexes of 9b,d.

The yellow powder of **13b** was dissolved in a minimum amount of THF and suitable crystals for a single crystal X-ray diffraction study were grown at +4°C. The compound **13b** crystallizes in a monoclinic unit cell in the space group $P2_1$. The crystal contains discrete molecules that lie on a crystallographic C_2 axis. The unit cell contains further four molecules of THF per molecule of **13b**. Two of the THF molecules show strong hydrogen bonding interactions with the hydroxy protons [O5-H2 1.91 Å and O7-H4 2.05 Å], whereas the third THF molecule interacts only weakly (O6-H29A 2.54 Å) with a hydroxy group and the fourth THF does not show any kind of interaction with the complex. Apart from these intermolecular interactions, there were no further particular inter- or intramolecular interactions observed. The palladium atom displays a square planar geometry with two chlorides and two phosphines completing the coordination sphere. The P-Pd-P array is nearly linear with an angle of 178.1º. The Pd-P distances (2.33 Å) are normal and the observation of rather long distances to the oxygen atom (more than 5 Å) in

2-position of the catechol ring ruled out the presence of any Pd-O interaction and thus demonstrated the P-only coordination mode. The phosphorus atom features a distorted tetrahedral geometry with the largest angle of 118.3º (C14-P1-Pd1). Thus, the crystal structure and solution NMR studies of **13b** unambiguously support the formation of a P-only coordinating palladium complex.

Bond lengths [Å]	Bond angle [º]
Pd-Cl2 2.307(1)	P1-Pd-P2 178.05(1)
Pd-Cl1 2.301(0)	C14-P1-Pd1 118.31(2)
Pd-P1 2.338(0)	
Cl1-O2 6.161(1)	

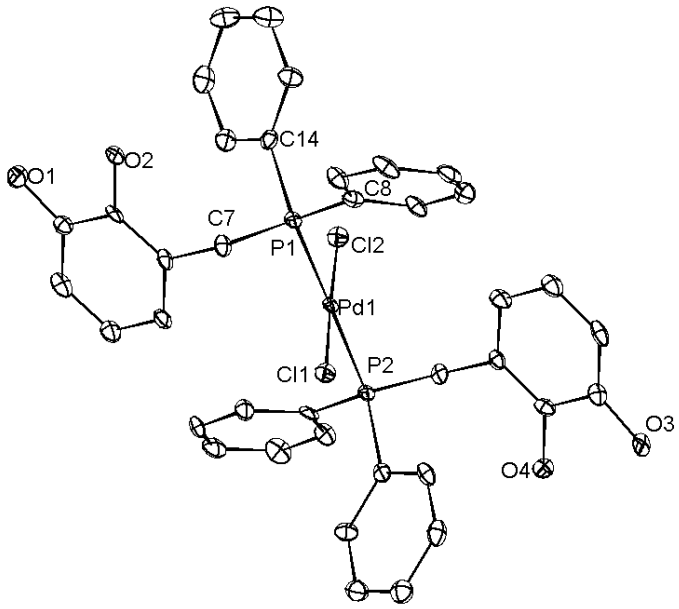

Fig. 2.4: Molecular structure of 13b (H-atoms omitted, 50% probability thermal ellipsoids), important bond angles and bond lengths are given in the table.

Complex **13d** was synthesized according to the procedure mentioned for **13b** and was isolated in 95% yield. The light yellow powder of **13d** melts at 223ºC. The ^{31}P NMR spectrum displayed a single resonance at 20 ppm indicating P-only coordination and a *trans* configuration. The ^{1}H NMR spectrum at ambient temperature in CD_3CN displayed a multiplet at 7.3-6.96 ppm accounting for 20 protons, which is attributed to the phenyl groups. Three catechol protons appear as distinct multiplets with three bond proton-proton

couplings of about 7 Hz at 6.38, 6.31 and 6.14 ppm. The two aliphatic protons displayed a doublet at 3.65 ppm with a $^2J_{PH}$ coupling of 12 Hz.

Suitable crystals for a single-crystal X-ray diffraction study were obtained from a concentrated THF solution of **13d** at +4ºC. The yellow monoclinic (space group $C_{2/c}$) crystals contain molecules of **13d** that lie on a crystallographic C_2 axis. The crystal contains further one disordered molecule of THF per molecule of **13d**, which does not show any kind of intermolecular interactions with the complex. The palladium atom displays a square planar geometry with 180.0º P1-Pd-P1^i and Cl-Pd-Cl angles. The P-Pd (2.30 Å) distance is a bit shorter compared to that found in **13b**. The catechol oxygen atom in 3-position is far away (approximately 6 Å) from having any kind of interaction with the palladium atom. The phosphorus atom displays a distorted tetrahedral geometry. The two catechol rings are trans to each other.

The silver complex **14b** was readily obtained by mixing two equivalents of ligand **9b** with one equivalent of silver triflate in THF (with a few drops of DMF). The reaction mixture was stirred at room temperature for one hour and the solvent was then evaporated in vacuum. The residue was dissolved in dichloromethane, a few drops of diethyl ether were added and the Schlenk tube was kept for crystallization at –28ºC overnight. White needle like crystals were isolated by filtration and dried in vacuum, which gave a white powder of **14b** in 73% yield with a melting point of 109ºC. The positive mode ESI-MS experiment showed a pseudo-molecular ion peak at m/e = 781.09, corresponding to the cation of **14b** $[M+NaCl-OTf]^+$. A peak attributable to $[M-OTf]^+$ was observed at m/e = 723, where M = **14b**. The ^{31}P NMR resonance of the complex **14b** at ambient temperature appeared as broad doublet centered at 6.2 ppm with a mean $^{107/109}Ag$-^{31}P coupling of 445 Hz. The line broadening is attributable to slow intermolecular ligand exchange which is a common feature for many silver complexes.[51] The downfield shift of the ^{31}P signal of **14b** compared to the free ligand is typical for the coordination of phosphorus to a silver center. The ^1H and ^{13}C chemical shifts appeared similar to those of the ligand **9b**.

Suitable crystals for single-crystal X-ray diffraction were obtained by recrystallizing **14b** from a CH_2Cl_2/Et_2O/DMF mixture at –28ºC. The colorless monoclinic crystals (space group $P2_1/n$) of **14b** contain two half crystallographically independent cations $[Ag(\mathbf{9b})_2]$

[51] R. Terroba, M. B. Hursthouse, M. Laguna, A. Mendia, *Polyhedron*, **1999**, 18, 807; E. L. Muetterties, C. W. Alegranti, *J. Am. Chem. Soc.* **1972**, 94, 18, 6386.

along with a triflate anion and one molecule of each CH_2Cl_2 and DMF in the asymmetric unit. The bonding parameters in the two cations do not deviate significantly. The hydroxy

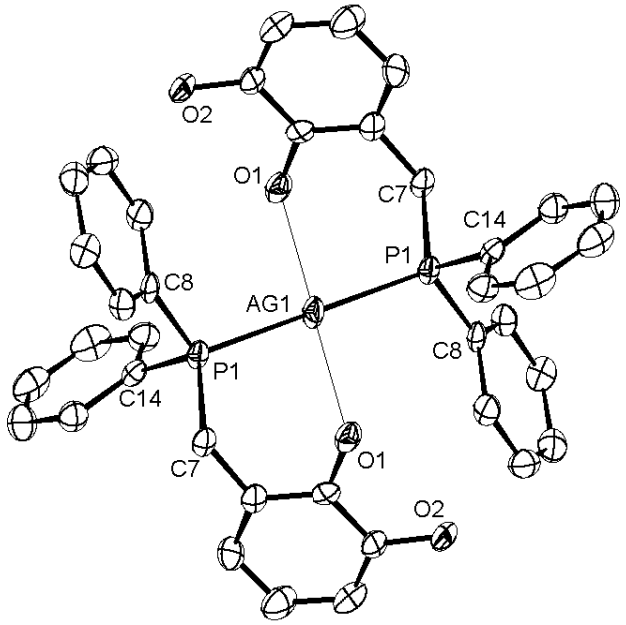

Bond lengths [Å]	Bond angles [°]	Bond angles [°]
Ag1-P1/P1^1 2.402(2)	P1-Ag1-P1^1 180.0	Ag1-P1-C7 111.2(1)
Ag1-O1/2 3.16-3.25	C8-P1-C14 102.5(2)	Ag1-P1-C8 114.0(2)
	C7-P1-C14 106.9(3)	

Fig. 2.5: Molecular structure of **14b** (H-atoms omitted, thermal ellipsoids with 50% probability), important bond angles and bond lengths are given in the table.

groups in 2-position of the catechol units show hydrogen bonding interactions to the chlorine atom of a molecule of CH_2Cl_2, and those in 3-positions to an oxygen atom of a triflate anion. Taking these interactions into account, the crystal packing can be described in terms of chains of alternating, weakly interacting cations and anions. The silver ions in the complex cations lie on a crystallographic center of symmetry (C_i-symmetry) and feature a linear coordination by the two phosphorus atoms. The Ag-P distances (2.40 Å) are normal. Rather short contacts to the oxygen atoms in 2-position of the catechol ring (Ag1-O1 3.16Å) compared to **13b-d** are interpreted in terms of additional weak secondary Ag…O interactions. The phosphorus atom displays a distorted tetrahedral geometry with larger Ag-P-C7/8 (111.2°/114.0°) angles compared to C14-P-C7/8 (106.9°/102.5°).

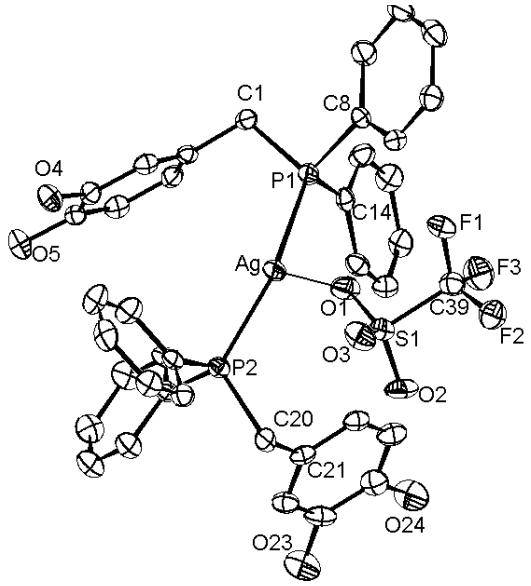

Bond lengths [Å]	Bond angles [°]
P2-Ag1 2.399(1)	P1-Ag1-P2 159.23(3)
P1-Ag1 2.401(1)	Ag1-P1-C1 112.57(1)
Ag1-O1 2.576(2)	P1-C1-C2 113.63(2)
P1-C1 1.841(2)	P2-C20-C21 110.99(2)

Fig. 2.6: Molecular structure of **14d** (H-atoms omitted, thermal ellipsoids with 50% probability), important bond lengths and bond angles are given in the table.

Complex **14d** was synthesized according to the procedure mentioned for **14b.** The product was isolated in 95% yield as a white solid melting at 112ºC. Positive mode ESI-MS produced a molecular ion peak m/e $[M]^+$ = 725 corresponding to the cationic silver complex. The ^{31}P NMR spectrum of **14d** at ambient temperature in $CDCl_3$ displayed a broad doublet ranging from 13 to 18 ppm, which may arise from a medium fast ligand exchange process. Cooling down the sample to –50°C split the broad doublet into two doublets of almost equal intensity centered at δ 16.41 due to ^{31}P coupling with the two naturally occurring silver isotopes (^{107}Ag, I = ½, 51.82%; ^{109}Ag, I = ½, 48.18%). The magnitude of these coupling constants of 501 Hz ($^1J_{107Ag-P}$) and 579 Hz ($^1J_{109Ag-P}$) is consistent with the linear P-Ag-P array and very weak coordination of one or two oxygen atoms.[52]

[52] R. G. Goel, P. Pilon, *Inorg. Chem.* **1978**, 17, 2876; R. Terroba, M. B. Hursthouse, M. laguna, A. Mendia, *Polyhedron*, **1999**, 18, 807; X. Sun, D. W. Hohnson, K. N. Raymond, E. H. Wong, *Inorg. Chem*. **2001**, 40, 4504.

Suitable crystals for single-crystal X-ray diffraction measurements were grown at room temperature from a THF solution. The unit cell contains two molecules of solvent (THF) per molecule of **14d**. The colorless monoclinic crystals (space group $P2_1/n$) of **14d** contain a silver center which is bonded to one of the oxygens of the triflate [Ag-O1 2.58 Å], thus producing [Ag(**9d**)$_2$OTf] as a neutral complex. The P-Ag-P array is slightly bent (P1-Ag-P2 159.2°) so as to accommodate the triflate, and the overall geometry around silver can be best described as intermediate between T-shaped and trigonal planar. No secondary Ag…O interactions like in **14b** were observed as all the Ag-O distances exceeded 5 Å.

Complex **15** was synthesized according to the procedure mentioned for **13b** except that a platinum complex [$(PhCN)_2PtCl_2$)] was employed instead of a palladium complex (see **Scheme 8**). The light yellow compound was isolated by crystallization from THF solution in quantitative yield and melts at 235°C. The ^{31}P NMR spectrum of the isolated product displayed two resonances at 18.8 and 11,0 ppm in 1:2 ratio along with two sets of platinum satellites. The resonance at 18.8 ppm with a $^1J_{Pt\text{-}P}$ coupling of 1296 Hz is attributed to a *trans* complex of **9b**, whereas signal at 11,0 ppm with a larger coupling of 1861 Hz is assigned to a *cis* complex. The proton NMR spectrum displayed two sets of multiplets for the aromatic as well as for the aliphatic protons due to the *cis*-*trans* isomerism. The positive mode ESI-MS spectrum revealed that the complex **15** spontaneously eliminates one molecule of HCl to give a P-O chelate. The pseudo-molecular ion peak at m/e = 810.14 $[(C_{38}H_{32}O_4P_2Pt = M)+H]^+$ corresponds to cation of **15** generated by eliminating one HCl and a chloride. Further pseudo-molecular ion peaks were observed at m/e = 832.13 $(M+Na)^+$, 873.06 $(M-H+NaCl+Li)^+$, 895.05 $(M-2H+2Na+Cl+Li)^+$.

Storing the sample for two months lead to a spontaneous conversion into a new product. The ^{31}P NMR spectrum of this complex displayed two doublets (AB spin system), which appeared at 49.7 and –0.6 ppm with a $^2J_{P\text{-}P}$ coupling of 21 Hz ($^1J_{Pt\text{-}P}$ = 2141, 1727 Hz respectively) and a singlet at 28.6 ppm ($^1J_{Pt\text{-}P}$ = 1942 Hz). The AB spin system observed can be best interpreted assuming that one of the ligand forms a P-O chelate while the other displays P-only coordination so that the two phosphorus atoms coordinating to platinum become inequivalent and display an AB spin system. The remaining singlet can be attributed to a fully chelated (P-O chelate only) complex.

2.5. Synthesis and characterization of a palladium complex of 3-[(Mesitylphenyl phosphanyl)-methyl]-benzene-1,2-diol:

Two equivalents of **9f** were dissolved in dry THF and one equivalent of $(COD)PdCl_2$ was added under constant stirring. After one hour, half of the THF was evaporated in vacuum and the Schlenk tube was kept at +4ºC overnight. Filtering the supernant solution, followed by 3 hours drying in vacuum, gave a yellow powdered compound, which was isolated quantitatively.

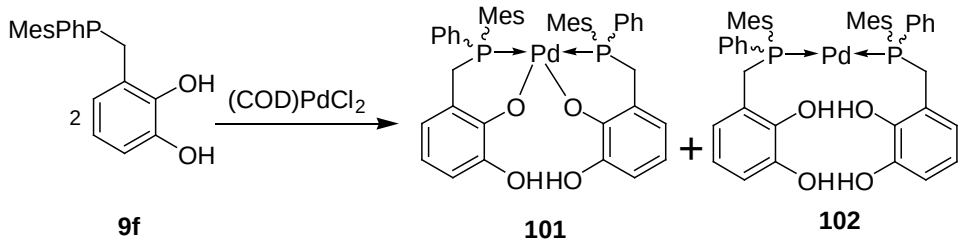

9f **101** **102**

Scheme 9: Synthesis of P-O chelating and P-only complex 102 and 102.

The ^{31}P NMR spectrum of the reaction mixture displayed two major signals at 5.4 and 4.3 ppm which are attributable to *diastereomers* (*meso* and *rac* pair) of the P-only coordinated complex **102**(see **Scheme 9**). The other two minor signals at 55.7 and 19.2 ppm (together about 1%) were hard to interpret. The ^{31}P NMR spectrum of the isolated product showed a major peak (about 95%) at 53.5 ppm, which is attributable to the P-O chelate complex **101**. The other two resonances at 1.3 and –0.9 ppm (together about 2%) can be assigned to *diastereomeric* (*meso* and *rac*) complexes **102**. The ESI-MS positive mode spectrum displayed a molecular ion peak at m/e = 805.2[**101**+H]$^+$, corresponding to the cation of chelated palladium complex **101**. A pseudo-molecular ion with sodium was observed at m/e 827.2. The above observations allow to state that increased steric bulk at phosphines presumably forces the diastereoisomeric complexes to eliminate HCl and to produce a P-O chelated complex **101** as the major product.

2.6. Conclusions:

It has been confirmed that the reaction of diphenyl phosphine with phenolic aldehydes proceeds via initial formation of α-phosphanyl-carbinols. The presence of OH-groups in p- or o-position destabilizes the adducts relative to the starting materials and facilitates their subsequent rearrangement into isomeric phosphine oxides. The latter may further be reduced to phenol-functionalized phosphines. The overall reaction permits to access

phosphines with pendant phenolic functionalities from readily available starting materials, without the necessity of additional efforts for the introduction and removal of protecting groups at the phenol functionalities. This procedure constitutes a substantial improvement over previously known synthetic protocols which required often more complicated approaches.[32,43] The application of this procedure should prove useful for the preparation of functional phosphines in applications as chelating ligands in catalysis or as supramolecular building blocks.

With the procedures outlined for the syntheses of transition metal complexes it was possible to selectively generate P-only coordinating transition metal complexes rather than P-O chelates. The neutral palladium complexes **13b**,**d,** and cationic silver complexes **14b,d** of the corresponding catechol phosphines (**9b,d** respectively) were easily prepared and isolated in good yields and thus demonstrated the P-only coordination mode of **9b,d**. The platinum complex **15** displayed a different behavior and can be very easily converted from a P-only to P-O coordination mode. Increasing the steric bulk at phosphorus lead to the preferential formation of a P-O chelated complex **101**.

3. Phosphine functionalized catechol borates and their Lewis-acid/base behavior

3.1. Introduction

It was envisioned that borate might be a useful template for the catechol-phosphine ligands and a good starting material to explore the template centered ligand-designing strategy. The most easily accessible tricoordinate boron compound to name is boric acid. The reaction between boric acid and alcohols is well established, in fact it is routine laboratory practice to use methyl borate as a qualitative test for boron, which colors the flame green confirming the presence of boron. Boric acid derivatives, e.g. phenyl boronic acid, are known to undergo likewise condensation with a variety of substrates such as penyldiamines[53], anthranilic acids[54] 1,2-diols[55] and with catechols[56] to yield the corresponding condensation products. These tricoordinated boron compounds can further act as Lewis acid centers. This Lewis acidity is attributable to the existence of an empty 2p orbital on boron. This orbital can be utilized to build Lewis acid-base adducts, where the

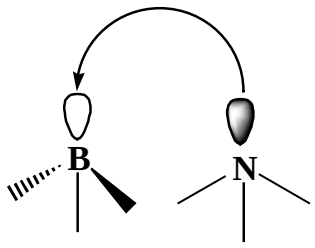

Fig. 3.1: Boron acid-base adducts

[53] W. R. Purdum, E. M. Kaiser, *Inorg. Chim. Acta* **1975**, 12, 45.
[54] M. Pailer, W. Fenzl, *Monatsh. Chem.* **1961**, 92, 1294.
[55] H. G. Kuivila, A. H. Keough, E. J. Soboczenski, *J. Org. Chem.* **1954**, 19, 780; R. A. Bowie, O. C. Musgrave, *J. Chem. Soc.* **1963**, 3945.
[56] M. Wieber, W. Kuenzel, *Z. Anorg. Allg. Chem.* **1974**, 403, 107.

base donates its electron pair to the vacant 2p orbital (**Fig. 3.1**) on boron [4,57]. Generally these tetra-coordinated adducts are in equilibrium with the tricoordinated species in solution (**Scheme 1**). The equilibrium can be shifted towards the product side by i) adding an excess of base, ii) using strong bases, iii) using sterically less bulky bases or iv) increasing the acidity of the boron center by electron withdrawing substituents such as pentaflurophenyl groups.[58, 70]

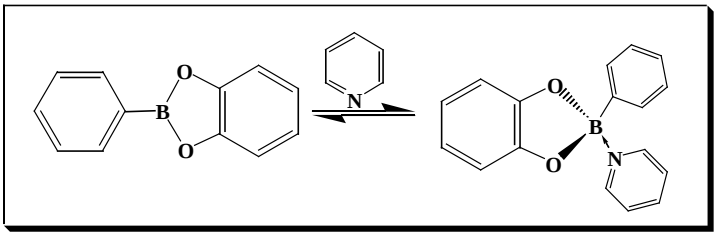

Scheme 1: Lewis acid-base equilibrium.

In recent years, boron acid base adducts have been rigorously studied owing to their ability to produce catalytically active centers for olefin polymerization.[59] The simple acid/base chemistry has been further extended to high-end applications such as photo switching.[60] Recently a new concept called "borate centered ligands" in which the boron bound hydrogen has been replaced by an alternative group such as tris(pyrazolyl) has emerged but it has not been intensively studied.[61] Apparently the newly synthesized catechol phosphine **9b** suffices all the criteria required to synthesize boron centered ligands. In order to contribute to this challenging and developing field a detailed investigation of the synthesis of esters of the catechol phosphines with boric and boronic esters, and the behavior of the latter as Lewis-acids in reactions with pyridine derivatives was carried out. The products

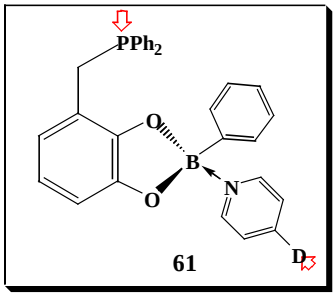

61

[57] F. Norberto, C. Rosalinda, *J .Chem. Soc. Perkin Tran. 2*, **1987**, 6, 771.
[58] H. Sakurai, N. Iwasawa, K. Narasaka, *Bull. Chem. Soc. Jpn.* **1996**, 69, 2585.
[59] F. Focante, P. Mercandelli, A. Sironi, L. Resconi, *Coord. Chem. Rev.* **2006**, 250-(1-2), 170.
[60] N. Kano, J. Yoshino, T. Kawashima, *Org. Lett.* **2005**, 7, 18, 3909.
[61] P. J. Bailey, D. Lorono-Gonzale, C. McCormack, F. Millican, S. Parsons, R. Pfeifer, P. P. Pinho, F. Rudolphi, A. S. Perucha, *Chem. Eur. J.* 2006, 12, 5293.

formed can be used as borate centered bidentate ligands such as **61**.

These boron centered ligands like **61** are promising candidates for building chelate complexes if the spatial arrangement of the donor sites can be made to fit accordingly. In the following, a detailed report on the synthesis, characterization and possible complex formation reactions will be given.

The second part of this chapter is focused on tetra-coordinate borate compounds. The above boron acid/base chemistry was explored to synthesize stable borate anions rather than just equilibrium reaction mixtures. The intramolecular interaction between tricoordinated boron and an oxygen donor produced a reasonably stable borate.[62] It was in 1925 when Meulenhoff first reported on the synthesis of catechol borates.[63] The ongoing controversy about tri or tetra coordinated boron[64] was recently resolved by White et al. who reported the first crystal structure of a catechol borate.[10,65] Since then tetra coordinated boron complexes have attracted much attention,[66] but reports on second donor substituted catechol-borates are very scarce.[67] Incidentally, the ligands **9b-d** carry a catechol function along with a phosphine donor. Section 2.3 demonstrated that coordinating complexes of **9b-d** with palladium and silver can be very easily accessed and that these catechol phosphines (**9b-d**) form P-coordinating complexes rather than chelating complexes.

In the following it will be demonstrated that, a tetrahedral BO_4 unit can be used as template to assemble two ligands **9b-d** to give an aggregate that behaves as/mimics a bidentate phosphine. Further the selection of the boron building blocks allows to control the molecular structure of the complexes formed, producing either a monometallic silver complex or a macrocycle.

[62] W. P. Griffith, A. J. P. White, D. J. Williams, *Polyhedron*, **1995**, 15, 17, 2835.
[63] J. Meulenhoff, *Rec. traav. Chim*., **1925**, 44, 150.
[64] D. F. Kuemmel, M. G. Mellon, *J. Am. Chem. Soc.* **1956**, 78, 4572.
[65] A. Mitra, L. J. DuPue, J. E. Struss, B. P. Patel, S. Parkin, D. A. Atwood, *Inorg. Chem.* **2006**, 45, 9213.
[66] E. Graf, M. W. Hosseini, *Angew. Chem. Int. Ed.* **1995**, 34, 1115.
[67] S. Mohr, G. Heller, U. Timper, K. H. Woller, *Z. Naturforsch.* **1990**, 45, 308.

3.2. Results and discussion:

3.2.1. Detailed investigations on the synthesis and Lewis acid/base behavior of Diphenyl-(2-phenyl-benzo[1,3,2]-dioxaborol-4-ylmethyl) phosphine:

The catechol functionalized phosphine **9b** was synthesized in two simple steps as reported earlier in chapter **2,** section **2.2.1-2.2.3**. The condensation reaction between phenyl boronic acid and **9b** with excess of triethyl amine as acid scavenger at room temperature produced Diphenyl- (2-phenyl-benzo [1,3,2]-dioxaborol-4-ylmethyl) phosphine **16a**. Evaporation of solvents followed by an hour vacuum drying gave a quantitative yield of a white solid. A single ^{11}B NMR resonance at 31.7 ppm in dichloromethane was observed, which is typical of tricoordinated borates.[68] The ^{31}P NMR resonance appeared as singlet at –11 ppm indicating the presence of a free phosphine and ruled thus out the formation of phosphine-borane adducts which might be expected. Detailed NMR studies of similar tetra/tri-coordinate boron compounds with nitrogen bases have been reported by Goetz *et al*.[69]

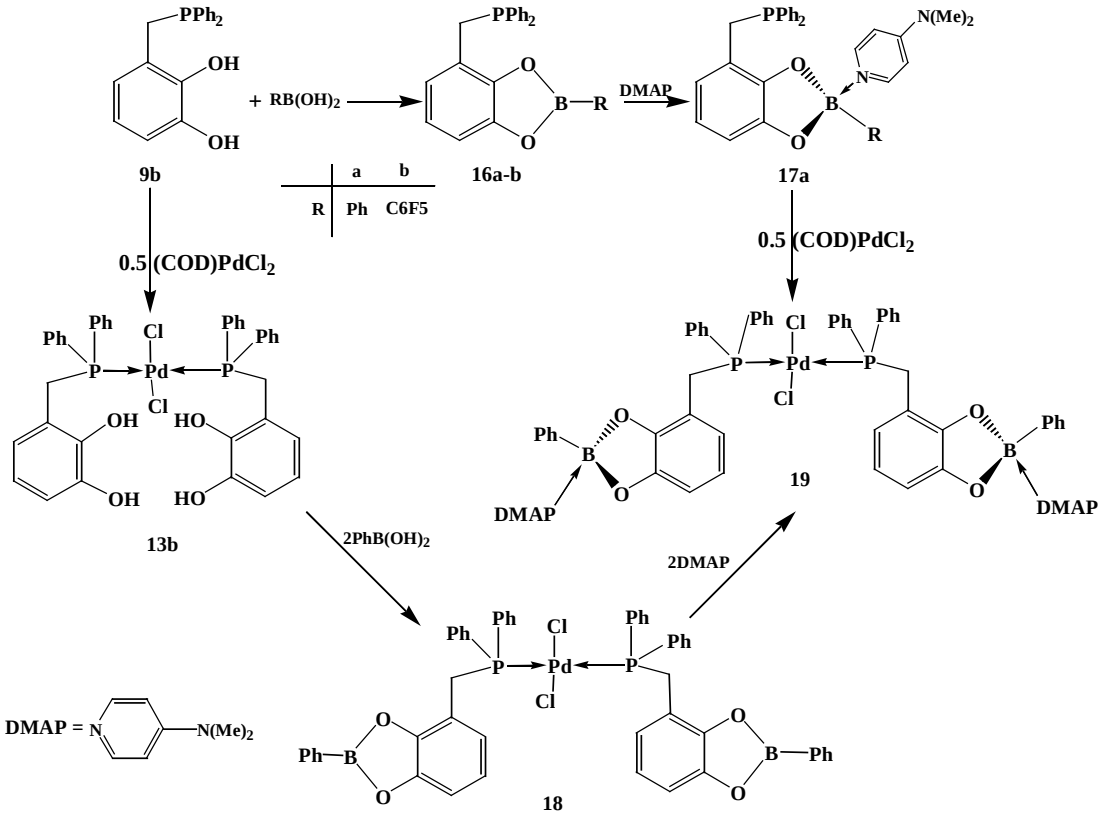

[68] F. Zettler, H. D. Hausen, H. Hess, *Acta Crystallog. Sect.B: Struct. Crystallogr.Cryst.Chem.* **1974,** 30, 1876.

[69] R. Goetz, H. Noeth, H. Pommerening, D. Sedlak, B. Wrackmeyer, *Chem. Ber*. **1981**, 114, 1884.

Scheme 2: Syntheses of boron-centered ligand and their complexes.

Having confirmed the formation of borane **16a,** it was of further interest to investigate its Lewis acid behavior towards various bases. The simple base pyridine was selected for the ease of availability of comparable ^{11}B NMR data.[70] One equivalent of borate **16a** was treated with one equivalent of pyridine, the ^{11}B NMR of this reaction mixture showed a peak similar to that of the starting material indicating that the equilibrium shown in **Scheme 1** is still shifted to the left side. A series of reactions with increasing equivalents of pyridine was found to produce an easy upfield shift of the ^{11}B resonance. A considerable change to δ = 11.9 in the ^{11}B NMR shift was observed when **16a** was mixed together with six equivalents of pyridine. Further addition of pyridine did not change the ^{11}B NMR shift, indicating saturation. These observations made it clear that the borane **16a** is too weak Lewis-acid to allow generation of a stable adduct with a stoichiometric quantity of pyridine.

In this case two strategies could be followed to obtain more stable adducts; i) introduction of an electron withdrawing substitutent on boron, making it more acidic, or ii) use of a stronger base. To perceive on the first strategy pentaflurophenyl boronic acid was chosen. Similar boron compounds of 2,3 dihydroxynaphthalene with pentaflurophenyl substituents were reported recently.[71] Reaction of the catechol phosphine **9b** and pentaflurophenyl boronic acid produced a white powder after stripping off the solvent. The ^{11}B NMR displayed four resonances at 21.6, 14.3, 9.9 and 5.3 ppm indicating formation of more than one product. The ^{31}P NMR spectrum displayed a single broad resonance ranging from – 10.6 to -8.5 ppm. The proton NMR displayed a multiplet at 7.7-7.2 ppm, which is attributed to the phenyl groups, and a second multiplet at 7.1-6.6 ppm which is assigned to the catechol protons. The aliphatic protons appear at 3.62 ppm as broad singlet. These spectral observations indicated formation of a dynamic equilibrium mixture of the expected boronic ester **16b** together with one (or more) B-P adducts.

Hoping that addition of a strong Lewis base may break the B-P adduct it was decided to go ahead without further characterizing the product. In a combined (i and ii) strategy, an equimolar amount of DMAP in dichloromethane was added to the isolated product (**16b)**. Evaporating the solvent under vacuum followed by vacuum drying produced a clean

[70] N. Farfan, R. Contreras, *J. Chem. Soc. Perkin Trans 2*, **1987**, 771.
[71] D. Vagedes, R. Froehlich, G. Erker, *Angew. Chem. Int. Ed.* **1999**, 38, 22, 3362.

product. The ^{11}B NMR spectrum displayed two major resonances, a singlet at 14.3 ppm and a doublet at 8.47 ppm in 1:1 ratio. The ^{31}P NMR spectrum showed two singlets at –12.6 and –13.9 ppm. On comparing with ^{11}B literature data[72] it appears that the former signal arising from a borane-DMAP adduct and the latter doublet could not be clearly assigned. The above observations indicated that the pentaflurophenyl substituent makes the boron much more acidic so that it may then coordinate to the phosphine. Considering that the formation of unwanted reaction products could not be suppressed, the focus was shifted to the second strategy, i.e. the use of a stronger base as donor.

To realize this approach, dimethyl amino pyridine was chosen, which is also of interest owing to the presence of a potential secondary donor site in the Me_2N-group. The reaction of a stoichiometric amount of the borate **16a** and DMAP produced a mixture whose ^{11}B NMR spectrum showed a single resonance at 11 ppm. This can be interpreted as a stable adduct arising from strong coordination of the base to the boron center. The product was isolated quantitatively by evaporating the solvent and drying the white powder under vacuum. The ^{31}P NMR spectrum showed a singlet at –17.1 ppm confirming the presence of a free phosphine. The proton NMR of a solution of the white powder in $CDCl_3$ showed a multiplet (broad doublet of triplets) at 8.25 ppm with $^3J_{H\text{-}H}$ of 7.4 Hz corresponding to the ortho protons of DMAP. Signals at 7.55 to 7.40 ppm and at 7.30 can be assigned to the phenyl substituents on boron and phosphorus. A multiplet at 6.55 to 6.35 ppm can be assigned to one catechol proton and two m-DMAP protons. Two doublets of triplets (6.62 and 6.39 with $^3J_{H\text{-}H}$ of 7.34 and 8 Hz respectively) were observed for the remaining catechol proton. In the aliphatic region, two singlets at 3.5 and 3 ppm were observed which can be assigned to the CH_2 protons of catechol phosphine and the CH_3 protons of DMAP, respectively.

Unambiguous support for the structure of the DMAP Lewis acid base adduct **17a** came from a single-crystal X-ray diffraction study. Shining white crystals were obtained after dissolving a small amount of the isolated white powder in a minimum amount of dichloromethane, addition of a few drops of THF, and crystallization at room temperature. The molecular structure of **17a** is shown in **Fig. 3.2**. The crystal structure determination showed that the compound crystallizes in the space group $P2_1/c$ along with one THF molecule in the periphery, without any hydrogen bonding interactions. No π-stacking

[72] W. Clegg, A. J. Scott, F. E. S. Souza, T. B. Marder, *Acta Crystallogr. Sect. C:* **1999**, C55, 11, 885.

interaction between any of the aromatic rings was observed, as none of the rings are parallel to each other. The phosphorus atom displays a distorted pyramidal geometry (sum of the angles is 302°) with two phenyl rings and a catechol substituent. The angle between C6-C7-P1 (116.0°) is by few degrees larger than in the free ligand (**9b**, 111.9°). The boron atom displays a distorted tetrahedral arrangement with the catechol

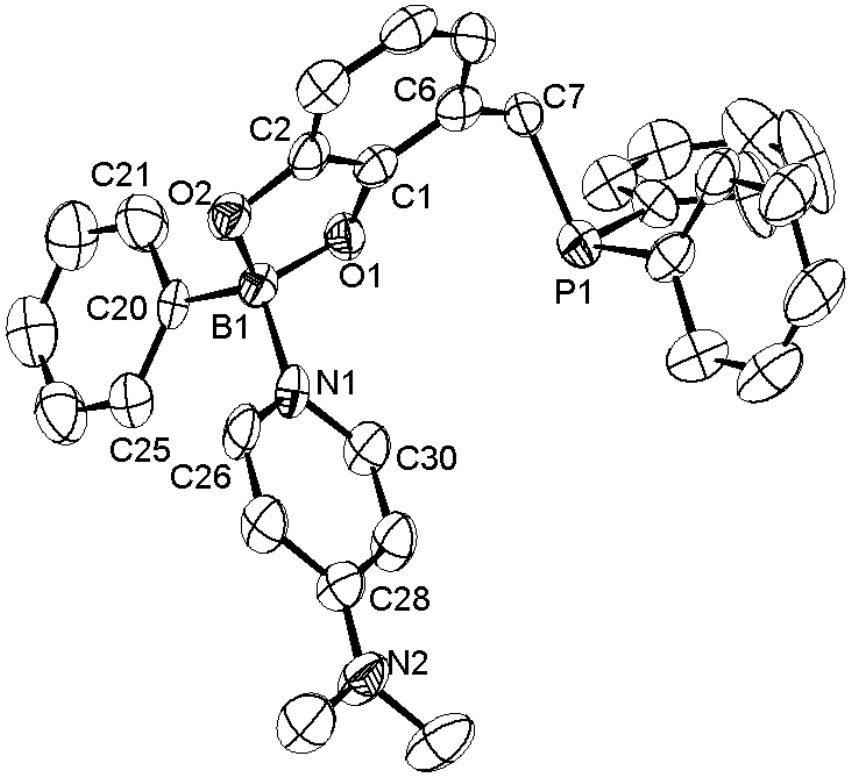

Bond lengths [Å]	Bond angles [°]
B1-O2 1.491 (1)	C20-B1-N1 111.6 (1)
B1-O1 1.475 (1)	O1-B1-O2 105.3 (1)
B1-N1 1.608 (1)	C6-C7-P1 116.0(4)
B1-C20 1.613(1)	O-B1-C20 111.86-114.70

Fig. 3.2: Crystal structure of 17a (50% probability thermal ellipsoids). Important bond lengths and angle are given in the table.

chelate, phenyl substituents, and the nitrogen donor atom completing the coordination sphere (**Fig. 3.2**). The catecholate unit gives an O1-B1-O2 angle of 105.2°, which is considerably sharper than the ideal tetrahedral angle of 109.5°. The remaining three angles (C20-B1-N1 111.5 and O1/2-B1-C20 111.9-114.7) are wider than the ideal one. The

phenyl substituent on boron is directing outwards with an angle of 111.5° (C20-B1-N1). Raising the boron coordination number from three to four in **17a** considerably lengthens the B1-O and B1-C20 bonds (1.47 to 1.49 Å, respectively) which are in accordance with the literature reported distances (1.48 and 1.58 Å, respectively).[68] The NMe_2 group and the aromatic ring in DMAP lie in the same plane with both nitrogen atoms.

Having shown that P-only complexation and B-complexation (**16a/b**) of **9b** in two independent reactions is feasible it was envisioned to combine both reactions to generate extended oligomers or coordination polymers. Such species are of great interest for preparing multimetallic complexes, molecular devices,[73] novel electronic, magnetic[74] or polymeric materials.[75] The first step to put this concept into reality was to synthesize a metal complex of **9b**, which has been demonstrated in section 2.3. The logical next step was to utilize the hydroxyl functionalities in order to incorporate an acidic boron center alongside. This was achieved simply by stirring **13b** with phenyl boronic acid. Subsequent solvent removal produced a yellow colored powder of **18** (**Scheme 2**) in quantitative yield. The yellow powder decomposes at 240ºC. A single ^{11}B NMR signal at 29.1 ppm was observed which indicated the presence of a trigonally planar coordinated boronic ester.[76] The ^{31}P NMR resonance appeared at 21.2 ppm, indicating that the phosphorus coordination to palladium remains unchanged from that of **13b.** The proton NMR of **18** displayed a slight downfield shift of all signals compared to the free ligand **9b**. A multiplet at 7.8 to 7.5 ppm is attributed to the phenyl and another multiplet at 7.1 to 6.7 ppm to the catechol protons. A broad doublet of triplets (ABX spin system) at 4.3 ppm with a $^2J_{PH}$ coupling of

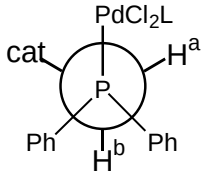

Scheme 3: Newman projection along the $Ph_2P\text{-}CH_2$ bond showing inequivalency of H^a and H^b.

[73] H. Sleiman, P. Baxter, J. M. Lehn, *J. Chem. Soc. Chem. Comm.* **1995**, 7, 715.
[74] T. Goslinski, C. Zhong, M. J. Fuchter, C. L. Stern, A. J. P. White, A. G. M. Barrett, B. M. Hoffman, *Inorg. Chem.* **2006**, 45, 9, 3686.
[75] Hoffman, M. Brian, Barrett, G. M. Anthony, U.S. (1999), 37 pp., Cont.-in-part of U.S. 5,675,001. CODEN: USXXAM US 5912341 A 19990615 Application: US 97-928415 19970912. Priority: US 95-403302 19950314. CAN 131:27113 AN 1999:384025
[76] P. Diehl, E. Fluck, R. Kosfeld, *Nuclear Magnetic spectroscopy of boron compounds*, Springer-Verlag, Berlin, Heidelberg, New York, **1978**, p. 144

11.3 Hz and a triplet at 4.2 ppm with $^2J_{PH}$ coupling of 3.8 Hz was observed and can be assigned to the CH_2 protons. The two signals are attributed as being due to diastereotopic protons, the presence of which can be explained by assuming that **18** exists in a preferred conformation as shown in a Newman projection model (**Scheme 3**). The species H^a and H^b are in a different chemical environment and hence appear as two distinct signals.

The yellow powder was dissolved in THF and crystals of X-ray quality were grown at 4ºC. The complex **18** crystallizes with two molecules of THF in a monoclinic unit cell in the space group $P2_{1/c}$ (**Fig. 3.3**). The palladium atom lies on a crystallographic C_2 axis and shows a typical square-planar coordination with the two catechol rings trans to each other and a normal P-Pd distance of 2.33Å. The boron atom is trigonal planar but the exocyclic angle O1-B1-O2 is reduced to 110.9° from the ideal angle of 120°. On the other hand, the two O1-B1-C20 angles (125.2°) are considerably larger than the standard angle. The

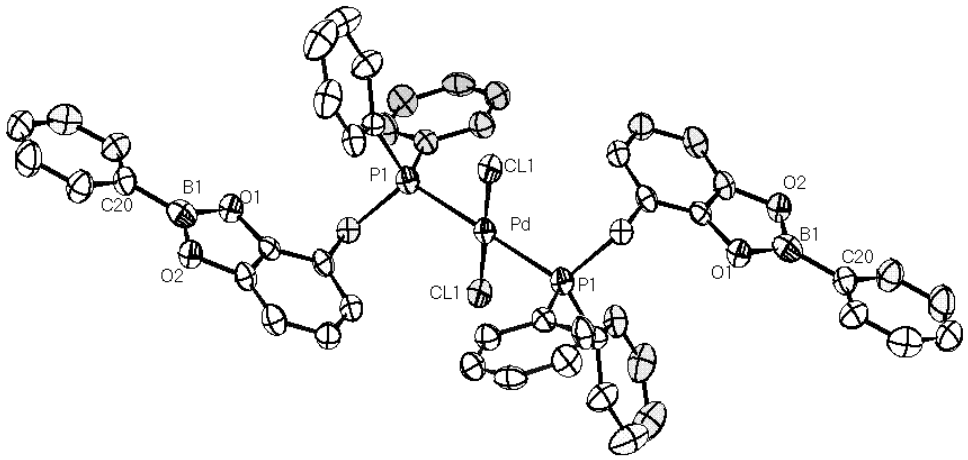

Bond angles [Å]	Bond lengths [°]
B1-O2 1.403(2)	O1-B1-C20 125.3(1)
B1-O1 1.394(2)	O1-B1-O2 110.91(1)
B1-C20 1.544(2)	Cl1'-Pd-P1 86.267(3)
P1-Pd 2.332(1)	Cl1-Pd-P1 93.72(2)

Fig. 3.3: Molecular structure of 18 in the crystal. (H-atoms omitted, 50% probability thermal ellipsoids); important distances and angles are given in the table.

torsional angle around the P-CH_2 unit is 118.3°. The B1-O bonds (1.39-1.40 Å) and the B1-C20 bond (1.53 Å) are in close agreement with previous reports on 2-phenyl-1,3,2-benzodioxaborol.[68]

After confirming the constitution of complex **18**, it was decided to explore the coordination of a base to the boron center as demonstrated for **17a**. Two simple methodologies can be designed to realize such complexes: i) Reaction of two equivalents of **17a** with one equivalent of (COD)$PdCl_2$, and ii) treating the complex **18** with two equivalents of DMAP. During the efforts to synthesize the adduct **19**, it was established that route i) gave better results (**Scheme 2**). Thus, reaction of two equivalents of **17a** with (COD)$PdCl_2$, in a THF/dichloromethane mixture gave within 5 minutes a yellow precipitate, which was filtered and dried in vacuum. The yellow powder was soluble in a mixture of acetonitrile and dimethyl formamide and in DMSO.

The ^{11}B NMR spectrum of the isolated powder in DMSO displayed a single resonance at 11 ppm confirming that the coordinated DMAP donors remain in place. However, ^{31}P NMR spectra showed two products; one giving a singlet signal at δ = 19.4 and the second one appears as AB spectrum with resonances of two chemically inequivalent phosphorus atoms at 82 and 29 ppm with a coupling of 31 Hz. It appears that the first signal could be the possible product although there is no further clear evidence. The AB spectrum is not yet assigned and hence the second product remains unknown. However, the ^{31}P NMR findings indicate in both cases that the phosphorus atoms are coordinated to palladium. At this stage deeper investigations are required in order to state the constitution of the product unambiguously.

3.2.2. Syntheses and characterization of Silver (I) bis {diphenyl- (benzo- [1,3]-dioxo-4-ylmethyl)-phosphane} 2-borate:

Motivated by the importance of borate esters in naturally occurring antibiotics such as boromycin,[77] aplasmomycin[78] and having understood that the smallest feasible templates are tetrahedrally coordinated second row elements, it was decided to explore the borate ester chemistry of **9b-d**. The idea behind this work is to synthesize borate esters of **9b-d,** which can mimic a bidentate ligand and the geometry of which can control the bite angle.

[77] R. Huetter, W. Keller-Schierlein, F. Knuesel, V. Prelog, G. C. Rodgers, P. Sutter, G. Vogel, W. Voser, H. Zaehner, *Helv. Chim. Acta.* **1967**, 50, 9, 1533.
[78] T. Okazaki, T. Kitahara, Y. Okami, *J. Antibiot.* **1975**, 28, 176; T. J. Stout, J. Clardy, I. C. Pathirana, W. Fenical, *Tetrahedron*, **1991**, 47, 22, 3511.

The three-components **9b,** $B(OH)_3$, and NEt_3 were reacted in THF to give the borate **20 (Scheme 4).** The reaction mixture was evacuated to dryness and a white powder of m. p. 92ºC was isolated in good yield (83%). The ^{11}B NMR displayed a resonance at 14.3 ppm which is typical for a tetra-coordinated borate.[79] The ^{31}P resonance at –13.2 ppm corresponds to the free phosphine. The proton NMR displayed signals between 7.60 and 7.26 ppm which can be easily assigned to the phenyl protons on phosphorus, and a multiplet between 6.44 and 6.34 ppm, which is assigned to the catechol ring protons. A doublet of doublets centered at 3.51 and a doublet at 3.44 ppm are attributed to the diastereotopic aliphatic CH_2 protons, as the group is prochiral. Excessive line broadening was observed for the NH proton of the triethyl amine counter ion, which appeared as a very broad singlet at 6.8 ppm.

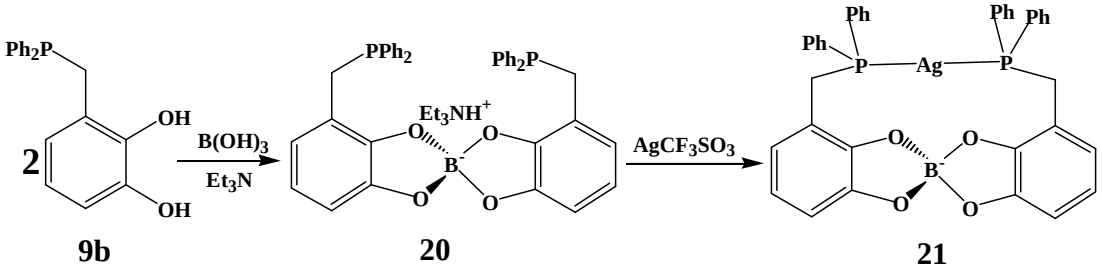

Scheme 4: Syntheses of catechol borate template 20 and its silver complex 21.

A quartet at 3.13 and a triplet at 1.23 ppm were assigned to the CH_2 and CH_3 protons of the triethyl ammonium ion, respectively. Coordination of the catechol units of **9b** to boron was further supported by the significant ^{13}C NMR downfield shift (5-10 ppm) of the C-O carbon atoms as compared to the free ligand **9b**. A Positive ion FAB-MS showed a triethyl ammonium cation at m/e = 102 $(Et_3NH)^+$, a protonated cation $[B(catphos)_2H_2]^+$, at m/e = 625 and the protonated complex **20** at m/e = 726 $[B(catphos)_2(H)(Et_3NH)]^+$. The negative FAB-MS ion spectrum displayed a peak at m/e = 623 arising from the borate anion $[B(catphos)_2]^-$.

White needle like crystals of **20** suitable for X-ray diffraction measurement were obtained from a THF solution at –28°C. The single crystal X-ray diffraction study revealed that the product crystallizes in a triclinic unit cell in the space group P*1(*bar). The crystal structure determination disclosed the presence of two crystallographically independent ion pairs whose constituents show minor differences in their bonding parameters. Both are

[79] R. A. Baber, J. P. H. Charmant, J. D. Moore, N. C. Norman, and A. G. Orpen, *Acta. Cryst. Sect. E, Stru. Rept.* **2004**, E60, o1140.

composed of a spirocyclic anion which is assembled around a central BO_4-tetrahedron, and a triethyl ammonium cation that interacts with the anion via a NH···O hydrogen bridge (**Fig. 3.4**). As a consequence of this interaction, the B–O2 bond (1.51 Å) is slightly longer than the other B–O bonds (1.46 – 1.48 Å); similar observations have been reported by

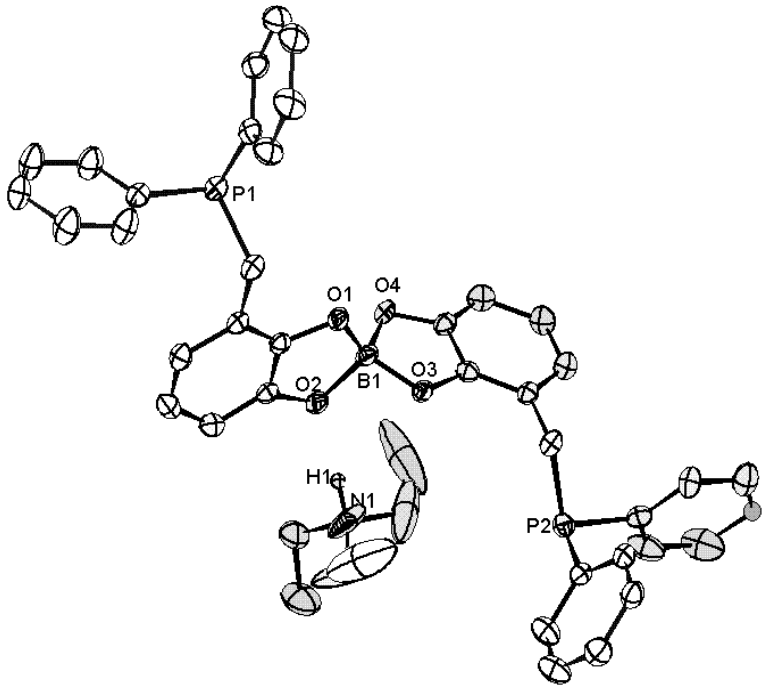

Bong lengths [Å]	Bond angles [°]
B1-O4 1.460 (4)	O4-B1-O3 105.7(2)
B1-O1 1.478 (4)	O1-B1-O2 103.4(2)
B1-O2 1.511(4)	O1-B1-O4 112.9(3)
H1-O2 1.83	O2-B1-O3 110.6 (2)

Fig. 3.4: Molecular structure of 20 (H-atoms omitted except the NH atom; 50% probability thermal ellipsoids); selected bond lengths and bond angles are given in the table.

Moore et al.[79] The catecholate chelating O1-B1-O2 array has a very acute angle of 103° which is considerably sharper than the ideal tetrahedral angle of 109.5°. On the other hand, the O1-B1-O4 angle is 112.8°, i. e. considerably larger than the tetrahedral angle. The distorted tetrahedral coordination at boron enforces further a mutually orthogonal arrangement of the catechol ring planes in the phosphine fragments, and the spatial

separation between the methylene carbon atoms was found to be 7.6 Å and the phosphorus donor atoms are separated by 10.6 Å. The successful isolation of the borate **20** (**Scheme 4**) proved that formation of a template is in principle feasible.

The isolated product was then treated with $AgSO_3CF_3$ in DMF and the solution was stirred at room temperature for an hour. Diethyl ether was added to produce a precipitate which was filtered and finally dried in vacuum to obtain a product that was characterized as the silver borate **21**. The soluble side product (triethyl ammonium triflate) was eliminated by filtration. NMR studies of **21** showed a single ^{11}B NMR resonance at 13.9 ppm corresponding to a tetra-coordinated boron atom. The ^{31}P resonance displayed two doublets centered at 2.9 ppm with silver couplings to ^{107}Ag (I = ½, 51.82 %) and ^{109}Ag (I = ½, 48.18 %) of 506 and 584 Hz, indicating that the two phosphorus atoms are equivalent

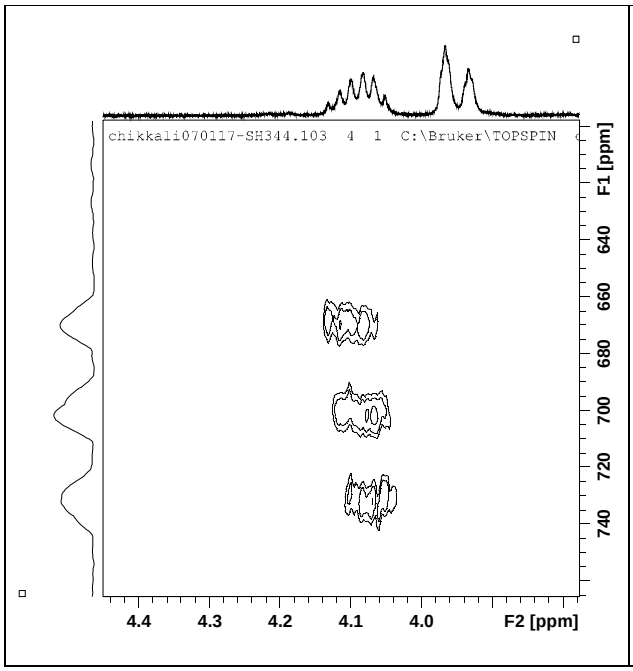

Fig. 3.5: ^{1}H-^{109}Ag 2D NMR displaying proton-silver cross peaks.

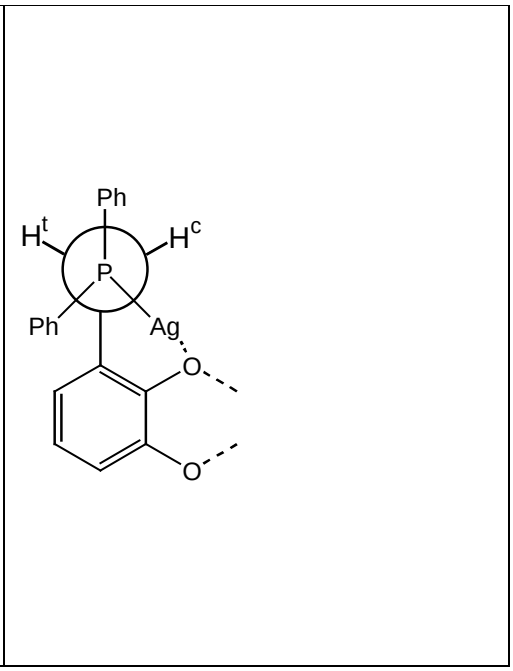

Fig. 3.6: Newman projection along the Ph_2P-CH_2 bond showing schematically the conformation of the chelate ring in the crystal. The benzylic protons are labeled as H^c and H^t respectively.

and are coordinating to the silver atom.[80] The proton NMR displayed only one set of signals for the aromatic catechol protons indicating equivalence of the catechol rings, whereas two sets of signals were observed for the phenyl groups and for the aliphatic CH_2 protons, which prove the geminal protons and arene rings in each Ph_2PCH_2-unit to be diastereotopic. It was possible to explain the splitting of the signal of one of the CH_2 protons (at δ = 3.95 in **Fig. 3.5**) by assuming coupling to the geminal proton ($^2J_{PH}$ = 13.3 Hz) and the phosphorus atoms, whereas the multiplet structure of the second signal (at δ = 4.01) suggested that coupling to an additional nucleus is present. The assignment of the extra interaction to scalar coupling with silver was established by a ^{1}H-^{109}Ag HMQC experiment (**Fig. 3.5**), and analysis of the cross peak profile permitted to determine $^3J_{Ag,H}$ = -7 Hz. The absence of a similar correlation for the second methylene proton indicated that $^3J_{Ag,H}$ is in this case close to zero. The diastereotopic nature of the methylene protons in **21** owes to the embedding of the CH_2-moiety into a non-planar chelate ring. The strict absence of dynamic exchange processes between both signals suggests that no ring inversion and concomitant racemization of the configuration at boron occur on the NMR time scale and led to conclude that the rigid conformation established for solid **21** (see below) persists at ambient temperature in solution. The imbalance of $^3J_{Ag,H}$ for the CH_2 protons is under these conditions attributable to a difference in Ag-P-C-H dihedral angles (**Fig. 3.6**; H^t is assigned to the proton with the larger absolute value of $^3J_{Ag,H}$). The ^{13}C NMR resonances remained similar to those of the boron template **20**. The formation of the silver complex **21** was further confirmed by ESI Mass spectra. A positive mode ESI experiment showed a pseudo molecular ion peak at m/e = 733.08 $(\mathbf{21}+H)^+$ formed by capture of a proton and one at m/e = 755.07 $(\mathbf{21}+Na)^+$ formed by capture of a sodium cation.

Crystals of compound **21** suitable for X-ray measurement were obtained by dissolving the white powder in DMF: diethyl ether (1:1) at room temperature. The monoclinic crystals (space group *Cc*) contain discrete mononuclear complexes consisting of one silver ion and one chelating bisphosphine moiety (see **Fig. 3.7**), along with one molecule of DMF per formula unit. An interesting feature to note is the deviation of the silver coordination from linearity, as the silver and phosphorus atoms in each complex form a distinctly non-linear array (P1-Ag-P2 154.4°). The Ag-P bonds (Ag-P ~2.45 Å) are longer than those in **14b,d**

[80] P. S. Pregosin, R. W. Kunz, In *^{31}P and ^{13}C of Transition Metal Phosphine Complexes*, Springer-verlag, New York, **1979**, p. 89.

(2.39 – 2.40 Å). The silver atom displays two additional short contacts to oxygen atoms in the borate unit at distances (Ag-O2/O3 2.81 – 2.85 Å) that exceed the secondary Ag-O interaction in **14b** but are still much shorter than the sum of van-der-Waals radii (3.55 Å). The phosphorus atom displays a distorted tetrahedral arrangement with the two phenyl groups, the catechol moiety and the silver atom completing the coordination sphere. The distorted tetrahedral coordination at the boron atom is characterized by a slight lengthening of the B-O bonds to the bridging oxygen atoms (1.49 – 1.50 Å for B-O2/3 vs. 1.47 – 1.48 Å for B-O1/4), and a contraction of the O2-B-O3 (107.0°) and a widening of the O1-B-O4

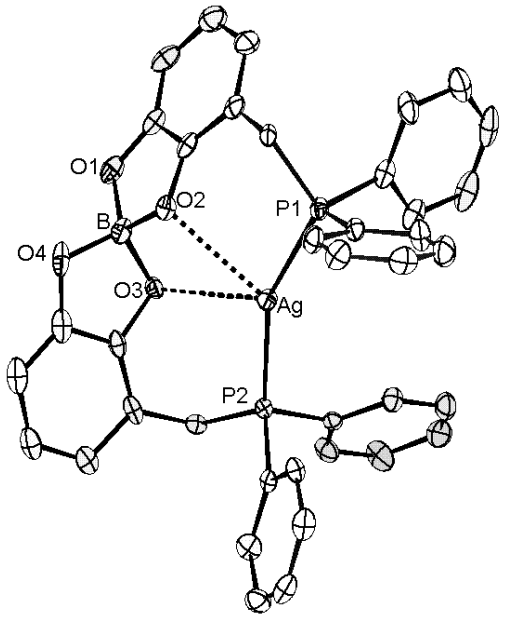

Bond lengths in [Å]	Bond angles [°]
B-O4/1 1.470-1.473	P1-Ag-P2 154.43(6)
B-O2/3 1.493-1.502	O1-B-O2 104.8 (4)
Ag-O2/3 2.802-2.849	O2-B-O3 107.0(5)
Ag-P1/2 2.446-2.450	O1-B-O4 112.4(5)

Fig. 3.7: Molecular structure of 21 (H-atoms omitted for simplicity; 50% probability thermal ellipsoids); selected bond lengths and angles are given in the table.

angle (112.4°), which deviate considerably from the ideal tetrahedral angle of 109.5°. All structural features together suggest that **21** represents, in a similar manner as **14b** and **d**, a bis-phosphine complex with a linear two-coordinate silver ion that exhibits additional, presumably electrostatic, interactions with oxygen atoms of the borate unit. It remains currently undecided if the Ag-P bond lengthening in **21** is a direct electronic consequence

of these secondary interactions, or is rather attributable to the presence of conformational strain in the chelate ring.

3.2.3. Synthesis and characterization of a Silver (I) bis {diphenyl- (benzo-[1,3]-dioxo-5-ylmethyl)-phosphane} 2-borate macrocycle:

In this section, another catechol phosphine **9d** will be utilized which differs from **9b** only in the relative position of the hydroxy groups to the phosphorus atom. The three components $B(OH)_3$, **9d** and Et_3N were reacted in THF to give the borate **22.** The reaction mixture was evacuated to dryness and a white powder of m. p. 197ºC was isolated in good yield (90%). The ^{11}B NMR displayed a resonance at 14.33 ppm, which is typical of a tetra-coordinated borate.[79] The ^{31}P resonance at –10.2 ppm corresponds to a free phosphine. The proton NMR spectrum displayed signals between 7.5 and 7.3 ppm which can be easily assigned to the protons of the phenyls at phosphorus. A broad singlet at 3.37 ppm is attributed to the aliphatic CH_2 protons. An excessive line broadening was observed for the NH proton, which appeared as a very broad singlet at 6.8 ppm. A quartet at 3.08 and triplet at 1.18 ppm were assigned to the CH_2 and CH_3 protons of triethyl ammonium, respectively. Coordination of the catechol units of **9d** to boron was further supported by the significant ^{13}C NMR downfield shift (5-10 ppm) of the C-OH carbon atoms as compared to the free ligand **9d**.

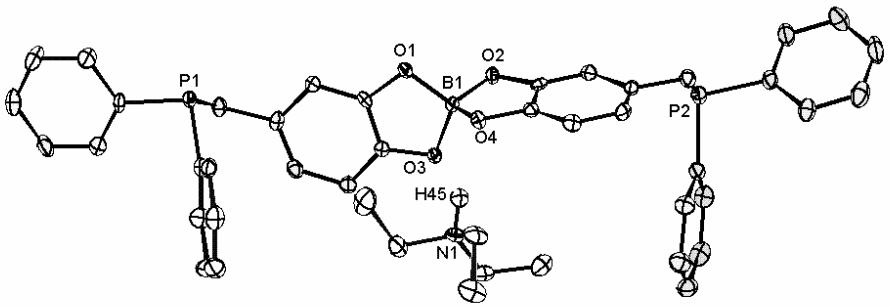

Bond lengths [Å]	Bond angles in [°]
O4-B1 1.496(4)	O1-B1-O3 105.88(2)
O3-B1 1.494(4)	O2-B1-O4 104.91(2)
O1-B1 1.476(1)	O3-B1-O4 109.45(2)
O4-H45 1.957(1)	O1-B1-O2 113.0(2)

Fig. 3.8: Molecular structure of 22. (H-atoms omitted except the NH atom; 50% probability thermal ellipsoids); selected bond lengths as given in the table.

Suitable single crystals for X-ray diffraction measurements were obtained from tetrahydrofuran solution at –28ºC. The molecular structure of **22** (monoclinic, space group Cc) disclosed as in the case of **20** the presence of two crystallographically independent ion pairs. Both are composed of a spirocyclic anion which is assembled around a central BO_4-tetrahedron, and a triethyl ammonium cation that interacts with the anion via a NH···O hydrogen bridge. As a consequence, the B-O4 (1.49 Å) bond is slightly elongated as compared to the other three B-O bonds (1.47-1.48 Å) although not significantly (**Fig. 3.8**). The spirocyclic ring structure induces also a contraction of the O-B-O angles in the five-membered rings (104 – 105°) and a concomitant widening of the remaining bond angles (109 – 112°C) with respect to the tetrahedral angle of 109.4°. Other bonding parameters in the spirocyclic catechol borate unit are similar to those observed in **20** but the distance between the two methylene carbon atoms (C9…C12 12.0 Å) and the phosphorus donor atoms (P1…P2 13.3 Å) shows, as a direct consequence of the different substituent pattern, a further substantial increase.

A stoichiometric reaction between template **22** and AgO_3SCF_3 in DMF at room temperature produced a colorless solution. The product was precipitated by adding excess

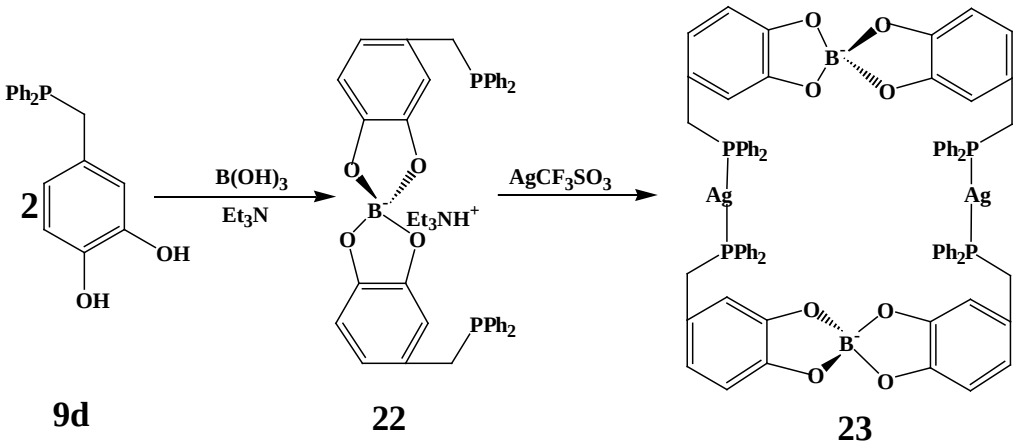

9d **22** **23**

Scheme 5: Syntheses of boron template 22 and boron-silver macrocycle 23.

diethyl ether. The white solid was filtered off, dried in vacuum, and characterized by NMR and Mass Spectroscopy. The material obtained melts at 272ºC and is sparingly soluble in highly polar solvents. The presence of a ^{11}B resonance at δ =14.8 confirms that the boron template **22** remained intact and a broad ^{31}P signal at 12.8 ppm with a splitting of 314 Hz due to P-Ag coupling indicates that the phosphorus is coordinated to the silver and is undergoing fast intermolecular ligand exchange. Cooling down the sample did not cause

simple sharpening of the signals but resulted in decoalescence to give a complicated pattern of several multiplets (due to coupling with $^{107/109}$Ag nuclei) that could not be fully analyzed. The ^{1}H NMR signals were likewise broad, but the appearance of a single signal for the benzylic protons indicated that a similar resolution of different environments of diastereotopic CH_2 protons as in **21** was unfeasible.

Starting with the assumption that formation of a *mononuclear* complex with similar constitution as **21** is incompatible with the arrangement of the donor sites in the template ligand **22**, it was concluded that the available analytical and spectroscopic data are best interpreted by assuming the presence of oligomeric complexes of composition $[(\mathbf{22})Ag]_n$ (n> 1) which are formed by μ-bridging coordination of n bis-phosphine units to n silver

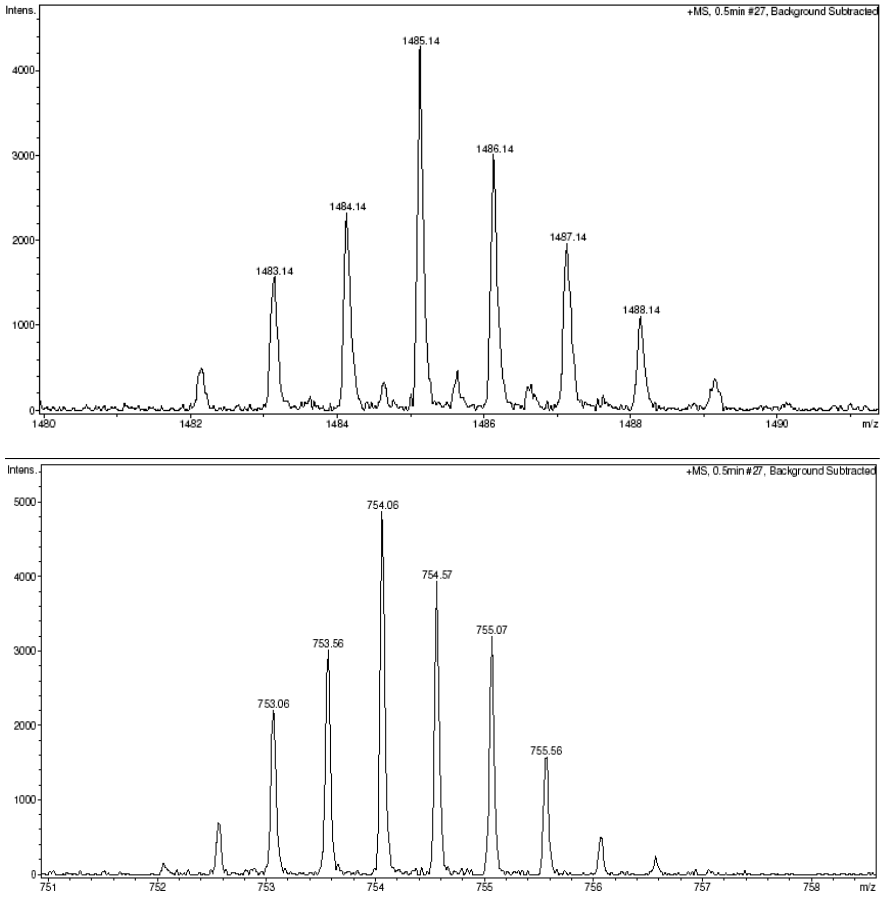

Fig. 3.9: Positive mode ESI-MS spectra displaying m/e = 1485.14 $(\mathbf{23}+Na)^{+}$ and 754.05 $(\mathbf{23}+Na)^{2+}$ with 13 C isotopic splitting of 1.0 Da and 0.5 Da respectively.

ions. Since each fragment **22** represents an axially chiral building block, the oligomeric assembly may exist in several diastereomeric forms, and mutual interconversion between

individual isomers via intermolecular ligand exchange and/or racemization of individual borate units can provide a satisfactory explanation for both the observed line broadening effects in the ^{1}H and ^{31}P NMR spectra and the observation of multiple ^{31}P NMR resonances at low temperature. Direct experimental evidence for the presence of the postulated oligomers was also obtained from a positive mode ESI mass spectrum of a DMF solution of the isolated product which displayed a peak at m/e = 1485.13 assigned to a pseudo-molecular ion (**23**+Na)$^{+}$ (**fig. 3.9** top trace). The small peaks at the bottom suggest that a small amount of a tetrameric complex is presumably also present. The ESI-MS spectra further displayed a doubly charged ion peak at 754.1 assigned as [**23**+2Na]$^{2+}$(**fig. 3.9** bottom trace).[81] These pseudo-molecular ions were unequivocally identified by comparison of observed and simulated isotope patterns. As at the same time no ions indicating the presence of mononuclear complexes were found we deduce that the predominant species present in solution is the dinuclear complex **23**.

The conclusions derived from the mass spectral studies of complexes **21** and **23** were further validated by diffusion coefficient measurements using Pulsed Gradient Spin Echo NMR experiments.[82]

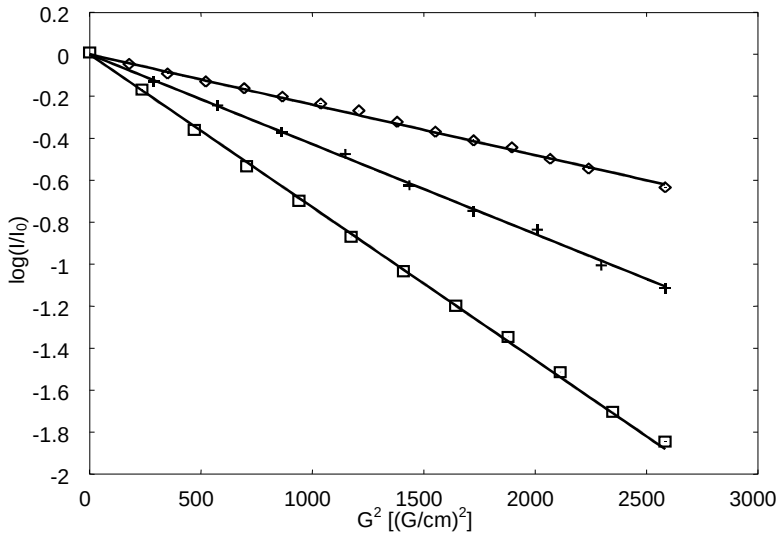

Fig. 3.10: Plots of log I/I0 for the signal of the benzylic protons vs. the square of gradient amplitude. Data refer to solutions of 21 in $CDCl_3$ (□) and DMF-d_7 (+), and to a solution of 23 in DMF-d_7 (◊). Diffusion coefficients were calculated from the slope of the straight lines, and values are given in text.

[81] A. P. Gies, D. M. Hercules, A. E. Gerdon, D. E. Cliffel, *J. Am. Chem. Soc.* **2007**, 129, 1095.
[82] P. S. Pregosin, P. G. Anil Kumar, I. Fernandez, *Chem. Rev.* **2005**, 105, 8, 2977.

The diffusion coefficient D allows one to compute hydrodynamic radii r_H via the Stokes-Einstein equation, $r_H = kT/6\pi\eta D$, and r_H may in turn be used to estimate molecular volumes. A common application of PGSE techniques in chemistry concerns the comparison of relative molecular sizes of species in solution and is based on the perception that the ratio of the diffusion coefficients of two molecules determined in the same solvent and at the same temperature is inversely proportional to the ratio of r_H, and thus the molecular volumes, of these species.[82]

Measurement of the diffusion coefficients of solutions of **21** and **23** in DMF-d_7 at 30°C (**Fig. 3.10**) gave values of $D = 4.3(1) \cdot 10^{-10}$ m^2/s for **21** and $D = 2.2(1) \cdot 10^{-10}$ m^2/s for **23**, respectively. These data suggest that the hydrodynamic radius of **23** is nearly twice as large as that of **21**, which is well in accord with the proposed nature of **23** as a dimer. Carrying out the experiment on a solution of **21** in $CDCl_3$ at the same temperature gave $D = 9.2(1) \cdot 10^{-10}$ m^2/s which indicated a higher mobility of the complex in $CDCl_3$ than in DMF. Although this is in principle to be expected as a consequence of the lower solvent viscosity,[83] the noticeable deviation of the measured ratio of diffusion coefficients of 4.3/9.2 = 0.47 from the inverse ratio of viscosities of 0.68 suggests that this effect is not attributable to the viscosity influence alone. A likely explanation for the deviation can be given by postulating that the silver ion in **21** is in DMF solution involved in additional donor-acceptor interactions with solvent molecules which should increase the hydrodynamic radius and thus lead to an overproportional decrease of the diffusion coefficient. Further support for this hypothesis is gained from the observation of a noticeable solvent dependence of the values of $\delta(^{109}Ag)$ and $^1J_{AgP}$ as well as the relative chemical shifts of the benzylic protons H^t and H^c (see Expt. section for details) in **21** which is interpreted to reflect directly the interaction between the metal ion and the additional solvent molecules.

[83] Dynamic viscosities at 30ºC from *Landolt Boernstein*, Springer, **2002**, 18B; η = 0.506 ($CDCl_3$), 0.743 (DMF-d_7) m Pa.s. The value for DMF-d_7 was interpolated from the available data in the temperature region between 15 and 45ºC.

3.3. Attempted synthesis of Triethyl ammonium [Dichloro palladium bis {diphenyl- (benzo- [1,3]-dioxo-4-ylmethyl)-phosphane}] 2-borate:

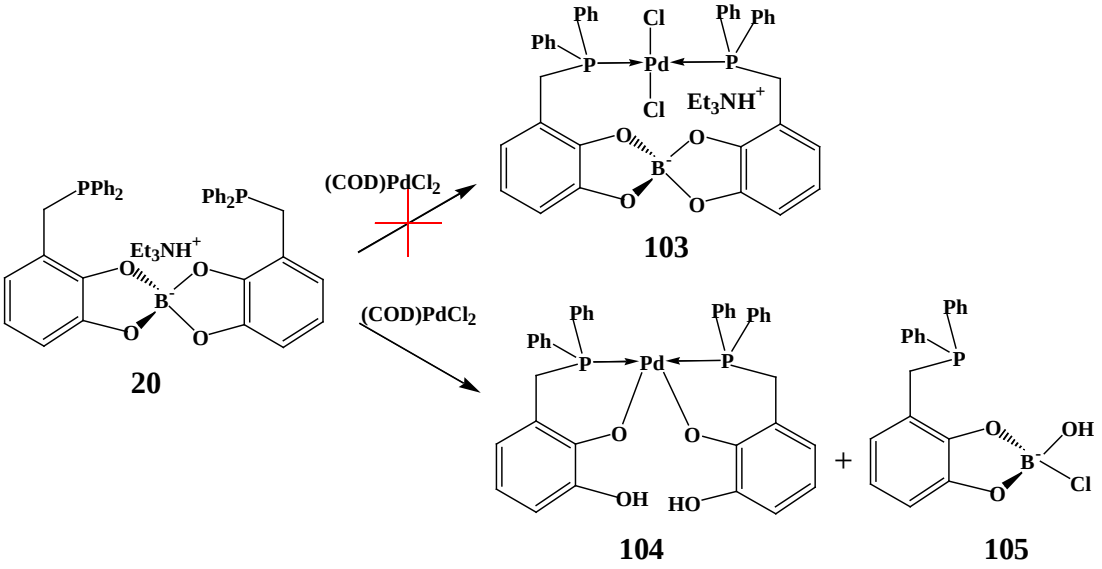

Scheme 6: Attempted synthesis of the palladium borate complex 103.

The isolated product **20** was treated with (COD)$PdCl_2$ in DMF and the solution was stirred at room temperature for 24 hours. Diethyl ether was added to produce a precipitate which was filtered and finally dried in vacuum to obtain an orange yellow powder of melting point 142ºC. NMR studies of **103** showed a single ^{11}B NMR resonance at 14.6 ppm corresponding to a tetra-coordinated boron atom. The ^{31}P NMR spectrum displayed three broad singlets at 40.7, 31.2, and 19.5 ppm indicating that a mixture of several products had formed. The ESI-MS positive mode experiment displayed quite surprising spectra. A pseudo-molecular ion peak was observed at m/e = 743.07 corresponding to $[(catphos)_2Pd+2H+Na]^+$, where (catphos) = $C_{19}H_{15}O_2P$. A further ion was observed at m/e = 1465.15 $\{[(catphos)_2Pd+2H]_2+Na\}^+$. The ESI-MS negative mode spectra displayed a pseudo-molecular ion peak at m/e 719.07 corresponding to $[(catphos)_2+HPd]^-$, another peak at 404.96 corresponding to $[(catphos)BOHCl]^-$ could also be assigned. The above observations suggest that complex **103** was not at all formed, whereas fragments containing separate palladium complex (**104**) and borate anion (**105**) were found in ESI-MS spectra. A likely explanation for the failure to observe **103** could be that the palladium atom likes to be square planar which induces more strain on the borate anion and forces it to open up, giving two separate fragments. Thus efforts to synthesize **103** were

unsuccessful.

3.4 Conclusions:

In Summary, the catechol phosphine **9b** reacts with phenyl boronic acid to give the corresponding borane **16a**. The moderately strong boron acidic center of **16a** required six equivalents of pyridine for complete conversion into the acid/base adduct, whereas only one equivalent of dimethyl amino pyridine was sufficient to obtain the corresponding adduct **17a**. Two equivalents of **17a** on treatment with one equivalent of palladium complex produced a mixture of products, one of them is likely to be **19**, though further evidence is required. The presented experimental findings allow to state that, by varying the substituent on boron, either a strongly acidic or a weakly acidic center can be generated, which can be further utilized to coordinate a bidentate base that can act as a building block for organometallic polymers.

It was demonstrated that the tetrahedral borate unit can be used to assemble the catechol phosphines **9b**,**d** to yield the supramolecular bis phosphines **20** and **22** respectively. These borates can act as bidentate ligands towards soft metals like Ag^{+} forming either a mononuclear complex **21** or a dinuclear complex **23**. The nature of the product is determined by the control of the bite angle of the bis-phosphine, which is in turn commanded by the relative arrangement of the catechol and phosphorus donor sites in the molecular backbone of the catechol phosphine. The observed product selectivity during the complexation step suggest that the template-based approach allows one not only to link two simple monodentate ligand fragments to form a bidentate donor, but that the resulting assemblies are sufficiently rigid to permit tuning of the geometric parameters of the ligand assembly. The procedures reported here should thus encourage further efforts to combine catechol phosphines **9b,d** with different main group or transition metal templates to generate ligand libraries whose geometric properties can be fine-tuned.

4. Transition metal complexes of templated symmetric bisphosphane ligands and potential application in catalysis

4.1. Introduction:

In Chapter 2 facile and rational syntheses of a series of functional catechol phosphine ligands was demonstrated (see **Fig. 4.1**). A peculiarity of these ligands is that they are composed of hard donors (oxygen atoms) at one end and soft donors (phosphine) at the other end. Important to note is the relative disposition of these donors, which are in close proximity to each other. The ligand can form a six-membered ring with a metal atom utilizing both a hard and soft donor available. Alternatively, hard acids may selectively react with the oxygen donors and soft acids with the soft phosphine.

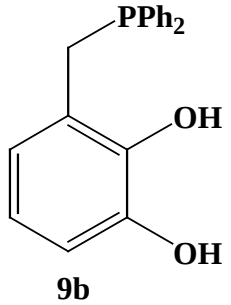

9b

Fig.4.1: Ligand 9b.

Another feature is that these ligands are equipped with a CH_2 unit which acts as a spacer to provide limited but sufficient flexibility. Chapter 3 demonstrated that a main group element such as boron may act as template to assemble two bifunctional ligands **9b** to give a bifunctional phosphine which may then react with a transition metal ion to form a complex. Recently Raymond and coworkers demonstrated that the relative placement of hard and soft donors could be exploited for designed syntheses of heterometallic clusters,

allowing to construct complex metal-ligand aggregates in a single step by "self-assembly".[84] Taking into account these features, it is highly likely that in the presence of a hard and soft acid, ligand **9b** may likewise undergo template directed self assembly to generate a di- or multinuclear complex. It is envisioned that alteration of the template center may allow the study of a series of complexes featuring ligands with different geometric properties. In particular, the size of the template may control the ligand bite angle, and varying the template size may provide better insights into the complexation properties of ligands with different bite angles. In order to study the effect of alteration of the template, various ions of group 3, 4, 13, 14 and 15 with three or four positive charges will be used. Though there is in principle a similar variability in the metal used for complexation, the studies in this chapter will focus on Pd(II) and Pt(II) because of the frequent use of these elements in catalysis. The final goal of this study is to employ the self-assembled complexes as catalysts for C-C coupling reactions.

Investigations on boron compounds, as detailed in chapter 2, indicated that the use of boron as a template is limited in view of its small size. Due to its large ion radius and high reactivity, gallium, the higher analogue of boron, was selected for further investigations. The close similarity of gallium (III) with iron (III) makes it further interesting, as iron is an important component in many biological processes.[85] It is assumed that gallium complexes may be useful as mimics for analogous iron complexes which may have useful properties owing to the redox activity of iron.[86] Shifting the focus from group 13 to 14, tin was selected owing to its larger size and higher chlorophilicity than gallium. Furthermore, tin is known to form penta- coordinated complexes with mixed O,S-donors and hexa-coordinated complexes with oxygen donors.[87] At the application end, tin compounds are known to show non-linear optical (NLO) properties,[88] and organo-tin halides are important alkyl transfer reagents in Stille type C-C coupling reactions.[89] Recently, Ishii and coworkers reported the oxidative carbonylation of phenols to diphenyl carbonate.[90] In this

[84] X. Sun, D. W. Johnson, K. N. Raymond, E. H. Wong. *Inorg. Chem.* **2001**, 40, 4504.
[85] a) B. Kersting, J. R. Relford, M. Meyer, K. N. Raymond, *J. Am. Chem. Soc*. **1996**, 118, 5712. b) M. Meyer, B. Kersting, R. E. Powers, K. N. Raymond, *Inorg. Chem.* **1997**, 36, 5179.
[86] T. B. Karpishin, T. M. Dewey, K. N. Raymond, *J. Am. Chem. Soc.* **1993**, 115, 1842.
[87] R. R. Holmes, S. Shafieezad, V. Chandrasekhar, A. C. Sau. J. M. Holmes, R. O. Day, *J. Am. Chem. Soc.* **1988**, 110, 1168.
[88] C. Lamberth, J. C. Machell, D. M. P. Mingos, T. L. Stolberg, *J. Mater. Chem.* **1991**, 1(5), 775.
[89] a) J. K. Stille, *Angew. Chem. Int. ed.* **1986**, 25, 508. b) T. N. Mitchell, *Synthesis* **1992**, 803. c) L. S. Hegedus, *Coord. Chem. Rev*. **1996**, 147, 443.
[90] H. Ishii, M. Ueda, K. Takuechi, M. Asai, *J. Mol. Catal. A: Chem.* **1999**, 138, 311.

reaction, a mixture of palladium and tin compounds was employed to generate complexes in situ and no further explanation on the composition of the complex was provided.

Bismuth was picked up as a representative of group 15, applying to similar size criteria as gallium and tin. Whereas trivalent arsenic and antimony catecholates are well studied,[91] less is known about bismuth compounds. Rosenheim in1931 reported coordination of three catechols to bismuth,[92] and Smith et al[93] reported a dimeric penta-valent bismuth catecholate complex $\{(NH_4)_2[Bi_2(C_6H_4O_2)_4].2C_6H_4O_2.2H_2O\}$. Lately, organo-bismuth compounds have attracted much interest,[94] due to the potential biological activity and their use as catalysts in organic synthesis.[95] Bismuth is the heaviest stable element in the periodic table, and bismuth compounds often show special behavior, both electronically and sterically.[96]

Moving from the main group elements to transition metals and considering the commercial importance of zirconium complexes in polymer industry,[97] zirconium was chosen as a possible template. To check out the reactivity of the lanthanides, which are known to be very oxophilic, the near neighbor yttrium was chosen. Detailed report on the reactivity of all above elements with the catechol phosphine **9b** will be provided in the following section.

4.2. Results and discussion:

4.2.1. Synthesis and characterization of self-assembled palladium-bis {diphenyl- (benzo- [1, 3]-μ-oxo-k-oxo-4-ylmethyl) phosphane)}-gallium chloride (25):

A reaction aiming at preparing a chelate complex by self-assembly was carried out by placing a mixture of **9b** (2 equivs.), $(COD)PdCl_2$, $GaCl_3$ and excess Et_3N (2.5 equivs.) into a Schlenk tube and dissolving this mixture in a suitable solvent. In view of the lower solubility of some of the reaction components and previous reports on similar reactions[98] dimethyl formamide was chosen as the most suitable solvent. The progress of the reaction

[91] A. Rosenheim, I. Baruttschisky, *Ber. Dtsch. Chem. Ges*. **1925**, 58, 891.
[92] A. Rosenheim, *Z. Anorg. Allg. Chem*. **1931**, 200, 173.
[93] G. Smith, A. N. Reddy, K. A. Byriel, C. H. L. Kennard, *Aust. J. Chem.* **1994**, 47, 1413.
[94] H. Suzuki, Y. Matano, Eds. *Organobismuth Chemistry*; Elsevier Science B. V.: Amstredam, **2001**.
[95] C. Silvestru, H. J. Breunig, H. Althaus, *Chem. Rev*. **1999**, 99, 3277.
[96] N. Guilhaume, M. Postel, *Heteroatom. Chem*. **1990**, 1(3), 233.
[97] M. J. Ferreira, A. M. Martins, *Coord. Chem. Rev*. **2006**, 250(1-2), 118.
[98] D. L. Caulder, R. E. Powers, T. N. Parac, K. N. Raymond, *Angew. Chem. Int. Ed.* **1998**, 37, 1840.

was monitored by ^{31}P NMR and showed complete conversion in 5 hours. A red solution with a white precipitate was obtained which was first filtered through a celite bed, followed by evaporation of the filtrate to dryness. The dried red powder was dissolved in 10 ml of dimethyl formamide and precipitated out by adding 60 ml of diethyl ether; this was repeated one more time. At the end of this procedure an orange red powder of m. p. 358ºC was isolated in 70% yield. The product was submitted to further characterization by analytical and spectroscopic methods.

A sharp singlet at 65 ppm in the ^{31}P NMR spectrum in $CDCl_3$ indicated the exclusive formation of a single product. The relatively large down field shift in phosphorus NMR as compared to complexes like **24** raised speculations about the formulation of the product. The observed deshielding is compatible with the formation of chelate complexes, as similar deshielding was reported for the palladium chelates of related phosphinoalcohols.[99]

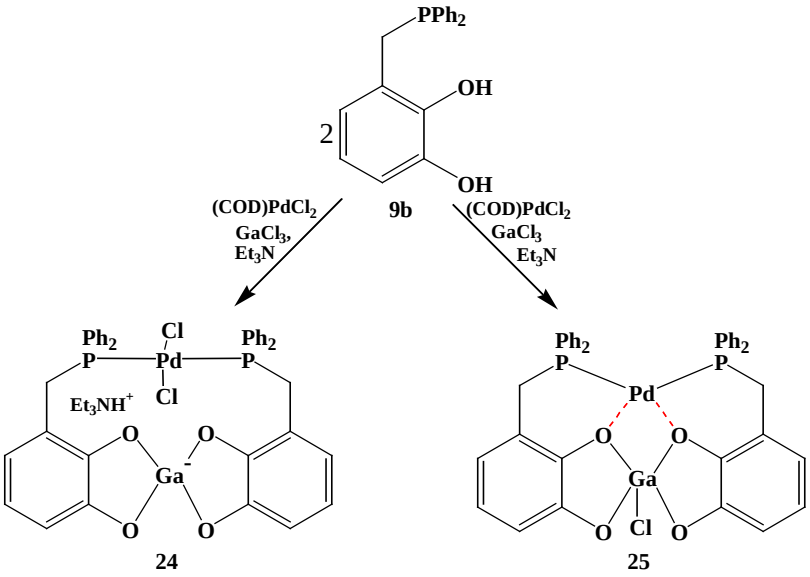

Scheme 4.1: Synthesis of palladium-gallium dinuclear complex 25.

The ^{1}H NMR spectrum was similar to that of the free ligand and no signals indicating an ammonium cation were visible, thus ruling out the expected constitution as **24**. Presumably, the triethyl ammonium cation present in **24** can abstract chloride from the palladium atom, spontaneously eliminating triethyl ammonium chloride and resulting in weak intramolecular palladium oxygen interactions to give complex **25** (see **Scheme 4.1**). The positive mode ESI-MS spectrum showed a pseudo-molecular ion peak at m/e = 825

[99] D. J. Brauer, P. M. Machnitzki, T. Nickel, O. Stelzer, *Eur. J. Inorg. Chem.* **2000**, 65.

$(M+H)^+$ where M = $C_{38}H_{30}O_4P_2GaPdCl$ (See 25, Scheme 4.1). Another pseudo-molecular ion peak was observed at m/e = 847 $(M+Na)^+$. An oxidation product was also observed at m/e = 857 $(M+O_2+H)^+$. The negative mode ESI-MS displayed two peaks corresponding to the pseudo-molecular ion at m/e = 823$(M-H)^-$ and 8589 $(M+Cl)^-$.

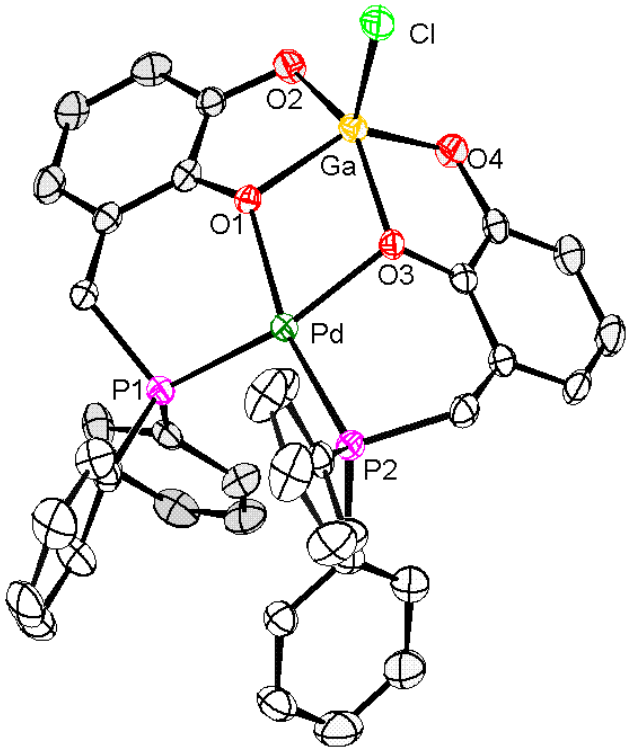

Bond lengths [Å]	Bond angles [°]	Bond angles [°]
Ga-O1 1.974(1)	O1-Ga-O2 83.56(1)	P2-Pd-O3 92.34(1)
Ga-O2 1.918(1)	O1-Ga-O3 76.26(1)	O1-Pd-O3 74.31(2)
Ga-O3 2.085(1)	O3-Ga-O4 83.86(1)	O2-Ga-Cl 104.64(1)
Ga-O4 1.885(1)	O2-Ga-O4 96.23(1)	O1-Ga-Cl 116.61(1)
Pd-O1 2.064(1)	P1-Pd-O1 92.18(1)	O3-Ga-Cl 110.42(1)
Pd-P1 2.250(1)	P1-Pd-P2 101.8(1)	O4-Ga-Cl 111.42(1)

Fig. 4.2: Molecular structure of complex 25, (H-atoms omitted, 50% probability thermal ellipsoids); selected bond lengths in and bond angles are given in table.

Unambiguous confirmation of the constitution of the product as complex **25** came from the crystal structure determination. Suitable crystals for single crystal X-ray diffraction were obtained from a highly concentrated solution of the isolated product in dichloromethane, tetrahydrofuran, and an equivalent amount of diethyl ether at room temperature. A single

crystal X-ray diffraction study disclosed the presence of complex **25** together with three molecules of solvent ($CDCl_3$ from the NMR) per formula unit in a monoclinic unit cell in the space group $P2_{1/n}$. One of the solvent molecules is weakly hydrogen bonded to the chloride on gallium, and the second one is weakly hydrogen bonded to the benzylic hydrogen via a chloride, whereas the third molecule does not show such interactions. The palladium atom displays a square planar geometry with the two phosphorus and two μ_2-bridging oxygen atoms completing the coordination sphere. The phosphine donors exhibit a cis-arrangement with a normal P-Pd bond length of 2.24 Å, but the bond angles deviate from the standard angle of 90º with a very acute O1-Pd-O3 angle of 74.3º and a larger P1-Pd-P2 angle of 101.8º. The most striking feature of the assembly are the oxygen atoms O1/O3 which act as μ_2-bridging ligands towards palladium and gallium. The PdO_2Ga four membered ring is planar. A space filling model displays nicely the cavity built by the two catechol rings and the phenyl substituents on phosphorus. This cavity allows easy access to palladium which would be of further interest in catalysis.[100]

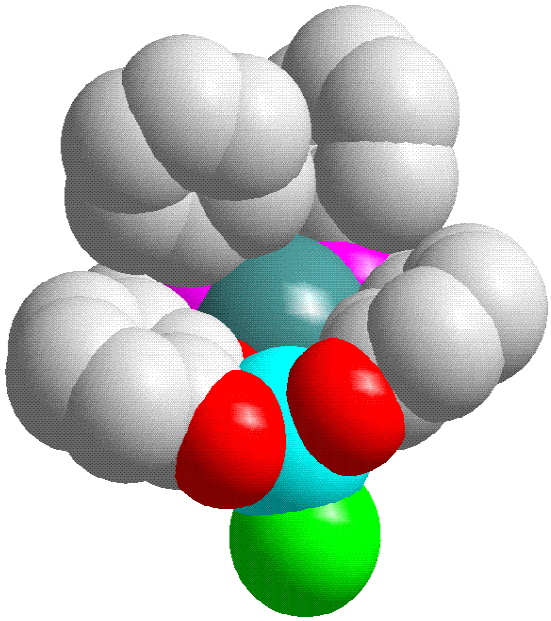

Fig. 4.2a: Space filling model of complex 25 displaying the cavity at palladium(center) made by the catechol and phenyl groups on phosphorus.

The phosphorus atom displays a distorted tetrahedral geometry. The phosphine donors bite into palladium with a bite angle of 101.7º. In order to have less steric hindrance, the phenyl

[100] E. Negishi, R. A. John, *J. Org. Chem.* **1983**, 48, 4098.

rings on phosphorus atom are oriented in a way to have minimum steric repulsive interactions and thus one phenyl ring from each phosphorus atom is oriented trans to the other while the other ring points out of the P-Pd-P plane.

Of particular interest is the distorted square pyramidal geometry at the gallium atom, in which the four oxygen atoms occupy the basal square and the chloride the top of the pyramid. The Holmes model[101] allows to estimate the deviation of the arrangement of ligands around a pentacoordinate central atom from ideal trigonal bipyramidal (TBP) and sqiare pyramidal (SP) geometries. By the dihedral angle method[102] to assess displacements, complex **25** is displaced 11% from an ideal SP toward a TBP coordination. Noteworthy is the displacement of the gallium above the oxygen plane by 0.8Å (O1/2/3-Ga), which reduces the sum of O-Ga-O angles to 340º, compared to a value of 360º for ideally square planar coordination. The observed distortion can be rationalized by the development of certain ring strain in the molecule forming the GaO_2Pd ring. Thus the four oxygen atoms are being pressed down out of the gallium plane. A similar observation was reported earlier[103] in case of the aliphatic 2,2-dimethylpropane-1, 3-diol (neol) gallium complex $[Ga_3(^tBu)_5(neol)_2]$. The oxygen bridging in **25** results in elongation of the O1/O3-Ga bonds (1.97-2.08 Å) compared to the non-bridging O2/O4-Ga bonds (1.88-1.91 Å). The Ga-O (terminal) bonds in **25** are also shorter than in similar cationic gallium catechol complexes[104] reported earlier [Ga-O:1.94 Å]. All four O-Ga-O angles are smaller than the standard square pyramidal angle of 90º, the smallest is O1-Ga-O3 with 76.3º. The inter-atomic distance between the two metals is Pd-Ga 3.21 Å, which is considerably larger than the sum of the covalent radii (2.53 Å) and thus rules out existence of any metal-metal interaction. Hexa- and tetracoordinate gallium complexes are well known in the literature,[105] but there are very few reports on square pyramidal, penta-coordinate gallium compounds.[103, 106]

---

[101] R. R. Holmes, *ACS Monogr*. **1980**, 175, Chapter 2; R. R. Holmes, J. A. Deiters, *J. Am. Chem. Soc*. **1977**, 99, 3318; R. R. Holmes, R. O. Day, A. C. Sau, J. M. Holmes, *Phosphorus, Sulfur, and Silicon and Related Elements*, **1995**, 98, 423.
[102] E. L. Muetterties, L. J. Guggenberger, *J. Am. Chem. Soc*. **1974**, 96, 1748.
[103] C. N. McMahon, S. J. Obrey, A. Keys, S. G. Bott, A. R. Barron, *J. Chem. Soc. Dalton Tans.* **2000**, 2151.
[104] T. B. Karpishin, T. D. P. Stack, K. N. Raymond, *J. Am. Chem. Soc.* **1993**, 115, 182.
[105] B. A. Borgias, S. J. Barclay, K. N. Raymond, *J. Coord. Chem*. **1986**, 15, 109; M. A. Brown, A. A. El-Hadad, B. R. McGarvey, R. C. W. Sunf, A. K. Trikha, D. G. Tuck, *Inorg. Chim. Acta.* **2000**, 300, 613.
[106] N. R. Bunn, S. Aldridge, C. Jones, *Appl. Organometal. Chem.* **2004**, 18, 425; W. Ziemkowska, P. Stella, R. Anulewicz-Ostrowska, *J. Organomet. Chem.* **2005**, 690, 722.

In summary, simple mixing of the four complementary reactants at room temperature produces selectively a single, neutral, palladium-gallium complex **25** by self-assembly. The complex **25** was fully characterized by ^{31}P, ^{1}H NMR, elemental analysis, electron spray ionization mass spectrometry, and a single crystal X-ray diffraction study. A very unique feature of the complex is the presence of μ_2-bridging oxygen atoms. It has been found that the complex **25** is the first palladium-gallium hetero-dinuclear complex with penta-coordinate square-pyramidal gallium, and it is believed that the ligand design is crucial for this special assembly.

4.2.2. Syntheses and characterization of self-assembled palladium–bis {diphenyl- (benzo-[1, 3]-μ-oxo-k-oxo-4-ylmethyl) phosphane)}-tin complexes:

In section 4.2.1, it was illustrated that ligand **9b** allows to produce a dinuclear palladium-gallium complex **25** in one straightforward step by self-assembly. It was envisioned that expanding a similar strategy to group 14 elements may provide more insight and may allow to study the effect of variation in the coordination geometry of the template center on the P-M-P bite angle in the product. Tin, principally larger than gallium and an important component of many catalytic reactions, was explored. Stille coupling is an effective cross-coupling reaction where an alkenyl tin compound undergoes coupling with a wide variety of organic halides in presence of a palladium catalyst.[107]

Mixing of 3-[(Diphenylphosphanyl) methyl] benzene-1, 2-diol (**9b**), tin tetrachloride, cyclooctadiene palladium dichloride and triethyl amine in a 2:1:1:2.5 ratio in 20 ml of dry dimethyl formamide and stirring the solution for 24 hours at room temperature produced a red suspension which was filtered through celite. The filtrate was evaporated in vacuum and the residue washed with dichloromethane and dissolved in little DMF. The same volume of dichloromethane and finally small portions of diethyl ether were added until a precipitate began to form. The mixture was stored over night at 4ºC to yield a microcrystalline solid which was collected by filtration and dried in vacuum for four hours at 70ºC to yield 40% of a red powder, melting at 214ºC (dec.). The powder was characterized as complex **26a** by means of spectroscopic data, analytical data, and a single

[107] a) S. Casson, P. Kocienski, *J. Chem. Soc. , Perkin Trans. 1* **1994**,1187, b) T. Takeda, Y. Kbasawa, T. Fujiwara, *Tetrahedron*, **1995**, 51, 2515.

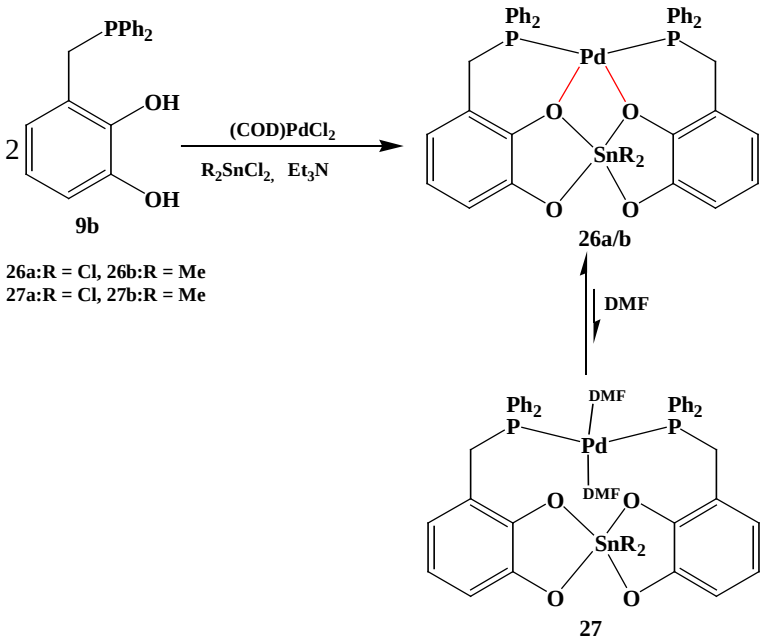

Scheme 4.2: Syntheses of palladium-tin complexes (26a/b) of ditopic catechol phosphine 9b.

crystal X-ray diffraction study. In an attempt to improve the yield, above reaction was repeated at 60ºC, and complex **26a** was isolated in 60% yield. It is interesting to note that complex **26a** was obtained even in the presence of an excess of ligand **9b,** suggesting that displacement of the chlorine atoms on tin by a third catechol phosphine ligand was unfeasible.

The ^{31}P NMR spectrum of the isolated compound at 30ºC in DMF-d_7 displayed a single broad resonance at 76.4 ppm. The considerable down field shift is similar as in **25**. The ^{1}H NMR spectra at 30ºC displayed broad signals with similar chemical shifts as the free ligand. The ^{119}Sn NMR signal was unobservable owing to the low solubility of the complex. Cooling down the sample to –30ºC eventually sharpened the ^{31}P NMR signal, and at the same time ^{1}H NMR resonances decoalesced into two sets of signals, indicating that the methylene groups and phenyl protons of Ph_2PCH_2 moieties become chemically equivalent.

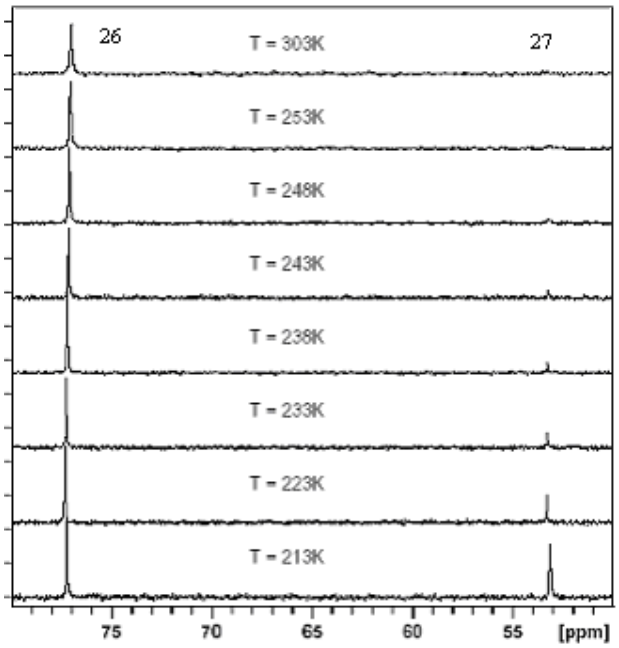

Fig. 4.3: $^{31}P\{^{1}H\}$ NMR spectra of 26/27 recorded between +30ºC and –60ºC.

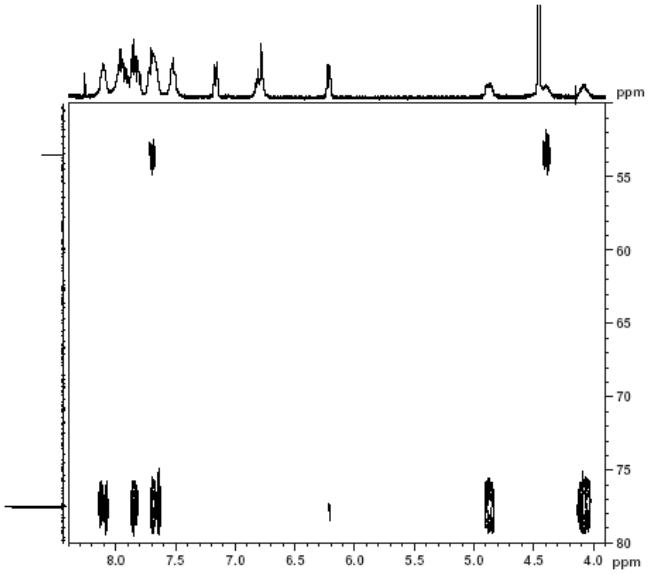

Fig. 4.4: ^{1}H, ^{31}P-HMQC (in DMF-d7) spectra of 26a/27a at –50ºC showing correlation between two sets of signals.

Surprisingly, cooling the sample below –30ºC resulted in the appearance of a new ^{31}P resonance at 55.5 ppm, which grew in intensity upon cooling to –55ºC (**see fig. 4.3**). All the changes were reversible upon warming up to ambient temperature. The above observations revealed that there should be two products **26a** and **27a**, which are in equilibrium at room temperature and give rise to separate signals at lower temperatures

which are according to 2D ^{31}P EXSY spectra still in dynamic exchange. Assignments of the ^{1}H NMR signals of the second product from 2D NMR spectra (see **Fig. 4.4**) reveals the methylene protons and phenyl groups in the CH_2PPh_2 fragment to remain chemically equivalent. The exchange can be described as pseudo-unimolecular reaction between **26a** and a second compound **27a**, and evaluation of the temperature dependence of the equilibrium constant K = **[27a]/[26a]** yielded values of ΔH = -5.4 kcal/mol and ΔS = -26 kcal/mol. The observed dynamic phenomena can be interpreted by assuming that **27a** arises from coordination of extra solvent molecules to **26a** in a process which is favored by enthalpy and disfavored by entropy.

The isolated compound was sparingly soluble in $CDCl_3$. The ^{31}P NMR spectrum at room temperature in $CDCl_3$ displayed two doublets (AB spin system) at 71.3 and 64.5 ppm with a $^{2}J_{P\text{-}P}$ coupling constant of 27 Hz each. Presumably, the observed compound is a C1 symmetric isomer of **26a** where the phosphorus atoms are inequivalent (an inherent property of C1 symmetry) and thus display an AB spin system. Details on the stereochemistry of complex **26a** will be discussed in chapter 5.

Crystals of the product suitable for single crystal X-ray measurements were grown in DMF: CH_2Cl_2 (8:2) at +4ºC. The crystals contain a discrete complex **26a** that lies on the crystallographic C2 axis in a monoclinic unit cell (space group $P_{2/c}$) (**Scheme 4.2** and **Fig. 4.5**). Further three solvent (CH_2Cl_2) molecules per molecule of complex were found in the asymmetric unit of the unit cell. The **26a** molecules are linked together via a weak hydrogen bond between a chloride on tin and the CH_2 hydrogen of a neighboring complex forming a chain. The tin atom features a distorted octahedral geometry being coordinated by the four oxygens of two chelating catechols and two chloride atoms. Three catechol oxygens (O1/2/2') and one chloride lie in the same plane as the tin atom forming a rectangle, and the remaining oxygen and chloride are positioned axially. The oxygen atoms O1/O1'act as μ_2-briding ligands towards tin and palladium, with the bridging Sn-O1 bonds being distinctly longer (2.17 Å) than the terminal Sn-O2 bonds (2.03 Å) (see **fig. 4.5**). Further, the terminal Sn-O bond distances are in fair accordance with literature reported values (2.05 Å).[87] The formation of two five membered rings and a four membered ring around tin is presumably responsible for the substantial bond angle distortion at tin (smallest O1'-Sn-O1 = 73.5º).

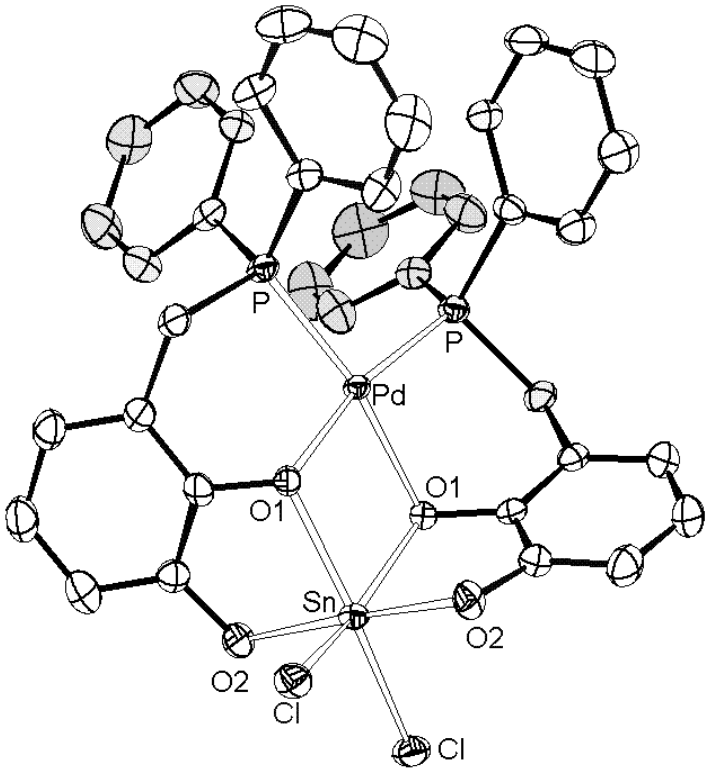

Bond lenghts Å	Bond angles [°]	Bond angles [°]
O1-Sn 2.171(2)	O1-Sn-O2 79.08(1)	P-Pd-P'98.79(1)
O2-Sn 2.033(3)	O1-Sn-O1'73.52(1)	
Cl-Sn 2.391(1)	O1-Pd-O1'76.96(1)	
O1-Pd 2.088(2)	Cl-Sn-O2 91.46(1)	
P1-Pd 2.251(3)	Cl-Sn-Cl'104.28(5)	

Fig. 4.5: Molecular structure of complex 26a (H-atoms omitted for clarity, 50% thermal ellipsoids), bond lengths in Å and angles in [°] are given in the table.

The palladium atom displays a square planar geometry with the two bridging oxygens and two phosphines completing the coordination sphere. The phosphine donors exhibit a *cis*-arrangement with a normal P-Pd bond length of 2.25 Å, whereas the bond angles deviate from the ideal angle of 90° with a very acute O1-Pd-O1' angle of 76.9° and a larger P1-Pd-P2 angle of 98.8°, probably due to the SnO_2Pd ring constraints. Of particular interest is the Pd- O1/O1' distance of 2.08 Å which is considerably larger than observed in the P- μ_1-O distances in chelate complexes (Pd-O 1.92 Å)[108] and falls into the known range for Pd-μ_2-O

[108] G. S. Ferguson, P. T. Wolczanskl, *Organometallics*, **1985**, 4, 1601.

bonds (2.02-2.17 Å).[109] The constraints of the polycyclic structure inflict a strictly pyramidal coordination at the μ_2-briding oxygen atoms (sum of the angles 323º) with a *trans*-arrangement of the exocyclic O-C bonds at the SnO_2Pd-ring, in contrast to the planar μ_2- bridging O-atoms in phenoxide or alkoxides. The above facts allow to conclude that the assembling of the complex goes along with the build-up of a certain ring strain. As expected, the increase in the size of the template center as compared to the gallium template in complex **25** results in a decrease of the bite angle: the gallium centered assembly **25** gave a bite angle of 101.7º, whereas in the tin centered assembly the bite angle decreases to 98.8º.

In order to obtain further details, solid state NMR experiments were carried out. The $^{31}P\{^1H\}$ CP-MAS spectrum displays two resonances at δ_{iso} = 79.5 and 74.1 with a $^2J_{PP}$ coupling of 41 Hz (from *J*-resolved 2D spctra), clearly indicating the presence of a AB spin system with two inequivalent phosphorus atoms. A likely explanation for this observation is that **26a** x DMF forms a pseudo-polymorph to the dichloromethane solvate that was characterized by X-ray diffraction, and that the crystallographic equivalence between the phosphorus atoms in the former is lost. The ^{119}Sn CP-MAS NMR spectrum of the solid sample shows a isotropic line at δ_{iso} = -455, indicating the presence of only one type of tin center. Thus, the above CP-MAS measurements allow to state that the second species observed in solution (**27a**) is not present in the solid state.

After knowing that **27a** exists only in solution, it was of further interest to decide if the new donors in **27a** bind preferably to tin or to palladium. In order to model the interaction of **26a** with formamide in gas phase, DFT calculations were performed with the B3LYP functional. Energy optimization of **26a** and of two different adducts with two molecules of formamide were carried out using a 3-21g* basic set. The relative energies E_{rel} of both adducts were obtained by computing the energy optimized molecular structure of formamide at the same level of theory and evaluating the difference, $\mathbf{E_{rel}}$ = E (adduct) – E (**26a**) – 2E (Formamide).

[109] J. S. Kim, A. Sen, I. A. Guzei, L. M. Liable-sands, A. L. Rheingold, *J. Chem. Soc. Dalton Trans.* **2002**, 4726.

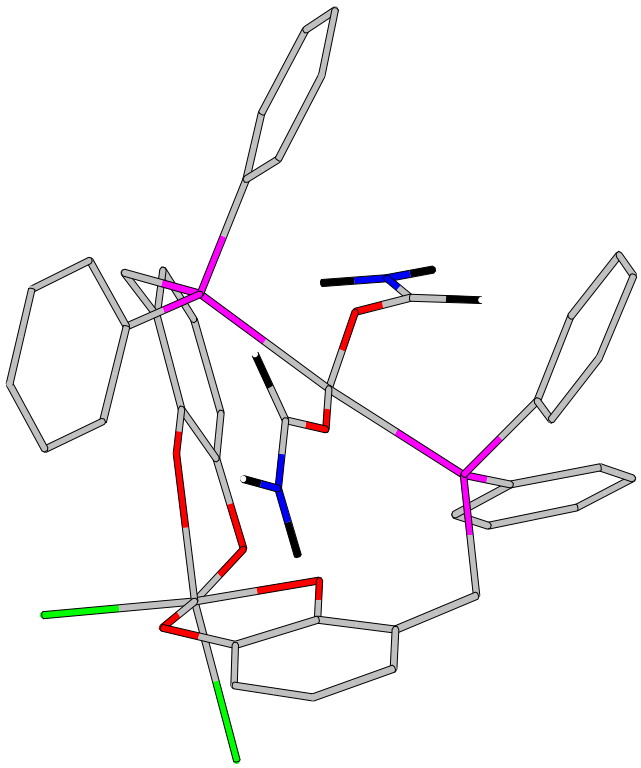

Fig. 4.14: Wire model of the energy optimized molecular structure of a solvent adduct of 26a X $2H_2NCHO$ (at the b3lyp/3-21g* level of theory).

Table 1: Relative energies in kcal/mol.

	E_{rel} (in kcal mol^{-1}):
Complex **26a** + 2 Formamide:	0.0
Complex **26a** × 2 Formamide (coordination at Pd, *trans*-isomer)	-15.0
Complex **26a** × 2 Formamide (Coordination at Sn)	-18.6

The outcome of these studies suggested that formation of a macrocyclic complex with *trans*-configuration at palladium (see fig.**4.14**) is favored by 3.6 kcal/mol over coordination of formamide to tin. Attempts to locate a structure with *trans*-coordination of the chloride ligands at tin did not lead to a minimum. Attempts to locate a complex with *cis*-coordination of the formamide ligands at palladium produced a strongly distorted structure with very low energy gradient at high relative energy. As all attempts to locate further stationary points representing complexes with *cis*-configuration at palladium or *cis/trans*-

configuration at tin on the energy hypersurface failed, it was concluded that the molecular structure displayed in fig. 4.14 is most likely to represent that of the transient complex **27a**.

Whereas all attempts to improve the yield of **26a** were unsuccessful, other tin (IV) compounds were explored in order to obtain improved yields and to reduce the reaction time. Dry DMF (20 ml) was thus added to a mixture of **9b** (2 eq.), Me_2SnCl_2 (1 eq.), $(COD)PdCl_2$ (1 eq.), and finally Et_3N (5 eq.) was injected. The reaction mixture was stirred at room temperature to give a red suspension. Monitoring the reaction by ^{31}P NMR revealed that the reaction took 3 hours for complete conversion. Dark red crystals were obtained after workup (refer to experimental details), which were dried in vacuum at 120ºC for four hours to give compound **26b** in 95% yield. The red powder melts at 310ºC and positive mode electron spray ionization mass spectrometry displayed pseudo-molecular ion peaks at m/e = 869.02 $(M+H)^+$, and 891.02 $(M+Na)^+$.

The ^{31}P NMR spectrum of **26b** at ambient temperature showed a single broad resonance at 74.6 ppm. Cooling the sample to 233K produced a very weak and broad singlet at δ = 51.6. Careful evaluation of low temperature NMR studies of solutions of **26b** suggested that similar dynamic equlibria as in the case of **26a**/**27a** are likewise present, even if the unambiguous identification of a transient species was in this case precluded due to its much lower concentration. The observation of tin satellites in the $^{31}P\{^1H\}$ NMR spectrum and a triplet in the $^{119}Sn\{^1H\}$ NMR spectrum (δ = -199.4, J_{Sn-P} = 15 Hz) disclosed that the bimetallic complex remains kinetically stable on the NMR time-scale and does not undergo ligand exchange.[111] The ^1H NMR spectrum at ambient temperature appeared very much similar to that of **26a** with an additional singlet at 0.53 ppm with $^{117/119}Sn$ satellites (J_{Sn-H} = 71 Hz) arising from the methyl protons at tin. The diastereotopic CH_2 protons were not detectable even at low temperature indicating rapid dynamic racemization of the chiral coordination environment at tin which is facilitated by the easy dissociation of the oxygen donors from palladium. A considerable down field shift (7-9 ppm) of the ^{13}C signals of the C-O carbon atoms in **26b** as compared to the free ligand **9b** indicate the coordination of the oxygen atoms to metals and thus further support the formation of complex **26b**. The methyl carbon ($SnCH_3$) on tin appeared as singlet at 25.6 ppm.

Dark red crystals suitable for a single crystal X-ray diffraction study were grown in a DMF diethyl ether mixture (1:4) at +4ºC. The discrete molecules of **26b** crystalizes in a monoclinic unit cell (space group $P2_{1/n}$) (see **fig. 4.6**) which contains further one molecule

of solvent (DMF). The crystal structure exposed similar features as that of **26a** with few differences. The Sn-C bonds are shorter than the Sn-Cl bonds, which can be attributed to the smaller covalent radius of a C as compared to Cl.

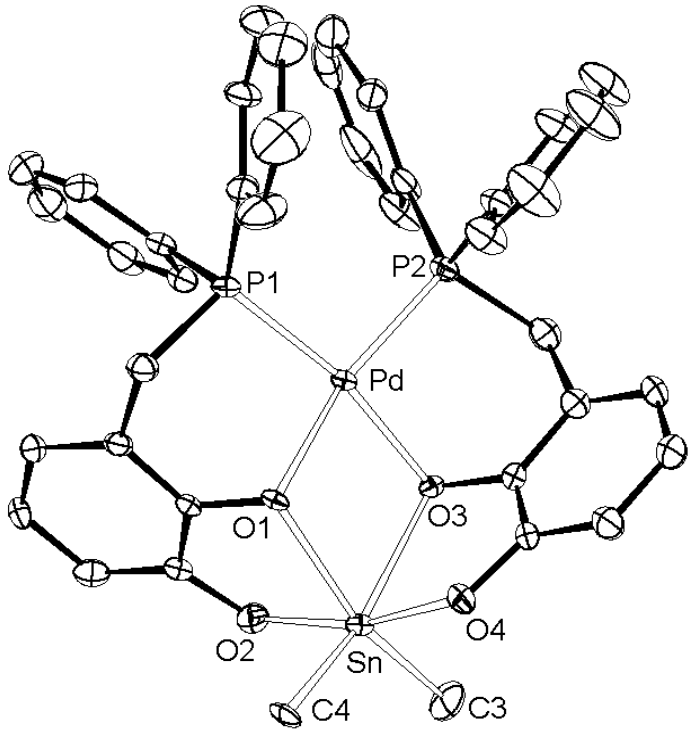

Bond lengths [Å]	Bond angles [°]	Bond angles [°]
Sn-O1 2.238(3)	O1-Sn-O2 75.59(1)	O4-Sn-C3 97.1(2)
Sn-O2 2.105(4)	O3-Sn-O4 74.93(1)	O1-Pd-O3 79.0(1)
Sn-O3 2.286(3)	O1-Sn-O3 70.83(1)	P1-Pd-O1 91.31(1)
Pd-O1 2.056(3)	O2-Sn-C4 94.73(2)	P1-Pd-P2 99.4(1)
Sn-C3 2.137(1)	C3-Sn-C4 114.2(2)	
Pd-P1 2.255(1)		
Pd-P2 2.244(1)		
Sn-C4 2.167(5)		
Sn-O4 2.103(5)		

Fig.4.6: Molecular stru.of 26b; (H-atoms omitted for simplicity, thermal ellipsoids at 50% probability) important bond distances and bond angles are given in the table.

Although the methyl groups are cis to each other, the C-Sn-C (114º) bond angle is considerably larger than the Cl-Sn-Cl (104º) angle. This observation is in accordance with Bent's rule (small bond angle are formed between electronegative ligands since the central atom to which the ligands are attached tends to direct bonding hybrid orbitals of greater p-

character towards its more electronegative substituents).[110] The presence of less electronegative substituents at tin (chlorides formally replaced by methyl groups) increases the Sn-O1/3 bond length by 0.10Å. A minor increase in bite angle (P-Pd-P) was also observed (**26a**: 98.8, **26b**: 99.4). The two catechol rings are inequivalent in the sense that one ring plane is bent towards tin by 15.5º (C11-C12-C13-C14) and the other by 12.1º (C64-C65-C66-C61). A similar deviation was also reported in $Me_2Sn(chelate)_2$ (where chelate can be picolinate or tropolonate) type complexes.[111]

In summary, it was established in this section that the flexible catechol phosphine **9b** effectively and selectively discriminates between hard and soft acids, and reacts to produce dinuclear tin-palladium complexes in good yields. Though the two complexes **26a**, **26b** appear very similar they also display a few differences which are attributable to the electronegativity difference between the methyl and chloride substituents.

4.2.3. Synthesis and characterization of a platinum -bis{diphenyl-(benzo-[1, 3]-µ-oxo-k-oxo-4-ylmethyl) phosphane)}-tin complex (28):

The two previous sections (4.2.1 and 4.2.2) demonstrated that variation in the template can have consequences on the bite angle of the ligand. Considering that alteration in the catalytic metal might shade light on further interesting aspects of the dinuclear complexes and in view of the catalytic importance of platinum,[112] a detailed investigation of platinum-tin complexes was undertaken. Reaction of 3-[(Diphenylphosphanyl) methyl] benzene-1, 2-diol (**9b**), tin tetrachloride, $LPtX_2$ (L = cyclooctadiene, bis-benzonitrile X = bromide, chloride) and triethyl amine in a 2:1:1:2.5 ratio in 20 ml of dry dimethyl formamide at room temperature produced a yellow suspension. Monitoring the reaction by ^{31}P NMR indicated completion of the reaction within 3 hours. A yellow solution was obtained after work-up which was evacuated to dryness to yield a yellow powder in almost quantitative yield. A concentrated DMF solution of the yellow residue at room temperature produced shining yellow needles, which were dried at 70ºC in vacuum for 4 hours.

[110] H. A. Bent, *Chem. Rev*. **1961**, 61, 275.
[111] C. Camacho-Camacho, R. Contreras, H. Noth, M. Bechmann, A. Sebald, W. Milius, B. Wrackmeyer, *Mag. Reson. Chem.* **2002**, 40, 31.
[112] M. Colladon, A. Scarso, G. Strukul, *Synlett.* **2006**, 20, 3515; M. V. Baker, D. H. Brown, P. V. Simpson, B. W. Skelton, A. H. White, C. C. Williams, *J. Organomet. Chem.* **2006**, 691, 26, 5845.

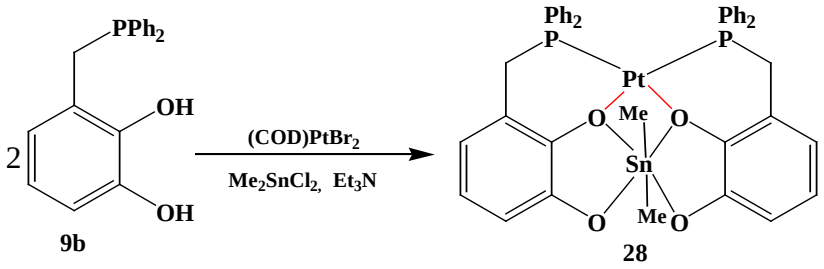

Scheme 4.3: self-assembly of 9b to dinuclear platinum-tin complex 28.

The product which was identified as compound **28** by spectral and X-ray diffraction studies melts at 354ºC and has one of the highest melting points among the series of complexes reported in this work. The ESI-MS positive mode experiment displayed two pseudo-molecular ions peaks at m/e = 957.08 $(M+H)^+$ and 979.07 $(M+Na)^+$. The ^{31}P NMR

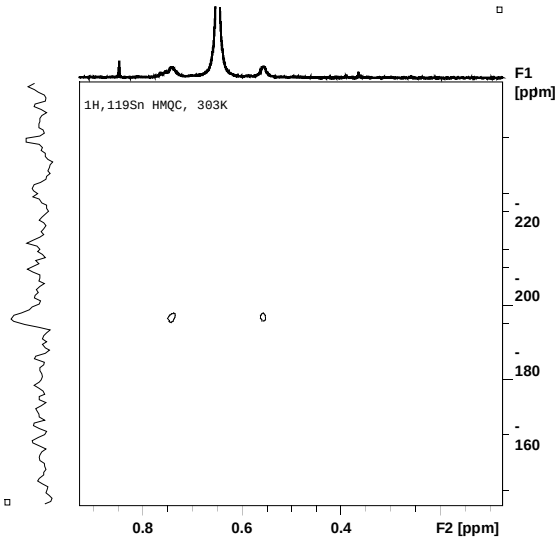

Fig.4.7: ^{1}H ^{119}Sn HMQC spectrum of **28** displaying cross peaks.

specturm of complex **28** in $CDCl_3$ at room temperature produced a singlet at 39.5 ppm with platinum satellites (J_{Pt-P} 4120 Hz), confirming the formation of only one product. The upfield shift with respect to **26a/b** is attributable to the lower coordination of shift of platinum as compared to palladium complexes. Both the ^{1}H, ^{119}Sn, HMQC (see **fig. 4.7**) and ^{119}Sn NMR spectra show a single ^{119}Sn resonance at –183.8 ppm indicating the formation of a single product. The proton NMR at room temperature in $CDCl_3$ displayed a similar signal pattern as that of **26b**, except that the methyl (CH_3) protons appeared at 0.62 ppm. Low temperature ^{1}H and ^{13}C NMR of **28** showed signal broadening, presumably due to the formation of solvent adducts.

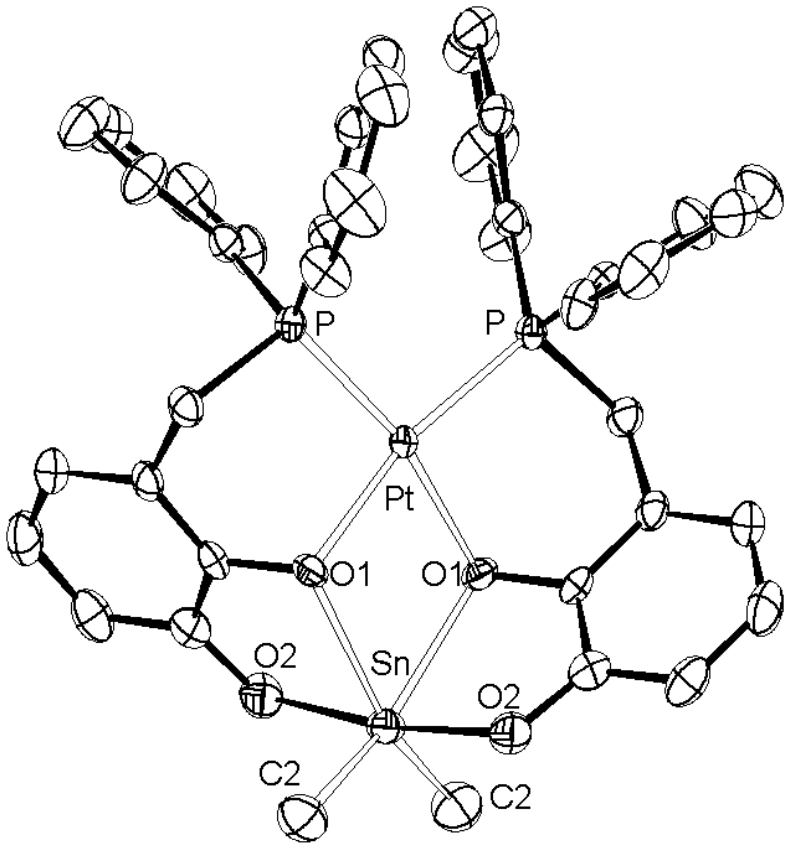

Bond lengths [Å]	Bond angles [°]
P-Pt 2.242(1)	O1-Sn-O2 74.17(4)
O1-Pt 2.064(3)	O2-Sn-C2 96.4(2)
O1-Sn 2.303(3)	C2-Sn-C2 120.0(4)
O2-Sn 2.110(4)	O1-Pt-O1 76.7(2)
C2-Sn 2.14(1)	P-Pt-P' 100.78(1)

Fig.4.8: Molecular structure of the platinum-tin complex 28. (H-atoms omitted for clarity, thermal ellipsoids at 50% probability), important bond lengths and bond angles are given in the table.

Shining yellow crystals were grown from a DMF: dichloromethane mixture at +4ºC. A single crystal X-ray diffraction study showed that the complex **28** crystalises in a monoclinic unit cell in space group $C_{2/c}$. The molecule lies on a crystallographic C2 axis (see **Fig. 4.8**). The tin atom displays octahedral geometry and the platinum atom is square planar. The observed bond lengths and bond angles closely match those found in complex **26b**, with few exceptions. Compared to **26b**, the bite angle (P-Pt-P) increases to 100.7º. The C2-Sn-C2 angle in **28** is 120.0º compared to the smaller angle of (114.2º) observed in complex **26b**. The two catecholate planes intersect at the tin center with an angle of 83.7º,

whereas in complex **26b** they intersect with a larger angle of 88.6º. These observations are attributed to the bigger size of the platinum compared to the palladium atom, which probably reduces the steric-repulsive interactions between the catechol phosphines.

In summary, the platinum-tin based heterodinuclear complex **28** was successfully synthesized in one simple step and in almost quantitative yield. Changing the transition metal center from palladium to platinum has a rather small effect on the structural properties of the complex.

4.2.4. Synthesis and characterization of a palladium- bis{diphenyl-(benzo-[1, 3]-μ-oxo-k-oxo-4-ylmethyl) phosphane)}-bismuth complex (29a):

The heavier elements of group 15 are particularly interesting as designing element in supramolecular chemistry due to the rare preference for a trigonal pyramidal coordination geometry, which is very difficult to obtain using transition metals.[113] Another aspect is their Lewis acidity, which increases markedly as one moves down the group. For example, bismuth predominantly behaves as a lewis-acid whereas the lighter nitrogen behave as base. Smith et. al. reported a penta-coordinated bismuth compounds and demonstrated the presence of a dimeric bismuth complex, which was reported as four coordinated bismuth earlier.[93] In the view of larger size, increased acidity, predefined geometry, a detailed investigation of the reaction of $BiCl_3$ with **9b** was undertaken.

The solid mixture of (COD) $PdCl_2$, $BiCl_3$ and **9b** (1:1:2, respectively) was dissolved in 8 ml of DMF, followed by addition of triethyl amine (5 eq.). Monitoring the reaction by ^{31}P NMR evidenced complete conversion of the starting material **9b** to a product **29a (**see **Scheme 4.4)** in 3 hours. The dark red product, which melted at 273ºC with decomposition, was isolated in good yield (70%) by following the standard procedure established for the previously discussed products. The ^{31}P NMR spectrum at ambient temperature in DMF-d_7 displayed two broad resonances at 70.8 and 52.1 ppm. The signal at 70.8 ppm is assigned to the complex **29a** and the resonance at 52.6 ppm is to a solvent adduct **29b** (see **scheme 4.4**) with an analogous constitution as **27a**. The ^{1}H NMR spectrum of **29b** at ambient temperature displayed similar chemical shifts as that of complex **26a**. Cooling down the sample eventually sharpened the ^{31}P and ^{1}H NMR signals of **29a** and **29b**, which were readily assigned by ^{31}P, ^{1}H HMQC and ^{1}H-COSY experiments, but the nuclei in Ph_2PCH_2

[113] W. J. Vickaryous, R. Herges, D. W. Jonson, *Angew. Chem. Int. Ed.* **2004**, 43, 5831.

moieties remained chemically equivalent, an effect that was observed in **27a** as well. The above observation revealed that there should be two products, which are in equilibrium at ambient temperature. The observed dynamic phenomena can be interpreted as pseudo-unimolecular reaction by assuming that **29b** arises from coordination of extra solvent molecules to **29a.** Electron spray ionization mass spectra in positive mode disclosed two pseudo-molecular ion peaks at m/e = 927.04 $(M\text{-}Cl)^+$, and the other at m/e = 969.03 $(M+Li)^+$ confirming the presence of a monomeric complex **29a.**[93]

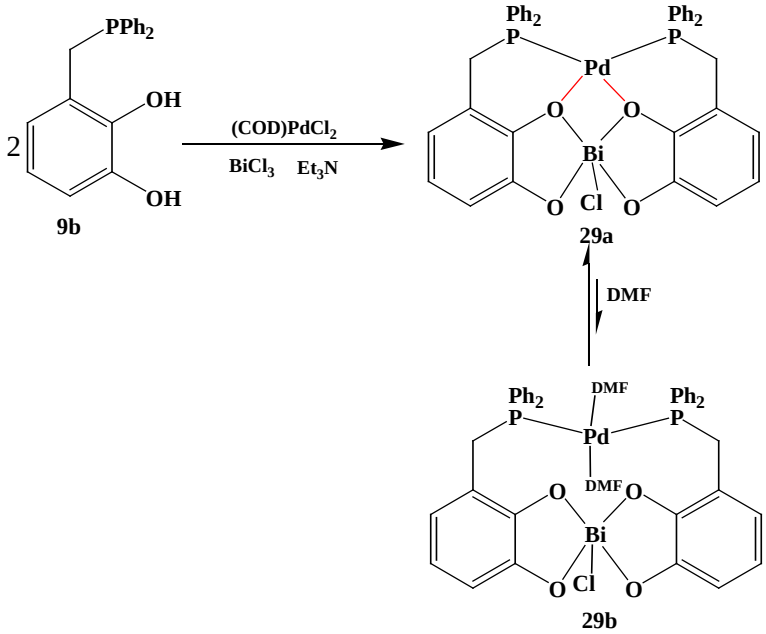

Scheme 4.4: assembling of palladium-bismuth dinuclear complex 29a.

Suitable single crystals for X-ray diffraction measurement were grown at room temperature from a concentrated dichloromethane solution. Complex **29a** crystallizes in the monoclinic crstal system in the space group $P2_{1/c}$ (see **Fig. 4.9**) with one molecule of solvent CH_2Cl_2). The solvent molecules form weak hydrogen bonds with the chloride on bismuth, and a chlorine atom in the CH_2Cl_2 molecule builds another weak hydrogen bridge to a CH_2- unit of the neighboring complex. Thus, the overall structure can be described as three-dimensional network of **29a** and solvent molecules that are held together by weak hydrogen bonds. (Surprisingly, the single-crystal X-ray diffraction study revealed that complex **29a** appears as a dimer with hexa-coordinated, strongly distorted octahedral bismuth atom. The dimer is a neutral, centrosymmetric entity with the chlorides bridging the two bismuth centers. The bridging Bi-Cl bond measures 3.30Å, indicating weak intermolecular bismuth-chloride interactions.

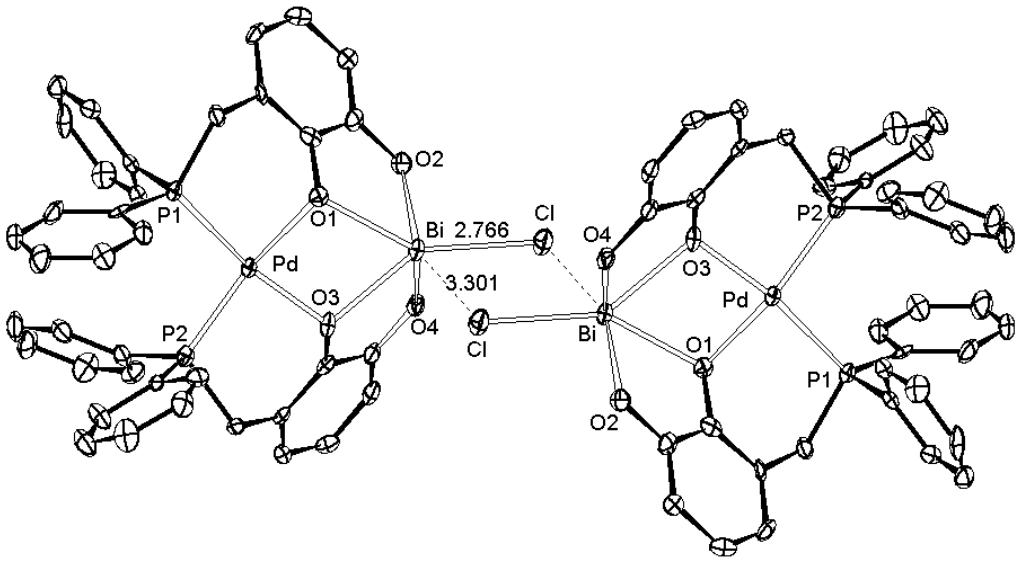

Bond lengths [Å]	Bond angles [°]	Bond angles [°]
O3-Bi 2.439(5)	O1-Bi-Cl 149.99(1)	O1-Bi-O3 66.03(2)
P1-Pd 2.256(2)	O4-Bi-Cl 83.29(2)	Bi-Cl-Bi1 102.444(2)
O2-Bi 2.175(1)	O2-Bi-Cl 89.48(1)	Cl-Bi-Cl1 77.56(2)
O3-Pd 2.089(5)	O2-Bi-O4 85.7(2)	
Cl-Bi 2.765(3)	P1-Pd-P2 97.14(5)	
μ.Cl-Bi 3.301(2)	O3-Bi-Cl 144.11(1)	

Fig. 4.9: Molecular structure of the dimeric palladium-bismuth dinuclear complex 29a. H-atoms are omitted for the clarity, thermal ellipsoids with 50% probability, important bond lengths and bond angles are given in the table.

However, in other respects, the coordination is unusual for bismuth (III), displaying a large coordination void of almost 149º, presumably occupied by the inert lone pair of electrons. Similar observation were reported by Smith et. al for a complex $\{(NH_4)_2[Bi_2(C_6H_4O_2)_4].2C_6H_4O_2.2H_2O\}$, where a third catechol ligand was found to bridge the two bismuth centers and a coordination void of 147º was observed.[93] The lone pair effect results for **29a** in a huge deviation of the O3-Bi-Cl angle (144.1º) from the ideal octahedral angle. The O2-Bi-O4 angle is 85.7º, whereas the O1-Bi-O3 angle is much smaller (66.0º). The effect of an increase in the size of the template center as compared to complex **26b** reflects on the μ_2-O-M bond lengthening so that the μ_2-O1/3-Bi bonds in **29a** are 0.26Å longer than the μ_2-O-Sn distances in **26b**. Thus, the combined effect of O1/3-Bi

bond lengthening (increases the P-Pd-P bite angle), the O1-Bi-O3 angle shortening (decreases the bite angle) and the presence of a lone pair (decreases the bite angle) is likely to be responsible for the observed overall reduction of the P1-Pd-P2 bite angle to 97.0º compared to 101.8º in the square pyramidal gallium-palladium assembly **25**. The palladium atom in **29a** displays a square planar geometry with a cisoid arrangement of the catechol phosphine moieties in the resulting planar BiO_2Pd four-membered ring, but the two BiO_2Pd units in the dimer display a trans-arrangement along the Bi-Bi axis. No metal-metal inter/intra molecular interactions were found as all distances exceeded the sum of their respective covalent radii (Bi-Bi: 4.74 Å, Pd-Bi: 3.64 Å). The dimeric structure makes the coordination at the template center very different from that of other complexes discussed so far.

In summary, a surprisingly dimeric, hexa-coordinated, palladium-bismuth complex was obtained in solid state, though the NMR and ESI-MS analysis showed a monomeric complex as the dimer presumably dissociates in solution. A large coordination void present on bismuth is assumed to be occupied by the inert lone pair.

4.2.5. Zirconium assisted synthesis of a trinuclear di-palladium zirconium complex of 3-[(Diphenylphosphanyl) methyl] benzene-1, 2-diol (30):

Detailed investigation was set to study the role of oxophilic transition metals as template centers. With respect to increasing interest in zirconium oxide materials[114] and zirconia supported palladium cross-coupling catalysts,[115] syntheses of heteromultinuclear transition metal complexes were targeted. As the group 4 metals are known to react with two or four units of a catechol to give di- or tetra-catecholato-complexes[116] it was of further interest to study the behavior of **9b**. 2 equivalents of **9b**, 1 equivalent of $(COD)PdCl_2$, 1 equivalent of $ZrCl_4$, and excess of the base Cs_2CO_3 (1.3 equiv) were dissolved in 15 ml of DMF and stirred for 6 days at room temperature. A dark red reaction mixture was formed which was filtered and taken to dryness. 5 ml each of DMF and dichloromethane was added and the solution diluted with 50 ml of diethyl ether to produce a reddish gray precipitate. The precipitate was filtered and dried in vacuum for 4 hours. The isolated powder that melts at

[114] K. G. Caulton, L. G. Hubert-Pfalzgraf. *Chem. Rev.* **1990**, 90, 969 ; C. N. R. Rao, B. Raveau, *Transition Metal Oxides*, VCH Publishers, New York, **1995**.
[115] D. Villemin, P. A. Jaffres, B. Nechab, F. Courivaud, *Tetra. Lett.* **1997**, 38(37), 6581; M. Xuebing, F. Xiangkai, *J. Mol. Cat. A: Chem*. **2004**, 208(1-2), 129; G. Potenzo, N. Cosimo-Francesco, M. Giovanni, L. G. Aldo, F. Carla, M. M. Antonietta, P. Pasquale, *J. Mol. Cat.*, **1989**, 53, 349.
[116] T. J. Boyle, L. J. Tribby, T. M. Alam, S. D. Bunge, G. P. Holland, *Polyhedron*, **2005**, 24, 1143.

390ºC with decomposition was identified as **30** (see **Scheme 4.5**) by analytical and spectroscopic studies.

The complex is insoluble even in polar solvents but was soluble in DMSO. The ^{31}P NMR spectrum recorded at ambient temperature in DMSO displayed a single resonance at 52.4 ppm, indicating phosphorus coordination to palladium. Interesting to note was the reasonably sharp ^{31}P signal at room temperature, in contrast to all previous complexes discussed so far. Likewise, the ^{1}H NMR spectrum displayed well separated phenyl proton signals at 7.5, 7.3 and 7.1 ppm, corresponding to ortho, para and meta groups respectively, The catechol ring protons could also be identified as a multiplet (6.0-6.2, m) and a doublet (5.9, $^{3}J_{HH}$ = 7.11 Hz).

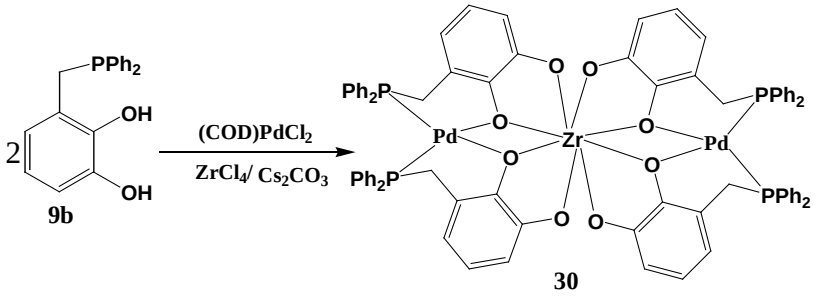

Scheme 4.5: Syntheses of trinuclear palladium-zirconium complex 30.

These spectral observations strongly suggested that the complex must be less prone to undergo addition of solvents than the previously reported complexes, where solvent adducts were easily observable. It is assumed that the extra stability of the complex may arise from the di-palladium-zirconium trinuclear complex, but further evidence was required in order to support this assumption. The positive mode ESI-MS displayed pseudo-molecular ions peaks at m/e = 1716.9 $(L_4Pd_2Zr+NaCl+Cs)^+$, 1662.17$(L_4Pd_2Zr+Cs)^+$, 1530.27 $(L_4Pd_2Zr+H)^+$, 1552.25 $(L_4Pd_2Zr+Na)^+$, 842.93 $(L_2PdZrCl)^+$, 788.01 $(L_4Pd_2Zr+2Na)^{2+}$ 777.02 $(L_4Pd_2Zr+H+Na)^{2+}$, 765.5 $(L_4Pd_2Zr+2H)^{2+}$, where is L = $C_{19}H_{15}O_2P$. The pseudo-molecular ion peak at 842.93 corresponds to a dinuclear

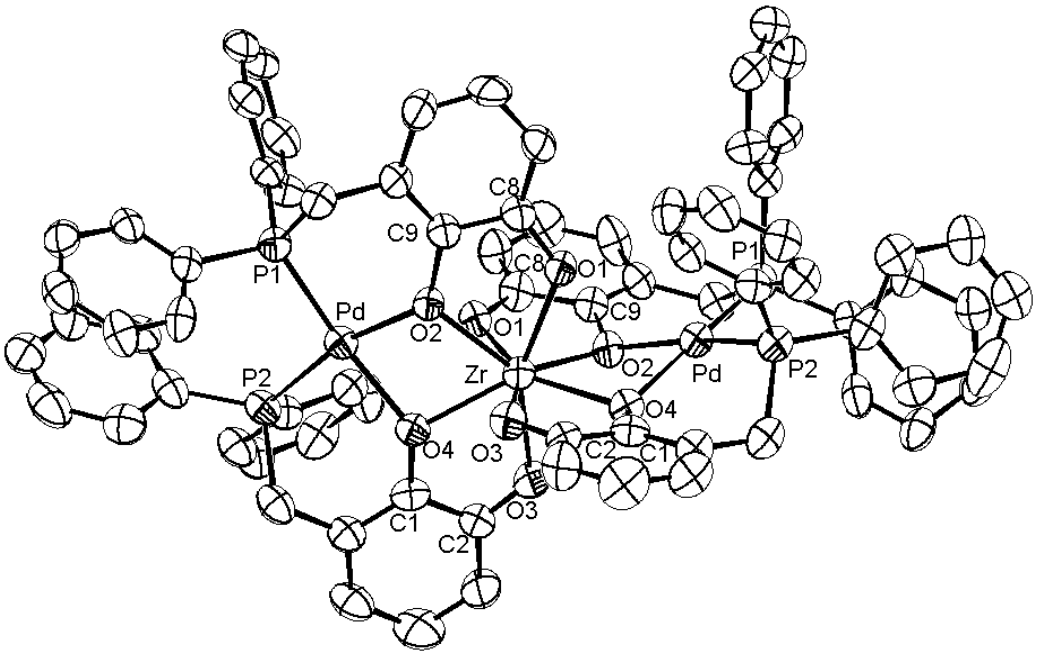

Bond lengths [Å]	Bond angles [°]
P1-Pd 2.223(1)	P1-Pd-P2 99.78(1)
O4-Pd 2.061(5)	O3-Zr-O4 70.7(1)
O2-Zr 2.296(1)	C2-O3-Zr 121.94(1)
O1-Zr 2.162(2)	C9-O2-Zr 116.92(2)
Zr-Pd 3.408(1)	O3-Zr-O4 70.80(1)
P2-Pd 2.230(1)	O1-Zr-O2 71.20(1)

.

Fig. 4.10A: Molecular structure of trinuclear palladium-zirconium complex 30 (H-atoms are ommited for clarity, thermal ellipsoids at 50% probability), important bond lengths and bond angles are given in the table.

palladium-zirconium complex. All other peaks are attributable to the tri-nuclear complex **30**. The pseudo-molecular ion peak at 1662.17 showed additional weak ^{13}C isotopic peak with a separation of 0.5 Da, which suggested the presence of a small amount of hexa-nuclear complex.

Slow evaporation of diethyl ether into the DMSO solution of **30** produced red colored needle like crystals suitable for X-ray studies. The X-ray crystal structure revealed indeed that the discrete molecules of **30** (see **Fig. 4.10A**) are formed by assembly of four catechol phosphine units around one zirconium center with two phosphines ending each on a palladium atom. The formation of this highly unexpected compound can be rationalized in

view of the size of the template, which can accommodate eight oxygen ligands and thus promotes the formation of a neutral, trinuclear complex **30**. The monoclinic unit cell (space group $C_{2/n}$) contains two molecules of solvent (DMF) per molecule of the complex. **Fig. 4.10B** illustrates that the central zirconium is octacoordinated by the catecholate oxygens and adopts a distorted square antiprismatic geometry as was observed in $[Zr(ETAM)_4]^{4-}$ (ETAM = N, N' diethyl-2,3-dihydroxyterepthalamide) by Raymond et al.[117] A closer look at the zirconium coordination sphere revealed that the four oxygen atoms (O1/2/3/4) form a square below the plane of this paper shown by dashed line in fig. 4.10B and the remaining four oxygen atoms (O1/2/3/4) forms a square above the plane of the paper shown with a continuous line in fig.4.10B. The catechol chelating ligands make

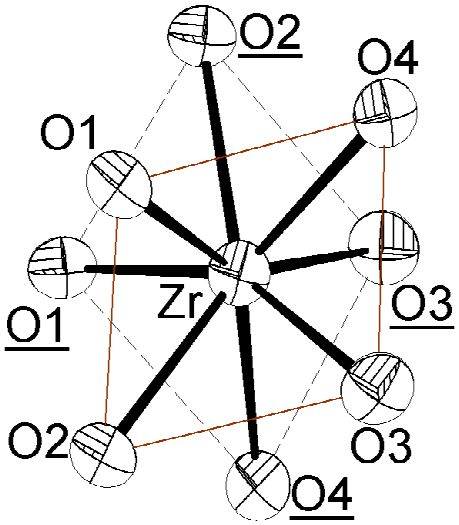

Fig. 4.10B: Closer view of zirconium coordination sphere in complex 30.

angles of 70.5-71.2º (O-Zr-O) with the central zirconium. The approach of the ligand to the zirconium center makes an angle of 116-121º between the catecholate plane(C8/9-O1/2-Zr) and zirconium with the central zirconium lying out of plane of the catechol rings by 0.17-0.26Å (e.g.O1-C8-C9-O2 x O1-Zr-O2). The bridging O-Zr bonds are approximately 0.12 Å longer than the non-bridging O-Zr bonds. The catecholic phenyl ring planes are tilted towards the central ZrO2 planes of each chelate ring by 4.4-5.5º. The two palladium atoms display a distorted square planar geometry and cap the zirconium centred ZrO8 polyhedraon. The P-Pd-P bite angle is ~99.7º, which does not differ by a significant extent from the other assemblies discussed in the present work. The bridging oxygen-

[117] C. J. Gramer, K. N. Raymond, *Inorg. Chem.* **2004**, 43, 6397.

palladium distances are between 2.05-2.06 Å. The two four membered Pd'O'2Zr vs. PdO2Zr rings intersecting at zirconium are almost perpendicular to each other with an angle of 85.8º. The Pd-Zr distance is 3.4 Å, considerably larger than the sum of covalent radii of the two atoms (2.73 Å), thus ruling out any metal-metal interaction.

In an attempt to synthesize $Cp_2Zr(catphos)_2$, 2 equivalents of **9b** (=catphos H_2), 1 equivalent of $(COD)PdCl_2$, 1 equivalent of Cp_2ZrCl_2 and excess of Et_3N (5 equiv.) were dissolved in 15 ml of DME:THF (1:1) and stirred for 2 hours at room temperature. A dark red reaction mixture was filtered and the precipitate was dissolved in THF. This was diluted by adding excess of diethyl ether, and the precipitate formed was filtered and dried in vacuum for two hours. Microcrystals of the product were obtained from THF: Et_2O solution at room temperature, which were dried in vacuum and characterized by NMR. The ^{31}P NMR spectrum displayed a very broad singlet around 50 ppm. The ^{1}H NMR in $CDCl_3$ displayed signals corresponding to catechol phosphine moiety only, no Cp proton signals were detectable. These observations ruled out formation of $Cp_2Zr(cat.phos)_2$ type complex and indicated that the product formed is presumably of similar composition as **30**. Detailed investigations are necessary in order to unambiguously assign the product.

In summary, a trimetallic dipalladium-zirconium complex was synthesized with an octa-coordinated zirconium. Interesting to note is the formation of L_4M_2M' type of assembly even when 2:1 ligand to metal (Zr) ratio was employed (i.e. less than stoichiometric amount of the ligand L). This observation underlines the basic principle of supramolecular self-assembly, which prefers the formation of a thermodynamically more stable product over stoichiometric control.

4.2.6. Stoichiometry controlled syntheses of tri- and octanuclear palladium-yttrium complexes of 3-[(Diphenylphosphanyl) methyl] benzene-1, 2-diol (31 and 32):

As lanthanides are a) oxophilic in nature and b) have found many applications in catalysis,[118] they make interesting candidates as template for catechol phosphine complexes. Yttrium was chosen for the further studies as 1) it has comparable size to Gadolinium (Gd) and 2) complexes are diamagnetic which facilitates NMR spectroscopic

[118] C. Benelli, D. Gatteschi, *Chem. Rev*. **1998**, 27, 2369; M. Shibasaki, N. Yoshikawa, *Chem. Rev*. **2002**, 102, 2187.

characterization.[119] In this respect it was worth exploring possibilities of synthesizing yttrium complexes of the catechol phosphine **9b.**

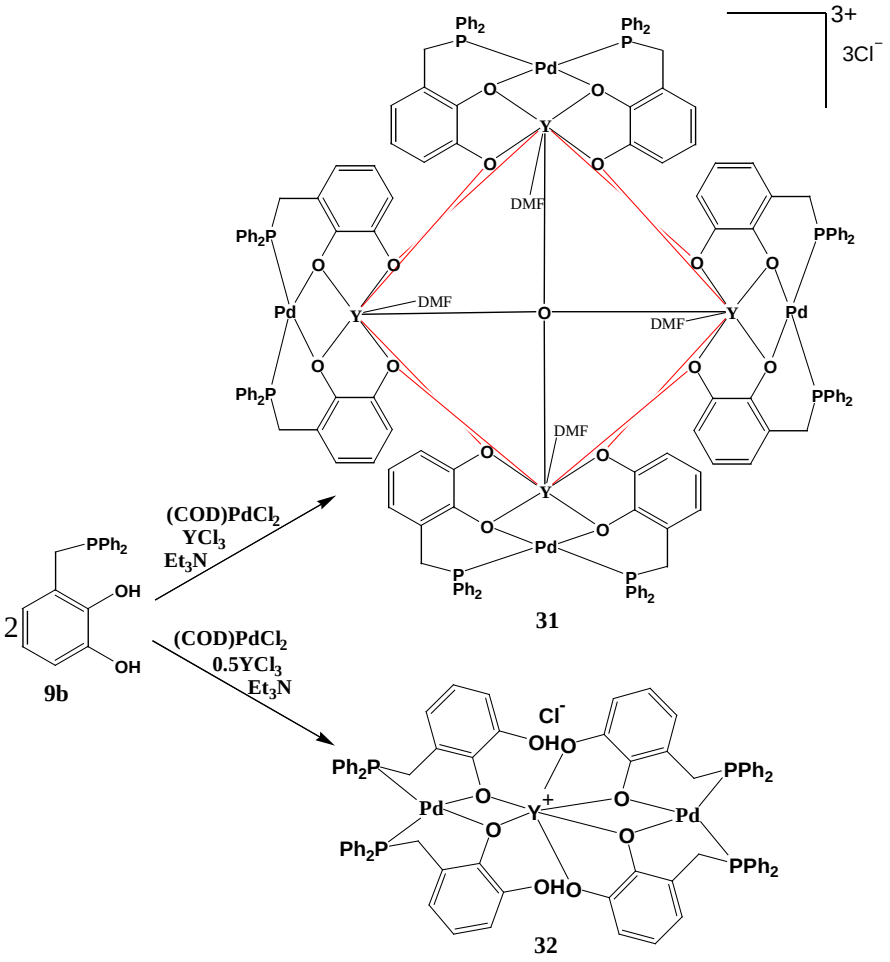

Scheme 4.6: Syntheses of octanuclear palladium-yttrium cluster 31 and trinuclear palladium yttrium complex 32.

Stoichiometric amounts of **9b**, (COD)$PdCl_2$, and YCl_3 (2:1:1 respectively) were dissolved in DMF and excess of triethyl amine was added. A dark red suspension was obtained after 3 hours of stirring at room temperature. The suspension was filtered and kept at –28ºC overnight. A white precipitate of triethyl ammonium chloride was separated by decantation and the filtrate was evaporated to dryness in vacuum. Finally, the residue was dried at 120ºC for 4 hours to obtain a red powder in good yield (60%). The red powder decomposes at 345ºC.

[119] P. W. Roesky, G. Canseco-Melchor, A. Zulys, *Chem. Commun*. **2004**, 738.

The ^{31}P NMR spectrum of the isolated product at ambient temperature in $CDCl_3$ displayed a single resonance at 69.7 ppm. A proton NMR spectrum similarly displayed a single set of aromatic protons but the aliphatic diastereotopic CH_2 protons are split into two groups and appear as broad doublets at 4.2-4.0 and 2.3-2.9 ppm. Solvent (DMF) signals were also observed. The NMR data are thus compatible with the presence of a bimetallic complex showing coordination of the phosphorus atoms of the catechol phosphine to the palladium metal and the oxygen atoms to the yttrium. The electron spray ionization spectra revealed the presence of a huge cluster molecule of composition $[C_{152}H_{120}O_{16}P_8Pd_4Y_4]^{3+}$, a tetranuclear cation with one excess oxygen atom, presumably an oxygen centered cluster. Three chlorides can be added to obtain a neutral species, which is compatible with the analytical data.

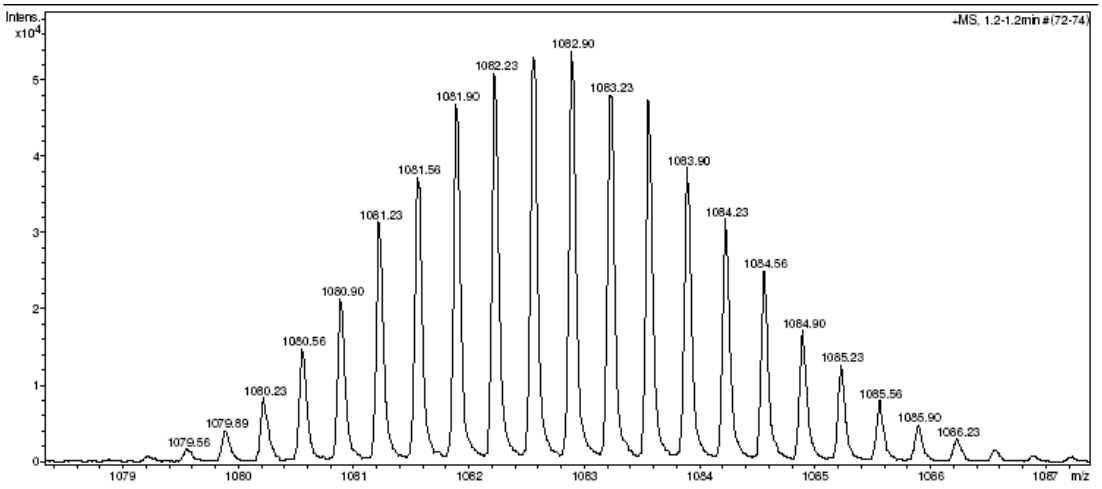

Fig. 4.11: ^{13}C isotopic splitting of a triply charged species of 31.

The positive mode spectrum displayed a triply charged pseudo-molecular ion peak at m/e = 1082.7 $(L_8Pd_4Y_4+OH)^{3+}$ (where L = $C_{19}H_{15}O_2P$) (see **Fig. 4.11**). Another peak at m/e = 1646.8 $(L_8Pd_4Y_4+OH+LiF_2)^{2+}$, with a ^{13}C isotopic splitting of 0.5 Da certainly indicating a doubly charged ion, was observed. Though the source of LiF cannot be stated, it might come from the impurities in the solvent used, or the glass tube, or as an impurity in the spectrometer itself. Nevertheless, ESI-MS observation can be very well correlated with the crystal structure data discussed below, allowing to assign the product as **31**.

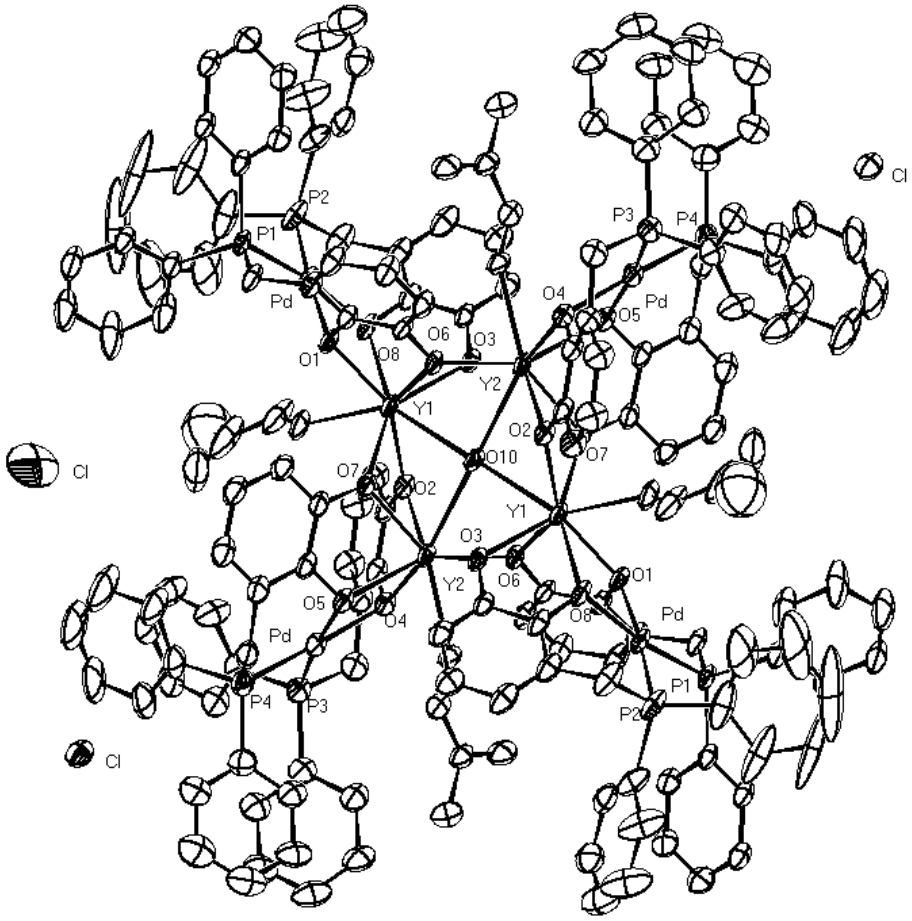

Bond lengths [Å]	Bond angles [º]	Bond angles [º]
O(1-8)-Y(1-4) 2.28-2.35	P1/3-Pd-P2/4 97.33-97.69	Y-O10-Y ~89.8-90.1
O10-Y(1-4) 2.46-2.47	Y1/1'-O10-Y2/2' 90	O2-Y2-O4 69.66(1)
O1/8/4/5-Pd1/2 2.07-2.09	O1-Y1-O6 68.7 (1)	O1-Y1-O6 68.68(2)
P(1-4)-Pd(1/2) 2.23-2.24	Y1-O3-Y2 97.0	

Fig. 4.12: Molecular structure of the octanuclear palladium-yttrium cluster 31 (H-atoms are omitted for clarity, thermal ellipsoids at 50% probability), important bond lengths and bond angles are given in the table.

The formation of a complex [**31]Cl$_3$** was unambiguously ascertained by single crystal X-ray diffraction study. Suitable triclinic crystals (space group P1 bar) were grown from a concentrated DMF solution at room temperature. The data revealed that, complex [**31]Cl$_3$** crystallizes together with four uncoordinated solvent (DMF) molecules that were found to be trapped in the periphery. The whole cluster **31** comprises four dinuclear subunits, each formed by two catechol phosphine units, an yttrium atom and a palladium atom. The four subunits are arranged around a central μ_4- bridging hydroxide anion. The central oxygen,

the yttrium atoms, and the peripheral palladium atoms are coplanar with the catechol phosphines in each subunit being stapled on each other. All together the molecule **31** is cationic, and three chlorides balance the charges to produce a neutral cluster **[31]Cl_3**. Though the source of hydroxide cannot be firmly named, the product can be considered as arising from partial hydrolysis, with the water originating from DMF or an impurity in YCl_3, and its presence seems to be necessary in order for the structure to be stable. The central μ_4- bridging oxygen atom displays a perfect square planar geometry with Y- μ_4O-Y angles of 89.8-90.1º and Y-O distances of ~2.4 Å. The unusual geometry of the central oxygen and the bond distance found are very commonly observed in oxygen bridged yttrium compounds.[120] Each yttrium atom in **31** displays a square antiprismatic arrangement and coordinates to four catechol oxygens, two oxygens from neighboring units, one solvent molecule, and the central oxygen atom. The catechol chelates form (O-Y-O) angles of 68.6-69.5º, which are the smallest catechol-chelating angles observed so for in this chapter. The increased steric crowding around yttrium is likely to be responsible for the reduced angles observed. The Y-Y distances are found to be ~ 3.48 Å, and the Y- μ_2O distances are 2.28-2.34 Å, which falls in the literature reported range (2.27-2.57 Å).[121] All four palladium atoms display square planar geometry with two sites occupied by bridging oxygens and two phosphorus atoms completing the coordination sphere with a normal Pd-P distance of 2.23-2.24 Å. The Pd- μ_2O distances are 2.07-2.09 Å and the P-Pd-P bite angle is found to be 97.3-97.6º, which is lower than that in zirconium complex (99.7º) but is nearly equivalent to that found in the dimeric bismuth complex **29** (97.0º).

Rational evaluation of the above facts suggested that one yttrium atom should also be able to accommodate four catechol phosphine ligands and might then form similar assemblies as complex **30**. The prerequisite for such a complex could be use of the starting materials in appropriate stoichiometry and strict exclusion of water. In an attempt to prove this hypothesis, four equivalents of the catechol phosphine were treated with one equivalent of yttrium trichloride and two equivalents of cyclooctadiene palladium dichloride. The reaction was carried in a similar manner as the synthesis of **31**. The isolated crude product was dissolved in little DMF, and diethyl ether was added dropwise until a precipitate

[120] P. Miele, J. D. Foulon, N. Hovnanian, L. Cot, *J. Chem. Soc. Chem. Commun.* **1993**, 29; B. A. Vaartstra, J. C. Huffman, W. E. Streib, K. G. Caulton, *J. Chem. Soc. Chem. Commun.***1990**, 1750; O. Poncelet, W. J. Sartain, L. G. Hubert-Pfalzgarf, K. Folting, K. G. Caulton, *Inorg. Chem*. **1989**, 28, 263.
[121] W. J. Evans, M. S. Sollberger, *J. Am. Chem. Soc*. **1986**, 108, 6095; M. R. Buergstein, P. W. Roeky, *Angew .Chem. Int. Ed*. **2000**, 39, 549.

started to form. An extra drop of DMF was added and the Schlenk tube kept for crystallization at room temperature. This procedure afforded a dark red powder which was dried at 70ºC for 4 hours and which melts at 197ºC.

The ^{31}P NMR spectrum in $CDCl_3$ at room temperature produced two broad resonances at 70.8 and 60 ppm. The ^{1}H NMR spectrum displayed two sets of well-separated catechol protons at 6.25, 6.17, 6.0, 5.93, 5.85, 5.7 and 5.6 ppm. Hydroxy protons were also detectable and appeared as broad singlet at 7.65 ppm, and the phenyl groups appeared as multiplet at 7.5-6.6 ppm. The aliphatic protons produced two broad doublets at 3.8-3.6 and 3.2-3.0 ppm. The ^{31}P and ^{1}H NMR signals of **32** were readily assigned by ^{31}P, ^{1}H HMQC

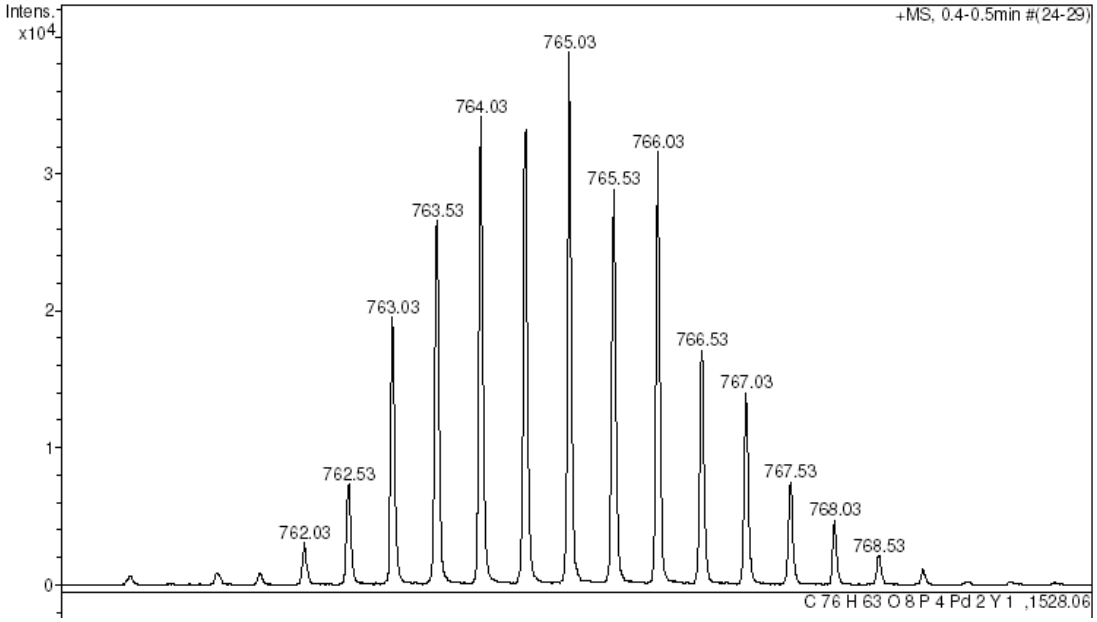

Fig. 4.13: Positive mod e ESI-MS ^{13}C isotopic splitting of a doubly charged species of 32.

and ^{1}H-COSY experiments. The above NMR observations indicated the presence of two different coordination modes of the catechol phosphines. The presence of free hydroxy groups indicated that the coordination of catecholate moieties to yttrium remained incomplete, thus displaying separate set of ^{31}P and ^{1}H NMR signals.

Positive mode ESI-MS spectra displayed two pseudo-molecular ion peaks at m/e = 1529.06, 765.1, which corresponds to ions of composition $[L_4Pd_2YCl+2H]^+$ and $[L_4Pd_2YCl+3H]^{2+}$ respectively. Further pseudo-molecular ion peaks were observed at m/e 776.05, 786.01, 743.07 and 510.35, corresponding ions of composition $[L_4Pd_2YCl+2H+Na]^{2+}$, $[L_4Pd_2YCl+H+2Na]^{2+}$, $(L_2Pd+2H+Na)^+$ and $[L_4Pd_2YCl+4H]^{3+}$

respectively, where L = $C_{19}H_{15}O_2P$. A pseudo-molecular ion peak at 1529.06 can be well assigned to $(M\text{-}Cl)^+$, where M = **32**. The second peak is a doubly charged pseudo-molecular ion peak at 765.1 $(M\text{-}Cl+H)^{2+}$ with an ^{13}C isotopic splitting of 0.5 Da. (see **fig. 4.13**). Other species observed at 776.05, 786.01 can be assigned to $(M\text{-}Cl+Na)^{2+}$, $(M\text{-}HCl+2Na)^{2+}$ respectively and a triply charged species at m/e 510.35 to $(M\text{-}Cl+2H)^{3+}$. The ESI-MS negative mode experiment displayed two pseudo-molecular ion peaks at m/e 1527 with the composition $[C_{76}H_{62}ClO_8P_4Pd_2Y\text{-}2H]^-$ that can be assigned for $(M\text{-}Cl\text{-}2H)^-$ and another at 719 $(C_{38}H_{32}O_4P_2Pd_1\text{-}H)^-$.

The formation of a complex **32** was unambiguously ascertained by a single crystal X-ray diffraction study. Suitable crystals were grown from a DMF diethyl ether (1:1) mixture at room temperature. The monoclinic unit cell (space group $P2_{1/n}$) contains three molecules of solvent (DMF) per molecule of the complex. One of the solvent molecules is coordinating to the central yttrium via oxygen donor, the other forms a hydrogen bridge with the chloride anion, and the third is trapped in the periphery of the complex. The X-ray crystal structure revealed indeed that the discrete molecule of **32** (see **Fig. 4.15**) is formed by assembly of two inequivalent (independent) catechol phosphine-palladium blocks around one yttrium center. The complex is a zwitterionic species with the chloride balancing the charge to produce neutral **32**. The chloride forms a hydrogen bridge with one of the catecholic hydroxides (H40-Cl 2.17 Å). The central yttrium atom displays a distorted antiprismatic geometry and is coordinated to eight oxygen ligands. In contrast to the zirconium complex **30,** only seven of the catechol oxygens are coordinated to the yttrium and the coordination sphere is completed by one molecule of DMF. The catechol chelating angles (O-Y-O: 68.2-69.0º) are similar to those in **31**. The non-bridging Y-O bonds are shorter (2.28-2.30 Å) than the bridging yttrium oxygen (2.35-2.37 Å) bonds. The oxygen atom O40 that carries a proton is very weakly coordinating to the yttrium and displays the longest Y-O distance of 2.44 Å observed in **32**. The palladium atoms display a distorted square planar geometry with very different P-Pd-P bite

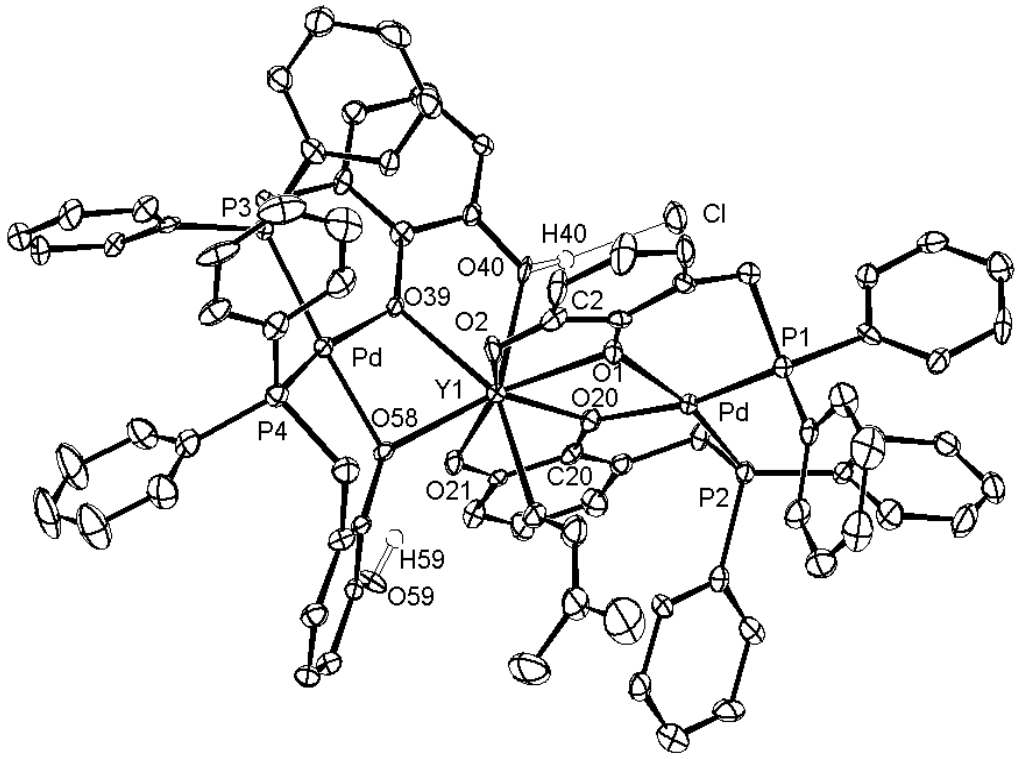

Bond lengths [Å]	Bond angles [º]
Y-O1D 2.346(4)	P1-Pd1-P2 102.6(1)
Y-O40 2.435(5)	P3-Pd2-P4 98.55(1)
Y-O21 2.281(4)	O20-Y-O21 68.4(1)
Y-O20 2.358(4)	O1-Y-O2 69.19(1)
Y-O2 2.307(4)	
Y-O39 2.371(4)	
H40-Cl 2.176(3)	

Fig. 4.15: Molecular structure of palladium-yttrium complex 32 (H-atoms except H59 & H40 are omitted for clarity, thermal ellipsoids at 50% probability), important bond lengths and bond angles are given in the table.

angles. The first block displays a considerably small P3-Pd2-P4 angle of 98.5º which can be attributed to the fact that the free and weakly coordinating hydroxy groups enable the phosphorus donors to come closer and thus reduce the bite angle. The other block displays a P1-Pd1-P2 angle of 102.6º. The two four membered YO_2Pd rings with a common yttrium are almost perpendicular to each other (interplanar angle of 83.8º). The formation of **32** can be attributed to the oxophilicity and the size of the template, which can

accommodate eight oxygen ligands and thus promotes the formation of a trinuclear complex.

In summary, an octanuclear palladium-yttrium cluster **31** stabilized on a central μ_4-oxygen atom was produced when **9b**:$LPdX_2$:YX_3 [L = (COD), X = Cl] were employed in 2:1:1 ratio. The cluster **31** displayed a P-Pd-P bite angle of 97º, which is smallest among all complexes discussed in this chapter. Except the central one, all oxygen atoms are μ_2-bridged and are equidistant from the metals and could not be differentiated as terminal and bridging ones, as in other complexes. Changing the ratio of **9b**:$LPdX_2$:YX_3 to 4:2:1 gave a trinuclear dipalladium-yttrium complex **32**. Interestingly, complex **32** is zwitterionic in contrast to the all other reported complexes in this chapter being neutral.

4.3. Investigations on the catalytic behavior of selected metal complexes:

In section 4.2.2 the occurrence of equilibrium reactions illustrated in **Scheme 4.7** was confirmed. The DFT calculation performed at the B3LYP/3-21g* level of theory suggested that formation of a macrocyclic complex with *trans*-configuration at palladium (see fig.**4.14**) is favored by 3.6 kcal/mol over coordination of formamide to tin. The outcome of these studies lead to conclude that the found molecular structure is most likely to represent that of the transient complex **27a**.

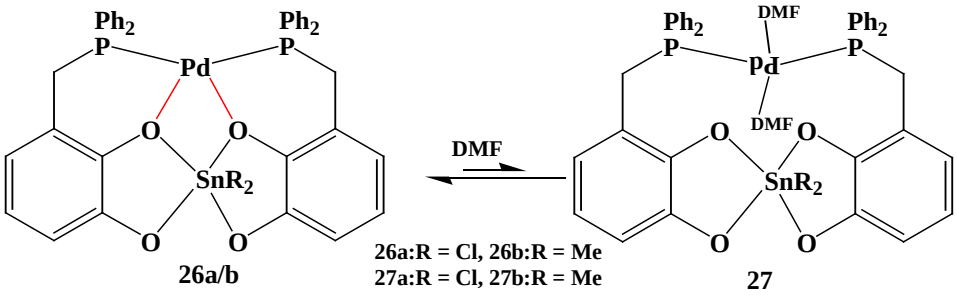

Scheme 4.7: Equilibrium reactions demonstrating hemilabile behavior of complexes 26a/b.

In view of the easy displacement of catechol oxygens from palladium, the complexes **26a/b** can be seen as palladium complexes with a hemilabile ligand that can switch between tetradentate O_2P_2- and bidentate P_2- coordination. Easy replacement of the solvent molecules by other donors is very much expected, and hence a similar catalytic activity as

for other palladium-phosphines complexes is anticipated.[122] Palladium complexes are effective catalysts in the coupling reaction between terminal alkynes and aryl halides (Sonogashira coupling).[123] A palladium bis-catechol phosphine complex similar to that of **26a** was recently employed in Sonogashira coupling reaction.[124] In order to demonstrate the potential of **26a** in catalysis, the Sonogashira[125] C-C coupling reaction was selected as a model reaction for further catalytic investigations.

Phenyl acetylene (0.44 mmol), copper iodide (0.056 mmol) and 3 mol% of **26a** (0.033 mmol) were added to a solution of 4-iodonitro-benzene (0.44 mmol) in 15 ml of triethyl amine/DMF (2:1). The mixture was stirred for 20 hours at room temperature. n-Hexane (20 ml) was then added and the precipitate filtered off. The filtrate was evaporated to dryness and the dark solid was purified by column chromatography using neutral silica as stationary phase and dichloromethane/hexane as eluent to give 94% of the coupled product 4-nitrophenyl-phenylacetylene (See **Scheme 4.8**). The isolated product was characterized by ^{1}H NMR.

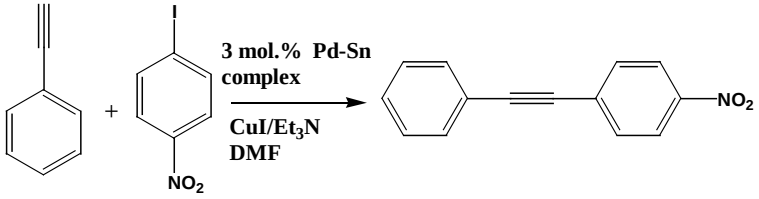

Scheme 4.8: Coupling of phenylacetylene to 4-iodonitro benzene with 26a/b as pre-catalyst

The corresponding reaction using **26b** as pre-catalyst was performed under identical conditions. In order to monitor the status of the reaction, ^{31}P NMR spectra were recorded after 1, 5 and 20 hours. All spectra displayed a single resonance at 76 ppm, confirming that **26b** remained intact during the reaction. After 24 hours, all volatiles were evaporated in vacuum. The residue was extracted with 10 ml of toluene. The suspension formed was allowed to settle for 15 minutes and the supernant toluene layer was decanted. The filtrate was evaporated to dryness and the dark solid was purified by column chromatography using neutral silica as stationary phase and dichloromethane/hexane as eluent to give 90% of the coupled product 4-nitrophenyl-phenylacetylene. The residue was dried in vacuum

[122] S. Braese, A. de Meijere, *Metal-catalyzed Cross-coupling Reactions* (Hrsg. F. Diederich, P. J. Stang), Wiley-VCH, Weinheim, **1998**, p. 99.
[123] C. C Tzschucke, C. Markert, H. Glatz, W. Bannwarth, *Angew. Chem. Int. Ed.* **2002**, 41, 4500.
[124] N. T. Lucas, A. M. McDonagh, I. G. Dance, S. B. Colbran, D. C. Craig, *Dalton Trans.* **2006**, 680.
[125] K. Sonogashira, *Compreh. Org. Synth.* **1991**, 3, 551.

and dissolved in 5 ml of DMF. The ^{31}P NMR spectrum of this solution still showed the broad signal of **26b** at 76 ppm as the only visible resonance. The residue of **26b** obtained after solvent evaporation was recovered and reused for further catalytic transformations. After the same reaction time and under same condition as the first batch the coupling product was produced in 75% yield, which was worked up according to the procedure mentioned for the first cycle. The ^{31}P NMR of the residue still showed the resonance of **26b** as the only visible product. The same cycle as above was repeated for the third time and the catalyst was reused for further transformations. Although the coupling product was observed in the proton NMR, the yield of this cycle was not determined. The above experiments clearly demonstrated the potential of **26a/b** as a C-C coupling catalyst.

4.4. Conclusions:

The syntheses of discrete di or polynuclear complexes containing hard and soft transition metal by self-assembly of simple metal precursors and bifunctional phosphine-catecholate ligands have been demonstrated. The most striking feature of the synthesized complexes is the presence of μ_2-bridging oxygen atoms which bridge the two metal centers. The coordination of the soft palladium center by μ_2-briding catecholate oxygen atoms that are easily displaced by donor solvents can be viewed in terms of hemilabile coordination. In this respect complexes **26a/b** mimic the behavior of complexes containing a supramolecular bis-phosphine ligand which is formed by the assembly of two phosphine-catecholate fragments on a main-group metal template and can switch between tetra dentate -O_2P_2 and bidentate -P_2 coordination.

The experimental findings allow to state that the coordination geometry of the template center and its size has great impact on the assembly process. A small template like gallium

Table 4.1: Template vs. properties

Template(E)	Cov.radii Å	No. Ligands	O-E termi.Å	O-E bridg.Å
Ga	1.25	5	1.898	2.027
Sn	1.4	6	2.033	2.171
Zr	1.45	8	2.145	2.273
Bi	1.52	6	2.173	2.448
Y	1.62	8	2.294	2.356

can accommodate only five donor atoms (see **table 4.1**), whereas larger templates like zirconium and yttrium can accommodate as many as eight donor atoms. In all complexes, the μ_2-briding oxygen-E bonds were found to be longer than the terminal oxygen-E bonds. The oxygen-E bond lengths (bridging and terminal) vary according to the size of the E, understandably, as the size increase the bond length increases (see **Table 4.1**). On the other hand, changing the transition metal from palladium to platinum had negligible effects on the properties of the complexes. A stoichiometry controlled synthesis of an octanuclear palladium-yttrium cluster and a tri-nuclear palladium-yttrium complex was also demonstrated.

Bite angle is an important factor in catalysis and can control regio- or stereo selectivity. Using the self-assembly tool, it was demonstrated that variable bite angles could be achieved using a single step synthetic protocol. **Diagram 4.1** shows the relation between covalent radii of group III, IV and V elements versus the P-Pd-P bite angle in the complexes **25**, **26a** and **29a** which all carry chloride substituents and hence can be rationally compared.

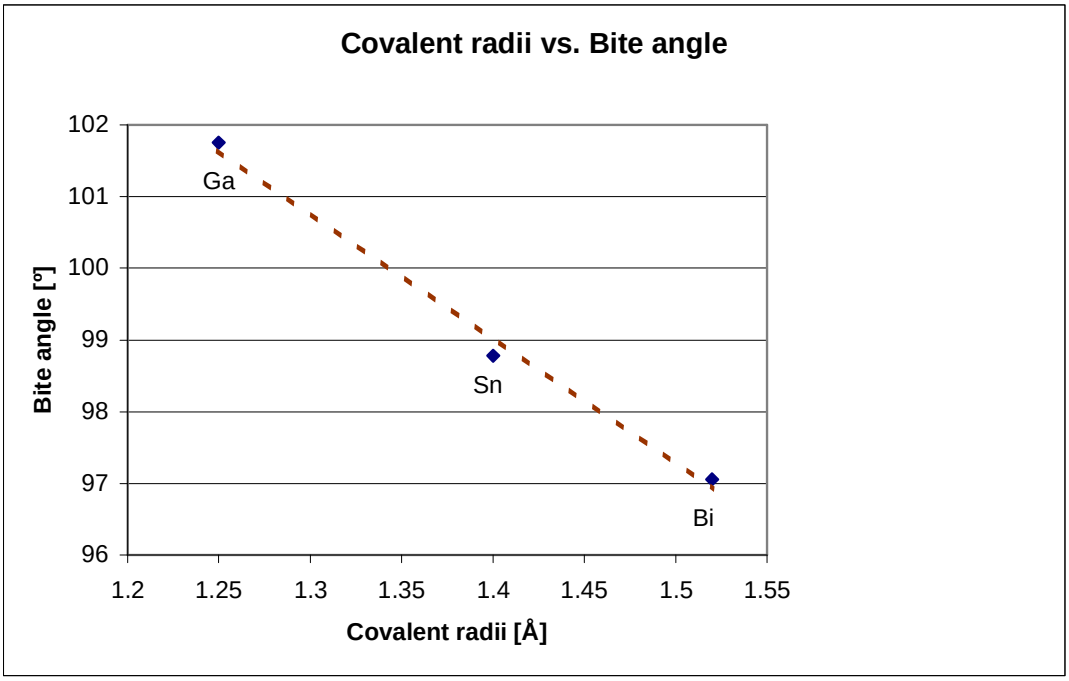

Diagram 4.1: covalent radii of main group elements vs. P-Pd-P bite angle in complexes 25, 26a, and 29

As can be seen, the bite angle decreases with increasing size of the main group element. It is postulated that the above trend can be utilized to predict the bite angles obtained by using other main group elements as templates. The transition metals zirconium (**30**) and yttrium (**31**) have different coordination numbers and hence displayed a different behaviour, giving P-Pd-P bite angles of 99.7 and 97-99º, respectively.

The rational ligand design allowed to synthesize a great variety of complexes wherein hard acids react with the hard oxygen donors and the soft phosphine donors coordinate to the soft acids. The products are distinguished from known heterometallic complexes of phosphinoalcohols in requiring neither the dedicated syntheses of a polydentate chelate ligand,[126] nor the need for introducing the metal atoms in separate reaction steps.[127] Finally, the hemilabile nature of the synthesized complexes promoted to study the catalytic behavior of these complexes and the first experimental proof of their catalytic potential was demonstrated by the application of **26a/b** in the Sonogashira C-C coupling reaction (section 4.3).

[126] A. Kless, C. Lefeber, A. Spangenberg, R. Kempe, W. Baumann, J. Holz, A. Boerner, *Tetrahedron*, **1996**, 52, 14599.
[127] G. S. Ferguson, P. T. Wolczanski, *J. Am. Chem. Soc*. **1986**, 108, 8293.

5. Some considerations on stereochemical aspects in bisphosphine complexes with octahedral tin templates

5.1. Introduction:

Objects or molecules that exist as pairs of enantiomers which are non-superimposable mirror images of each other are regarded as chiral. The existence of chirality in nature is of utmost importance. Let us take a simple example of limonene, which exists in two different isomeric forms, namely, the R-(+) or S-(–) isomers, with the same molecular formula but with different spatial arrangements (see **Fig. 5.1**).[128] Certainly the two forms have different characteristics: R-limonene has orange odor whereas S-limonene has lemon odor. In medicinal and pharmaceutical sciences, chiral discrimination is an important subject, because many drugs consist of chiral molecules, and often only one of them carries a certain desired chemical activity while the other often causes unwanted side effects. An example is the anti-emetic activity of one of the enantiomers of thalidomide while the other can cause death.[129]

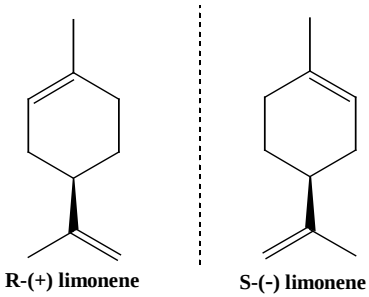

Fig. 5.1: Orange and lemon odor of R-(+) and S-(-) limonene, respectively.

[128] L. Friedman, J. G. Miller, *Science*, **1971**, 172, 1044.
[129] T. Nakanishi, N. Yamakawa, T. Asahi, N. Shibata, B. Ohtani, T. Osaka, *Chirality*, **2004**, 16, S36.

Although nature simply generates chiral molecules and assemblies in enantiopure form, designing and enantioselective synthesis of chiral entities presents an active challenge to synthetic chemists. As a rule of thumb, chirality can be induced in a molecule via *chiral* precursors, or via *achiral* precursors which assemble to give a chiral product. Importantly, highly symmetric architectures, such as the quartz minerals present in nature, are generated from the self-assembly of identical achiral subunits. Inspired by this fact, chemists have created chiral assemblies that can act as reaction vessels[130] for storage and recognition of ions [131] or molecules,[132] and for various chemical transformations.[133] A selective synthesis of desired architectures is another area of high interest. At this application end of chirality, chemists around the world have developed methodologies which enable them to synthesize the desired architectures.[134]

5.1.1. Stereochemistry in octahedral complexes with two chelating ligands:

Chirality in inorganic chemistry often deals with coordination compounds.[135] The metal-ligand interactions are generally kinetically more labile and dynamically more flexible than covalent interactions. The two enantiomers of an enantiomeric pair are usually separated by a very low energy barrier, which results in a spontaneous interconversion process called racemization. Isomerization of the racemates to give different diastereomers is another important process. The energy barriers between the individual enantiomers and diastereomers determine if the separation of individual isomers is in principle possible or not.

The above mentioned stereoisomers can racemize mainly by two pathways, 1) intermolecular or dissociative racemization, 2) intramolecular racemization. Now, in octahedral tris-chelate complexes the latter can occur via two mechanisms, namely a) Bailar twist, b) Ray-Dutt twist. [136] Both mechanisms proceed via trigonal prismatic transition states. Though it is difficult to predict which mechanism will be followed,

---

[130] N. Takeda, K. Umemoto, K. Yamaguchi, M. Fujita, *Nature*, **1999**, 398, 794.
[131] A. Caneschi, A. Cornia, A. C. Fabretti, S. Foner, D. Gatteschi, R. Grandi, L. Schenetti, *Chem. Eur. J.* **1996**, 2, 1379; B. Hasenknopf, J-M. Lehn, B. O. Kneisel, G. Baum, D. Fenske, *Angew. Chem. Int. Ed.* **1996**, 35, 1838; J. S. Fleming, K. L. V. Mann, C. A. Carraz, E. Psillakis, J. C. Jeffery, J. A. McCleverty, M. D. Ward, *Angew. Chem. Int. Ed.* **1998**, 37, 1279.
[132] D. Fiedler, D. H. Leung, R. G. Bergman, K. N. Raymond, *J. Am. Chem. Soc*. **2004**, 126, 3674.
[133] D. Fiedler, D. H. Leung, R. G. Bergman, K. N. Raymond, Acc. Chem. Res. **2005**, 38, 349; T. Kusukawa, M. Fujita, *J. Am. Chem. Soc*. **1999**, 121, 1397.
[134] A. von Zelewsky, *Stereochemistry of Coordination Compounds*, **1996**, Wiley, New York.
[135] G. Seeber, B. E. F. Tiedemann, K. N. Raymond, *Top. Curr. Chem.* **2006**, 265, 147.
[136] D. L. Kepert, *Prog. Inorg. Chem.* **1977**, 23, 1.

theoretical studies have indicated that delicate ligands with small bite angles will prefer Bailar twist, whereas those with large bite angles favor the Ray-Dutt mechanism. [137]

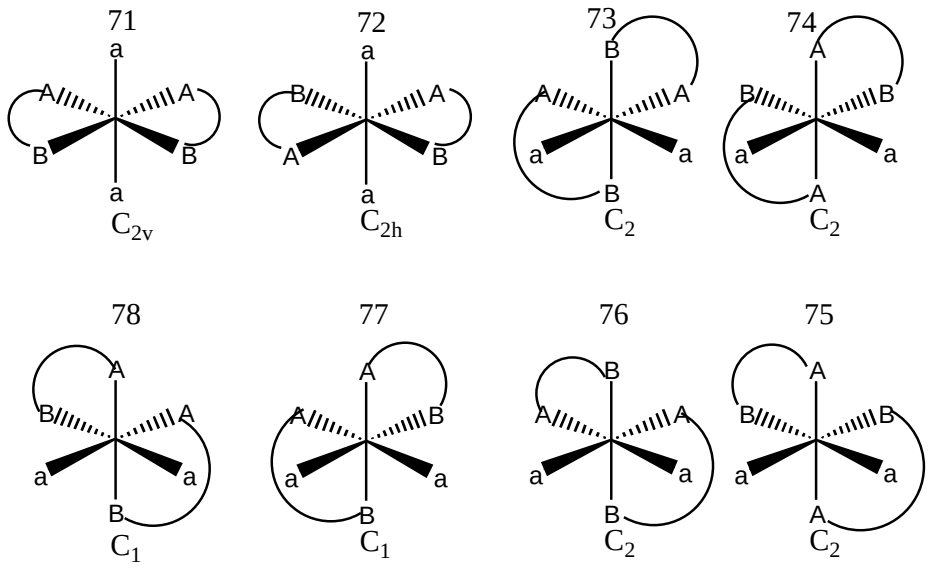

Diagram 5.1: Stereoisomers in $M(A=B)_2a_2$ type octahedral complexes.

As the present work mainly deals with bis-chelating catechol phosphine ligands with an octahedral metal center, it is of atmost importance to know their stereochemistry. Consider a coordination of two catechol phosphine units with an $SnCl_2$ unit. **Diagram 5.1** displays all theoretically possible stereoisomers in complex **26a**, where "A=B" represents the stereochemically inequivalent oxygen atoms of a catechol phosphine unit and "a" represents the chloride ligands. In total eight isomers (71-78) of which six form three chiral pairs 73/74, 75/76, 77/78 with C_2, C_2 and C_1 symmetry, respectively, are possible. In complex **26a**, the presence of the stereoisomers 72, 73 and 75 can be ruled out as the oxygen atoms (A) coordinating to palladium are trans to each other. The remaining 5 stereoisomers with 2 chiral pairs (73/76-C_2 and 77/78-C_1) might be observed. As mentioned in sect. 4.2.2, the $CDCl_3$ soluble material may possibly contain a mixture of stereoisomers 77 and 78. Clear differentiation of each isomer was impossible as medium-fast exchange between all isomers resulted into line broadening.

Having understood the importance of chirality and considering (chapter 3 and 4) that the tin centered complexes can be created in a single step via self-assembly, it is envisioned to

[137] A. Rodger, B. F. G. Johnson, *Inorg. Chem*. **1988,** 27, 3061.

explore mainly two aspects in this chapter, namely 1) variation in the stereochemistry at tin center by employing $(A=B)_2ab$ type ligand coordination, where A=B is the chelating catechol ligand and "a" is a methyl group and "b" a chloride substituent, 2) employing catechol phosphines with chiral phosphorus centers. The catechol phosphine **9f** is presumed to be a good candidate for such a modification.

Now, the $(A=B)_2ab$ type coordination at tin can possibly produce 11 isomers with 5 chiral pairs[134] i. e. in a complex **33a** (see following section). But assuming that the cis-disposition of the catechol oxygens "A" is a necessary and sufficient condition, four isomers can be ruled out and only the remaining seven (80-86) should be theoretically observable (see **Diagram 5.2**).

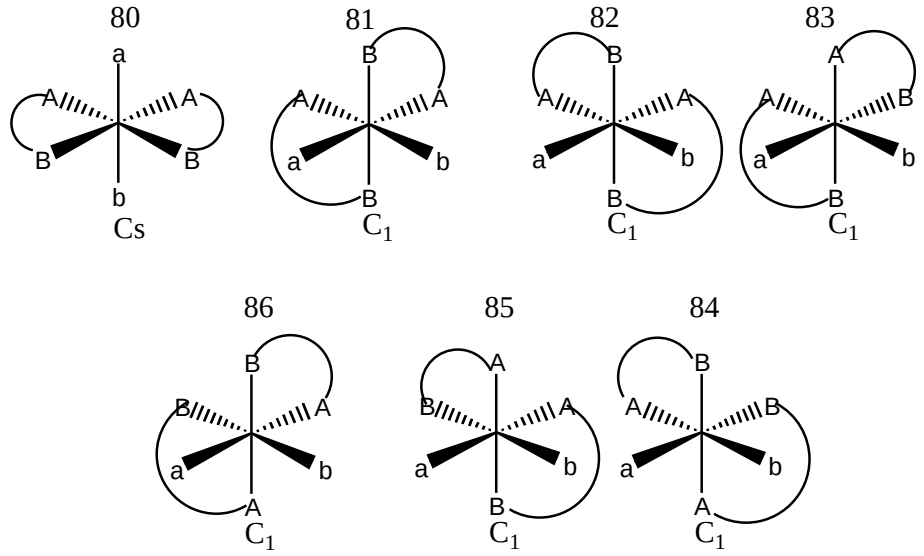

Diagram 5.2: Theoretically observable Stereoisomers of complex 33.

The chiral ligand **9f** on complex formation with $(COD)PdCl_2/Cl_2SnMe_2$ can produce the diastereoisomers with the backbones 87-91 which are further differentiated by the possibility to accommodate phosphine ligands with R and S configuration. The diastereoisomer 87 can thus exist as RR/SS-C_2 or RS/SR-C_s isomers. Assuming that 88 has a clockwise rotational axis Δ, and 89 has an anticlockwise rotational axis Λ, they can produce altogether 20 stereoisomers of which 16 form 8 pairs (refer to **Diag. 5.3**). Although the complex **34b** can produce all these diastereoisomers, only a very few were detectable (refer to sect. 5.2.2). In a likewise manner a complex **34a** featuring two distinguishable monodentate ligands a + b can produce 28 diastereoisomers (12 chiral pairs) based on the seven stereoisomers presented in diagram 5.2.

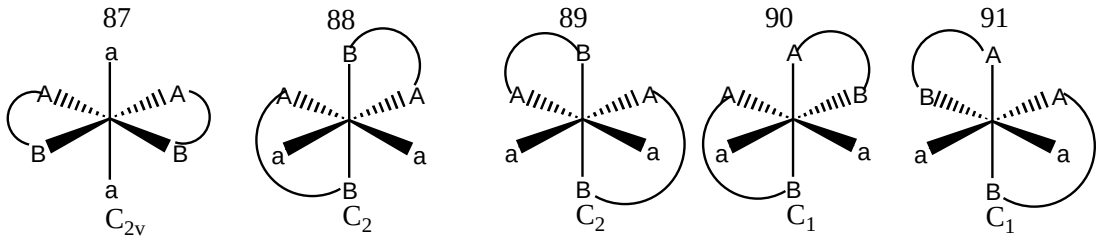

Diastereoisomers of 87	Diastereoisomers of 88/89	Pairs in 88/89	Diastereoisomers in 90/91	Pairs in 90/91
RR	ΔRR		ΔRR	
RS/SR	ΔRS		ΔRS	
	ΔSR	ΔRR/ ΛSS-C_2	ΔSR	ΔRR/ ΛSS-C_1
	ΔSS	ΔSS/ ΛRR-C_2	ΔSS	ΔSS/ ΛRR-C_1
	ΛRR	ΔRS/ ΛSR-C_1	ΛRR	ΔRS/ ΛSR-C_1
	ΛRS	ΛSR/ ΔRS-C_1	ΛRS	ΛSR/ ΔRS-C_1
	ΛSR		ΛSR	
	ΛSS		ΛSS	

Diagram 5.3: Representation of diastereoisomers of complex 34.

5.2. Results and discussion:

5.2.1. Chiral tin templated assemblies of 3-[(Diphenylphosphanyl)-methyl]-benzene-1, 2-diol (33):

Mixing of 3-[(Diphenylphosphanyl) methyl] benzene-1, 2-diol (**9b**), $MeSnCl_3$, $(COD)PdCl_2$ and triethyl amine in a 2:1:1:2.5 ratio in 20 ml of dry dimethyl formamide

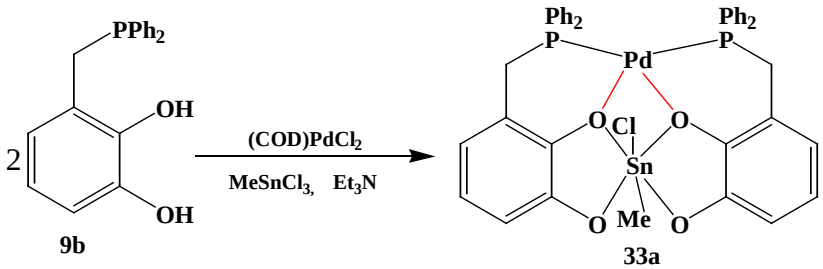

Scheme 5.1: Synthesis of tin centered chiral palladium-tin complex 33a.

and stirring the solution for 3 hours at room temperature produced a dark red suspension which was filtered through celite (**Scheme 5.1**). The filtrate was dried in vacuum and the residue redissolved in DMF. Upon dilution with excess diethyl ether, the precipitate formed again and was filtered and dried in vacuum at 70ºC for 4 hours. The complex **33a** was thus isolated in good yield, melting at 255ºC with decomposition.

Suitable crystals for single crystal X-ray diffraction were grown from a concentrated DMF: diethyl ether (2:1) mixture at room temperature. The complex **33a** crystallizes in a monoclinic unit cell in space group $P2_{1/n}$ with one molecule of solvent (DMF) per molecule of complex. The units of **33a** are linked together by weak hydrogen bonds between the chloride on tin and phenyl hydrogens of neighboring complexes in a 1D chain-like motif. The tin atom displays a distorted octahedral coordination by a chloride, a methyl and four oxygen ligands (see **Fig. 5.6**). The non chelating substituents make a C-Sn-Cl angle of 106.6º that is considerably smaller than the 114º C-Sn-C angle observed in **26b,** and slightly larger than the Cl-Sn-Cl angle of 104º in **26a**. No disorder of the chloride and methyl substituents was observed. The Sn-C bond distance in **33a** is 0.10 Å longer than in **26b**. The electronegativity difference between the methyl and chloride group are likely to be responsible for the observed bond angle and bond distance variation in **33a** compared to that in **26a, 26b** (Bent's rule). The two catechol planes intersect at tin with an angle of 88.6º. The palladium atom displays a distorted square planar geometry with a P-Pd-P bite angle of 98.8º which is comparable to that observed in **26a** (98.8º) and **26b** (99.4º). The SnO_2Pd ring is planar with an O1-Pd-O3 angle of 78.7º.

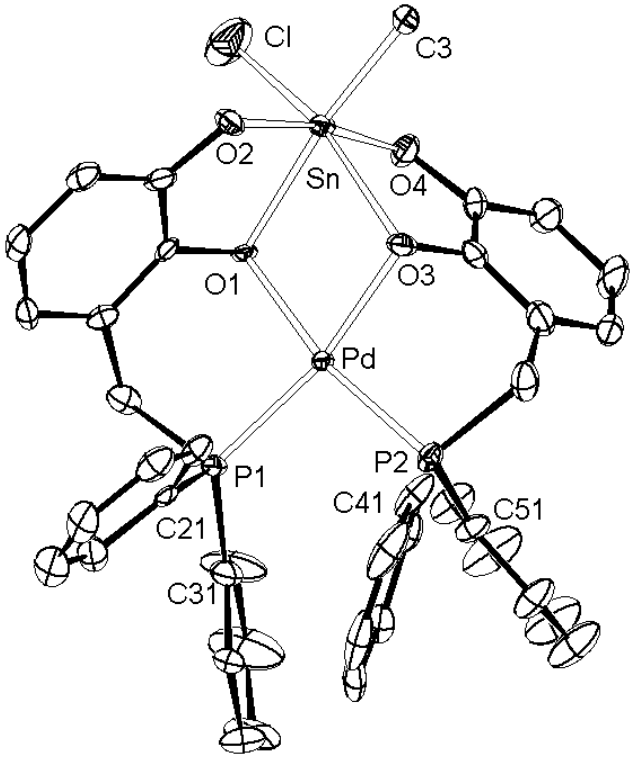

Bond lengths [Å]	Bond angles [°]
O3-Sn 2.207(5)	P1-Pd-P2 98.87(7)
O4-Sn 2.083(5)	O1-Sn-O2 77.41(2)
O3-Pd 2.081(5)	O1-Sn-O3 73.57(2)
P1-Pd 2.255(2)	Cl-Sn-C3 106.6(2)
Cl-Sn 2.358(3)	O1-Pd-O3 78.78(2)
C3-Sn 2.227(6)	Cl-Sn-O2 92.27(2)
O1-Sn 2.192(1)	O3-Sn-O4 77.32(1)
O2-Sn 2.075(1)	O2-Sn-O4 170.53(1)
O1-Pd 2.070(1)	
P2-Pd 2.243(1)	

Fig. 5.6: Molecular structure of the chiral complex 33a; (H-atoms omitted for clarity, thermal ellipsoids with 50% probability), important bond lengths and bond angles are given in the table.

The positive mode electron spray ionization mass spectra displayed two distinct pseudo-molecular ion peaks at m/e = 852.9 corresponding to a cation (**33a**-Cl)$^+$, and at 894.9, corresponding to a cation (**33a**+Li)$^+$.

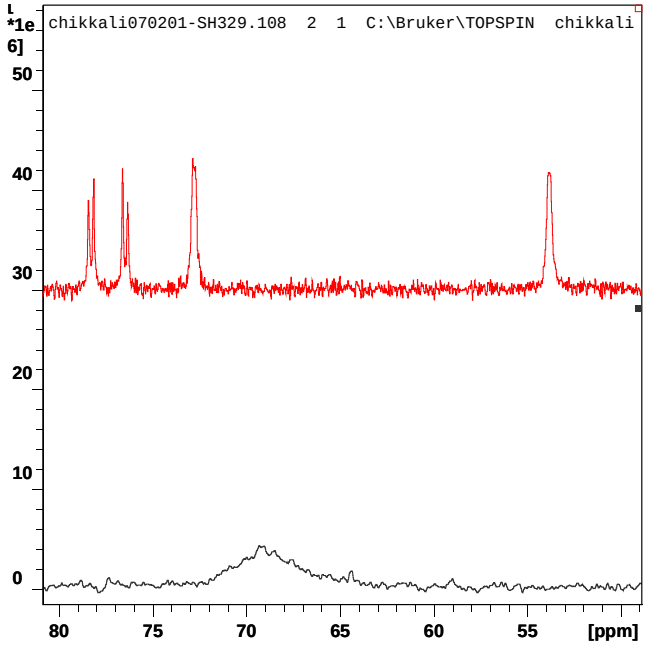

Fig. 5.5: ^{31}P NMR of complex 33a/33b at 303 (bottom) and 203K (top).

The ^{31}P NMR spectrum of **33a** in DMF-d_7 at ambient temperature displayed a single broad resonance at 69.6 ppm (bottom trace in **Fig. 5.5**). At the same time, the ^{119}Sn ^{1}H HMQC NMR spectrum displayed a broad ^{119}Sn singlet at –327 ppm with tin satellites to the CH_3 protons. The ^{31}P NMR signal sharpens eventually upon cooling to 203ºK and the single broad signal split into four resonances which make up two AB spin systems with chemical shifts at 78.2, 76.4 ppm and $^{2}J_{P\text{-}P}$ of 45 Hz, and at 72.8, 53.8 ppm with $^{2}J_{P\text{-}P}$ 22 Hz, respectively (top trace in **Fig. 5.5**). A ^{31}P NOESY experiment revealed the presence of intermolecular and intramolecular exchange between the four phosphorus sites as shown in **Fig. 5.7.** As can be seen in the NOESY spectrum with the longer mixing time, all four phosphorus sites displayed mutual correlation peaks indicating intermolecular and intramolecular exchange processes taking place (**Fig. 5.7,** right). When the mixing time was shortened the exchange was restricted to the intramolecular interconversion of the signals at 72.8, 53.8 ppm. In this spectrum, the absence of any exchange correlations between the nuclei of the second AB spin system suggests that this isomer is configurationally more stable and the interconversion of the two phosphorus sites requires first isomerization to the other diastereomer. In a likewise manner, the ^{1}H NMR spectrum at 203ºK displayed two singlets at 0.9 and 0.7 ppm ($^{2}J_{Sn\text{-}H}$ 105, 99 Hz respectively) corresponding to the Sn-CH_3 protons of two different products. Integrating the ^{31}P and ^{1}H peaks disclosed that the proton signal at 0.7 ppm corresponds to the AB spin system at 78.2

and 76.4 ppm and the proton signal at 0.9 ppm to the 72.8/53.8 AB spin system. All the proton phosphorus correlations were established from a ^{1}H ^{31}P HMQC experiment.

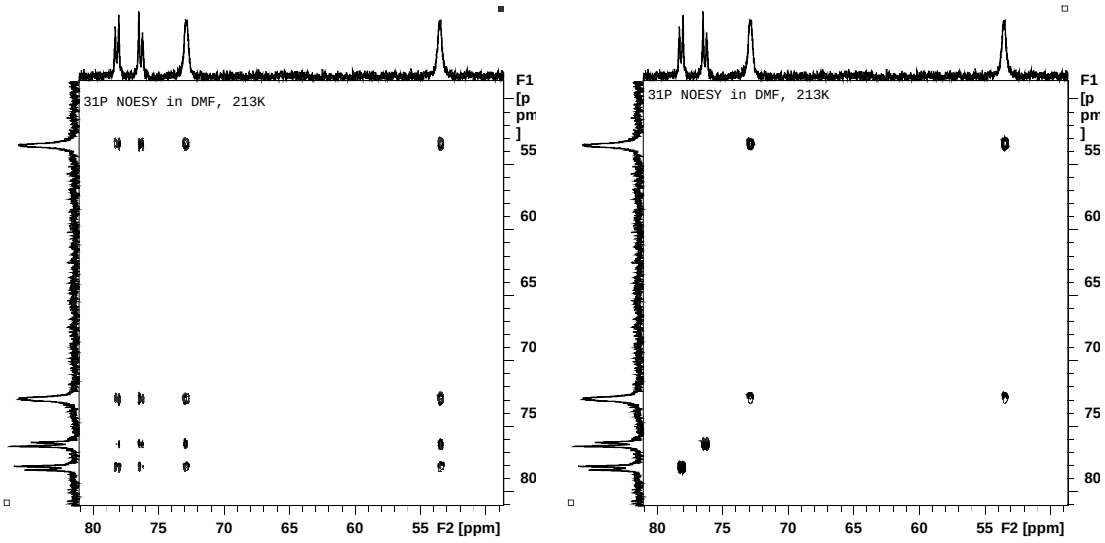

Fig.5.7: $^{31}P\{^{1}H\}$ NOESY Spectra of 33a recorded with different mixing times (right: 40ms. left: 12,5ms.) for chemical exchange.

Careful evaluation of the low temperature NMR data showed the presence of two of the three possible enantiomeric pairs. There was no clear evidence for the presence of the Cs symmetric isomer. Further, no clear evidence for the Pd-O bond breaking was obtained although the isomer with upfield resonance could possibly be **33b**.

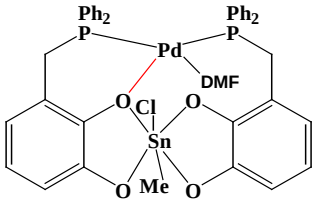

33b

Piecing together the NMR, ESI-MS and crystal structure results allow to state that, a chiral palladium-tin complex **33a** was synthesized in good yields. Low temperature NMR experiments proved very useful in order to evaluate that the product formation occurred stereoselective in the sense that not all possible stereoisomers were observed although the nature of all isomers present could not be unambiguously established.

5.2.2. Tin templated chiral assemblies of 3-{[Phenyl- (2,4,6-trimethyl-phenyl)-phosphanyl]-methyl}-benzene-1, 2-diol (34):

The chiral catechol phosphine 3-[(Mesitylphenyl phosphanyl)-methyl]-benzene-1, 2-diol (**9f**) was synthesized in two simple steps as reported in chapter 2. Appropriate amounts (2:1:1) of **9f**, (COD)$PdCl_2$, and dimethyl tin-dichloride were dissolved together with an excess of triethyl amine in DMF, and the mixture stirred at room temperature. The reaction progress was monitored by ^{31}P NMR and showed complete conversion in 3 hours. The reaction mixture was filtered and the Schlenk tube was kept at –28ºC overnight. White needles of triethyl ammonium chloride formed were separated by filtration. The filtrate was diluted by adding excess diethyl ether and the precipitate formed filtered off and dried at 70ºC in vacuum for 6 hours. The dark red powder was isolated in moderate yields (70%) and melts at 230ºC with decomposition.

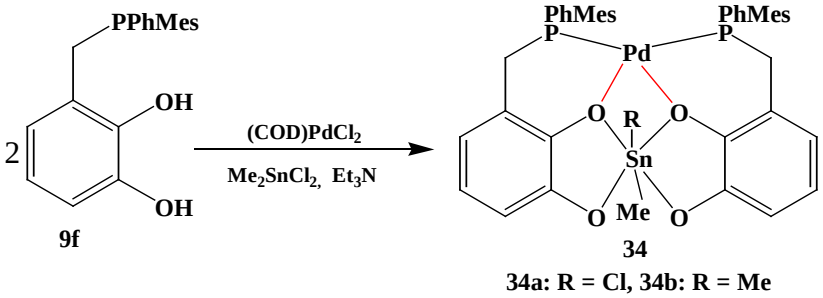

9f **34**

34a: R = Cl, 34b: R = Me

Scheme 5.2: Synthesis of chiral palladium-tin complex 34.

Fig. 5.3 displays a solid-state 2D ^{31}P CP/MAS J-resolved spectrum of the product at a spinning speed of 15.000 kHz. The spectrum shows signals attributable to an AB spin system with chemical shifts at δ = 57.4 and 55.4, and a $^2J_{PP}$ coupling of 40 Hz. As the chiral phosphorus atoms can have RR, SS or RS/SR configuration, chemical inequivalence and the observance of an AB spin system is possible. A ^{119}Sn CP/MAS spectrum displayed two signals at –207 and –308 ppm. The ^{119}Sn CP/MAS NMR data indicate that the sample must consist of a mixture of two components: the signal at –207 is attributable to a tin center carrying two methyl substituents, i.e. complex **34b** (see scheme 5.2 and the tin NMR data in sec. 4.2.2.2), and the peak at –308 ppm can be assigned to a tin center carrying a methyl and a chloride substituent in (**34a**). This interpretation was further confirmed by the results of elemental analysis.

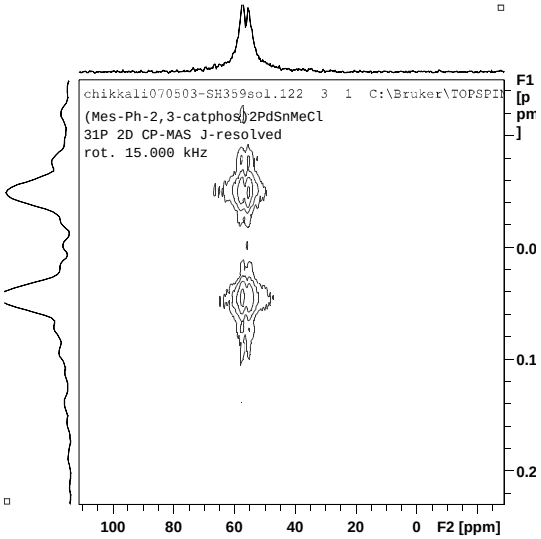

Fig. 5.3: Solid state ^{31}P CP/MAS 2D NMR spectra of 34.

Positive mode ESI-MS spectra displayed two peaks at m/e = 937.08 and 994.14. The peak at 937 corresponds to a cation of composition $(L_2PdSnMe)^+$ generated by taking off either a methyl group or a chloride resp., from **34a,b**. The peak at m/e = 994 is attributed to a cationic species $(L_2PdSnMeCl+Na)^+$ generated by attachment of a sodium ion to **34a**. No definite proof for the presence of **34b** was thus obtained from the ESI-MS experiment.

Suitable crystals for single crystal X-ray diffraction were grown from DMF, diethyl ether 1:1 mixture at room temperature. The X-ray diffraction study of one of the monoclinic crystals (space group $P2_{1/n}$) revealed the presence of complex **34a** (**Fig. 5.4**). The discrete molecules are linked together via weak Cl-H intramolecular hydrogen bridges between two units, forming zigzag, head to tail linked chains. The crystal structure disclosed that the tin atom carries one chloride and one methyl substitutent instead of two methyl groups, along with two catechol phosphine units, and displays a distorted octahedral geometry. The Sn-Cl distance of 2.34Å is close to that found in **26a** (2.39 Å), **34a** (2.35 Å) and is also in accordance with the literature reported Sn-Cl distance (2.30 Å) in phenoxy-cholorostannates.[138] The two-catechol planes intersect at tin with an angle of 84.7º.

[138] H. Jolibois, F. Theobald, R. Mercier, C. Devin, *Inorg. Chim. Acta.* **1985**, 97, 119.

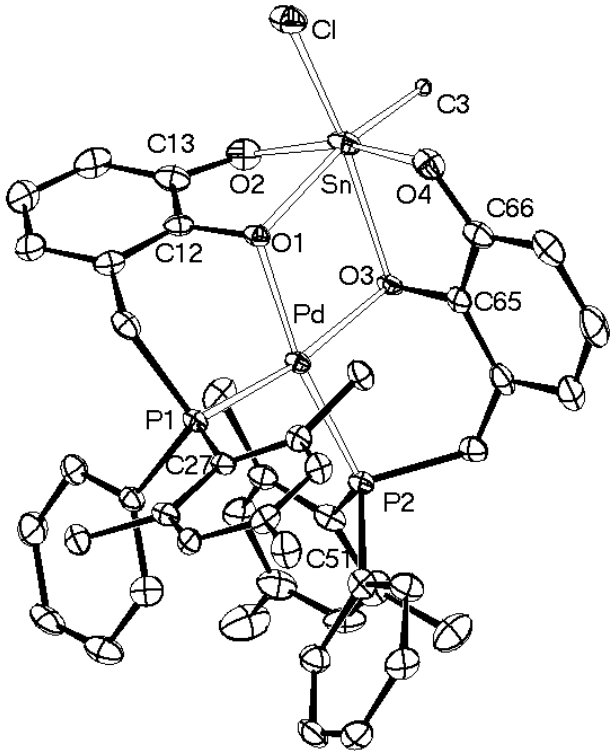

Bond lengths [Å]	Bond angles [°]	Bond angles [°]
O1-Sn 2.248(4)	P1-Pd-P2 104.64(5)	C27-P1-Pd 118.43(2)
O2-Sn 2.083(5)	O1-Pd-O3 80.23(2)	Cl-Sn-O4 90.86(1)
Cl-Sn 2.344(2)	Cl-Sn-C3 105.91(1)	Cl-Sn-O3 159.48(1)
P1-Pd 2.290(2)	O3-Sn-O4 76.63(2)	P1-Pd-O1 88.29(1)
O1-Pd 2.081(4)	C13-O2-Sn 114.2(4)	C3-Sn-O2 91.3(2)
C3-Sn 2.214(5)	C12-O1-Sn 108.8(3)	C3-Sn-O1 159.39(2)
O3-Sn 2.277(1)	O1-Sn-O2 75.57(2)	
O4-Sn 2.066(1)	O1-Sn-O3 72.65(1)	
O3-Pd 2.081(1)	O2-Sn-O4 162.95(0)	
P2-Pd 2.285(1)	O1-Sn-C3 159.38(2)	

Fig. 5.4: Molecular structure of 34a; (50% thermal ellipsoids, H-atoms omitted for clarity), important bond lengths and bond angles are given in the table.

The palladium atom displays a distorted square planar geometry with the two bridging oxygens and the two phosphorus atoms completing the coordination sphere. The Pd-P bond distance of 2.28-2.29 Å are slightly elongated with respect to **34a** (2.25 Å). The P-Pd-P bite angle of 104.6º in complex **34a** is the largest bite angle of all complexes discussed in chapter 4 and 5. The increased steric bulk of the mesityl groups at the phosphorus atoms is presumably responsible for these features. The two tetrahedrally coordinated phosphorus atoms dispose a trans-arrangement of the phenyl and mesityl substituents in order to have minimum steric hindrance. Thus, only one stereoisomer (**34a**)

out of 28 as indicated in sect. 5.2.1 was found in the measured crystal. It could be that other stereoisomers might have crystallized as well but the crystal picked up for measurement was accidentally one of **34a**.

The ^{31}P NMR spectrum of the isolated product in DMF-d_7 at room temperature displayed a broad singlet at 63.8 ppm, suggesting the presence of a dynamic equilibrium between different diastereoisomers. Cooling the sample to 243ºK split the ^{31}P line into two lines that appeared at 62.1 and 65 ppm. The ^{1}H, ^{119}Sn HMQC experiment showed two correlation signals at –202 and –206 ppm that correspond to tin bound methyl groups (see **Fig. 5.2,** right trace).

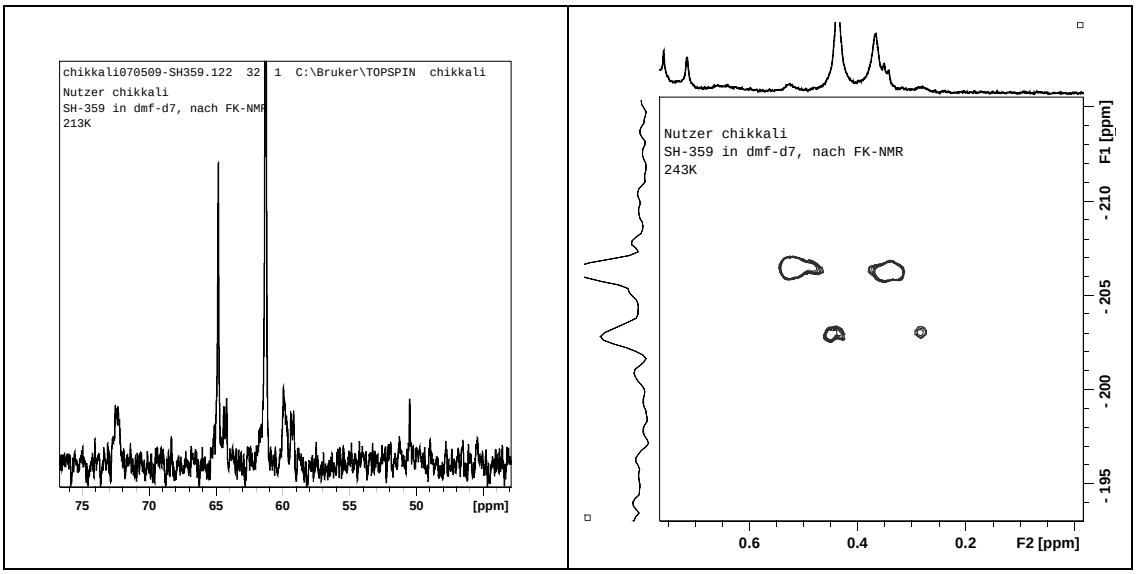

Fig. 5.2: ^{31}P NMR of 34 at 213K (left) and ^{1}H, ^{119}Sn HMQC (right) plot of complex 34 at 243K.

Further cooling down to 213ºK led to the appearance of additional ^{31}P NMR signals at 72, 64, 60, 59 and 50 ppm. Two singlets at 64.8 and 61.3 ppm were observed, whereas the signals at 64.2 and 59.2 were found to be an AB spin system with a J_{PP} coupling of 32 Hz. Another pair of broadened lines was tentatively assigned to a second AB spin system with the chemical shifts at 72.4, 59.8 ppm and an unresolved coupling (see **fig. 5.2**). A very weak singlet at 50 ppm which was not unequivocally assigned was also observable. The two broad singlets can be attributed to the C2 symmetric enantiomeric pair of the dimethyl tin complex **34b.** The two AB spin systems can be tentatively assigned to **34a** although the presence of C_1 isomers of **34b** could not be completely ruled out.

Warming up to 333ºK led to irreversible decomposition of the complex, producing several new species which were not further characterized. Thus, the NMR experiments showed the presence equilibrium mixture of diastereoisomers of **34a** and **34b** in solution even at lower temperatures indicating a very low energy difference between the diastereoisomers.

In summary, complex **34a** can have theoretically 28 diastereoisomers (12 chiral pairs + 4 meso isomers) and **34b** 19 diastereoisomers (8 chiral pairs + 3 mesoisomers). The solid state NMR spectrum of an isolated sample suggested the presence of a mixture of **34a** and **34b**. A diastereoselective reaction was achieved. The major isomers of **34b** are found to be homochiral ones (either RR or SS). Though the crystal structure displayed **34a** as one of the stable diastereoisomers, its formation is mechanistically unclear. Hence it is necessary to repeat the experiment to avoid formation of **34a,** and to get unequivocal results on the diastereoselectivity.

5.3. Conclusions:

The complex **33a** was synthesized in good yield and was characterized by NMR, ESI-MS and a single crystal X-ray diffraction study. The crystal displayed the presence of one of the stereoisomers 81 or 82 (depending on the sense of the rotational axis through chiral center) (see **Diag. 5.2**) with planar arrangement of O1/3, C3 and Cl and axially situated O2/4 atoms. Low temperature NMR experiments proved very useful in order to observe the existence of at least two possible stereoisomers of **33a**.

A mixture of chiral complexes **34a/b** with three chiral elements was synthesized and obtained in good yield utilizing the established one pot synthetic methodology. The solid state NMR of the crystals of **34** showed the presence of mixture of **34a** and **34b,** suggesting that accidental replacement of one methyl group had occurred during the synthesis. The solution NMR showed the presence of diastereoisomers of **34b** with broad singlets at 64.8 and 61.3 ppm. At least two diastereoisomers of **34a** could also be observed at 64.2, 59.2 and 72.4, 59.8 ppm as AB spin systems indicating inequivalent phosphorus atoms. Crystal structure measurements revealed presence of one of the diastereoisomer of **34a** (either 81or 82) with ΔRR or ΔSS configuration (see **Diag. 5.2**) and planar arrangement of O1/3, C3 and Cl and axially situated O2/4. Thus, easy syntheses of chiral assemblies was achieved although it is necessary to repeat the reaction to obtain pure **34b**.

Such chiral complexes are known to perform selective transformations such as asymmetric syntheses.[139] The catalytic potential of complexes **34** and **33a** has to be explored.

[139] J. Okuda, S. Verch, R. Stuermer, T. P. Spaniol, *J. Organomet. Chem.* **2000**, 605, 55; J. P. Genet, N. Kopola, S. Juge, J. Ruez-Montes, O. A. C. Antunes, S. Tanier, *Tetra. Lett.* **1990**, 31, 22, 3133.

6. Experimental details

6.1. General remarks:

As primary and secondary phosphines are known to undergo oxidation in air and metal alkoxides or phenolates may easily hydrolyze, most of the intermediates, and compounds studied are air and moisture sensitive. In order to avoid the oxidation or hydrolysis, all manipulations were therefore carried out under dry argon atmosphere, and solvents were dried by standard procedures if required.[140] The compounds are fully characterized by NMR, the prefixes *i, o, m, p* denote phenyl ring positions of *P*-C_6H_5 substituents.

Chemicals:

The following chemicals were synthesized according to experimental procedures reported in the literature:

Diphenyl phosphine,[141] Mesityl phenylphosphine,[41] Pentafluro-phenyl boronic acid,[142] Dichloro-[1,5-cyclooctadien] palladium,[143] Dibromo-[1,5-cyclooctadien] platinum,[144] and Bis-{benzonitrile}-palladium dichloride.[145]

All other chemicals were commercially available and purchased from Acros, Merck, Fluka, Strem, Chempure, Aldrich and Riedel-deHaehn.

Nuclear Magnetic Resonance Spectroscopy:

---

[140] D. D. Perrin, W. L. Armarego, L. F. Willfred, *Purification of Laboratory Chemicals*, Oxford: Pergamon Pr. **1988**.
[141] D. Wittenberg, H. Gilman, *J. Org. Chem.* **1958**, 23, 1063; Diphenyl phosphine was synthesized as reported in the above literature with little modification. Triethyl amine hydrochloride was employed as proton source instead of water.
[142] H. J. Frohn, N. Y. Adonin, V. V. Bardin, V. F. Starichenko, *Z. Anorg. Allg. Chem.* **2002**, 628, 2827.
[143] P. M. Maitlis, *The Organic Chemistry of Palladium Metal Complexes, V.1*, **1971**, Academic Press, New York; and references there in.
[144] J. Chatt, L. M. Vallarino, L. M. Venanzi, *J. Chem. Soc.* **1957**, 2496.
[145] M. Schlosser, Organometallics in Synthesis: A Manual; Wiley, **2002**.

The Solution NMR spectra were recorded on Bruker Avance 400 (^{1}H, ^{13}C, ^{31}P, ^{11}B, ^{119}Sn, ^{195}Pt) or AC 250 spectrometers (^{1}H, ^{13}C, ^{31}P, ^{19}F) with Tetramethylsilane as external standard.

^{1}H-NMR: 250,0/300,0/400,0 MHz, sec. Standard: Tetramethylsilane (TMS); δ = 0,0 (Ξ = 100,000000 MHz)

^{11}B-NMR: 128,4 MHz, sec. Standard: $Et_2O.BF_3$; δ = 0,0 (Ξ = 32,083974 MHz)

^{13}C-NMR: 62,9/75,5/100,6 MHz, sec. Standard: TMS; δ = 0,0 (Ξ = 25,1454004 MHz)

^{31}P-NMR: 101,2/121,5/161,9 MHz, sec. Standard: 85% H_3PO_4; δ = 0,0 (Ξ = 40,480737 MHz)

^{195}Pt-NMR: 86,7 MHz, sec. Standard: H_2PtCl_6 in D_2O; δ = 0,0 (Ξ = 21,497426MHz)

^{119}Sn-NMR: 148.7 MHz, sec. Standard: Tetramethyltin ($SnMe_4$); δ = 0,0 (Ξ = 37.290632 MHz)

^{109}Ag-NMR: 14.0 MHz, sec. Standard $AgNO_3$ in D_2O/sat. (Ξ = 4.653533 MHz)

In ambiguous cases assignments were derived from 2D experiments such as gs^{1}H^{31}P HMQC, gs^{1}H^{13}C HSQC, gs^{1}H-COSY, ^{31}P gsNOESY and gs^{1}H^{119}Sn HMQC. Solid state MAS NMR spectra were recorded on a Bruker Avance 400 instrument equipped with a 4 mm MAS probe and using spinning rates between 3 and 14 kHz. Cross polarization with a ramp-shaped contact pulse and mixing times between 3 and 5 ms was used for signal enhancement. MAS NMR spectra aiming at the determination of $^{1}J_{P,H}$ couplings were recorded under frequency-shifted Lee–Goldburg decoupling of homonuclear proton–proton interactions[146] which scales the visible splitting by a factor of 0.577. All coupling constants are given as absolute values. The resonances of OH protons were not always detectable, presumably as a consequence of chemical exchange, and data are not listed when unequivocal assignment was unfeasible.

Elemental Analysis: The C, H, N analyses were recorded on a Perkin-Elmer 240 CHSN/O Analyzer, and Cl was determined by argentometric titration.

---

[146] A. Bielecki, A. C. Kolbert, M. H. Levitt, *Chem. Phys. Lett.* **1989**, 155, 341; M. H. Levitt, A. C. Kolbert, A. Bielecki, S. J. Ruben, *Solid State NMR*, **1993**, 2, 151.

IR: IR spectra were measured between 4400 and 400 cm^{-1} on a Perkin Elmer FTIR Paragon 1100 spectrometer either as nujol paste or as KBr pallet.

EI-Mass-spectroscopy: Varian MAT 711, EI, 70 eV.

ESI-Mass-spectroscopy: Bruker Daltonics-micrOTOF-Q.

Melting point: Melting points were determined in sealed capillaries on a Büchi B-545 melting point apparatus.

Single Crystal X-ray Measurements: The Diffractometer Nonius Kappa CCD and Siemens P4 were used and the structure solutions and refinements were carried out using SHELXS, SHELXL and SHELXTL programs.

6.2. General procedure for the syntheses of phenol functionalized phosphane oxides (5a-e and 10a):

Diphenyl phosphine **2** (12 mmol) was added to a solution of the appropriate aldehyde **3a**–**e** (12 mmol) in DME (10 ml). The solution was stirred for five minutes at room temperature. A catalytic amount of *p*-toluenesulfonic acid (approx. 3–6 mmol) was added and the stirring continued for 48 h. The colorless precipitate formed was isolated by filtration, washed twice with 5 ml of DME, and dried in vacuo for 4 hours.

6.2.1. 2-[(Diphenyl phosphinoyl) methyl] phenol (5a):

Yield: 2.59 g (70 %); **Melting point:** 177°C.

Elemental analysis: $C_{19}H_{17}O_2P$ (308.32): calcd. C 74.02 H 5.56 found: C 73.90 H 5.37. Spectroscopic data are identical with the values reported in the literature.[147]

[147] N. A. Bondarenko, E. N. Tsvetkov, E. I. Matrosov, M. I. Kabachnik, *Izv. Akad. Nauk. SSSR, Ser. Khim.* **1979**, 432; V. I. Evreenov, V. E. Baulin, Z. N. Vostroknutova, N. A. Bondarenko, T. Kh. Syundyukova, E. N. Tsvetkov, *Izv. Akad. Nauk. SSSR, Ser. Khim.* **1989**, 1990.

6.2.2. 3-[(Diphenyl phosphinoyl) methyl] benzene-1, 2-diol (5b):

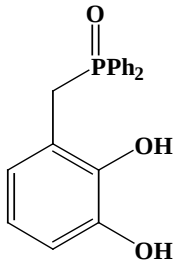

Yield: 3.31 g (85 %); **Melting point:** 194°C

Elemental analysis: $C_{19}H_{17}O_3P$ (324.32): calcd. C 70.37 H 5.28 found: C 70.44 H 5.35.

^{31}P NMR (101 MHz, $CDCl_3$): δ = 40.4 (s).

^{1}H NMR (400 MHz, $CDCl_3$): δ = 8.2 (br., 2 H, OH), 7.74 (m, 4 H, *o*-Ph), 7.58 (m, 2 H, *p*-Ph), 7.50 (m, 4 H, *m*-Ph), 6.81 (ddd, $^{3}J_{HH}$ = 8.0 Hz, $^{4}J_{HH}$ = 1.7 Hz, $^{6}J_{PH}$ = 1.7 Hz, 1 H, C_6H_3), 6.63 (dt, $^{3}J_{HH}$ = 8.0 Hz, $^{5}J_{PH}$ = 0.9 Hz, 1 H, C_6H_3), 6.34 (dddm, $^{3}J_{HH}$ = 7.7 Hz, $^{4}J_{HH}$ = 1.7 Hz, $^{4}J_{PH}$ = 1.7 Hz, 1 H, C_6H_3), 3.73 (d, $^{2}J_{PH}$ = 12.8 Hz, 2 H, CH_2).

^{13}C{^{1}H} NMR (100 MHz, $CDCl_3$): δ = 148.2 (d, J_{PC} = 2.7 Hz), 143.9 (d, J_{PC} = 4.2 Hz), 133.2 (d, J_{PC} = 2.7 Hz, *p*-C), 131.6 (d, J_{PC}= 9.6 Hz, *o*-C), 130.9 (d, J_{PC} = 100.4 Hz, *i*-C), 129.4 (d, J_{PC} = 12.1 Hz, *m*-C), 122.9 (d, J_{PC} = 6.3 Hz), 121.7 (d, J_{PC} = 1.9 Hz), 119.9 (d, J_{PC} = 8.4 Hz), 114.6 (d, J_{PC} = 2.5 Hz), 35.6 (d, J_{PC} = 67.1 Hz, CH_2).

MS (EI = 70 eV): *m/e* (%) = 324.1 (100) $[M]^+$; 202.1 (38) $[Ph_2POH]^+$; 201 (54) $[Ph_2PO]^+$.

6.2.3. 4-[(Diphenyl phosphinoyl) methyl] phenol (5c):

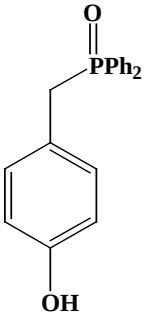

Yield: 2.22 g (60 %); **Melting point:** 223°C.

Elemental analysis: $C_{19}H_{17}O_2P$ (308.32): calcd. C 74.02 H 5.56 found: 74.19 H 5.82.

^{31}P NMR (162 MHz, $CDCl_3$): δ = 32.2 (s).

^{1}H NMR (400 MHz, $CDCl_3$): δ = 8.2 (br., 1 H, OH), 7.76 (m, 4 H, *o*-Ph), 7.57 (m, 2 H, *p*-H), 7.49 (m, 4 H, *m*-Ph), 6.82 (m, 2 H, C_6H_4), 6.56 (m, 2 H, C_6H_4), 3.62 (d, $^{2}J_{PH}$ = 12.2 Hz, 2 H, CH_2).

^{13}C{^{1}H} NMR (100 MHz, $CDCl_3$): δ = 156.9 (d, J_{PC} = 1.7 Hz), 132.7 (s), 131.8 (d, $^{2}J_{PC}$ = 9.2 Hz, *o*-C), 131.6 (d, J_{PC} = 4.8 Hz), 129.3 (d, $^{3}J_{PC}$ = 11.7 Hz, *m*-C), 128.6 (d, J_{PC} = 99.6 Hz), 120.7 (d, J_{PC} = 7.5 Hz), 117.0 (d, J_{PC} = 2.1 Hz), 37.4 (d, J_{PC} = 72.1 Hz, CH_2).

6.2.4. 4-[(Diphenyl phosphinoyl) methyl] benzene-1, 2-diol (5d):

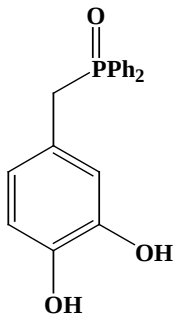

Yield: 3.50 g (90 %); **Melting point:** 192℃

Elemental analysis: $C_{19}H_{17}O_3P$ (324.32): calcd. C 70.37 H 5.28 found: C 69.98 H 5.17.

^{31}P NMR (101 MHz, $CDCl_3$): δ = 40.4 (s).

^{1}H NMR (250 MHz, $CDCl_3$): δ = 7.47 to 7.23 (m, 10 H, C_6H_5), 6.53 (s, 1 H, C_6H_3), 6.31 (d, $^{3}J_{HH}$ = 8.1 Hz, 1 H, C_6H_3), 6.12 (d, $^{3}J_{HH}$ = 8.1, 1 H, C_6H_3), 3.42 (d, $^{2}J_{PH}$ = 12.9 Hz, 2 H, CH_2).

^{13}C{^{1}H} NMR (62 MHz, $CD_3CN/CDCl_3$): δ = 143.8 (d, J_{PC} = 2.3 Hz), 143.2 (d, J_{PC} = 3.1 Hz), 131.7 (d, J_{PC} = 1.8 Hz, *p*-C), 130.3 (d, J_{PC} = 9.4 Hz, *o*-C), 128.1 (d, J_{PC} = 11.7 Hz, *m*-C), 126.9 (d, J_{PC} = 101.8 Hz, *i*-C), 121.2 (d, J_{PC} = 6.1 Hz), 120.9 (d, J_{PC} = 8.4 Hz), 116.6 (d, J_{PC} = 4.8 Hz), 114.4 (d, J_{PC} = 2.3 Hz), 35.1 (d, J_{PC} = 68.2 Hz).

6.2.5. 3-[(Diphenyl phosphinoyl) methyl] phenol (5e):

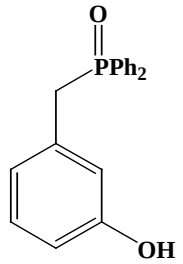

Yield: 2.22 g (60 %); **Melting point:** 198°C.

Elemental analysis: $C_{19}H_{17}O_2P$ (308.32): calcd. C 74.02 H 5.56 found: C 74.10 H 5.60.

$^{31}P\{^1H\}$ NMR (101 MHz, $CDCl_3$): δ = 31.4.

^1H NMR (250 MHz, CD_3CN/ $CDCl_3$): δ = 7.55 (m, 4 H, *o*-Ph), 7.40 to 7.25 (m, 6 H, *m*/*p*-Ph), 6.80 (t, $^3J_{HH}$ = 8.0 Hz, 1 H, C_6H_4), 6.59 (s, 1 H, C_6H_4), 6.44 (d, $^3J_{HH}$ = 8.0 Hz, 1 H, C_6H_4), 6.41 (d, $^3J_{HH}$ = 8.0 Hz, 1 H, C_6H_4), 3.50 (d, $^2J_{PH}$ = 13.4 Hz, 2 H, CH_2).

$^{13}C\{^1H\}$ NMR (62 MHz, $CD_3CN/CDCl_3$): δ = 157.1 (d, J_{PC} = 2.6 Hz), 132.4 (d, J_{PC} = 2.9 Hz, *p*-C), 131.2 (d, J_{PC} = 9.5 Hz, *o*-C), 131.0 (s), 130.9 (d, J_{PC} = 102.3 Hz, *i*-C), 129.5 (d, J_{PC} = 2.1 Hz), 128.9 (d, J_{PC} = 11.8 Hz, *m*-C), 121.8 (d, J_{PC} = 5.8 Hz), 117.5 (d, J_{PC} = 5.0 Hz), 114.2 (d, J_{PC} = 2.9 Hz), 37.1 (d, J_{PC} = 67.1 Hz).

6.2.6. 3-[(Mesitylphenylphosphinoyl) methyl] benzene-1, 2-diol (4f):

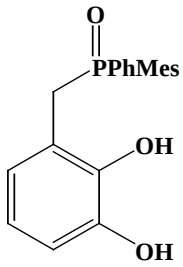

Yield: 3.73 g (85 %); **Melting point:** 220°C.

Elemental analysis: $C_{22}H_{23}O_3P$ (366.40): calcd. C 72.12 H 6.33 found: C 72.21 H 6.41.

^{31}P NMR (250 MHz, $CDCl_3$): δ = 46.38 (s).

^1H NMR (400 MHz, $CDCl_3$): δ = 7.65-7.38 (m, 5 H, Ph), 6.86 (d, $^4J_{HH}$ = 3.65 Hz, 2 H, *mes*-H), 6.78 (dt, $^3J_{HH}$ = 8.0 Hz, 1 H, Ph), 6.56 (t, $^3J_{HH}$ = 7.9 Hz, 1 H, Ph), 6.18 (dt, $^3J_{HH}$ =

7.7 Hz, 1 H, Ph), 3.83 (p, $^2J_{HH}$ = 12.6 Hz, 2 H, CH_2), 2.31 (d, $^2J_{HH}$ = 16.9 Hz, 9 H, *Mes*-CH_3).

$^{13}C\{^1H\}$ NMR (250 MHz, $CDCl_3$): δ = 147.5 (d, J_{PC} = 3 Hz. C_6H_3), 143.4 (d, J_{PC} = 4 Hz C_6H_3), 143.0 (d, J_{PC} = 10.5 Hz C_6H_3), 142.4 (d, J_{PC} = 2.8 Hz C_6H_3), 134.9 (s, *p*-Mes), 133.4 (s, *p*-Ph), 132 (d, J_{PC}= 2.8 Hz, C_6H_3), 131.3 (d, J_{PC} = 11.5 Hz, *m*-Ph), 129.9 (d, J_{PC} = 9.8 Hz, *i*-Ph/Mes), 128.8 (d, J_{PC} = 12 Hz, *m*-Mes), 122.2 (d, J_{PC} = 6 Hz, *o*-Mes), 120.9 (d, J_{PC} = 2.3 Hz, *o*-Ph), 119.9(s, *o*-Ph), 113.7 (d, J_{PC} = 2.8 Hz, *o*-Mes), 36.2 (d, J_{PC} = 65.3 Hz, CH_2), 23.5 (d, J_{PC} = 3.8 Hz, *o*-CH_3-Mes), 20.9 (d, J_{PC} = 1.3 Hz, *p*-CH_3-Mes).

MS (EI = 70 eV): *m*/*e* (%) = 366.1 (100%) [M].

6.2.7. 2-[(Diphenylphosphanyl)hydroxymethyl]phenol Hydrochloride (6a):

2-Hydroxybenzaldehyde (0.64 ml, 6 mmol) was added to a solution of diphenyl phosphine (1.05 ml, 6 mmol) in diethyl ether (10 ml). This mixture was stirred for five minutes at room temperature and an excess of conc. hydrochloric acid (2 ml, 24 mmol) was added. A colorless precipitate formed immediately. The reaction mixture was then stirred for further 60 minutes, the precipitate filtered off, washed twice with diethyl ether (5 ml), and dried for 1 h in vacuo.

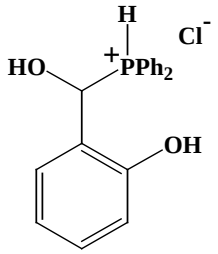

Yield: 1.86 g (90 %); **Melting point:** 104°C.

Elemental analysis: $C_{19}H_{18}ClO_2P$ (344.78): calcd. C 66.19 H 5.26 Cl 10.28 found: C 66.76 H 5.38 Cl 8.54.

$^{31}P\{^1H\}$ NMR (solid, 162 MHz, CP/ MAS): δ_{iso} = –0.8.

6.2.8. 4-[(Diphenylphosphanyl) hydroxymethyl] phenol (4c):

A solution of diphenyl phosphine (**2**) (1.43 ml, 8.2 mmol) and 4-hydroxybenzaldehyde (**3c**) (1.00 g, 8.2 mmol) in methanol (10 ml) was stirred for 5 minutes at room temperature and conc. hydrochloric acid (0.25 ml, 3 mmol) was added. A colorless precipitate formed

immediately. The reaction mixture was stirred for further 60 minutes, the precipitate filtered off and dried for 1 h in vacuo.

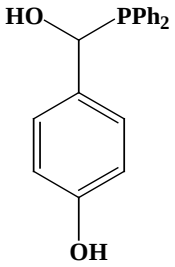

Yield: 2.27 g (90 %); **Melting point:** 168°C.

Elemental analysis: $C_{19}H_{17}O_2P$ (308.32): calcd. C 74.02 H 5.92 found: 74.29 H 5.92.

^{31}P NMR (101 MHz, THF): δ = –2.3 (s).

^{31}P{^{1}H}NMR (solid, 162 MHz, CP/MAS): δ_{iso} = –7.2.

6.2.9. Bis [hydroxy (3-hydroxyphenyl) methyl] diphenyl phosphonium Toluenesulfonate (7e/7e_):

A solution of diphenylphosphane (1.43 ml, 8.2 mmol) and 3-hydroxy benzaldehyde (1.00 g, 8.2 mmol) in DME (5 ml) was stirred for 5 minutes at room temperature and *p*-toluenesulfonic acid (0.60 g, 3.2 mmol) was added. A colorless precipitate began to form after 10 minutes. The reaction mixture was stirred for 12 h, the precipitate filtered off, washed twice with DME, and dried for 4 h in vacuo.

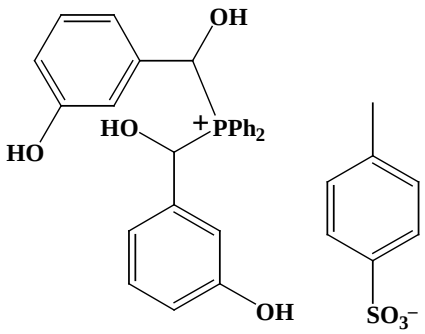

Yield: 1.73 g (90 %); **Melting point:** 121°C.

Elemental analysis: $C_{33}H_{31}O_7PS$ (602.64): calcd. C 65.77 H 5.19 found: 65.39 H 5.30.

^{31}P{^{1}H}NMR (solid, 162 MHz, CP/MAS): δ_{iso} = 30.5, 29.9.

6.3. General procedure for the synthesis of phenol-functionalized phosphanes 9a-d and 101:

The appropriate phosphine oxide **5a–d or 9f** (10 mmol) was dissolved in dry THF (100 ml). Methyl iodide (0.69 ml, 11 mmol) was added via a syringe and the solution stirred for 2 h at room temperature. The mixture was then cooled to 0°C and solid LiAlH4 (1.7 g, 45 mmol) added in several small portions. The reaction mixture was warmed to ambient temperature, and stirring was continued for another 5–6 h. The progress of the reaction was monitored by TLC. The reaction flask was again cooled to 0°C, and 50 ml of 1M. hydrochloric acid was added in several portions (the first few drops had to be added very carefully until the exothermic reaction became less violent). The organic layer was separated and the aqueous layer washed with ethyl acetate (3×50 ml). The combined organic phases were dried overnight with Na_2SO_4 and all volatiles evaporated in vacuo. The crude products were purified by column chromatography (silica, petroleum ether: ethyl acetate = 7:3).

6.3.1. 2-[(Diphenylphosphanyl) methyl] phenol (9a):

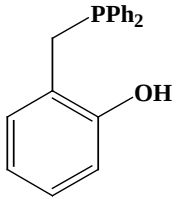

Yield: 1.81 g (62 %); colorless oil.

Elemental analysis: $C_{19}H_{17}OP$ (292.32): calcd. C 78.07 H 5.86 found: C 74.33 H 5.91.

^{1}H NMR (250 MHz, [D$_8$] toluene): δ = 6.8 to 7.5 (m, 10 H, C_6H_5), 6.80 (t, 1 H, $^3J_{HH}$ = 7.7 Hz), 6.74 (d, 1 H, $^3J_{HH}$ = 7.7 Hz), 6.61 (d, 1 H, $^3J_{HH}$ = 7.8 Hz), 6.50 (t, 1 H, $^3J_{HH}$ = 7.5 Hz), 3.32 (s, 2 H, CH_2). The ^{1}H NMR spectroscopic data match those published earlier.[126]
^{31}P{^{1}H} NMR (101 MHz, [D$_8$] toluene): δ = –15.0.

6.3.2. 3-[(Diphenylphosphanyl) methyl] benzene-1, 2-diol (9b):

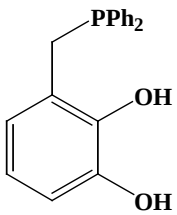

Yield: 1.85 g (60 %); **Melting point:** 82°C.

Elemental analysis: $C_{19}H_{17}O_2P$ (308.32): calcd. C 74.02 H 5.56 found: C 73.91 H 5.73.

^{31}P NMR (101 MHz, $CDCl_3$): δ = –13.1 (s).

^{1}H NMR (400 MHz, $CDCl_3$): δ = 7.52 to 7.30 (m, 10 H, C_6H_5), 6.78 (dm, $^{3}J_{HH}$ = 7.9 Hz, 1 H, C_6H_3), 6.64 (tm, $^{3}J_{HH}$ = 7.9Hz, 1 H, C_6H_3), 6.43 (dm, $^{3}J_{HH}$ = 7.9 Hz, 1 H, C_6H_3), 6.02 (br., 1 H, OH), 5.86 (br., 1 H, OH), 3.52 (d, $^{2}J_{PH}$ = 1.7 Hz, 2 H, CH_2).

^{13}C{^{1}H} NMR (100 MHz, $CDCl_3$): δ = 145.0 (d, J_{PC} = 1.6 Hz), 141.7 (d, J_{PC} = 3.7 Hz), 132.8 (d, $^{3}J_{PC}$ = 17.4 Hz, *m*-C), 130.9 (d, $^{2}J_{PC}$ = 9.5 Hz), 129.3 (s, *p*-C), 128.9 (d, $^{3}J_{PC}$ = 12.1), 128.6 (d, J_{PC} = 7.4 Hz, *o*-C), 122.4 (d, J_{PC} = 6.3 Hz), 121.0 (d, J_{PC} = 1.6 Hz), 113.6 (d, J_{PC} = 2.6 Hz), 30.7 (d, $^{1}J_{PC}$ = 10.5 Hz, CH_2).

MS (EI = 70 eV): *m*/e (%) = 308.1 (100) [M^+], 186.1(45) [Ph_2PH^+], 185.1 (44) [Ph_2P^+], 183.0 (54) [Ph_2P^+–H_2], 123.1 (45) [M^+–PPh_2], 108.1 (54).

6.3.3. 4-[(Diphenylphosphanyl) methyl] benzene-1, 2-diol (9d):

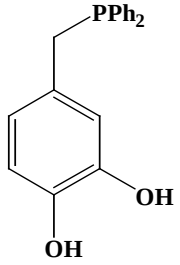

Yield 2.16 g (70 %); **Melting point**: 144°C.

Elemental analysis: $C_{19}H_{17}O_2P$ (308.32): calcd. C 74.02 H 5.56 found: C 74.06 H 5.59.

^{1}H NMR (400 MHz, [D_8]- THF): δ = 7.68 (s, 1 H, OH), 7.53 (s, 1 H, OH), 7.41 (m, 4 H, *o*-H), 7.33 to 7.25 (m, 6 H, *m*/*p*-H), 6.58 (dd, $^{4}J_{HH}$ = 1.7 Hz, $^{4}J_{PH}$ = 1.7 Hz, 1 H, C_6H_3), 6.52 (d, $^{3}J_{HH}$ = 8.1 Hz, 1 H, C_6H_3), 6.38 (dm, $^{3}J_{HH}$ = 8.0 Hz, 1 H, C_6H_3), 3.31 (s, 2 H, CH_2).

^{13}C{^{1}H} NMR (100 MHz, [D_8] THF): δ = 145.6 (d, J_{PC} = 1.5 Hz), 144.2 (d, J_{PC} = 2.9 Hz), 139.9 (d, J_{PC} = 16.8 Hz, *i*-C), 133.3 (d, J_{PC} = 18.7 Hz, *m*- C), 129.1 (d, J_{PC} = 8.8 Hz), 128.7 (s, *p*-C), 128.6 (d, J_{PC} = 6.3 Hz, *o*-C), 120.9 (d, J_{PC} = 7.1 Hz), 116.7 (d, J_{PC} = 7.6 Hz), 115.3 (d, J_{PC} = 1.5 Hz), 35.6 (d, J_{PC} = 15.1 Hz).

$^{31}P\{^{1}H\}$ NMR (162 MHz, $CDCl_3$): δ = –10.4.

MS (EI = 70 eV): *m*/e (%) = 308.1 (48) [M^+], 186.1 (38) [Ph_2PH^+], 183.0 (27) [Ph_2P^+–H_2], 123.1 (100) [M^+ _PPh_2], 108.1 (27).

6.3.4. 3-[(Mesitylphenyl phosphanyl)-methyl]-benzene-1, 2-diol (9f):

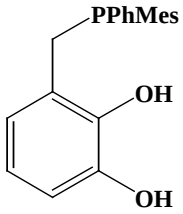

Yield: 2.45 gms (70%), **Melting point:** 93ºC.

Elemental analysis: $C_{22}H_{23}O_2P$, Calcd. C 75.41 H 6.62 Found: C 74.73 H 6.83

^{31}P NMR (250 MHz, $CDCl_3$): δ = -27.64 (s).

^{1}H-NMR ($CDCl_3$) δ = 7.35 to7.20 (m, 5 H Ph), 6.9 (d $^4J_{HH}$ = 1.9 Hz, 2 H, Mes), 6.73 (d, $^2J_{HH}$ = 7.5 Hz, 1 H C_6H_3), 6.66 (t, $^2J_{HH}$ = 7.8 Hz 1 H C_6H_3), 6.59 (d, $^2J_{HH}$ = 7.5 Hz, 1 H C_6H_3), 6.5 (broad s, 2 H, OH), 3.76 (broad, s, 1 H, CH_2), 3.52 (dd, $^2J_{PH}$ = 13.5 Hz 1 H, CH_2), 2.30-2.28 (m, 9 H, Mes-CH_3).

^{13}C-NMR (CDCl3) δ = 145.3 (s, C_6H_3), 145.1 (s, C_6H_3), 144.8 (d, $^4J_{PC}$ = 1.5 Hz, C_6H_3), 142.1 (d, $^3J_{PC}$ = 3.8 Hz, C_6H_3), 140.5 (s, C_6H_3), 140.3 (s, C_6H_3), 139.9 (d, $^4J_{PC}$ = 1.5 Hz, *p*-Mes.), 129.8 (d, $^3J_{PC}$ = 4.5 Hz, *m*-Ph.), 129.5 (s, *o*-Ph), 128.4 (d, $^3J_{PC}$ = 4.3 Hz, *m*-Mes), 126.8 (d, $^4J_{PC}$ = 1 Hz, *p*-Ph), 125.3 (d, $^1J_{PC}$ = 8.5 Hz, *i*-Ph), 122.0 (d, $^1J_{PC}$ = 7.3 Hz, *i*-Mes), 120.7 (d, J_{PC} = 2 Hz, *o*-Mes), 113.3 (d, $^3J_{PC}$ = 4.5 Hz, *m*-Mes.), 28.3 (d, $^1J_{PC}$ = 14.56 Hz CH_2), 21.1 (s, Mes-CH_3).

6.4. General procedure for the syntheses of transition metal complexes of 9b-d:

To the THF (20 ml) solution of 200 mg (0.64 mmol) of 3/4-[(Diphenylphosphanyl)-methyl]-benzene-1,2-diol was added 0.32 mmol of the corresponding transition metal complex. The reaction mixture was stirred for two hours at room temperature and then concentrated in vacuum to approximately half of the total volume. Storage of the

remaining solution at +4°C gave shining needle like crystals that were isolated nearly quantitatively by filtration.

6.4.1. Bis {3-[(Diphenylphosphanyl)-methyl]-benzene-1, 2-diol} Palladium dichloride, 13b:

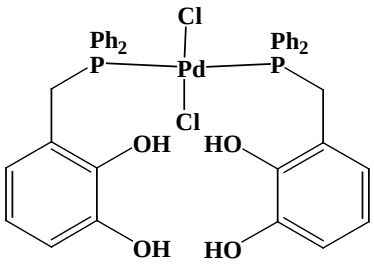

Elemental analysis: Calcd. for $PdCl_2$(**9b**)$_2$ × THF: C 58.25 H 4.89 Found: C 58.06 H 5.27.

Yield: 240 mg (95%); **Melting point:** 176ºC.

^{31}P{^{1}H}-NMR (CD_3CN): δ = 19.1 (s).

^{1}H NMR (CD_3CN): δ = 7.8 to 7.1 (m, 20 H, Ph), 7.0 to 6.5 (m, 6 H, C_6H_3), 4.23 (d, $^{2}J_{PH}$ = 11.6 Hz, 4 H, CH_2).

^{13}C{^{1}H} NMR (CD_3CN): δ = 145.28 (2C, C_6H_3), 144.6 (2C, C_6H_3), 134.88-134.48 (m, 8 C, *o*-Ph), 131.8 (d, ^{1}Jpc = 11.05 Hz, 4 C, *i*-Ph), 129-130.71 (m, 2 C, C_6H_3), 128.9(t, ^{3}Jpc = 7.4 Hz, *m*-Ph), 123.9 (d, $^{2}J_{PC}$ = 15.8 Hz, C_6H_3), 120-121 (m, *p*-Ph), 115.2 (s, 2C C_6H_3), 114.7 (s, 2 C, C_6H_3), 26.24 (s, 4C, CH_2).

6.4.2. Bis {4-[(Diphenylphosphanyl)-methyl]-benzene-1, 2-diol} Palladium dichloride, 13d:

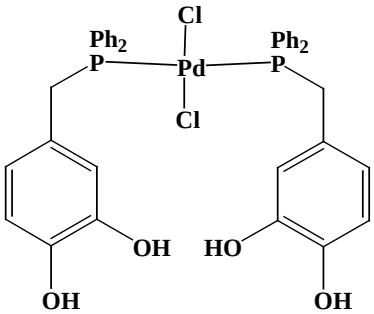

Yield: 240 mg (95%); **Melting Point:** 223ºC

^{31}P{^{1}H}-NMR (CD_3CN): δ = 20.0 (s).

^{1}H (CD3CN): δ = 7.30-6.96 (m, 20 H, Ph), 6.38 (d, $^{3}J_{HH}$ = 7.93 Hz, 2 H, C_6H_3), 6.31 (d, $^{3}J_{HH}$ = 7.47 Hz, 2 H, C_6H_3), 6.14 (d, $^{3}J_{HH}$ = 8.24 Hz, 2 H, C_6H_3), 3.65 (d, $^{2}J_{PH}$ = 11.59 Hz, 4 H, CH_2).

6.4.3. Silver- bis {3-[(Diphenylphosphanyl)-methyl]-benzene-1, 2-diol}, 14b:

Crystals were grown from a dichloromethane: diethyl either mixture (10:1).

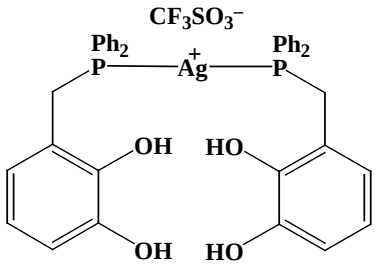

Elemental analysis: Calcd. for [$C_{39}H_{34}$ AgO_7P_2S X DMF X CH_2Cl_2] : C 50.07 H 4.20 N 1.36 Found: C 51.51 H 4.39 N 1.76.

ESI-MS (positive mode): m/e = 781.09 $(M\text{-}OTf+NaCl)^{+}$, 723.09 $(M\text{-}OTf)^{+}$, 725 $(M\text{-}OTf)^{+}$.

Yield: 261 mg (95%); **Melting Point:** 109ºC.

^{31}P{^{1}H}-NMR ($CDCl_3$, 303K): δ = 6.16 (d, broad, $^{1}J_{Ag\text{-}P}$, 444.5 Hz).

^{1}H NMR ($CDCl_3$): δ = 7.55 to 7.3 (m, 20 H, Ph), 6.70 (dd, $^{3}J_{HH}$ = 7.8 Hz, 2 H, C_6H_3.), 6.4 (t, $^{3}J_{HH}$ = 7.9 Hz, 2 H, C_6H_3), 6.1 (dd, $^{3}J_{HH}$ = 7.5 Hz, 2 H, C_6H_3), 5.29 (s), CH_2Cl_2, 3.7 (broad, s, 4 H, CH_2).

^{13}C{^{1}H} NMR ($CDCl_3$): δ = 144.2 (s, C_6H_3), 142.8 (s, C_6H_3), 133.1(broad, 8 C, Ph), 130.8 (broad, 4 C, Ph), 128.9 (broad, 4 C, Ph), 122.2(s, 2 C, C_6H_3), 120.8 (s, 2 C, C_6H_3.), 119.9 (s, 2 C, C_6H_3), 116.9 (s, 8 C Ph), 114.2 (s, 2 C, C_6H_3), 28.9 (broad, 4 C, CH_2).

6.4.4. Silver- bis {4-[(Diphenylphosphanyl)-methyl]-benzene-1, 2-diol}, 14d:

Crystals were grown from THF solution at room temperature.

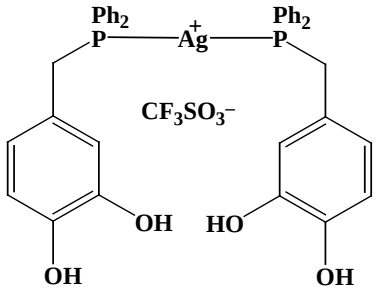

Elemental analysis: Calcd. for [$C_{39}H_{34}AgF_3O_7P_2S$ X 1.5 THF]: C 55.47 H 4.95 Found: C 55.48 H 4.95.

Yield: 261 mg (95%); **Melting Point:** 112ºC

ESI-MS (positive mode): m/e = 723.09 $(M\text{-}OTf)^+$, 725 $(M\text{-}OTf)^+$

$^{31}P\{^1H\}$-NMR ($CDCl_3$, 300K): δ = 16.5 (broad d, $^1J_{Ag\text{-}P}$ = 465 Hz).

$^{31}P\{^1H\}$-NMR ($CDCl_3$, 223K): δ = 16.4 (dd, $^1J_{P\text{-}Ag}$ = 580 Hz).

^1H NMR ($CDCl_3$): δ = 7.5 to 7.2 (m, 20 H, Ph), 7.02 (s, 2 H, C_6H_3.), 6.58 (d, $^3J_{HH}$ = 8.24 Hz, 2 H, C_6H_3), 6.08 (dd, $^3J_{HH}$ = 6.4 Hz, 2 H, C_6H_3), 3.53 (broad, s, 4 H, CH_2).

$^{13}C\{^1H\}$ NMR ($CDCl_3$): δ = 144.9 (s, C_6H_3), 144.3 (s, C_6H_3), 133.6 (broad, Ph), 131.6 (broad, Ph), 130.9 (broad, Ph), 129.7 (s, Ph), 126.5 (s, C_6H_3), 121.8 (s, C_6H_3), 116.3 (s, Ph), 115.8 (s, C_6H_3), 34.5 (broad, CH_2).

6.4.5. Bis {4-[(Diphenylphosphanyl)-methyl]-benzene-1, 2-diol} platinum dichloride, 15:

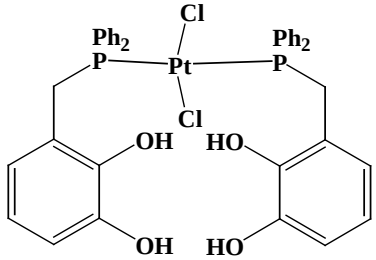

Elemental analysis: Calcd. for ($C_{38}H_{34}Cl_2O_4Pt$ + PhCN): C 54.87 H 3.99 N 1.42 Found: C 54.17 H 4.43 N 1.03.

Yield: 268 mg (95%); **Melting point:** 235ºC.

$^{31}P\{^1H\}$-NMR ($CDCl_3$) δ = 18.8 (s, $^1J_{Pt\text{-}P}$ 1296 Hz, 33%), 11.0 (s, $^1J_{Pt\text{-}P}$ 1861 Hz, 66%).

^{1}H NMR ($CDCl_3$): δ = 7.8 to 6.9 (m, 25 H, Ph + PhCN), 6.81 (t, $^{3}J_{H-H}$ = 8.24 Hz, 2 H, C_6H_3.), 6.6-6.4 (m, 2 H, C_6H_3.), 6.0-5.7 (m, 2 H, C_6H_3.), 4.14 (d, $^{2}J_{P-H}$, 11 Hz, 3 H, CH_2), 3.5 to3.4 (br, s, 1 H, CH_2).

The same sample (solid) was stored for two months in inert atmosphere, ^{31}P NMR of this displayed following chemical shifts.

^{31}P{^{1}H}-NMR ($CDCl_3$) δ = 28.6 (s, $^{1}J_{Pt-P}$ = 1942 Hz), 24.5 (dd, $^{1}J_{Pt-P}$ = 2141, 1727 Hz).

6.4.6. Bis{3-[(Mesitylphenyl phosphanyl)-methyl]-benzene-1, 2-diol} palladium(II), 101:

To the THF (20 ml) solution of 100 mg (0.28 mmol) of 33-[(Mesitylphenyl phosphanyl)-methyl]-benzene-1, 2-diol was added 0.14 mmol of (COD)$PdCl_2$. The reaction mixture was stirred for one hour at room temperature and then concentrated in vacuum to approximately half of the total volume. Storage of the remaining solution at +4°C gave yellow powder that was isolated nearly quantitatively by filtration and drying in vacuum.

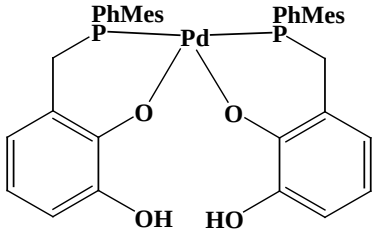

Yield: 107 mg (95%).

ESI-MS (positive mode): m/e = 805.2$[M+H]^+$, 827.2$[M+Na]^+$.

^{31}P{1H}-NMR ($CDCl_3$) δ = 55.7 (s), 19.2 (br, s), 5.4 (s), 4.3 (s).

^{31}P{1H}-NMR ($CDCl_3$) δ = 53.5 (br, s), 1.3 (s), -0.9 (s). of isolated product.

^{1}H NMR ($CDCl_3$): δ = 7.7-7.3 (m, 8 H, Ph/Mes), 6.9-6.6 (m, 6 H, Ph/Mes), 6.56-5.9 (m, 4 H, C_6H_3), 5.7-5.5 (m, 2 H, C_6H_3), 4.3-4.0 (br, d, 2 H, CH_2), 3.65-3.5 (br, d, 2 H, CH_2), 2.26 (br, s, 9 H, Mes-CH_3).

Though the proton signals of the cis-trans complexes where observable, it was hard to assign them.

6.5. General procedure for the syntheses of boranes:

620 mg (2 mmol) of solid 3-[(Diphenylphosphanyl)-methyl]-benzene-1, 2-diol was dissolved in 20 ml of dry dichloromethane. 245 mg (2 mmol) of aryl boronic acid was dissolved in 10 ml of dichloromethane in another schlenk tube and was transferred to the diol solution. The reaction mixture was stirred for 30 minutes, the solvent was evaporated to dryness and the white, powdered product was obtained in quantitative yield.

6.5.1. (a) Diphenyl- (2-phenyl-benzo [1,3,2]-dioxaborol-4-ylmethyl)-phosphane 16a:

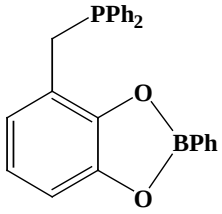

Elemental analysis: Calcd. for ($C_{25}H_{20}BO_2P$): C 76.12 H 511 Found: C 75.50 H 5.11.

Yield: 773 mg (98%.).

$^{31}P\{^1H\}$-NMR (CH_2Cl_2) δ = -11.1(s).

^{11}B-NMR (CH_2Cl_2) δ = 31.7 (br, s).

^1H NMR ($CDCl_3$): δ = 8.05-7.9(m, 2 H, BC_6H_5), 7.57 (t, $^3J_{HH}$ = 1.5 Hz, 1 H, BC_6H_5), 7.54 (t, $^3J_{HH}$ = 2.7 Hz, 1 H, BC_6H_5), 7.51 (t, $^3J_{HH}$ = 1.5 Hz, 1 H, BC_6H_5), 7.5-7.4 (m, 5 H, Ph), 7.35-7.25 (m, 5 H, Ph), 7.07 (dt, $^3J_{HH}$ = 7.8 Hz, 1 H, C_6H_3), 6.93 (t, $^3J_{HH}$ = 7.9 Hz, 1 H, C_6H_3), 6.82 (t, $^3J_{HH}$ = 7.9 Hz, 1 H, C_6H_3), 3.62 (br., s, 2 H CH_2).

6.5.1 (b) Diphenyl- (2-pentaflurophenyl-benzo [1,3,2]-dioxaborol-4-ylmethyl)-phosphane 16b:

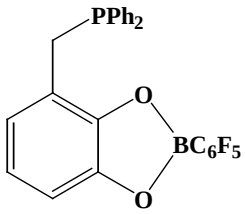

Yield: 891 mg (92%).

Elemental analysis: Calcd. for ($C_{25}H_{15}BF_5O_2P$): C 66.26 H 3.34 found: C 64.53 H 3.99.

$^{31}P\{^{1}H\}$-NMR ($CDCl_3$) δ = -9.3 (broad, s).

^{11}B-NMR (CH_2Cl_2) δ = 21.6 (broad, s) 14.3 (broad, s), 9.9 (broad, s), 5.3 (broad, s).

^{1}H NMR ($CDCl_3$): δ = 7.7 -7.2 (m, 10 H, Ph), 7.1-6.6 (broad, m, 3 H, cat.), 3.62 (s, CH_2).

6.5.2. (a) Synthesis of Diphenyl- (2-phenyl-benzo [1,3,2]-dioxaborol-4-ylmethyl)-phosphane-3- (Dimethyl amino pyridine) 17a:

To 560 mg (1.42 mmol.) of Diphenyl- (2-phenyl-benzo [1,3,2]-dioxaborol-4-ylmethyl)-phosphane was added 15 ml of dichloromethane. Stirring for 5 minutes was followed by addition of 172 mg (1.42 mmol.) of 4-dimethyl amino pyridine. The reaction mixture was stirred for another 30 minutes, dichloromethane was stripped off, and the white powder was dried for another 30 minutes. The residue was obtained quantitatively and was characterized by spectroscopic techniques (see below). The white powder was again dissolved in a minimum amount of dichloromethane, and few drops of THF were added. Storing the solution at room temperature gave crystals suitable for single crystal X-ray diffraction study.

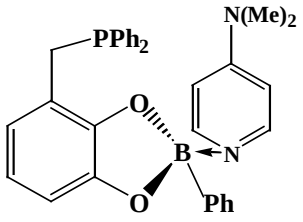

Yield: 697 mg (95%); **Melting point:** 167ºC.

Elemental analysis: Calcd. for ($C_{32}H_{30}BN_2O_2P$): C 74.43 H 5.86 N 5.43 Found: C 74.20 H 5.93 N 5.41.

$^{31}P\{^{1}H\}$-NMR ($CDCl_3$) δ = -17.14 (s).

^{11}B-NMR ($CDCl_3$) δ = 11.07 (s).

^{1}H NMR ($CDCl_3$): δ = 8.25 (d, $^{3}J_{HH}$ = 7.34 Hz, 2 H, DMAP), 7.55-7.40 (m, 6 H), 7.30-7.20 (m, 9 H), 6.62 (dt, $^{3}J_{HH}$ = 7.34 Hz, 1 H, C_6H_3), 6.55-6.45 (m, 3 H), 6.39 (dt, $^{3}J_{HH}$ = 8.03 Hz, 1 H, C_6H_3), 3.5 (br, s, 2 H, CH_2), 3.01 (br, s, 6 H, DMAP).

6.5.2 (b) Synthesis of Diphenyl- (2-pentaflurophenyl-benzo [1,3,2]-dioxaborol-4-ylmethyl)-phosphane-3- (Dimethyl amino pyridine) 17b:

To 428 mg (0.9 mmol.) of Diphenyl- (2-phenyl-benzo [1,3,2]-dioxaborol-4-ylmethyl)-phosphane was added 10 ml of dichloromethane. Stirring for 5 minutes was followed by addition of 110 mg (0.9 mmol.) of 4-dimethyl amino pyridine. The reaction mixture was stirred for another 30 minutes, dichloromethane was stripped off, and the white powder was dried for another 30 minutes. The residue was obtained in quantitative yields.

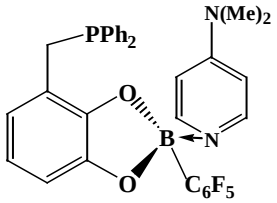

^{31}P{1H}-NMR ($CDCl_3$) δ = -12.6 (s), -13.9 (s).

^{11}B-NMR ($CDCl_3$) δ = 18.0 (br, s), 14.25 (s, major), 8.47 (d).

6.5.3. Synthesis of Dichloro bis {Diphenyl- (2-phenyl-benzo [1,3,2]-dioxaborol-4-ylmethyl)-phosphane}-palladium, 18:

To the THF solution of 397 mg (0.5 mmol) of bis-diphenyl-{2-phenyl-benzo (1,3,2) dioxaborol-4-ylmethyl}-phosphane palladium dichloride was added 122mg (1mmol) of Phenyl boronic acid. This reaction mixture was stirred for two hrs at room temperature. Finally the solvent was evaporated in vacuum to give a yellow powder. The powder was then dissolved in THF and the saturated solution kept at +4ºC. Microcrystals of orange yellow color were obtained, dried in vacuum, and characterized by analytical techniques.

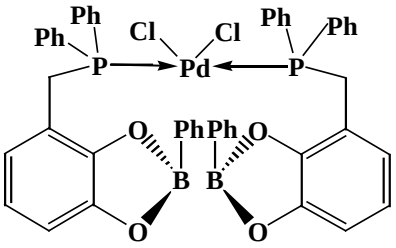

Yield: 333 mg (69%); **Melting point:** 240°C (dec).

Elemental Analysis: Calcd. for ($C_{50}H_{40}B_2Cl_2O_4P_2Pd$): C 62.19 H 4.18 Found: C 61.2 H 4.68.

^{31}P{^{1}H}-NMR ($CDCl_3$) δ = 21.2.

^{11}B-NMR ($CDCl_3$) δ = 29.06.

^{1}H NMR ($CDCl_3$): δ = 7.8-7.25 (m, 30 H, Ph), 7.1-6.7 (m, 6 H, C_6H_3), 4.3 (br, d, $^{2}Jp_H$, = 11.24 Hz, 2 H, CH_2), 4.2 (t, $^{2}J_{PH}$ = 3.8 Hz, 2 H, CH_2).

6.5.4. Synthesis of Dichloro palladium bis {Diphenyl- (2-phenyl-benzo [1,3,2]-dioxaborol-4-ylmethyl)-phosphane-3- (Dimethyl amino pyridine)}, 19:

In a dry schlenk was taken 300 mg (0.6 mmol) of Diphenyl-(2-phenyl-benzo[1,3,2]-dioxaborol-4-ylmethyl)-phosphane-3-(Dimethyl amino pyridine), 10 ml

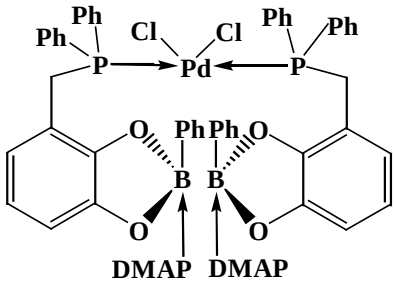

of dry THF was added to it. In another flask (COD)$PdCl_2$ [85 mg (0.3 mmol)] was dissolved in 5 ml of dichloromethane and added to the above schlenk. Within few minutes yellow precipitate starts falling out, which was filtered, dried and characterized by NMR.

Yield: 272 mg (75%).

^{31}P{^{1}H}-NMR (DMSO) δ = 82.1 (d, $^{2}J_{PP}$ = 32 Hz), 29.3 (d, $^{2}J_{PP}$ = 30 Hz), 19.4 (s).

^{11}B-NMR (DMF) δ = 10.4 (s).

6.5.5. General procedure for the syntheses of borates 20 and 22:

Catechol phosphines **9b-d** (355 mg, 1.15 mmol) dissolved in 10 ml of dry DMF were stirred for 5 minutes. To these solutions was added 35.6 mg (0.57 mmol) of boric acid and the reaction mixture was then heated to 40°C under slight (12 torr) vacuum. After 30 minutes DMF was taken off, the obtained white residue was washed thrice with diethyl ether and finally dried in vacuum. The remaining solid was then dissolved in 5 ml acetonitrile and 0.35 ml (2.5 mmol) of triethylamine was added. The resulting solution was again stirred at room temperature under slight vacuum (12 torr) for 15 minutes. Finally the reaction mixture was taken to dryness.

Crystals of **20** and **22** were grown from a concentrated THF solution at –28°C.

Triethyl Ammonium [Bis- diphenyl phosphane {benzo (1, 3) dioxa-4-methyl}] 2-borate (20):

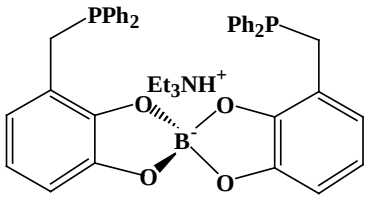

Elemental analysis: Calcd. for: [$C_{44}H_{46}$ BNO_4P_2): C 72.83 H 6.39 N 1.93 Found: C 70.83 H 6.78 N 1.70.

Yield: 343 mg (83%). **Melting point:** 92ºC.

^{31}P{^{1}H}-NMR (CD_3CN) δ = -13.1 (s).

^{11}B-NMR (CD_3CN) δ = 14.33 (s).

^{1}H NMR (CD_3CN): δ = 7.6 to 7.26 (m, 20 H, Ph), 6.8 (broad, 1 H, NH), 6.44 to 6.34 (m, 6 H, C_6H_3), 3.51 (dd, 2 H, $^{2}J_{HH}$ = 13.9 Hz, $^{2}J_{PH}$ = 0.9 Hz, CH_2), 3.44 (d, 2 H, $^{2}J_{PH}$ = 13.9 Hz, CH_2), 3.13 (q, 6 H, $^{3}J_{HH}$ = 7.3 Hz, NCH_2), 1.23 (t, 9 H, $^{3}J_{HH}$ = 7.4 Hz, CH_3).

^{13}C{^{1}H} NMR (CD_3CN): δ = 151.3 (d, J_{PC} = 1.2 Hz, C_6H_3), 149.9 (d, J_{PC} = 4.2 Hz, C_6H_3), 139.5 (d, $^{1}J_{PC}$ = 16.5 Hz, *i*-C), 139.2 (d, $^{1}J_{PC}$ = 16.3 Hz, *i*-C), 132.78 (d, $^{2}J_{PC}$ = 18.9 Hz, *m*-C), 132.76 (d, $^{2}J_{PC}$ = 18.9 Hz, *m*-C), 128.53 (s, *p*-C), 128.48 (s, *p*-C), 128.40 (d, $^{2}J_{PC}$ = 6.5 Hz, *o*-C), 128.38 (d, $^{2}J_{PC}$ = 6.7 Hz, *o*-C), 118.9 (d, J_{PC} = 8.4 Hz, C_6H_3), 117.1 (d, J_{PC} = 1.5 Hz, C_6H_3), 105.9 (br, C_6H_3), 47.0 (s, NCH_2), 27.5 (d, $^{1}J_{PC}$ = 13.4 Hz, PCH_2), 8.2 (s, $NCCH_3$).

Triethyl Ammonium [Bis- diphenyl phosphane {benzo (1, 3) dioxa-5-methyl}] 2-borate (22):

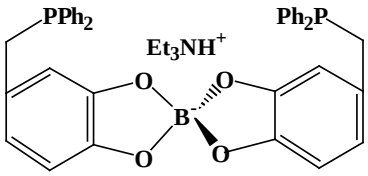

Elemental analysis: Calcd. for ($C_{44}H_{46}BNO_4P_2$): C 72.83 H 6.39 N 1.93. Found: C 72.90 H 6.39 N 1.90.

Yield: 372 mg (90%); **Melting point:** 197ºC.

$^{31}P\{^1H\}$-NMR (CD_3CN) δ = -10.2 (s).

^{11}B-NMR (CD_3CN) δ = 14.3 (s).

^1H NMR (CD_3CN): δ = 7.50 to 7.40 (m, 8 H, C_6H_5), 7.40 to 7.30 (m, 12 H, C_6H_5), 6.8 (broad, 1 H, NH), 6.37 to 6.30 (broad m, 6 H, C_6H_3), 3.37 (s, 4 H, CH_2), 3.08 (q, 6 H, $^3J_{HH}$ = 7.3 Hz, NCH_2), 1.18 (t, 9 H, $^3J_{HH}$ = 7.3 Hz, $NCCH_3$).

$^{13}C\{^1H\}$ NMR (CD_3CN): δ = 152.5 (d, J_{PC} = 1.3 Hz, C_6H_3), 151.0 (d, J_{PC} = 2.7 Hz, C_6H_3), 140.2 (d, $^1J_{PC}$ = 17.3 Hz, *i*-C), 133.8 (d, $^3J_{PC}$ = 18.6 Hz, *m*-C), 129.6 (s, *p*-C), 129.3 (d, $^2J_{PC}$ = 6.5 Hz, *o*-C), 127.4 (d, J_{PC} = 8.3 Hz, C_6H_3), 119.3 (d, J_{PC} = 7.5 Hz, C_6H_3), 110.3 (d, J_{PC} = 6.7 Hz, C_6H_3), 108.3 (s, C_6H_3), 47.9 (s, NCH_2), 35.6 (d, $^1J_{PC}$ = 13.6 Hz, PCH_2), 9.12 (s, $NCCH_3$).

6.5.6. Synthesis of the silver complex [Ag (20)], 21:

To a solution of 130 mg (0.179 mmol) of solid **20** was added 5 ml of DMF, and the mixture was stirred for 5 minutes. 46 mg (0.179 mmol) of silvertriflate was then added with constant stirring. After an hour, the reaction mixture was diluted with 60 ml of diethyl ether. A white precipitate was produced immediately which was filtered off and dried at 40°C/0.001 mbar for 3 hours. White crystals were obtained from DMF: Ether (1:1) mixture at room temperature.

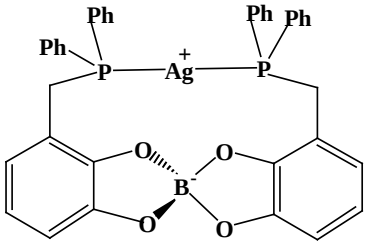

Elemental Analysis: Calcd. for [$C_{38}H_{30}AgBO_4P_2$ (731.28)]: C 62.41 H 4.14 Found: C 60.81 H 4.12.

ESI-MS (positive): m/e = 733.06 $(M+ H)^+$, 755.07 $(M+Na)^+$.

Yield: 91.6 mg (70%); **Melting point:** 253ºC.

$^{31}P\{^{1}H\}$-NMR ($CDCl_3$): δ = 2.9 ($^{1}J_{P-107/109Ag}$ = 585/507 Hz).

$^{11}B\{^{1}H\}$-NMR ($CDCl_3$) δ = 14.3.

^{109}Ag NMR ($CDCl_3$): δ = 645.

^{1}H NMR ($CDCl_3$): δ = 7.6 to 7.22 (m, 20 H, Ph), 6.80 (broad d, $^{3}J_{HH}$ = 7.7 Hz, 2 H, C_6H_3), 6.53 (dd, $^{3}J_{HH}$ = 7.7 Hz, 2 H, C_6H_3), 6.21 (broad d, $^{3}J_{HH}$ = 7.8 Hz, 2 H, C_6H_3), 3.95 (d of pseudo-t, $^{2}J_{HH}$ = 13.3 Hz, ΣJ_{PH} = 4.6 Hz, 2 H, CH_2), 3.51 (dd pseudo-t, $^{2}J_{HH}$ = 13.3 Hz, $^{3}J_{AgH}$ = 7.5 Hz, ΣJ_{PH} = 12.3 Hz, 2 H, CH_2).

$^{13}C\{^{1}H\}$ NMR ($CDCl_3$): δ = 151.4 (m, C_6H_3), 149.0 (m, C_6H_3), 133.1 (m, ΣJ_{PC} = 16.2 Hz, $^{4}J_{AgC}$ = 2.4 Hz, *m*-C), 132.5 (m, ΣJ_{PC} = 15.3 Hz, $^{4}J_{AgC}$ = 2.4 Hz, *m*-C), 132.2 (*i*-C), 131.9 (*i*-C), 131.0 (s, *p*-C), 129.8 (s, *p*-C), 129.1 (pseudo-t, ΣJ_{PC} = 9.6 Hz, *o*-C), 128.9 (pseudo-t, ΣJ_{PC} = 10.2 Hz, *o*-C), 119.5 (m, C_6H_3), 118.9 (m, C_6H_3), 113.2 (s, C_6H_3), 109.6 (m, C_6H_3), 30.8 (d, $^{1}J_{PC}$ = 0.8 Hz, CH_2).

$^{31}P\{^{1}H\}$ NMR (DMF-d_7): δ = 3.0 ($^{1}J_{P-107/109Ag}$ = 571/494 Hz).

^{109}Ag NMR (DMF-d_7): δ = 702.

^{1}H NMR (DMF-d_7): δ = 8.00 to 7.86 (m, 12 H, Ph), 7.68 (m, 4 H, Ph), 7.58 (m, 4 H, Ph), 6.72 (broad d, $^{3}J_{HH}$ = 7.7 Hz, 2 H, C_6H_3), 6.57 (dd, $^{3}J_{HH}$ = 7.7/7.7 Hz, 2 H, C_6H_3), 6.48 (broad d, $^{3}J_{HH}$ = 7.8 Hz, 2 H, C_6H_3), 4.09 (m, $^{2}J_{HH}$ = 13.3 Hz, $^{3}J_{HAg}$ = 7 Hz, ΣJ_{PH} = 14 Hz, 2 H, CH_2), 3.95 (d pseudo-t, $^{2}J_{HH}$ = 13.3 Hz, ΣJ_{PH} = 4 Hz, 2 H, CH_2).

6.5.7. Synthesis of the Ag-B macrocycle $Ag_2(22)_2$, 23:

To 330 mg (0.455 mmol) of **22** was dissolved under stirring (15 min) in13 ml of DMF. To this solution was added 117 mg (0.455 mmol) of silver triflate and stirring was continued for an hour at room temperature. 40 ml of diethyl ether was added and white precipitate was produced immediately. The precipitate was filtered off and dried at 50°C/0.001 mbar for 3 hours.

Yield: 470.9 mg (70%); **Melting Point:** 180ºC.

Elemental analysis: Calcd. for [$C_{76}H_{60}Ag_2B_2O_8P_4$ X 2DMF (1460.15)]: C 61.22 H 4.64 N 1.74 Found: C 60.03 H 4.83 N 2.27.

ESI-MS (positive mode) : m/e = 1485.13 $(M + Na)^+$, 754.06 $(M + Na)^{2+}$.

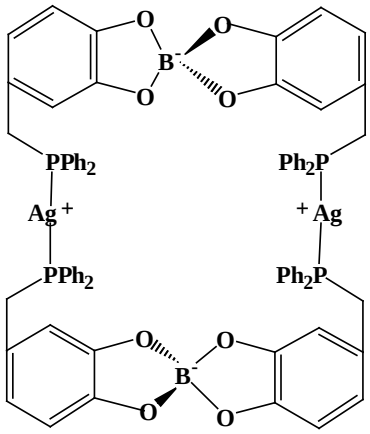

$^{31}P\{^1H\}$-NMR (DMF-d_7) δ = 12.8 (d-broad, $^1J_{Ag\text{-}P}$ = 313.7 Hz).

$^{11}B\{^1H\}$-NMR (DMF-d_7) δ = 14.6.

^1H NMR (DMF-d_7): δ = 7.8 to 7.3 (m, 40 H, Ph), 6.42 (s, 4 H, C_6H_3.), 6.34 (d, $^3J_{HH}$ = 8.1 Hz, 4 H, C_6H_3), 6.24 (dd, $^3J_{HH}$ = 7.7 Hz, 4 H, C_6H_3), 3.76 (broad, s, 8 H, CH_2).

6.5.8. Triethyl ammonium [Dichloro palladium bis {diphenyl- (benzo- [1,3]-dioxo-4-ylmethyl)-phosphane}] 2-borate(104):

To the 130 mg(0.179mmol) of solid, Bis[{benzo(1, 3, 2) dioxaborol-3-methyl}-diphenyl phosphane] was added 5ml of DMF and was stirred for 5 mins. To this solution was added 51mg (0.179mmol) of (COD)$PdCl_2$ with constant stirring. The reaction mixture was stirred at room temp. for another 24 hours. To the DMF solution was added 60ml of diethyl ether. Immediately a orange precipitate falls out. This was filtered out and dried at 40^0C at 0.001 mbar for 3 hours. The dried orange-red powder was than characterized using different analytical techniques.

M.P 142ºC

$^{31}P\{^1H\}$-NMR (DMF-d_7) δ = 40.7 (s), 31.2 (s), 19.5(s).

$^{11}B\{^1H\}$-NMR (DMF-d_7) δ =14.6.

ESI-MS(positive): m/e = 743.07 $[(catphos)_2Pd+2H+Na]^+$, where (catphos) = $C_{19}H_{15}O_2P$, 1465.15 $\{[(catphos)_2Pd+2H]_2+Na\}^+$.

ESI-MS (negative mode): m/e = 719.07 $[(catphos)_2+HPd]^-$, 404.96 $[(catphos)BOHCl]^-$.

6.6. Transition metal complexes of templated symmetric bisphosphine ligands and their potential application in catalysis

6.6.1. Synthesis of palladium-bis {diphenyl- (benzo- [1, 3]-µ-oxo-k-oxo-4-ylmethyl) phosphane)}- gallium chloride (25):

400 mg (1.29 mmol) of 3-(Diphenyl-phosphinoylmethyl)-benzene-1, 2-diol, 114 mg (0.64 mmol) of gallium trichloride, 185 mg (0.64 mmol) cyclooctadienyl palladium dichloride and 0.5 ml (3.25 mmol) of triethyl amine were placed in a dried 100ml Schlenk tube, 10 ml of dried DMF was added and the reaction mixture was stirred at room temperature for 3 hours. The precipitate was filtered through a P4 glass filter frit with a celite bed. The filtrate was dried in vacuum. The red powder was dissolved in 10 ml DMF, diluted by adding 80 ml of diethyl ether and filtered; this was repeated one more time. The remaining residue was dried in vacuum at 70ºC.

Crystals were grown from a 1:1 mixture of dichloromethane: diethyl ether or THF: diethyl ether.

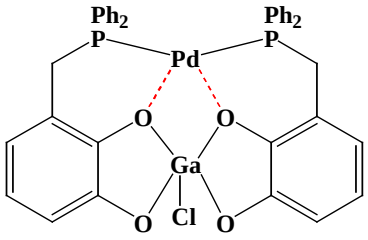

Yield: 369mg (70%); **Melting Point:** 358ºC.

Elemental analysis: Calcd. for $[C_{38}H_{30}ClGaO_4P_2Pd$ (824.17 g/mol)]: C 55.38 H 3.67 Found: C 53.02 H 3.50.

ESI-MS (positive mode): m/e = 825.0 $(M+H)^+$, 847.0 $(M+Na)^+$, 857.0 $(M+2O+H)^+$.

ESI-MS (negative mode): m/e = 823.0 $(M-H)^-$, 856.9 $(M+Cl)^-$.

$^{31}P\{^1H\}$-NMR ($CDCl_3$) δ = 64.7 (s).

^{1}H NMR ($CDCl_3$): δ = 7.5-6.80 (m, 20 H, Ph), 6.80 (broad, C_6H_3), 6.51 (t, $^{3}J_{HH}$ = 7.8 Hz, C_6H_3), 6.1 (d, $^{3}J_{HH}$ = 7.4, C_6H_3), 3.55 (d, $^{2}J_{PH}$ = 12.4 Hz, 2 H, CH_2), 3.2-3.1 (br, s, CH_2).

6.6.2. Synthesis of palladium-bis {diphenyl- (benzo- [1, 3]-μ-oxo- k-oxo-4-ylmethyl)-phosphane)}-tin dichloride (26a):

A mixture of 3-(Diphenyl-phosphinoylmethyl)-benzene-1, 2-diol (600 mg, 1.95 mmol), $SnCl_4$ (1.1 ml, 0.97 mmol), $(COD)PdCl_2$ (280 mg, 0.97 mmol), and NEt_3 (0.8 ml, 5.7 mmol) in dry DMF (20 ml) was stirred for 6 days at room temperature. The red suspension was filtered through celite. Solvents were evaporated in vacuum. The residue was washed with CH_2Cl_2 (10 ml) and dissolved in little DMF. The same volume of CH_2Cl_2 and, finally, small portions of diethyl ether were added until a precipitate began to form. The mixture was stored overnight at +4°C to yield a microcrystalline solid which was collected by filtration and dried in vacuum for 4 hours at 70°C to yield 40% of **26a.** Increasing the reaction temperature to 60ºC improved the yield and **26a** was isolated 60%.

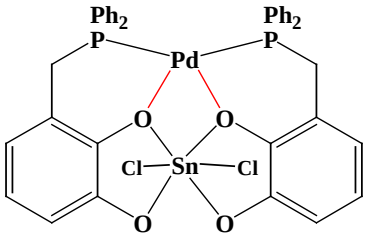

Yield: 528 mg (60%); **Melting point:** 214°C.

Elemental analysis: Calcd. for (**26a** × DMF): C 50.16 H 3.80 N 1.43 found: C 49.92 H 3.77 N 1.58.

^{119}Sn{^{1}H} CP-MAS NMR: δ_{iso} = -455.

^{31}P{^{1}H} CP-MAS NMR: δ_{iso} = 79.5, 74.1; J_{PP} = 41 Hz (from 2D-*J*-resolved).

^{31}P{^{1}H}-NMR (DMF-d_7) δ = 77,00 (br, s).

^{1}H NMR (DMF-d_7) δ = 7.7 to 7.25(m, broad, 20 H, C_6H_5), 6.9 (d, $^{3}J_{HH}$ = 8.0 Hz, 2 H), 6.58 (broad, s, 2 H), 6.1 to 6.03 (broad, s, 2 H), 4.0 to 3.7 (broad, 4 H, CH_2).

Cooling down the **26a** to –30ºC results into appearance of a new ^{31}P resonance at 55.5 ppm, which grew in intensity upon cooling to –55ºC. This observation revealed that there should be two products that are in fast equilibrium at room temperature and can be access

at reduced temperatures. The theoretical calculations (DFT) and 2D NMR measurements revealed the formation of solvent (DMF) adduct of **26a** at lower temperatures, which is designated as **27a**.

^{1}H NMR (DMF-d7, 223K): assignments were derived from ^{1}H-TOCSY, ^{1}H-NOESY, ^{1}H, ^{31}P-HMQC NMR spectra):

26a:

^{31}P{^{1}H}-NMR (DMF-d_7, 223K) δ = 77,0 (br, s).

^{1}H NMR (DMF-d_7, 223K) δ = 7.87, 7.73, 7.62 (all br, 10 H, C_6H_5), 7.57, 7.43, 7.28 (all br, 10 H, C_6H_5), 6.93 (br d, 2 H, C_6H_3), 6.55 (br t, 2 H, C_6H_3), 5.98 (br d, 2 H, C_6H_3), 4.64 (br m, 2 H, PCH_2), 3.86 (br m, 2 H, PCH_2).

27a:

^{31}P{^{1}H}-NMR (DMF-d_7, 223K) δ = 55,5 (br, s).

^{1}H NMR (DMF-d_7, 223K) δ = 7.74, 7.68, 7.43 (all br, 10 H, C_6H_5), 7.6 – 6.5 (br, 6 H, C_6H_3), 4.16 (br, 4 H, PCH_2).

6.6.3. Synthesis of palladium-bis {diphenyl- (benzo- [1, 3]-μ-oxo- k-oxo-4-ylmethyl)-phosphane)}-dimethyl tin (26b):

Dry DMF (20 ml) was added to a mixture of **9b** (550 mg, 1.79 mmol), Me_2SnCl_2 (196 mg, 0.89 mmol), $(COD)PdCl_2$ (250 mg, 0.89 mmol) and Et_3N (0.93 ml, 5.34 mmol). The reaction mixture was stirred for 3 hours at room temperature to give a red suspension, which was filtered through a celite bed in a P4 glass filter frit. The red filtrate was stored overnight at –28ºC. The colorless crystalline precipitate formed was separated by decantation, the solution diluted by addition of 50 ml of diethyl ether, and stored at +4ºC. Dark red crystals formed which were collected by decantation and dried in vacuum at 120ºC for 4 hours.

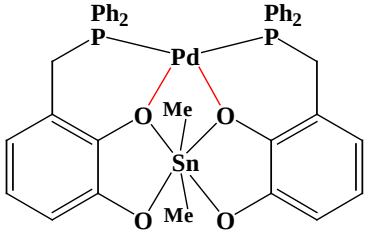

Elemental analysis: Calcd. for ($C_{40}H_{36}O_4P_2PdSn$ + DMF): C 54.78 H 4.81 N 1.49 Found: C 54.68 H 4.78 N 1.41.

Yield: 733 mg (95%); **Melting point:** 310ºC.

ESI-MS (positive mode): m/e = 869.02 (100%) $(M+H)^+$.

$^{31}P\{^1H\}$ NMR ($CDCl_3$, 303 K): δ = 74.6 (broad, s).

^1H NMR ($CDCl_3$, 303 K): δ = 7.96 (broad, s, 1 H, DMF), 7.4-6.8 (m, 20 H, Ph), 6.74 (d, $^3J_{HH}$ = 8.0 Hz, 2 H, C_6H_3), 6.34 (t, $^3J_{HH}$ = 7.91 Hz, 2 H, C_6H_3), 5.61 (d, $^3J_{HH}$ = 7.8 Hz, 2 H, C_6H_3), 3.6-3.2 (broad, 4 H, CH_2), 2.89 (s, 3 H, DMF), 2.82 (s, 3 H, DMF), 0.53 (s, 6 H, SnMe).

$^{13}C\{^1H\}$ NMR ($CDCl_3$, 303 K): δ = 162.6 (s, DMF), 154.5 (br., s), 148.9 (s), 132.4 (br., s), 131.7 (s), 128.5 (t, J_{PC} = 4.6 Hz), 120.7 (s), 119.4 (s), 115.8 (s) 115.6 (s), 36.4 (s, DMF), 33.4 (br., CH_2), 31.4 (s, DMF), 25.6 (s, $SnCH_3$).

6.6.4. Synthesis of platinum -bis {diphenyl- (benzo- [1, 3]-µ-oxo-k-oxo-4-ylmethyl) phosphane)}-dimethyl tin (28):

Complex **28** was synthesized under identical condition as described in section 6.6.3 for **26b**. Crystals were grown from a concentrated DMF solution of the light yellow colored product at room temperature.

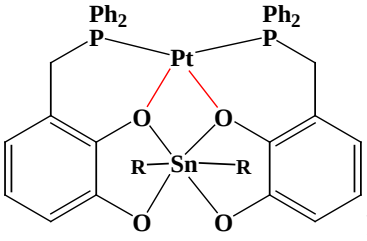

R = Me

Yield: 809 mg (95%); **Melting point:** 354°C (dec).

Elemental analysis: Calcd. for ($C_{40}H_{36}O_4P_2PtSn$ + DMF): C 50.17 H 4.21 N 1.36 Found: C 50.09 H 4.21 N 1.41.

ESI-MS (positive): m/e = 957.08 $(M+H)^+$, 979.07 $(M+Na)^+$.

$^{31}P\{^1H\}$-NMR ($CDCl_3$) δ = 39.5 (s, $^1J_{Pt-P}$ = 2041 Hz).

$^{31}P\{^{1}H\}$-NMR ($CDCl_3$, 213K) δ = 41.7 (s, $^{1}J_{Pt\text{-}P}$ = 2042 Hz).

$^{119}Sn\{^{1}H\}$-NMR ($CDCl_3$) δ = -183.8 (s).

^{1}H NMR ($CDCl_3$) δ = 7.99 (br, s, 1 H, DMF), 7.4 - 6.9(m, 20 H, Ph), 6.77 (d, $^{3}J_{HH}$ = 7.7 Hz, 2 H, C_6H_3), 6.39 (t, $^{3}J_{HH}$ = 7.78 Hz, 2 H, C_6H_3), 5.64 (d, $^{3}J_{HH}$ = 7.24 Hz, 2 H, C_6H_3), 3.6 - 3.2 (br., s, 4 H, CH_2), 2.92 (s, 3 H, DMF), 2.85 (s, 3 H, DMF), 0.62 (broad, s, 6 H, Sn-Me).

6.6.5. Syntheses of palladium- bis {diphenyl- (benzo- [1, 3]-μ-oxo-k-oxo-4-ylmethyl) phosphane)}-bismuth chloride (29):

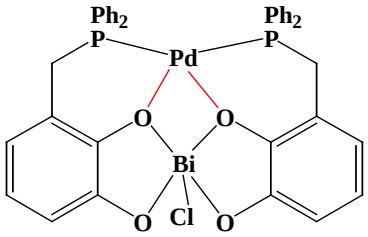

The mixture of 280 mg (0.90 mmol) of 3-(Diphenyl-phosphinoylmethyl)-benzene-1, 2-diol, 143 mg (0.45 mmol) of $BiCl_3$, 130 mg (0.45 mmol) of $(COD)PdCl_2$ and 0.32 ml (2.27 mmol.) of Et_3N was dissolved in 8 ml of dry DMF. Though the ^{31}P NMR indicated completion of the reaction in 3 hours, stirring was continued overnight. The dark-red suspension was filtered through a P4 glass filter frit; the filtrate was kept at –28ºC overnight. White needle like crystals of triethyl ammonium chloride were decanted off. The filtrate was diluted with excess of ether and the precipitate obtained was dissolved in dichloromethane. Dark red crystals of good quality were grown from a concentrated dichloromethane solution at room temperature. The crystals were filtered off and dried in vacuo.

Yield: 303 mg (70%); **Melting point:** 273ºC (dec).

Elemental analysis: Calcd. for ($C_{38}H_{30}BiO_4P_2Pd$ + CH_2Cl_2): C 44.68 H 3.08 Found: C 44.51 H 3.03.

ESI-MS (positive mode): m/e: 927.04 $(M\text{-}Cl)^+$, 969.03 $(M+Li)^+$.

$^{31}P\{^{1}H\}$-NMR (DMF-d7) δ = 70.8 (br, s), 52.1 (br, s).

^{1}H NMR (DMF-d7) δ = 8.3 (br, s, 1 H, DMF) 7.9 - 7.2 (m, 20 H, Ph), 6.8 - 6.1 (br., s, 6 H, C_6H_3), 6.0 (s, 2 H, CH_2Cl_2), 3.9 - 3.70 (br., d, 4 H, CH_2), 3.1 - 2.8 (br., 6 H, DMF).

^{31}P{^{1}H}-NMR (DMF-d7, 223K) δ = 69.8 (s), 50.0 (s).

^{1}H NMR (DMF-d7, 223K) δ = 8.0 (s, 1H, DMF), 8.0-7.9 (br, s, *o*-Ph), 7.7 (t, $^{3}J_{HH}$ = 6.9 Hz, Ph), 7.6 (t, $^{3}J_{HH}$ = 7 Hz, Ph), 7.5 (t, $^{3}J_{HH}$ = 7.1 Hz, Ph), 7.3 (t, $^{3}J_{HH}$ = 7.2 Hz, Ph), 7.2-7.1 (br, s, Ph), 6.6 (t, $^{3}J_{HH}$ = 7.3 Hz, C_6H_3), 6.5 (t, $^{3}J_{HH}$ = 7.1 Hz, C_6H_3), 6.3 (t, $^{3}J_{HH}$ = 7.2 Hz, C_6H_3), 6.2 (s, CH_2Cl_2), 3.9 (br, s, CH_2), 3.8 (d, $^{2}J_{PH}$ = 11.1 Hz, CH_2).

6.6.6. (a) Synthesis of bis {palladium- bis {diphenyl- (benzo- [1, 3]-μ-oxo-k-oxo-4-ylmethyl) phosphane)}- zirconium (30):

200 mg (0.64 mmol) of 3-(Diphenyl-phosphinoylmethyl)-benzene-1, 2-diol, 75.6 mg (0.32 mmol) of zirconium-tetrachloride, 124 mg (0.32 mmol) Bis (benzonitrile) palladium dichloride and 423 mg (1.3 mmol) of Cesium carbonate were placed in a Schlenk tube. The solid mixture was dissolved in 15 ml of DMF and stirred for 6 days at room temperature.

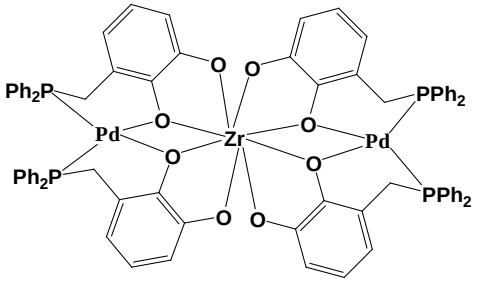

The red colored suspension was filtered, and the filtrate evacuated to dryness. The red residue was dissolved in DMF: dichloromethane (1:1), and diluted with 50 ml of ether. The formed precipitate was filtered off and dried in vacuum. Crystals suitable for X-ray measurements were grown by slow diffusion of diethyl ether into a concentrated DMF solution of **30**. As similar reactions with gallium (**25**) and tin (**26b**), with triethyl amine as base have shown that the reaction time can be reduced to 3 hours, similar behavior is expected with zirconium as well.

Yield: 293 mg (60%); **Melting point:** 390°C (dec).

Elemental analysis: Calcd. for ($C_{76}H_{60}O_8P_4Pd_2Zr$ + 3DMSO): C 55.85 H 4.46 Found: C 55.38 H 4.40.

^{31}P{^{1}H}-NMR (DMSO-d6) δ = 52.4 (s).

^{1}H NMR (DMSO-d6): δ = 7.53 (t, $^{3}J_{PH}$ = 8.72 Hz, 16 H, Ph), 7,36 (t, $^{3}J_{HH}$ = 7.34 Hz, 8 H, Ph), 7.15 (t, $^{3}J_{HH}$ = 6.8 Hz, 16 H, Ph), 6.0 - 6.2 (m, 8 H, C_6H_3), 5.97 (d, $^{3}J_{HH}$ = 7.11 Hz, 4 H, C_6H_3), 3.64 (br, d, 8 H, CH_2).

6.6.6 (b) Synthesis of dicyclopentadienyl {palladium- bis {diphenyl- (benzo- [1, 3]-μ-oxo-k-oxo-4-ylmethyl) phosphane)}- zirconium (30A):

In a Schlenk was added 190mg (0.62 mmol.) of 3-(Diphenyl-phosphinoylmethyl)-benzene-1,2-diol, 90 mg (0.31 mmol.) of Cp_2ZrCl_2, 118 mg (0.31 mmol.) Bis(benzonitrile) palladium dichloride and 0.21ml (1.5 mmol.) of Et_3N. This was dissolved in 15 ml of dried DME:THF and stirred for 2 hours at room temperature. A dark red reaction mixture was filtered and the precipitate was dissolved in THF. This was diluted by adding excess of diethyl ether, the residue formed was filtered and dried in vacuum for two hours. Microcrystals of the product were obtained from THF: Et_2O solution at room temperature, dried in vacuum and characterized by NMR.

^{31}P{^{1}H}-NMR (DMSO-d_6) δ = 49.8(s).

^{1}H NMR (DMSO-d6): δ = 8.0-6.9 (m, Ph), 6.7-5.6(br., m, C_6H_3), 3.7-3.5 (br, d, CH_2).

6.6.7. Synthesis of tetrakis {palladium- bis {diphenyl- (benzo- [1, 3]-μ-oxo-k-oxo-4-ylmethyl) phosphane)- yttrium} μ_4-hydroxy tri-chloride (31):

To a mixture of 320 mg (1.04 mmol) of 3-(Diphenyl-phosphinoylmethyl)-benzene-1,2-diol, 101 mg (0.52 mmol) of YCl_3, 148 mg (0.52 mmol) of $(COD)PdCl_2$ and 0.36 ml (2.59 mmol) of Et_3N was added 10 ml of dry DMF. This reaction mixture was stirred for 3 hours at room temperature to give a dark red suspension, which was filtered through celite bed in a P4 glass filter frit. The red filtrate was kept at –28ºC overnight, to give needle like white crystals. The solution was decanted to another Schlenk tube and kept at room temperature for crystallization. The dark red colored square crystals separated within 24 hours. The product was dried at 120ºC for 4 hours.

Yield: 275 mg (60%); **Melting point:** 345ºC (dec).

Elemental analysis: Calcd. for ($C_{164}H_{148}Cl_3N_4O_{21}P_8Pd_4Y_4$): C 54.02 H 4.09 N 1.54 Found: C 53.14 H 4.04 N 1.20.

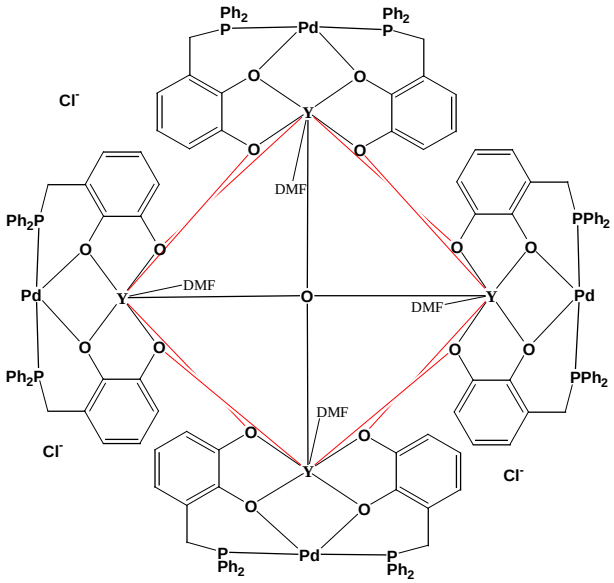

ESI-MS (positive mode): m/e = 1644.95 $(M\text{-}Cl+LiF_2)^{2+}$, 1082.7 $(M\text{-}3Cl)^{3+}$.

$^{31}P\{^{1}H\}$-NMR ($CDCl_3$): δ = 69.8 (s).

^{1}H NMR ($CDCl_3$) δ = 7.95 (s, broad, DMF) 7.7 - 6.7(m, 80 H, Ph), 6.25 (t, $^{3}J_{HH}$ = 7.2 Hz, 8 H, C_6H_3), 6.13 (q, $^{3}J_{HH}$ = 8.70 Hz, 8 H, C_6H_3), 5.79 (t, $^{3}J_{HH}$ = 6.65 Hz, 8 H, C_6H_3), 4.2 - 4.0 (br., d, 8 H, CH_2), 3.1 - 2.90 (br., d, 8 H, CH_2), 2.85 to 2.9 (br, DMF).

6.6.8. Synthesis of bis {palladium- 3-[(Diphenyl phosphanyl)-methyl]-2-{4-[(diphenyl phosphanyl)-methyl]-benzo[1,3,3'] µ-oxo- µ'-oxo k-oxo -2-yloxy}-phenol]}- yttrium chloride (32):

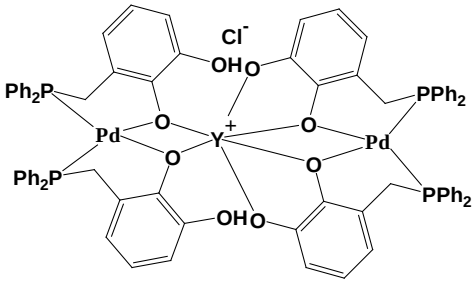

To a mixture of 450 mgs (1.4 mmol) of 3-(Diphenyl-phosphinoylmethyl)-benzene-1,2-diol, 71 mg (0.36 mmol) of YCl_3, 208 mg (0.7 mmol) of $(COD)PdCl_2$ and 0.51 ml (3.65 mmol) of Et_3N was added 12 ml of dry DMF. This mixture was stirred for 3 hours at room temperature, giving a dark red suspension. The suspension was filtered through a celite bed and the filtrate was kept at –28ºC overnight, to give needle like white crystals. The solution was decanted to another Schlenk tube, an equal amount of diethyl ether was added

and the solution kept at room temperature for crystallization. Dark red colored prismatic crystals of X-ray quality were obtained. The residue was dried at 100ºC for 4 hours.

Yield: 741mg (65%); **Melting point:** 197ºC (dec).

ESI-MS (positive mode): m/e = 1529.06 $(M\text{-}Cl)^{+}$, 765 $(M\text{-}Cl+H)^{2+}$, 776.05 $(M\text{-}Cl+Na)^{2+}$, 786.01 $(M\text{-}HCl+2Na)^{2+}$, 510.35 $(M\text{-}Cl+2H)^{3+}$, 743.07 $(C_{38}H_{32}O_4P_2Pd_1+Na)^{+}$

ESI-MS (negative mode) m/e : 1527 $(M\text{-}2H)^{-}$, 719.1 $(C_{38}H_{31}O_4P_2Pd)^{-}$.

$^{31}P\{^{1}H\}$-NMR ($CDCl_3$) δ = 70.8 (br, s), 66.0 (br, s).

^{1}H NMR ($CDCl_3$) δ = 8.2 (s, broad, 1 H, DMF) 7.5-6.6 (m, 40 H, C_6H_5), 6.25 (t, $^{3}J_{HH}$ = 8.1 Hz, 2 H, C_6H_3), 6.17 (d, $^{3}J_{HH}$ = 7.7 Hz, 2 H, C_6H_3), 6.0 (d, $^{3}J_{HH}$ = 7.0 Hz, 2 H, C_6H_3), 5.93 (d, $^{3}J_{HH}$ = 7.3 Hz, 2 H, C_6H_3), 5.85 (br, s, 1 H, C_6H_3), 5.7 (d, $^{3}J_{HH}$ = 7.6 Hz, 1 H, C_6H_3), 5.6 (d, $^{3}J_{HH}$ = 7.6 Hz, 2 H, C_6H_3), 3.3 (d, $^{2}J_{PH}$ = 13.5 Hz, 4 H, CH_2), 3.0 (d, $^{2}J_{PH}$ = 14.4 Hz, 4 H, CH_2), 2.85 to 2.9 (broad, 6 H, DMF).

6.6.9. Investigations on the catalytic behavior of selected metal complexes: Sonogashira C-C coupling reaction:

The palladium-tin complexes **26a** and **26b** synthesized according to the procedures reported in section 6.6.2, 6.6.3 respectively were employed as catalysts for the Sonogashira coupling of phenyl acetylene and 4-iodo nitrobenzene. The reaction was carried out under standard condition as follows:

Phenyl acetylene (44 mg, 0.44 mmol), copper iodide (33 mg, 0.16 mmol), and **26a** (30 mg, 3 mmol %) were added to a solution of 4-iodo-nitrobenzene (98 mg, 0.44 mmol.) in 15 ml of triethyl amine/DMF (2:1). The mixture was stirred for 20 hours at room temperature. N-Hexane (20 ml) was then added and the precipitate filtered off. The filtrate was evaporated to dryness and the dark residue purified by column chromatography using neutral silica as stationary phase and dichloromethane/hexane (3:7) as eluent to give 92 mg (94%) of 4-nitrophenyl-phenylacetylene. The coupling product was characterized by ^{1}H NMR.

The corresponding reaction using **26b** as (pre)catalyst was performed under identical conditions except that the ratio of **26b**: CuI was changed to 2:1. ^{31}P NMR spectra which were recorded after 1, 5 and 20 hours in order to monitor the status of the catalyst showed a single resonance at 76 ppm confirming that **26b** remained intact during the reaction.

After 24 hours, all volatiles were evaporated in vacuum. The residue was extracted with 10 ml of toluene. The suspension formed was allowed to settle for 15 minutes and the supernant toluene layer decanted, which on purification (by column chromatography as in **26a**) gave the coupling product in (88 mg) 90% yield. The residue was dried in vacuum and dissolved in 5 ml of DMF. The ^{31}P NMR spectrum of this solution still showed the resonance of **26b** at 76 ppm. The residue obtained after evaporation of the solvent was recovered and reused for the second catalytic cycle that produced (73 mg) 75% of the coupling product. The same cycle as above was repeated for the third time and the catalyst was reused for further transformations.

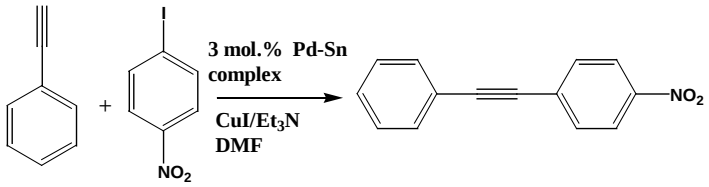

^{1}H NMR ($CDCl_3$): δ = 8.22 (m, 2 H, $C_6H_4NO_2$), 7.67 (m, 2 H, $C_6H_4NO_2$), 7.55 (m, 2 H, Ph.), 7.35 - 7.45 (m, 3 H, Ph).

6.7. Transition metal complexes of templated bisphosphine ligands with diastereotopic donor sites:

6.7.1. Synthesis of palladium -bis {phenyl, 2,4,6-trimethyl-phenyl (benzo- [1, 3]-μ-oxo-k-oxo-4-ylmethyl) phosphane)}-dimethyl tin (34a/b):

3-[(Mesitylphenyl phosphanyl)-methyl]-benzene-1, 2-diol (0.69 mmol) was dissolved in 8 ml of dimethyl formamide. Addition of 98 mgs (0.34 mmol) of 1,5-cyclooctadiene-palladium dichloride, 75 mg (0.34 mmol) of dimethyl tin dichloride followed by 0.24 ml (1.7 mmol) of triethyl amine gave a dark deep red suspension. Monitoring the reaction by ^{31}P NMR indicated completion of the reaction after 3 hours. The suspension was then filtered and the filtrate diluted with an excess of diethyl ether. The dark red colored powder formed was filtered off, and dried in vacuum at 80°C.

According to the spectroscopic and analytical data (see below) a mixture of two products was obtained. The X-ray crystal structure determination showed a product with methyl and chloride substituents at tin center.

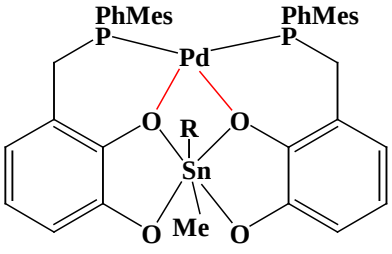

R =Me/Cl

Yield: 231mg (70%); **Melting point:** 230°C (dec).

Elemental analysis: Calcd. for ($C_{46}H_{48}O_4P_2PdSn$ + $C_{45}H_{45}ClO_4P_2PdSn$) C 56.80 H 4.87 Found: C 57.08 H 5.22.

ESI-MS (positive mode): m/e = 937.08 $(M-Cl)^+$, 973.04 $(M+H)^+$, 994.14 $(M+Na)^+$.

$^{31}P\{^1H\}$-NMR (DMF-d7) δ = 63.6 (s).

$^{31}P\{^1H\}$-NMR (DMF-d7, 273K) δ = 65.0 (s), 62.3 (s).

$^{31}P\{^1H\}$-NMR (DMF-d7, 243K) δ = 64.3 (s), 61.1 (s), 50.5 (s).

$^{31}P\{^1H\}$-NMR (DMF-d7, 213K) δ = 72.6 (s), 64.83 (s), 61.8 (dd, J_{PP} = 32 Hz) 61.3 (s), 59.9 (s), 50.5 (s).

^1H NMR (DMF-d7, 243K) (the assignments were made from ^1H, ^{31}P and ^1H, ^{119}Sn 2D experiments) δ = 8.0-6.7 (br, m, Ph), 6.65 (d, $^3J_{HH}$ = 7.7 Hz, C_6H_3), 6.53 (t, $^3J_{HH}$ = 7.6 Hz, C_6H_3), 6.05 (d, $^3J_{HH}$ = 7.6 Hz, C_6H_3), 3.8-3.4 (br. m, CH_2), 0.82 (br, s, $SnCH_3$), 0.77(br, s, $SnCH_3$), 0.43 (br, s, $SnCH_3$), 0.34 (br, s, $SnCH_3$).

$^{31}P\{^1H\}$ CP-MAS NMR: δ_{iso} = 55.

$^{119}Sn\{^1H\}$ CP-MAS NMR: δ_{iso} = -207, -308.

6.7.2. Synthesis of palladium -bis {biphenyl- (benzo- [1, 3]-μ-oxo-k-oxo-4-ylmethyl) phosphane)}-methyl tin chloride (33a):

To a DMF solution of 200 mg (0.65 mmol) of 3-(Diphenyl-phosphinoylmethyl)-benzene-1, 2-diol was added 78 mg (0.32 mmol) of methyl tin trichloride and 93 mg (0.32 mmol) of 1,5 cyclooctadiene palladium dichloride. Short stirring followed by addition of 2.5 equivalents (1.6 mmol) of triethyl amine resulted in formation of a red suspension. The reaction mixture was filtered and volatiles were evaporated in vacuum. The red colored

residue was dissolved in a minimum amount of DMF, few drops of diethyl ether were added and the solution was kept for crystallization at room temperature. Shining red crystals formed which were collected by filtration.

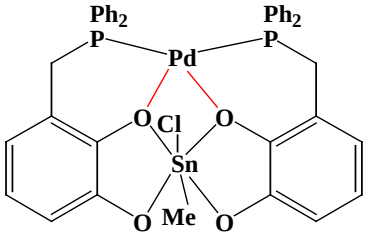

Elemental analysis: Calcd. for ($C_{39}H_{33}ClO_4P_2PdSn$ + 2DMF): C 52.25 H 4.58 N 2.71 Found: C 52.19 H 4.56 N 2.37.

Yield: 199 mg (70%); **Melting point:** 255°C (dec).

ESI-MS (positive mode): m/e = 852.99(100%) $(M-Cl)^+$, 894.98 $(M+Li)^+$.

$^{31}P\{^1H\}$-NMR (DMF-d7) δ = 69.6 (br, s).

$^{119}Sn\{^1H\}$-NMR (DMF-d7, 213K) δ = -327 (br, s).

^1H NMR (DMF-d7) δ = 7.9-7.2 (m, 20 H, Ph), 6.8 (d, $^3J_{HH}$ = 7.7 Hz, 2 H, C_6H_3), 6.6 (t, $^3J_{HH}$ = 7.8 Hz, 2 H, C_6H_3), 6.3 (d, $^3J_{HH}$ = 7.6 Hz, 2 H, C_6H_3), 4.1 to 3.8 (broad, d, 4 H, CH_2), 0.9 (broad, t, $^2J_{SnH}$, 106 Hz, 3 H, $SnCH_3$).

$^{31}P\{^1H\}$-NMR (DMF-d7, 213K) δ = 77.5 (dd, $^2J_{PP}$ = 297 Hz), 72.64 (broad, s), 54.24 (broad, s).

^1H NMR (DMF-d7, 213K) δ = 8.0-6.3 (br, m), 6-5.8 (br, m), 4.8-4.5 (br, s, CH_2), 4.3-4.0 (br, s, CH_2), 0.92 (t, $^2J_{SnH}$ = 105.1 Hz, $SnCH_3$), 0.72 (t, $^2J_{SnH}$ = 99.4 Hz, $SnCH_3$).

6.8. Results of computational studies on complex 26a/27a:

All DFT-computations were performed with the program package Gaussian 03[148] using the B3LYP functional and a normal grid for numeric integration. Energy optimizations of **26a**

[148] Computations were performed at the B3LYP/3-21g* level of theory with the Gaussian program suite: Gaussian 98 (Rev. A.7), M. J. Frisch, G. W. Trucks, H. B. Schlegel, G. E. Scuseria, M. A. Robb, J. R. Cheeseman, V.G. Zakrzewski, J. A. Montgomery, R. E. Stratmann, J. C. Burant, S. Dapprich, J. M. Millam, A. D. Daniels, K. N. Kudin, M.C. Strain, O. Farkas, J. Tomasi, V. Barone, M. Cossi, R. Cammi, B. Mennucci, C. Pomelli, C. Adamo, S. Clifford, J.Ochterski, G. A. Petersson, P. Y. Ayala, Q. Cui, K.

and of two different adducts with two molecules of formamide were carried using a 3-21g* basis set. The relative energies E_{rel} of both adducts were obtained by computing the energy-optimized molecular structure of formamide at the same level of theory and evaluating the difference E_{rel} = E(adduct) – E(**3**) – 2 E(formamide). Attempts to locate a structure with *trans*-coordination of the Chloride ligands at Sn did not lead to a minimum. Attempts to locate a complex with a cis-coordination of formamide ligands at Pd lead to the location of a strongly distorted structure at high energy (Erel = 28.7 kcal mol-1), which is not reported here. A short summary of the computational study is listed below. An electronic version of the computed structures and energies of **26a** and its formamide adducts is saved in a CD which is attached at the end of the thesis.

Complex **26a** (point group C_2): **E** = -14270.3118843 HartreeComplex **26a** × 2 Formamide (Coordination at Sn) (point group C_2): **E** = -14608.2311568 Hartree

Complex **26a** × 2 Formamide (coordination at Pd, *trans*-isomer) (point group C_2)

E = -14608.2368014 Hartree

Formamide (point group C_s): **E** = -168.9476573 Hartree

Relative Energies $\mathbf{E_{rel}}$ (in kcal mol^{-1}):

	E_{rel} (in kcal mol^{-1}):
Complex **26a**+ 2 Formamide:	0.0
Complex **26a** × 2 Formamide (coordination at Pd, *trans*-isomer)	-15.0
Complex **26a**× 2 Formamide (Coordination at Sn)	-18.6

Morokuma, D. K. Malick, A. D. Rabuck, K. Raghavachari, J. B.Foresman, J. Cioslowski, J. V. Ortiz, B. B. Stefanov, G. Liu, A. Liashenko, P. Piskorz, I. Komaromi, R. Gomperts, R. L.Martin, D. J. Fox, T. Keith, M. A. Al-Laham, C. Y. Peng, A. Nanayakkara, C. Gonzalez, M. Challacombe, P. M. W. Gill, B.G. Johnson, W. Chen, M. W. Wong, J. L. Andres, M. Head-Gordon, E. S. Replogle and J. A. Pople, Gaussian, Inc., Pittsburgh PA, 1998.

7. Summary and outlook

7.1. Summary:

The present work deals with the syntheses of functionalized phosphine ligands and their self-assembly to produce di- or multinuclear complexes. A bifunctional ligand with a phosphine functionality at one end and a catechol unit at the other end was designed. The rationale behind the design was to have a ligand which can differentiate between hard and soft metals, and react with a combination of both selectively to produce hetero di-nuclear assembly in single a step.

In an effort to synthesize the desired ligands, it was found that the reaction of diphenyl phosphine with phenolic aldehydes proceeds via initial formation of α-phosphanyl-carbinols. The presence of OH-groups in p- or o-position destabilizes the adducts relative to the starting materials and facilitates their subsequent rearrangement into isomeric phosphine oxides. $LiAlH_4$ treatment followed by hydrolysis further allowed to reduce the latter to phenol-functionalized phosphines (see **Scheme 7.1**). The overall reaction sequence permits to access phosphines with pendant phenolic functionalities from readily available starting materials, without the necessity of additional efforts for the introduction and removal of protecting groups at the phenol functionalities. This procedure constitutes a substantial improvement over previously known synthetic protocols which required often more complicated multi-step approaches.[43]

The catechol-phosphines **9b** and **9d** were shown to coordinate to soft acids such as palladium(II) and silver(I) selectively via the phosphorus atom.

Though the major goal of this work is to self-assemble the catechol-phosphines to generate multinuclear complexes, it was also planned to explore the Lewis base behavior of these catechol-phosphines itself. A boric acid ester **16a/b** was generated by reaction of

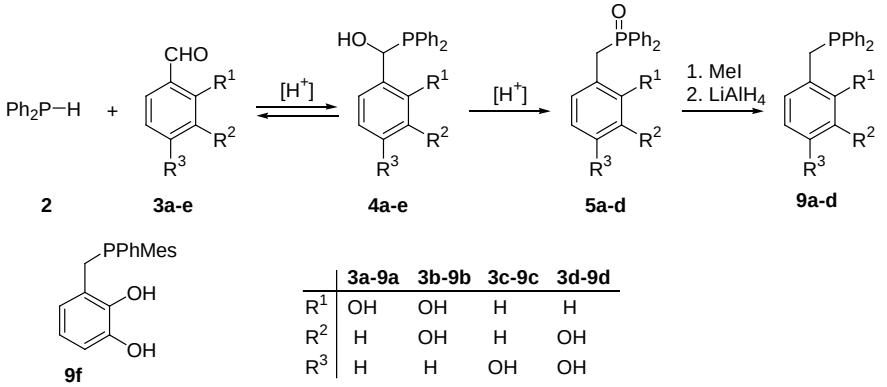

	3a-9a	3b-9b	3c-9c	3d-9d
R^1	OH	OH	H	H
R^2	H	OH	H	OH
R^3	H	H	OH	OH

Scheme 7.1: Syntheses of catechol functionalized phosphine ligands.

9b with aryl boronic acid and its reactivity with hard and soft donors was reported. The catechol-phosphine reacts readily, giving the corresponding alkyl borate. It is envisioned that the phosphine can coordinate to a soft acid and the boron to a hard base, this enable the species to act as a building block for inorganometallic coordination polymers. Thus, six equivalents of pyridine were required to convert **16a** quantitatively into the amine adduct **17c**, whereas only one equivalent of dimethyl amino pyridine was sufficient to obtain a similar acid-base adduct **17a** (see **Scheme 7.2**). These experimental findings allow to state that the alkyl borate unit behaves as a moderately strong Lewis acid. A strongly electron withdrawing substituent on boron (R = C_6F_5) makes **17b** a stronger acid, leading to intramolecular acid base interactions.

A palladium complex of **9b** on treatment with phenyl boronic acid produced the corresponding palladium borate complex in good yields, which on treatment with a strong base like dimethyl amino pyridine likewise produced a mixture of products. One of them is likely to be **19**, though further evidence is required **(Scheme 7.2)**. An adduct like **19** with appropriately modified donor functions might be of interest as an building block for supramolecular complexes with unsymmetric bidentate “pseudo” ligand.

Taking advantage of the selective reactivity of **9b** towards hard and soft donors, boron templated metal complexes were synthesized in a stepwise manner. Reacting two equivalents of the catechol-phosphine with one equivalent of boric acid in the presence of a base generated the borate templates **20/22**, which were characterized by NMR, ESI-MS and crystal structure. A crystal structure study of **20/22** revealed that changing the relative position of the hard hydroxy donors with respect to the phosphine fragment lead to borate templates with distinctly different P-P distances. The corresponding borate template of **9b**

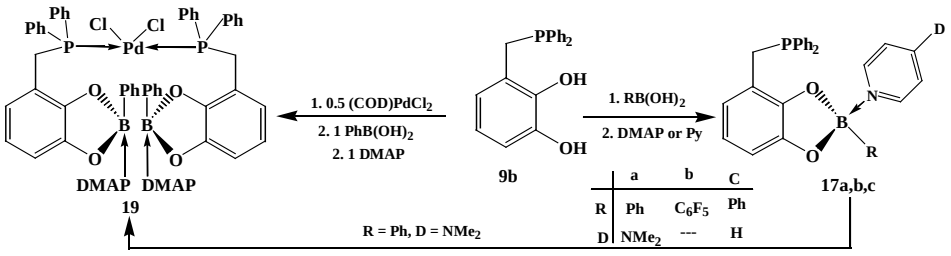

Scheme 7.2: Lewis acid-base behavior of catechol-phosphine.

showed a relatively small P-P distance (10.6 Å), whereas **9d** produced a borate template with P-P distance of 13.3Å. The difference in P-P distance is reflected in differences in

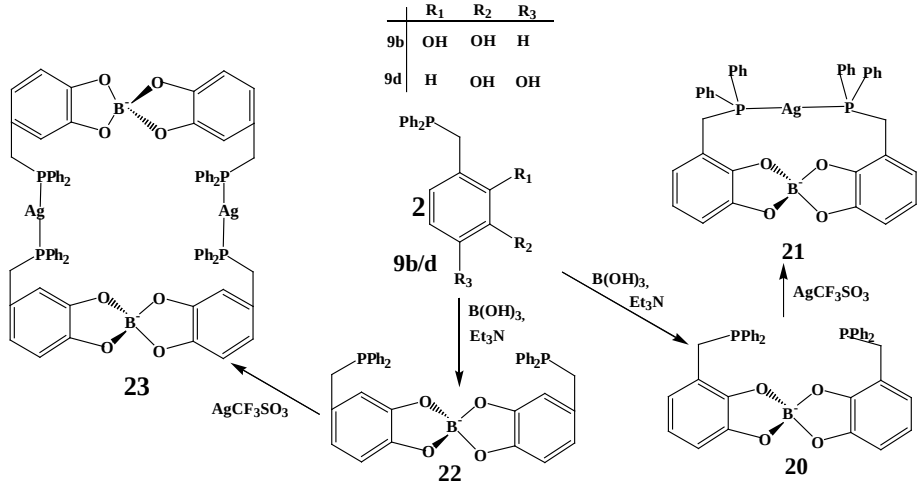

Scheme 7.3: Synthesis of borate templates 20, 22, monometallic silver complex 21 and a dimmer 23.

their activity. **20** reacts with silver triflate to produce the complex **21** whereas **22** reacted in 2:2 ratio and gave **23** (see **Scheme 7.3**). The monometallic silver complex **21** showed unusual secondary oxygen-silver interactions, which led to a visible deviation of P-Ag-P moiety from linearity. The macrocyclic complex **23** was difficult to crystallize and its constitution was hence established by ESI-MS and DOSY NMR measurements.

The main focus of the present work was on performing the assembly of catechol phosphine fragments on a hard acid center and the coordination to a catalytic metal in one step. This working concept was successfully demonstrated by using various hard acid centers and catalytically relevant metals (**Scheme 7.4)**.

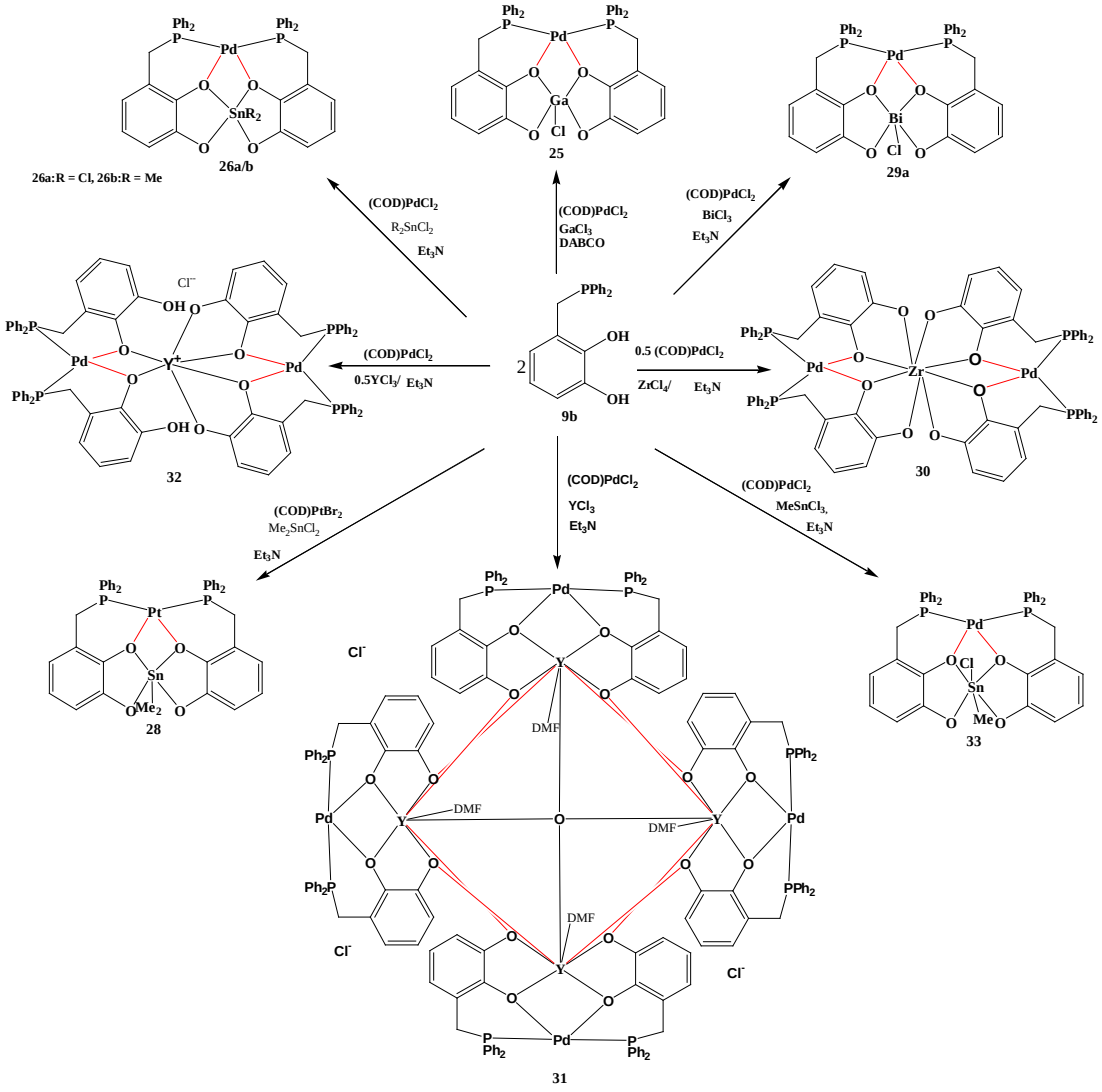

Scheme 7.4: Schematic of self-assembly of 9b to produce various metal complexes.

A four-component reaction between gallium (III) chloride, cyclooctadienyl palladium dichloride, catechol phosphine (**9b**) and excess base produced a heterobimetallic assembly **25** in good yields. Interesting to note is the presence of μ_2-bridging oxygen atoms which connect the two metal centers. Complexes **26a/b, 28, 29, 30, 31and 32** were synthesized under identical conditions. The products are distinguished from known heterometallic complexes of phosphinoalcohols in requiring neither the dedicated syntheses of a polydentate chelate ligand,[126] nor the need for introducing the metal atoms in separate reaction steps.[149,152]

[149] G. S. Ferguson, P. T. Wolczanski, *Organometallics*, **1985**, 4, 1601; G. S. Ferguson, P. T. Wolczanski, *J. Am. Chem. Soc*. **1986**, 108, 8293; G. S. Ferguson, P. T. Wolczanski, L. Parkanyi, M. C. Zonnevylle, *Organometallics*, **1988**, 7, 1967.

The experimental findings allow to state that the coordination geometry of the template center and its size have considerable impact on the assembly process. For example, a small template like gallium can accommodate only five donor atoms whereas a larger template like zirconium can accommodate as many as eight donor atoms. In the case of bismuth, increasing the size of the template center leads to formation of a dimer in the solid state. In the reaction of **9b** with yttrium trichloride it was possible to direct the assembly of multinuclear complexes by controlling the stoichiometric ratio of the starting materials. On the other hand, changing the transition metal from palladium to platinum had negligible effects on the complex formation. The chiral catechol phosphine **9f** produced a mixture of diastereoisomeric bimetallic palladium-tin complexes which were characterized by NMR and crystal structure determination.

All synthesized complexes displayed μ_2-briding oxygen donors and the μ_2-briding oxygen-template center bonds were found to be longer than the terminal oxygen-template center bonds. The oxygen-template center bond lengths (bridging and non-bridging) vary according to the size of the template center. The complexes studied here allowed to vary the P-Pd-P bite angles between 97º to 102º depending on the size and nature of the substituents on the template.

The solution behavior of **26a/b** was fully explored by NMR studies which allow to conclude that complexes **26a/b** mimic the behavior of complexes containing a supramolecular bis-phosphine ligand which is formed by the assembly of two catecholate phosphine fragments on a hard acidic metal template and can switch between tetra-dentate O_2P_2- and bidentate P_2- coordination. This hemilabile behavior stimulated a study of the application of these complexes in catalysis and the first experimental proof for the catalytic potential was demonstrated by the application of **26a/b** in the Sonogashira C-C coupling reaction (section 4.3).

7.2. Outlook:

7.2.1. Prospective ligands:

Throughout the present work it was assumed that the ligand design and the selection of the right template center are crucial for controlling the self-assembly. It is believed that fine-tuning of the ligands may offer further opportunities to study the steric, electronic and

stereochemical properties of the assemblies. In this view, the synthesis of further types of ligands is proposed (see **Scheme 7.5**) as outlined below.

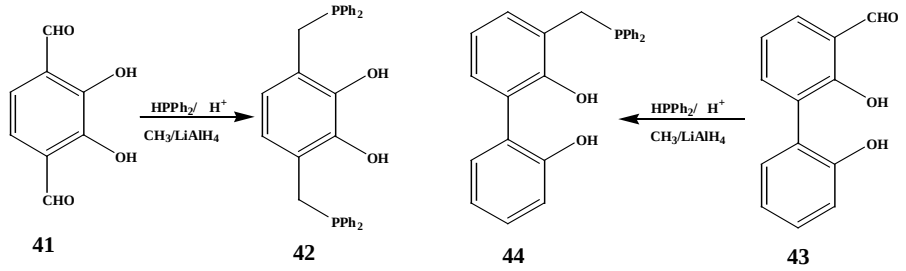

41 **42** **44** **43**

Scheme 7.5: Proposed synthesis of a bis phosphine-catechol 42 and biphenyl ligand 44.

Ligand **42** can be considered as multifunctional ligand with two phosphine donors and two hydroxy donors and can be employed in various organometallic transformations. Ligand **44** with hydroxy functionality on two aryl rings can be chiral when the aryl rings are not in one plane and may behave very differently. Further, it is envisioned that employing these ligands in complexation may produce either M1L2M'2 type trinuclear complexes or M2L6M'3 (M = Main group elements, M' = transition metals) type multinuclear complexes.

Rigid ligands with suitable metals can produce a desired architecture and hence rigidity is another area of great interest in self-assembly process. Increasing the spacer length between the phosphine and the catechol moieties may enable to produce complexes with hard-hard and soft-soft combinations of donors and metal centers. In **51** the donor atoms are directly bound to the aromatic rings, providing rigidity and the biphenyl moiety ensures the separation between the hard and the soft donors. Due to its enhanced rigidity and increased spacer length, ligand **51** will be a promising candidate to study the bite angle, steric and electronic properties of the resulting assemblies.

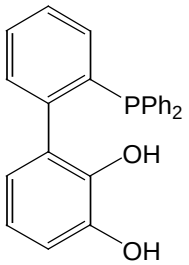

51

Scheme 7.6: 51.

7.2.2. Extending the self-assemblies:

Inspection of the present work pointed out a few loopholes. Whereas the described work dealt mostly with varying the template center, changing the transition metal (including metals like Rh, Ir, Ru, Cu, Au and Ni) may shade further light on the redox and catalytic properties of these complexes. As indicated in compound **23**, ligand **9d** can be a suitable candidate to synthesize macrocyclic assemblies that can be used as host capsule to encapsulate a guest molecule.

Section 3.2.1 dealing with the Lewis-acid/base behavior of **9b** demonstrated that a palladium complex of **9b** with two boron acidic centers **18**, can be synthesized and isolated. The complex **18** can be coordinated to a bidentate base, thus can act as a building block (as a bifunctional monomer) for organometallic polymers. In chapter 5 syntheses of diastereomeric bimetallic complexes **33** and **34** was discussed, but the isolation of these complexes proved very difficult. It is highly anticipated that similar complexes with other template centers such as Ga, Ge, Bi, Y and Zr can be synthesized and may enable better isolation of the diastereoisomers. These chiral assemblies can be employed as catalysts in asymmetric syntheses.

7.2.3. Applications:

The catalytic potential of **26a/b** was demonstrated in section 4.3. Complexes **26a/b** were found to be catalytically active in a C-C coupling reaction. Detailed mechanistic investigations and theoretical calculations may help to outline the energy profile of the catalytic cycle and thus provide further insights into the behavior of **26a/b** during the catalytic process.

All the complexes presented in this work are dinuclear, which can be seen as an asset of these assemblies. The transition metal moiety may activate nucleophiles and at the same time the Lewis acid center (Ga, Sn, Y, Zr) may activate electrophiles. Thus, the heterodinuclear complexes discussed in the present work may provide double activation.[150] As an example, synthesis of diphenyl carbonate is catalyzed by palladium-tin complexes, though the mechanism is not clearly established.[90] In this regards, it can be postulated that complexes **26a** may catalyze the phenol coupling reaction to give diphenyl carbonate. The postulated catalytic cycle is represented in **Scheme 7.7**. A electron rich CO can break the

[150] M. Shibasaki, N. Yoshikawa, *Chem. Rev*. **2002**, 102, 2187.

bridging oxygen palladium bonds and addition of CO on palladium can take place. In the next step a phenolate ion adds to the tin center giving out Base.H^+ and repeatdely generating an intermediate like **52** (when R = Cl), and finally add itself to the CO the same sequence would continue to produce the diphenyl carbonate (DPC). Thus, there is a lot of scope to explore the phenol coupling reaction and to prove the feasibility of the above hypothesis.

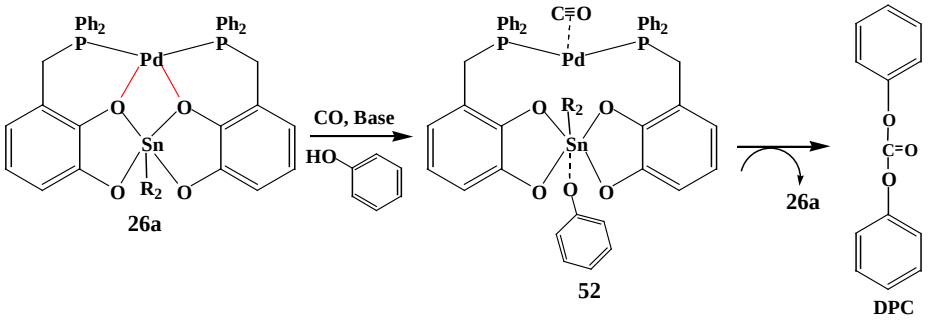

Scheme 7.7: Postulated reaction mechanism of phenol coupling reaction.

In view of recent reports on chiral ligands in bifunctional asymmetric catalysis,[151] similar transformations are expected from complex **33** and **34**. A direct aldol reaction of hydroxyketones can be considers as a good starting point to explore the potential of **33** and **34**.

In short, using catechol-phosphines as ligands, various catalytic reactions can be realized by modifying transition metals, template centers, organic spacers and peripheral substituents on the phosphorus donor.

[151] M. Shibasaki, S. Matsunaga, *Chem. Soc. Rev*. **2006**, 35, 269.

7.3. Zusammenfassung:

Die vorliegende Arbeit behandelt die Synthese funktionalisierter Phosphane und ihrer Aggregation zu zwei- oder mehrkernigen Komplexen. Es wurde ein bifunktioneller Ligand mit einer Phosphanfunktionalität an einem und einer Katecholeinheit am anderen Ende entworfen. Dieser Ligand sollte die Fähigkeit besitzen, sowohl zwischen harten und weichen Metallen zu unterscheiden als auch in einem einzelnem Schritt selektiv mit diesen Metallen zu Heterozweikern-Komplexen reagieren zu können.

Im Verlauf von Bemühungen zur Synthese der gewünschten Liganden stellte sich heraus, dass die Reaktion von Diphenylphosphan mit phenolischen Aldehyden über die Bildung von α-Phosphanylcarbinolen verläuft. Die Anwesenheit der OH-Gruppen in p- oder o-Position destabilisiert die Addukte im Vergleich zu den Ausgangsmaterialien, erleichtert aber im Folgenden die Umlagerung zu isomeren Phosphanoxiden. Durch Umsetzung mit $LiAlH_4$ und nachfolgende Hydrolyse können diese zu entsprechenden phenolfunktionalisierten Phosphanen reduziert werden (**Scheme 7.1)**. Die Gesamtreaktion ermöglicht es, Phosphane mit freien (flexiblen) phenolischen Funktionalitäten aus leicht verfügbaren Ausgangsmaterialien zugänglich zu machen, und zwar ohne die Einführung von Schutzgruppen an den Phenolgruppen. Dieses Verfahren stellt gegenüber der bekannten Literatur, in der häufig komplizierte Mehrstufensynthesen beschrieben wurden, eine erhebliche Verbesserung dar.[43] Es wurde auch gezeigt, dass die Katecholphosphane **9b** und **9d** selektiv über das Phosphoratom an weiche Säuren wie Palladium (II) und Silber(I) koordinieren können.

Obwohl das Hauptziel dieser Arbeit die Selbstassoziation von Katecholphosphanen zu mehrkernigen Komplexen war, wurde auch das Lewis Säure/Base Verhalten der Katecholphosphane untersucht. Boronsäureester **16a/b** wurden durch Reaktion von **9b** mit Arylboronsäuren erzeugt und ihre Reaktivität gegenüber harten und weichen Donormolekülen untersucht. Dabei wurde davon ausgegangen, dass das Phosphoratom an eine weiche Säure und das Bor an eine harte Base koordinieren kann und das Katecholphosphan so als Baustein für metall**an**organische Koordinationspolymere dienen kann. So wurden sechs Äquivalente Pyridin benötigt, um **16a** quantitativ in das Aminaddukt **17c** umzuwandeln, während zur Bildung des analogen Säure-Base Addukts **17a** (**Scheme 7.2**) ein Äquivalent Dimethylaminopyridin ausreicht.

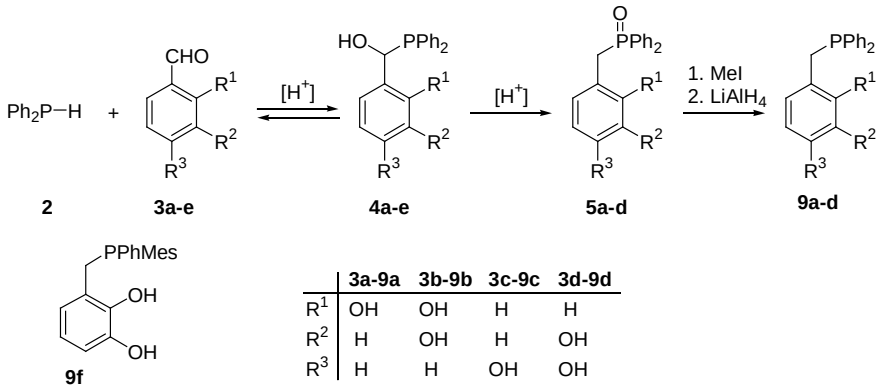

Scheme 7.1: Synthese katecholfunktionalisierten phosphanLiganden.

Diese experimentellen Ergebnisse zeigen, dass sich die Alkylboronateinheit als mäßig starke Lewis-Säure verhält. Ein stark elektronenziehender Substituent (R = C_6F_5) am Bor macht 17b zu einer starken Lewis-Säure und induziert intermolekulare Säure-Base-Wechselwirkungen.

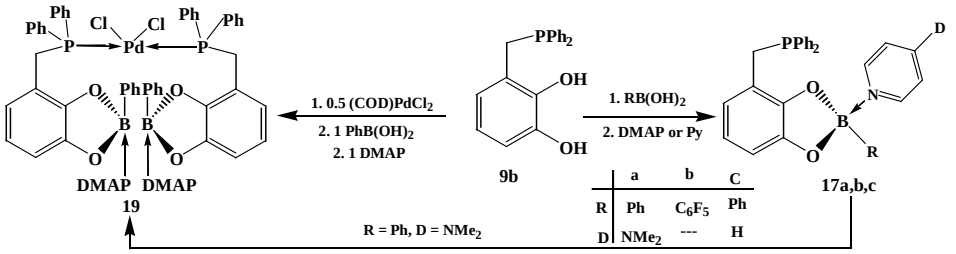

Scheme 7.2: Lewis Säure-Base Reaktionen von Katecholphosphinen.

Der Palladiumkomplex von **9b** lieferte mit Phenylboronsäure in guter Ausbeute den entsprechenden Borsäureester. Die Reaktion mit einer starken Base wie Dimethylaminopyridin ergab eine Mischung verschiedener Produkte. Eines dieser Produkte könnte der Komplex **19** sein, obwohl zu dessen eindeutigem Nachweis noch weiter Beweise notwendig sind. (**Scheme 7.2**). Ein Addukt wie **19** mit entsprechend modifizierten Donorfunktionen könnte als Baustein für supramolekulare Komplexe mit unsymmetrischen, zweizähnigen „Pseudo-“Liganden interessant sein.

Unter Ausnutzung der selektiven Reaktivität von **9b** gegenüber harten und weichen Donormolekülen wurden Metallkomplexe schrittweise an Bortemplaten synthetisiert. Die Reaktion von zwei Äquivalenten Katecholphosphan mit einem Äquivalent Borsäure in Anwesenheit einer Base erzeugte die Borattemplate **20/22**, die durch NMR, ESI-MS und Kristallstrukturanalysen charakterisiert wurden. Die Kristallstrukturen von **20/22** zeigen, dass die Änderung der Position der harten Hydroxyldonatoren relativ zu dem

Phosphanfragment zu deutlich unterschiedlichen P-P Abständen führt. Das Borat **20** zeigt einen deutlich kleineren P-P-Abstand (10.6Å) als **22** (13.3 Å). Der Unterschied im P-P Abstand wird in den unterschiedlichen Reaktivitäten von **20**/**22** reflektiert. Der Ligand **20** reagiert mit Silbertriflat zum Komplex **21**, während **22** im Verhältnis 2:2 reagiert und den Makrozylus **23** liefert. Der einkernige Silberkomplex **21** zeigt ungewöhnliche sekundäre-Sauerstoff-Silber-Wechselwirkungen, die zu einer sichtbaren Abweichung der P-Ag-P Einheit von der Linearität führen. Der makrozyklische Komplex **23** war schwierig zu kristallisieren, und sein chemischer Aufbau wurde durch ESI-MS und DOSY NMR Messungen etabliert.

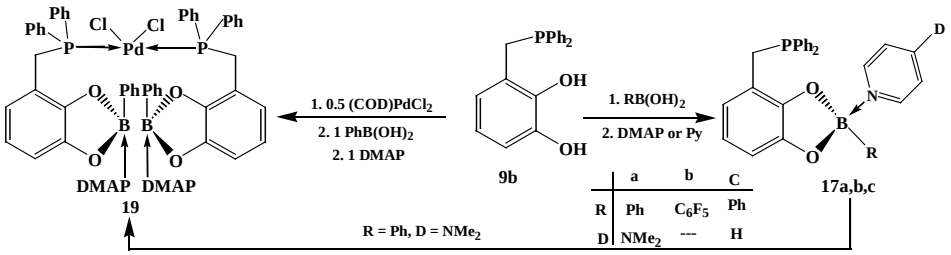

Scheme 7.2: Lewis Säure-Base Reaktionen von Katecholphosphinen.

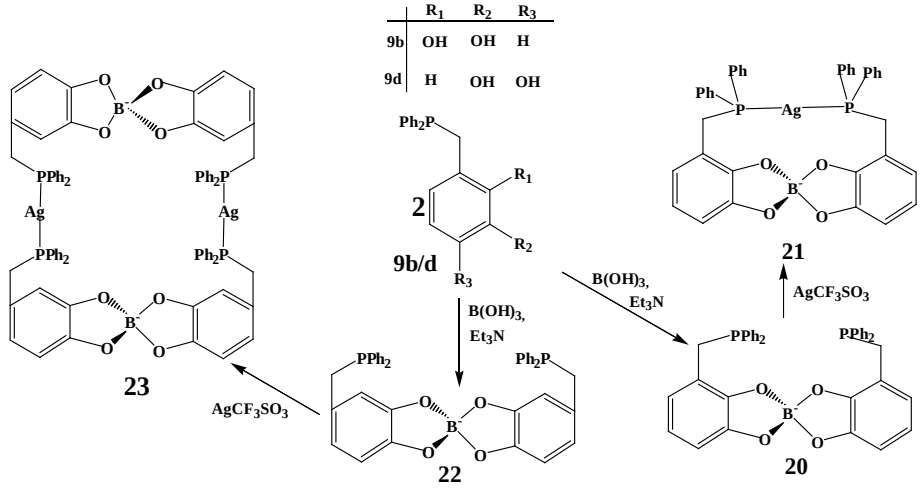

Scheme 7.3: Synthese der Bormatrix **20**/**22**, des einkernigen Silberkomplexes **21** und des Dimeren **23**.

Das Hauptziel der vorliegenden Arbeit war es, in einem Schritt die Bildung von Katecholphosphanfragmenten an einem harten Säurezentrum und die Koordination des P-atoms an ein katalytisch aktives Metall zu erreichen. Dieses Arbeitskonzept wurde unter Nutzung verschiedener harter Lewis-Säuren und katalytisch aktiver Metalle erfolgreich durchgeführt (**Scheme 7.4**). Eine Reaktion zwischen Gallium(III)chlorid, Cyclooctadienpalladiumdichlorid, Katecholphosphan **9b** und überschüssiger Base lieferte

den Heterozweikernkomplex **25** in guten Ausbeuten. Besonders erwähnenswert ist die Anwesenheit der μ_2-verbrückenden Sauerstoffatome, die die beiden Metallzentren verbinden. Die Komplexe **26a/b, 28, 29, 30, 31** und **32** wurden unter identischen Bedingungen hergestellt. Die Produkte sind gegenüber bekannten Heterometall-komplexen von Phophanylalkoholen bemerkenswert, da ihre Darstellung weder die aufwendige Synthese eines vielzähnigen Chelatliganden[126] noch die Notwendigkeit zur Einführung von Metallatomen in unterschiedlichen Reaktionsschritten erfordert.[152]

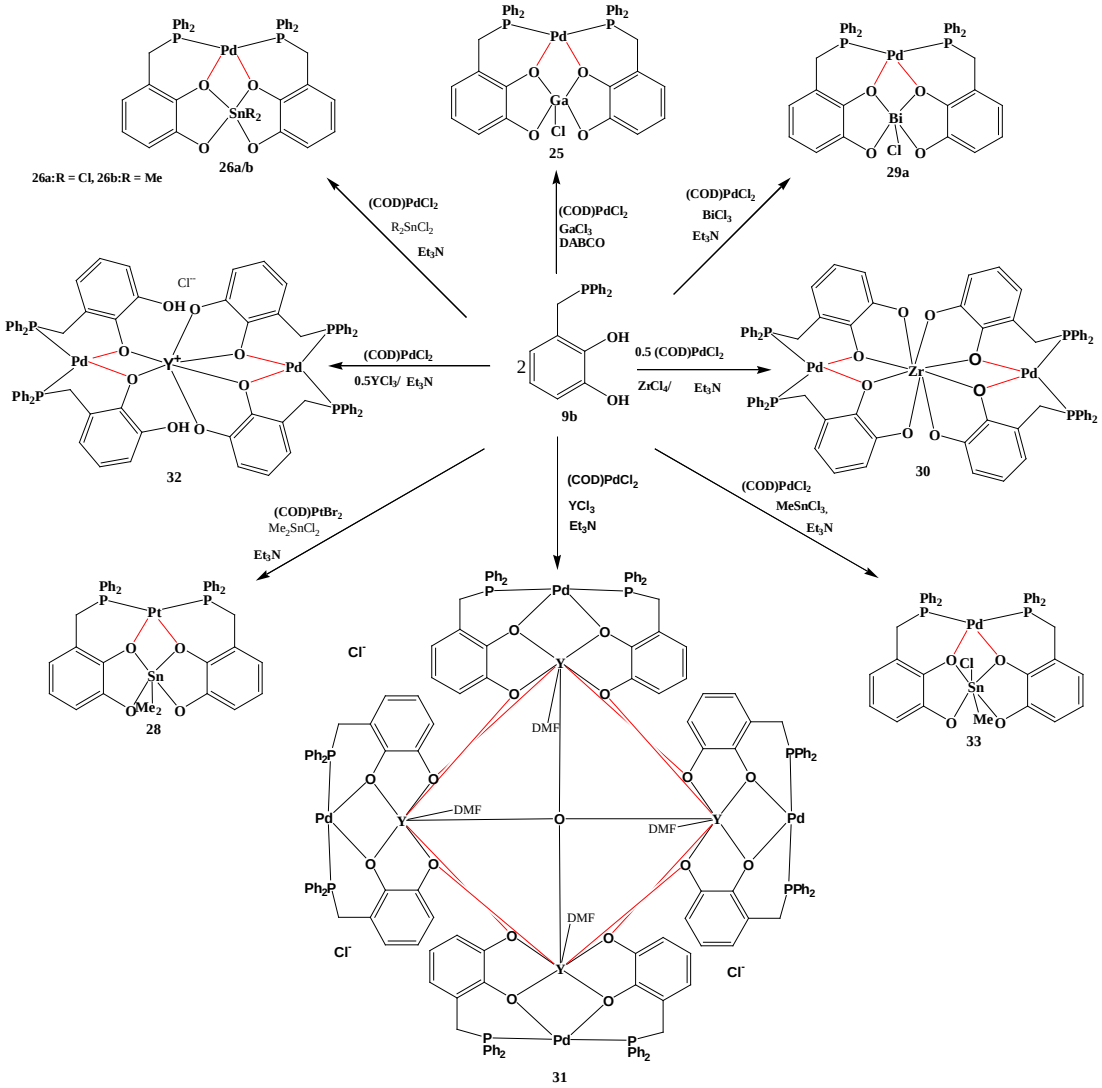

Scheme 7.4: Zusammenlagerung von **9b** zu verschieden Metallkomplexen

Die experimentellen Befunde zeigen, dass die Koordinationsgeometrie und die Größe des Templatzentrums beträchtliche Auswirkungen auf den Aufbauprozess haben.

[152] O. Kühl, S. Blaurock, J. Sieler, E. Hey-Hawkins, *Polyhedron*, **2001**, 20, 2171.

Beispielsweise kann ein kleines Templat wie Gallium nur fünf Liganden binden, während ein größeres Templat wie Zirkonium bis zu acht Liganden aufnehmen kann. Im Falle von Wismut führt die Vergrößerung des Templatzentrums zur Bildung von Dimeren im Festkörper. In der Reaktion von **9b** mit Yttriumtrichlorid gelanes, den Aufbau multinuklearer Komplexe durch die Variation des stöchiometrischen Verhältnis der Ausgangsmaterialien zu bestimmen. Die Variation des Übergangsmetalls von Palladium zu Platin hatte keinen wesentlichen Einfuss auf die Komplexstruktur. Das chirale Katecholphosphin **9g** lieferte eine Mischung diastereoisomerer, zweikerniger Palladium-Zinn-Komplexe, die durch NMR- Daten und eine Kristallstrukturanalyse charakterisiert wurden.

Alle dargestellten Komplexe zeigen μ_2-verbrückende Sauerstoffatome, deren Bindungen zum Zentralatom länger sind als die entsprechenden Bindungen zu terminalen O-Atomen. Die Bindungslängen (sowohl zu verbrückenden als auch nicht-verbrückenden O-Atomen) schwanken außerdem entsprechend der Größe des Zentralatoms. Die untersuchten Komplexe gestatten es, den Winkel P-Pd-P je nach Größe und Typ des Substituenten zwischen 97º und 102º zu verändern.

Das Verhalten von **26a/b** in Lösung wurde umfassend durch NMR- Experimente untersucht. Es ist festzustellen, dass sich die Komplexe **26a/b** ähnlich verhalten wie Komplexe mit einem supramolekularen Bisphosphan-Liganden, der aus der Anlagerung zweier Katecholatphosphan-Fragmente an ein hartes Lewis-acides Metalltenplat resultiert, und der zwischen vierzähniger O_2P_2- und zweizähniger P_2-Koordination wechseln kann. Dieses hemilabile Verhalten regte eine Studie der Anwendung dieser Komplexe in der Katalyse an, und der erste experimentelle Beweis ihres katalytischen Potentials wurde durch die Anwendung von **26a/b** in der Sonogashira C-C Kupplungsreaktion erhalten (Kap. 4.3).

8. Crystallographic Appendix

Crystal data including atom coordinates, bond distances, bond angles, torsion angles is saved as electron data files. The CD is attached at the end of chapter 9 in this dissertation. Primary information on the crystals reported in this work is provided in the following tables.

Crystal data and structural refinement for 5b with 0.5 THF:

Identification code	Chi01
Empirical formula	C21 H21 O3.5 P1
Formula weight	360.35
Temperature	173(2) K
Wavelength	0.71073 A
Crystal system, space group	Triclinic, P1(2)/c (no.14)
Unit cell dimensions	a = 12.551(3) A alpha = 83.17(3) deg.
	b = 12.623(3) A beta = 73.50(3) deg.
	c = 12.767(3) A gamma = 74.13(3) deg.
Volume	1863.6(6) A^3
Z, Calculated density	4, 1.284 Mg/m^3
Absorption coefficient	0.167 mm^-1
F(000)	760
Crystal size	0.30 x 0.30 x 0.20 mm
Theta range for data collection	1.67 to 27.00 deg.

Limiting indices	0 =< h =< 16, -15 =< k =< 16, -15 =< l =< 16
Reflections collected / unique	82031 / 4396 [R(int) = 0.0280]
Completeness to theta = 27.00	99.9 %
Absorption correction	None
Refinement method	Full-matrix least-squares on F^2
Data / restraints / parameters	8127 / 0 / 506
Goodness-of-fit on F^2	1.312
Final R indices [I>2sigma(I)]	R1 = 0.0647, wR2 = 0.1296
R indices (all data)	R1 = 0.0479, wR2 = 0.1214
Largest diff. peak and hole	0.448 and -0.334 e.A^-3

Crystal data and structure refinement for 9b.

Identification code	dg007_hy
Empirical formula	C19 H17 O2 P
Formula weight	308.30
Temperature	123(2) K
Wavelength	0.71073 A
Crystal system, space group	Monoclinic, P2(1)/c (no.14)
Unit cell dimensions	a = 12.369(2) A alpha = 90 deg. b = 8.320(1) A beta = 101.61(1) deg. c = 15.596(3) A gamma = 90 deg.
Volume	1572.1(4) A^3
Z, Calculated density	4, 1.303 Mg/m^3
Absorption coefficient	0.179 mm^-1
F(000)	648
Crystal size	0.45 x 0.30 x 0.25 mm
Theta range for data collection	2.97 to 27.48 deg.

Limiting indices	-15<=h<=16, -10<=k<=10, -20<=l<=20
Reflections collected / unique	15742 / 3524 [R(int) = 0.0230]
Completeness to theta = 25.00	98.4 %
Absorption correction	None
Refinement method	Full-matrix least-squares on F^2
Data / restraints / parameters	3524 / 3 / 207
Goodness-of-fit on F^2	1.058
Final R indices [I>2sigma(I)]	R1 = 0.0318, wR2 = 0.0756
R indices (all data)	R1 = 0.0453, wR2 = 0.0832
Largest diff. peak and hole	0.385 and -0.256 e.A^-3

Crystal data and structure refinement for 13b.

Identification code	scsep04_cif
Empirical formula	C38 H34 O4 P2Cl2Pd
Formula weight	793.89
Temperature	293(2) K
Wavelength	0.71073 A
Crystal system, space group	Monoclinic, P2(1)/c (no.4)
Unit cell dimensions	a = 10.2633(2)A alpha = 90 deg. b = 22.7369(4)A beta = 112.5860(10) deg. c = 11.6400(2) A gamma = 90 deg.
Volume	2507.93(8)A^3
Z, Calculated density	2, 1.34515 Mg/m^3
Absorption coefficient	0.568 mm^-1
F(000)	808
Theta range for data collection	2.10 to 28.27deg.
Limiting indices	-12<=h<=13, -30<=k<=30, -15<=l<=15

Reflections collected / unique	42973 / 10252
Completeness to theta = 28.27	98.9%
Absorption correction	None
Refinement method	Full-matrix least-squares on F^2
Data / restraints / parameters	12092 / 1 / 749
Goodness-of-fit on F^2	1.032
Final R indices [I>2sigma(I)]	R1 = 0.0699, wR2 = 0.1263
R indices (all data)	R1 = 0.0534, wR2 = 0.1179

Crystal data and structure refinement for 13d.

Identification code	scdez05a
Empirical formula	C44 H42 P2PdCl2 O5 THF (C4H8O)
Formula weight	866.07
Temperature	100(2) K
Wavelength	0.71073 A
Crystal system, space group	Monoclinic, C2(1)/n (no.15)
Unit cell dimensions	a = 18.54740(110)A alpha = 90 deg. b = 10.39230(70) A beta = 110.2944(39)deg. c = 26.20550(150)A gamma = 90 deg.
Volume	4737.555(518)A^3
Z, Calculated density	4, 1.23323 Mg/m^3
Absorption coefficient	0.60 mm^-1
F(000)	1684
Crystal size	0.70 x 0.20 x 0.40 mm
Theta range for data collection	1.018 to 28.283 deg.
Limiting indices	-22<=h<=24, -13<=k<=13, -34<=l<=34

Reflections collected / unique	28824 / 5642 [R(int) = 0.1731]
Max theta	= 56.65
Absorption correction	Mulit-scan
Refinement method	Full-matrix least-squares on F^2
Data / restraints / parameters	5642 / 0 / 261
Goodness-of-fit on F^2	1.029
R indices (all data)	R1 = 0.1122, wR2 = 0.3573
Largest diff. peak and hole	2.42 and -1.18 e.A^-3

Crystal data and structure refinement for 14b.

Identification code	dg004_hy
Empirical formula	C43 H43 Ag Cl2 F3 N O8 P2 S
	[C38 H34 Ag O4 P2]+ [CF3SO3]-,
	CH2Cl2, DMF (C3H7NO)
Formula weight	1031.55
Temperature	123(2) K
Wavelength	0.71073 A
Crystal system, space group	Monoclinic, P2(1)/n (no.14)
Unit cell dimensions	a = 13.818(1) A alpha = 90 deg.
	b = 22.343(2) A beta = 104.46(1) deg.
	c = 15.085(1) A gamma = 90 deg.
Volume	4509.7(6) A^3
Z, Calculated density	4, 1.519 Mg/m^3
Absorption coefficient	0.747 mm^-1
F(000)	2104
Crystal size	0.40 x 0.24 x 0.12 mm
Theta range for data collection	2.93 to 25.03 deg.

Limiting indices	-16<=h<=16, -26<=k<=26, -17<=l<=17
Reflections collected / unique	37390 / 7908 [R(int) = 0.0473]
Completeness to theta = 25.03	99.3 %
Absorption correction	Mulit-scan
Max. and min. transmission	0.9157 and 0.6172
Refinement method	Full-matrix least-squares on F^2
Data / restraints / parameters	7908 / 27 / 561
Goodness-of-fit on F^2	1.045
Final R indices [I>2sigma(I)]	R1 = 0.0592, wR2 = 0.1375
R indices (all data)	R1 = 0.1064, wR2 = 0.1603
Largest diff. peak and hole	1.391 and -2.510 e.A^-3

Crystal data and structure refinement for 14d:

Identification code	gudat141
Empirical formula	C47 H50 Ag F3 O9 P2 S [C38 H34 Ag O4 P2]+ [CF3SO3]- 2 thf
Formula weight	1017.74
Temperature	123(2) K
Wavelength	0.71073 A
Crystal system, space group	Monoclinic, P2(1)/c (No.14)
Unit cell dimensions	a = 14.3659(3) A alpha = 90 deg. b = 16.1257(4) A beta = 92.338(1) deg. c = 19.8458(6) A gamma = 90 deg.
Volume	4593.7(2) A^3
Z, Calculated density	4, 1.472 Mg/m^3

Absorption coefficient	0.621 mm^-1
F(000)	2096
Crystal size	0.15 x 0.10 x 0.05 mm
Diffractometer	Nonius KappaCCD
Theta range for data collection	3.06 to 25.02 deg.
Limiting indices	-16<=h<=17, -19<=k<=18, -15<=l<=23
Reflections collected / unique	25126 / 8092 [R(int) = 0.0462]
Completeness to theta = 25.02	99.7 %
Absorption correction	None
Refinement method	Full-matrix least-squares on F^2
Data / restraints / parameters	8092 / 110 / 580
Goodness-of-fit on F^2	0.910
Final R indices [I>2sigma(I)]	R1 = 0.0324, wR2 = 0.0555
R indices (all data)	R1 = 0.0705, wR2 = 0.0612
Largest diff. peak and hole	0.499 and -0.349 e.A^-3

Crystal data and structure refinement for 17a:

Identification code	gudat139
Empirical formula	C36 H38 B N2 O3 P
Formula weight	588.46
Temperature	173(2) K
Wavelength	0.71073 A
Crystal system, space group	Monoclinic, P2(1)/c (No.14)
Unit cell dimensions	a = 14.7942(4) A alpha = 90 deg.
	b = 9.5746(4) A beta = 93.558(2) deg.
	c = 22.8934(7) A gamma = 90 deg.
Volume	3236.57(19) A^3

Z, Calculated density	4, 1.208 Mg/m^3
Absorption coefficient	0.122 mm^-1
F(000)	1248
Crystal size	0.12 x 0.06 x 0.03 mm
Diffractometer	Bruker KappaAPEXII
Theta range for data collection	3.05 to 25.03 deg.
Limiting indices	-17<=h<=17, -10<=k<=11, -27<=l<=27
Reflections collected / unique	10492 / 5703 [R(int) = 0.1450]
Completeness to theta = 25.03	99.8 %
Absorption correction	None
Refinement method	Full-matrix least-squares on F^2
Data / restraints / parameters	5703 / 96 / 390
Goodness-of-fit on F^2	1.103
Final R indices [I>2sigma(I)]	R1 = 0.1199, wR2 = 0.1846
R indices (all data)	R1 = 0.2273, wR2 = 0.2272
Largest diff. peak and hole	0.385 and -0.335 e.A^-3

Crystal data and structure refinement for 18:

Identification code	gudat143
Empirical formula	C58 H56 B2 Cl2 O6 P2 Pd
	(C25 H20 B O2 P)2 Pd Cl2 - 2 thf
Formula weight	1109.89
Temperature	123(2) K
Wavelength	0.71073 A
Crystal system, space group	Monoclinic, P2(1)/c (no.14)
Unit cell dimensions	a = 11.7333(7) A alpha = 90 deg.
	b = 22.9485(17) A beta = 111.424(4) deg.

	c = 10.3897(5) A gamma = 90 deg.
Volume	2604.2(3) A^3
Z, Calculated density	2, 1.415 Mg/m^3
Absorption coefficient	0.572 mm^-1
F(000)	1144
Crystal size	0.20 x 0.10 x 0.05 mm
Theta range for data collection	3.25 to 25.03 deg.
Limiting indices	-12<=h<=13, -27<=k<=24, -12<=l<=12
Reflections collected / unique	22106 / 4480 [R(int) = 0.1020]
Completeness to theta = 25.03	97.5 %
Absorption correction	None
Refinement method	Full-matrix least-squares on F^2
Data / restraints / parameters	4480 / 66 / 322
Goodness-of-fit on F^2	0.862
Final R indices [I>2sigma(I)]	R1 = 0.0475, wR2 = 0.0753
R indices (all data)	R1 = 0.1307, wR2 = 0.0884
Largest diff. peak and hole	0.672 and -0.429 e.A^-3

Crystal data and structure refinement for 20:

Identification code	gudat117
Empirical formula	C48 H56 B N O6 P2
Formula weight	815.69
Temperature	123(2) K
Wavelength	0.71073 A
Crystal system, space group	Triclinic, P-1 (No.2)
Unit cell dimensions	a = 16.3386(2) A alpha = 84.929(1) deg.
	b = 16.3500(2) A beta = 88.028(1) deg.

	c = 16.7372(2) A gamma = 89.833(1) deg.
Volume	4450.97(9) A^3
Z, Calculated density	4, 1.217 Mg/m^3
Absorption coefficient	0.146 mm^-1
F(000)	1736
Crystal size	0.40 x 0.30 x 0.20 mm
Diffractometer	Nonius kappaCCD
Theta range for data collection	2.94 to 27.48 deg.
Limiting indices	-21<=h<=20, -21<=k<=21, -21<=l<=21
Reflections collected / unique	46944 / 19875 [R(int) = 0.0334]
Completeness to theta = 27.48	97.4 %
Absorption correction	None
Refinement method	Full-matrix least-squares on F^2
Data / restraints / parameters	19875 / 353 / 1045
Goodness-of-fit on F^2	1.102
Final R indices [I>2sigma(I)]	R1 = 0.0733, wR2 = 0.2187
R indices (all data)	R1 = 0.1036, wR2 = 0.2398
Largest diff. peak and hole	1.813 and -1.281 e.A^-3

Crystal data and structure refinement for 22:

Identification code	scnov05
Formula	C38 H30 B O4 P2, C6 H16 N
Formula Weight	725.57
Crystal System	Monoclinic
Space group	Cc (No. 9)
a, b, c [Angstrom]	8.1733(2) 43.277(1) 11.0401(3)
alpha, beta, gamma [deg]	90 94.894(2) 90

V [Ang**3] 3890.82(17)

Z 4

D(calc) [g/cm**3] 1.239

Mu(MoKa) [/mm] 0.155

F(000) 1536

Crystal Size [mm] 0.20 x 0.10 x 0.20

Temperature (K) 100

Radiation [Angstrom] MoKa 0.71073

Theta Min-Max [Deg] 4.0, 28.3

Dataset -10: 10 ; -57: 57 ; -14: 14

Tot., Uniq. Data, R(int) 32901, 9084, 0.090

Observed data [I > 2.0 sigma(I)]7638

Nref, Npar 9084, 476

R, wR2, S 0.0561, 0.1140, 1.05

w = 1/[\s^2^(Fo^2^)+(0.0256P)^2^+7.4395P] where P=(Fo^2^+2Fc^2^)/3

Max. and Av. Shift/Error 0.00, 0.00

Flack x -0.02(8)

Min. and Max. Resd. Dens. [e/Ang^3] -0.26, 0.29

Crystal data and structure refinement for 21:

Identification code scjan07

Empirical formula C38H30Ag1B1O4 P2 + C3H7N1O1 (DMF)

Formula weight 804.34.69

Temperature 100(2) K

Wavelength 0.71073 A

Crystal system, space group Monoclinic, Cc

Unit cell dimensions a = 18.8664(8) Å alpha = 90.00 deg.

b = 15.1936(5) Å beta = 124.062(2) deg.

c = 15.0136(5) Å gamma = 90.00 deg.

Volume	3565.3(2) A^3
Z, Calculated density	4, 1.498 Mg/m^3
Absorption coefficient	0.703 mm^-1
F(000)	16486
Crystal size	0.80 x 0.50 x 0.50 mm
Diffractometer	Nonius kappaCCD
Theta range for data collection	1.018 to 28.283 deg.
Limiting indices	-24<=h<=24, -20<=k<=19, -20<=l<=19
Reflections collected / unique	8102 / 4325 [R(int) = 0.0989]
Completeness to theta = 28.29	97.6 %
Absorption correction	None
Refinement method	Full-matrix least-squares on F^2
Data / restraints / parameters	8102 / 2 / 458
Goodness-of-fit on F^2	1.032
Final R indices [I>2sigma(I)]	R1 = 0.0715, wR2 = 0.1292
R indices (all data)	R1 = 0.0562, wR2 = 0.1217
Largest diff. peak and hole	0.77 and -1.06 e.A^-3
Rms deviation from mean =	0.10 e/A^3

Crystal data and structure refinement for 25:

Identification code	chi06
Empirical formula	C38H30Pd1Ga1O4 P2 + 3CDCl3
Formula weight	1182.23
Temperature	173(2) K
Wavelength	0.71073 A
Crystal system, space group	Monoclinic, P2

Unit cell dimensions	a = 16.125(4) Å alpha = 90.00 deg.
	b = 14.211(4) Å beta = 106.642(19) deg.
	c = 21.533(5) Å gamma = 90.00 deg.
Volume	4728(2) A^3
Z, Calculated density	4, 1.61429 Mg/m^3
Absorption coefficient	1.623 mm^-1
F(000)	2352.0
Crystal size	0.35 x 0.30 x 0.15 mm
Diffractometer	Nonius kappaCCD
Theta range for data collection	1.74 to 28.00 deg.
Limiting indices	0<=h<=20, 0<=k<=18, -27<=l<=26
Reflections collected / unique	7304 / 10308 [R(int) = 0.0497]
Completeness to theta = 28.00	99.8 %
Absorption correction	None
Refinement method	Full-matrix least-squares on F^2
Data / restraints / parameters	10308 / 0 / 535
Goodness-of-fit on F^2	1.032
Final R indices [I>2sigma(I)]	R1 = 0.0883, wR2 = 0.1017
R indices (all data)	R1 = 0.0514, wR2 = 0.1148
Largest diff. peak and hole	0.79 and -0.89 e.A^-3
Rms deviation from mean =	0.12 e/A^3

Crystal data and structure refinement for 26a:

Identification code	chi06
Formula	C38 H30 Cl2 O4 P2 Pd Sn
Formula Weight	908.59
Crystal System	Monoclinic

Space group	P2/c (No. 13)
a, b, c [Angstrom]	12.227(2) 11.707(2) 16.475(3)
alpha, beta, gamma [deg]	90 102.516(12) 90
V [Ang**3]	2302.2(7)
Z	2
D(calc) [g/cm**3]	1.311
Mu(MoKa) [/mm]	1.149
F(000)	900
Crystal Size [mm]	0.00 x 0.00 x 0.00
Temperature (K)	173
Radiation [Angstrom]	MoKa 0.71073
Theta Min-Max [Deg]	2.2, 28.0
Dataset	-16: 15 ; -5: 15 ; -21: 21
Tot., Uniq. Data, R(int)	6056, 5523, 0.024
Observed data [I > 2.0 sigma(I)]	4516
Nref, Npar	5523, 220
R, wR2, S	0.0445, 0.1248, 1.04
w = 1/[\S^2^(FO^2^)+(0.0844P)^2^] WHERE P=(FO^2^+2FC^2^)/3'	
Max. and Av. Shift/Error	0.00, 0.00
Min. and Max. Resd. Dens. [e/Ang^3]	-1.08, 1.94

Crystal data and structure refinement for 26b:

Identification code	scnov06
Formula	C40 H36 O4 P2 Pd Sn, C3 H7 N O
Formula Weight	940.85
Crystal System	Monoclinic

Space group	P21/n (No. 14)
a, b, c [Angstrom]	10.8862(2) 19.1979(3) 20.0183(3)
alpha, beta, gamma [deg]	90 102.811(1) 90
V [Ang**3]	4079.52(12)
Z	4
D(calc) [g/cm**3]	1.532
Mu(MoKa) [/mm]	1.176
F(000)	1896
Crystal Size [mm]	0.00 x 0.00 x 0.00
Temperature (K)	100
Radiation [Angstrom]	MoKa 0.71073
Theta Min-Max [Deg]	3.3, 28.3
Dataset	-14: 12 ; -25: 25 ; -26: 26
Tot., Uniq. Data, R(int)	56490, 10028, 0.142
Observed data [I > 2.0 sigma(I)]	8455
Nref, Npar	10028, 483
R, wR2, S	0.0633, 0.1568, 1.10
w = 1/[\s^2^(Fo^2^)+(0.0589P)^2^+22.3688P] where P=(Fo^2^+2Fc^2^)/	
Max. and Av. Shift/Error	0.00, 0.00
Min. and Max. Resd. Dens. [e/Ang^3]	-2.17, 2.20

Crystal data and structure refinement for 28:

Identification code	chi10
Formula	C40 H36 O4 P2 Pt Sn
Formula Weight	956.42
Crystal System	Monoclinic
Space group	C2/c (No. 15)

a, b, c [Angstrom]	11.4113(14) 22.727(3) 16.324(2)
alpha, beta, gamma [deg]	90 107.695(10) 90
V [Ang**3]	4033.2(9)
Z	4
D(calc) [g/cm**3]	1.575
Mu(MoKa) [/mm]	4.199
F(000)	1864
Crystal Size [mm]	0.20 x 0.25 x 0.25
Temperature (K)	173
Radiation [Angstrom]	MoKa 0.71073
Theta Min-Max [Deg]	2.1, 28.0
Dataset	-15: 14 ; 0: 30 ; 0: 21
Tot., Uniq. Data, R(int)	5227, 4865, 0.064
Observed data [I > 2.0 sigma(I)]	3479
Nref, Npar	4865, 222
R, wR2, S	0.0358, 0.0906, 0.91
w = 1/[\S^2^(FO^2^)+(0.0448P)^2^] WHERE P=(FO^2^+2FC^2^)/3'	
Max. and Av. Shift/Error	0.00, 0.00
Min. and Max. Resd. Dens. [e/Ang^3]	-1.05, 1.80

Crystal data and structure refinement for 29:

Identification code	dg002_hy
Empirical formula	C39 H32 Bi Cl3 O4 P2 Pd
	C38 H30 Bi Cl O4 P2 Pd - CH2Cl2
Formula weight	1048.32
Temperature	123(2) K
Wavelength	0.71073 A

Crystal system, space group	Monoclinic, P2(1)/c (no.14)
Unit cell dimensions	a = 11.264(1) A alpha = 90 deg.
	b = 17.247(1) A beta = 98.52(1) deg.
	c = 19.346(1) A gamma = 90 deg.
Volume	3716.9(4) A^3
Z, Calculated density	4, 1.873 Mg/m^3
Absorption coefficient	5.554 mm^-1
F(000)	2032
Crystal size	0.15 x 0.06 x 0.04 mm
Theta range for data collection	2.99 to 25.03 deg.
Limiting indices	-13<=h<=13, -20<=k<=19, -23<=l<=23
Reflections collected / unique	21315 / 6485 [R(int) = 0.0695]
Completeness to theta = 25.03	98.7 %
Absorption correction	Semi-empirical from equivalents
Max. and min. transmission	0.8084 and 0.4579
Refinement method	Full-matrix least-squares on F^2
Data / restraints / parameters	6485 / 0 / 451
Goodness-of-fit on F^2	1.033
Final R indices [I>2sigma(I)]	R1 = 0.0472, wR2 = 0.0837
R indices (all data)	R1 = 0.0979, wR2 = 0.0978
Largest diff. peak and hole	2.226 and -0.989 e.A^-3

Crystal data and structure refinement for 30:

Identification code	scfeb06
Formula	C76 H60 O8 P4 Pd2 Zr, 4(C3 H7 N O), C2 O
Formula Weight	1861.58
Crystal System	Monoclinic

Space group	C2/c (No. 15)
a, b, c [Angstrom]	25.0208(7) 15.3922(5) 25.6866(5)
alpha, beta, gamma [deg]	90 107.045(2) 90
V [Ang**3]	9458.0(5)
Z	4
D(calc) [g/cm**3]	1.307
Mu(MoKa) [/mm]	0.610
F(000)	3808
Crystal Size [mm]	0.00 x 0.00 x 0.00
Temperature (K)	293
Radiation [Angstrom]	MoKa 0.71073
Theta Min-Max [Deg]	3.2, 28.3
Dataset	-33: 33 ; -19: 20 ; -34: 33
Tot., Uniq. Data, R(int)	45844, 11301, 0.107
Observed data [I > 2.0 sigma(I)]	6855
Nref, Npar	11301, 510
R, wR2, S	0.1020, 0.3134, 1.08

Crystal data and structure refinement for 31:

Identification code	scokt06
Formula	4 O21 P8 Pd4 Y4, 10(C3 H N O), 2(C4 N), 3(C3), 3(Cl), 4(C)
Formula Weight	4572.82
Crystal System	Triclinic
Space group	P-1 (No. 2)
a, b, c [Angstrom]	16.3740(2) 18.8825(2) 20.6120(3)
alpha, beta, gamma [deg]	67.152(1) 70.115(1) 74.181(1)

V [Ang**3]	5449.58(13)
Z	1
D(calc) [g/cm**3]	1.393
Mu(MoKa) [/mm]	1.538
F(000)	2295
Crystal Size [mm]	0.00 x 0.00 x 0.00
Temperature (K)	293
Radiation [Angstrom]	MoKa 0.71073
Theta Min-Max [Deg]	3.8, 28.3
Dataset	-21: 21 ; -25: 25 ; -27: 27
Tot., Uniq. Data, R(int)	121778, 26741, 0.119
Observed data [I > 2.0 sigma(I)]	19288
Nref, Npar	26741, 1180
R, wR2, S	0.0730, 0.2075, 1.03

Crystal data and structure refinement for 32:

Identification code	dg018_hy
Empirical formula	C88 H86 Cl N4 O12 P4 Pd2 Y [C76 H62 O8 P4 Pd2 Y]+ Cl- dmf, 3 free dmf
Formula weight	1852.65
Temperature	123(2) K
Wavelength	0.71073 A
Crystal system, space group	Monoclinic, P21/n
Unit cell dimensions	a = 19.804(4) A alpha = 90 deg. b = 20.246(4) A beta = 98.08(2) deg. c = 21.280(4) A gamma = 90 deg.

Volume	8448(3) A^3
Z, Calculated density	4, 1.457 Mg/m^3
Absorption coefficient	1.272 mm^-1
F(000)	3784
Crystal size	0.25 x 0.15 x 0.10 mm
Theta range for data collection	2.94 to 25.03 deg.
Limiting indices	-23<=h<=23, -24<=k<=21, -25<=l<=24
Reflections collected / unique	56587 / 14752 [R(int) = 0.0849]
Completeness to theta = 25.03	98.9 %
Absorption correction	Semi-empirical from equivalents
Max. and min. transmission	0.8833 and 0.6347
Refinement method	Full-matrix least-squares on F^2
Data / restraints / parameters	14752 / 171 / 1015
Goodness-of-fit on F^2	1.112
Final R indices [I>2sigma(I)]	R1 = 0.0631, wR2 = 0.1012
R indices (all data)	R1 = 0.1344, wR2 = 0.1210
Largest diff. peak and hole	0.734 and -0.822 e.A^-3

Crystal data and structure refinement for 33a:

Formula	C39 H33 Cl O4 P2 Pd Sn, C3 H7 N O		
Formula Weight	961.27		
Crystal System	Monoclinic		
Space group	P21/n (No. 14)		
a, b, c [Angstrom]	10.8914(3)	19.0086(5)	20.1077(6)
alpha, beta, gamma [deg]	90	103.320(2)	90
V [Ang**3]	4050.9(2)		
Z	4		

D(calc) [g/cm**3]	1.576
Mu(MoKa) [/mm]	1.250
F(000)	1928
Crystal Size [mm]	0.00 x 0.00 x 0.00
Temperature (K)	100
Radiation [Angstrom]	MoKa 0.71073
Theta Min-Max [Deg]	3.8, 28.3
Dataset	-14: 14 ; -25: 25 ; -26: 26
Tot., Uniq. Data, R(int)	55811, 10000, 0.153
Observed data [I > 2.0 sigma(I)]	7137
Nref, Npar	10000, 481
R, wR2, S	0.0769, 0.1622, 1.06
w = 1/[\s^2^(Fo^2^)+(0.0430P)^2^+43.0179P] where P=(Fo^2^+2Fc^2^)/	
Max. and Av. Shift/Error	3.78, 0.01
Min. and Max. Resd. Dens. [e/Ang^3]	-3.21, 5.31

Crystal data and structure refinement for 34a:

Crystal System	Monoclinic
Space group	P21/n (No. 14)
a, b, c [Angstrom]	12.2118(3) 22.0395(5) 14.6819(4)
alpha, beta, gamma [deg]	90 94.379(2) 90
V [Ang**3]	3939.98(17)
Z	4
D(calc) [g/cm**3]	1.628
Mu(MoKa) [/mm]	1.265
F(000)	1948
Crystal Size [mm]	0.00 x 0.00 x 0.00

Temperature (K)	100
Radiation [Angstrom]	MoKa 0.71073
Theta Min-Max [Deg]	3.6, 28.3
Dataset	-16: 16 ; -29: 29 ; -19: 19
Tot., Uniq. Data, R(int)	51594, 9673, 0.147
Observed data [I > 2.0 sigma(I)]	7659
Nref, Npar	9673, 490
R, wR2, S	0.0731, 0.1520, 1.14
w = 1/[\s^2^(Fo^2^)+(0.0350P)^2^+28.7466P] where P=(Fo^2^+2Fc^2^)/	
Max. and Av. Shift/Error	0.03, 0.00
Min. and Max. Resd. Dens. [e/Ang^3]	-1.31, 2.03

9. References:

[1] P. J. E. Peebles, D. N. Schramm, E. L. Turner, R. G. Kron, *Nature*, **1991**, 352, 769; S. W. Hawking, G. F. R. Ellis, 1968, *The Astrophysical journal*, **1968**, 152, 25. G. L. Schroeder, *"Genesis and the big bang" Bantam Books, New York*, **1990**.

[2] H.-J. Schneider, A. K. Yatsimirsky, *Principles and Methods in Supramolecular Chemistry*, Wiley-VCH, New York, **2000**.

[3] G. Suess-Fink, J. L. Wolfender, F. Neumann, H. Stoeckli-Evans, *Angew. Chem. Int. Ed.* **1990**, 29, 429.

[4] G. Newton, I. Haiduc, R. B. King, C. Silvestru, *J. Am. Chem. Soc*. **1993**, 115, 1229.

[5] S. Gambarotta, C. Floriani, A. Chiesi-Villa, C. Guastini, *J. Am. Chem. Soc.* **1983**, 105, 1156.

[6] S. K. Mandal, L. K. Thompson, M. J. Newlands, E. J. Gabe, F. L. Lee, *J. Chem. Soc. Chem. Commun.* **1989**, 744.

[7] A. W. Maverick, M. L. Ivie, J. H. Waggenspack, F. R. Fronczek, *Inorg. Chem*. **1990**, 29, 2403.

[8] A. W. Kleij, J. N. H. Reek, *Chem. Eur. J.* **2006**, 12, 4218.

[9] D. Fiedler, H. van Halbeek, R. G. Bergman, K. N. Raymond, *J. Am. Chem. Soc.* **2006**, 128, 10240.

[10] J. M. Lehn, Supramolecular Chemistry: Concepts and Perspectives, VCH, Weinheim **1995**.

[11] D. L. Caulder, K. N. Raymond, *Angew. Chem. Int. Ed.* **1997**, 36, 1440.

[12] F. M. Mulder, T. A. Stegink, R. C. Thiel, L. J. de Jongh, G. Schmid, *Nature*, **1994**, 367, 716.

[13] M. N. Vargaftik, I. I. Moiseev, D. I. Kochubey, K. I. Zamaraev, *Faraday Discuss*. **1991**, 92, 13.

[14] C. A. Tolman, *Chem. Rev*. **1977**, 77, 313.

[15] C. A. Tolman. *J. Am. Chem. Soc*. **1970**, 92, 2953.

[16] P. W. N. M. van Leeuwen, P. C. J. Kamer, J. N. H. Reek, P. Dierkes, *Chem. Rev.* **2000**, 100, 2741; P. W. N. M. van Leeuwen, P. C. J. Kamer, J. N. H. Reek, *Pure Appl. Chem*. **1999**, 71, 1443.

[17] A. J. Sandee, J. N. H. Reek, *J. Chem. Soc. Dalton. Trans*, **2006**, 3385.

[18] J. M. Tackas, D. S. Reddy, S. A. Moteki, D. Wu, H. Palencia, *J. Am. Chem. Soc*. **2004**, 126, 14, 4494.

[19] B. Breit. *Angew. Chem. Int. Ed.* **2005**, 44, 6816.

[20] B. Breit, W. Seiche, *Angew. Chem. Int. Ed.* **2005**, 44, 1640.

[21] V. F. Slagt, M. Roeder, P. C. J. Kamer, P. W. N. M. van Leeuwen, J. N. H. Reek, *J. Am. Chem. Soc*. **2004**, 126, 4056.

[22] F. Chevallier, B. Breit, *Angew. Chem. Int. Ed*. **2006**, 45, 1599.

[23] M. Kuil, P. E. Goudriaan, P. W. N. M. van Leeuwen, J. N. H. Reek, *J. Chem. Soc. Chem. Commun.* **2006**, 4679.

[24] B. Breit, W. Seiche, *J. Am. Chem. Soc*. **2003**, 125, 6608.

[25] P. A. Duckmanton, A. J. Blake, J. B. Love, *Inorg. Chem*. **2005**, 44, 7708.

[26] L. K. Knight, Z. Freixa, P. W. N. M. van Leeuwen, J. N. H. Reek, *Organometallics*, **2006**, 25, 954.

[27] M. J. Wilkinson, P. W. N. M. van Leeuwen, J. N. H. Reek, *Org. Bio. Chem.* **2005**, 3, 2371.

[28] R. G. Pearson, J. Chem. Ed. 1987, 64, 561.

[29] J. Tsuji, Palladium Reagents and Catalysts, Wiley, **2000.**

[30] I. V. Komarov, A. Borner, *Angew. Chem. Int. Ed*. **2001**, *40*, 1197; T. Hayashi, *Acc. Chem. Res.* **2000,** *33*, 354.

[31] M. Epstein, S. A. Buckler, *Tetrahedron*, **1962**, 18, 11, 1231.

[32] K.V. Katti, H. Gali, C.J. Smith, D.E. Berning, *Acc. Chem. Res*. **1999**, *32*, 9.

[33] D. Gudat, A. Haghverdi, M. Nieger, *Angew. Chem*. **2000**, *112*, 3211; S. Burck, D. Gudat, M. Nieger, W.W. Du Mont, *J. Am. Chem. Soc*., **2006**, 128, 12, 3946.

[34] V.I. Evreinov, V.E. Baulin, Z.N. Vostroknutova, N.A. Bondarenko, T.Kh. Syundyukova, E.N. Tsvetkov, *Izv. Akad. Nauk SSSR, Ser. Khim*. **1989**, 1990.

[35] S. Trippett, *J. Chem. Soc*. **1961**, 1813.

[36] P. Y. Renard, P. Vayron, C. Mioskowski, *Organic Lett.* **2003**, *5*, 1661; A.N. Bovin, A.N. Yarkevich, A.N. Kharitonov, E.N. Tsvetkov, *Chem. Commun*. **1994**, 973.

[37] X. Sun, D. W. Johnson, D. L. Caulder, K. N. Raymond, E. H. Wong, *J. Am. Chem. Soc*. **2001**, *123*, 2752.

[38] N. T. Lucas, J. M. Hook, A. M. McDonagh, S. B. Colbran, *Eur. J. Inorg. Chem*. **2005**, 496; N. T. Lucas, A. M. McDonagh, I. G. Dance, S. B. Colbran, D. C. Craig, *Dalton Trans*. **2006**, 680.

[39] J. Fawcett, John; P. A. T. Hoye, R. D. W. Kemmitt, D. J. Law, D. R. Russell, *J. Chem. Soc. Dalton Trans.* **1993**, 2563.

[40] P. Perez-Lourido, J. A. Gracia-Vazquez, J. Romero, A. Sousa, *Inorg. Chem*. **1999**, 38, 538.

[41] I. Kovacik, D. K. Wicht, N. S. Grewal, D. S. Glueck, C. D. Incarvito, I. A. Guzei, A. L. Rheingold, *Organometallics*, **2000,** *19,6*, 950.

[42] T. Imamoto, S.-I. Kikuchi, T. Miura, Y. Wada, *Org. Lett.* **2001,** *3, 1*, 87.

[43] K. Kellner, S. Rothe, E. M. Steyer, A. Tzschach, *Phosphorus, Sulfur, Relat. Elem.* **1980**, 9, 269.

[44] J. J. Daly, *J. Chem. Soc*. **1964**, 3799.

[45] T. S. Cameron, B. Dahlen, *J. Chem. Soc. Perkin Trans. 2*, **1975**, 1737.

[46] E. C. Alyea, J. Malto, *Phosphorus, Sulfur and silicon*, **1989**, 46, 175.

[47] J. Heinicke, M. Koehler, N. Peulecke, M. K. Kindermann, W. Keim, M. Kockerling *Organometallics*, **2005**, 24, 344.

[48] L. Dahlenburg, Herbst, K.; Liehr, G., *Zeitschrift fuer Kristallographie - New Crystal Structures* **1998**, 213(1), 209.

[49] H. D. Impsall, B. L. Shaw and B. L. Turtle, *J. C. S. Dalton. Trans.* **1976**, 1500.

[50] S. Priya, M. S. Balakrishna and J. T. Mague, *J. Organomet. Chem.* **2004,** 689, 3335.

[51] R. Terroba, M. B. Hursthouse, M. Laguna, A. Mendia, *Polyhedron*, **1999**, 18, 807; E. L. Muetterties, C. W. Alegranti, *J. Am. Chem. Soc*. **1972**, 94, 18, 6386.

[52] R. G. Goel, P. Pilon, *Inorg. Chem.* **1978**, 17, 2876; R. Terroba, M. B. Hursthouse, M. laguna, A. Mendia, *Polyhedron*, **1999**, 18, 807; X. Sun, D. W. Hohnson, K. N. Raymond, E. H. Wong, *Inorg. Chem*. **2001**, 40, 4504.

[53] W. R. Purdum, E. M. Kaiser, *Inorg. Chim. Acta* **1975**, 12, 45.

[54] M. Pailer, W. Fenzl, *Monatsh. Chem.* **1961**, 92, 1294.

[55] H. G. Kuivila, A. H. Keough, E. J. Soboczenski, *J. Org. Chem.* **1954**, 19, 780; R. A. Bowie, O. C. Musgrave, *J. Chem. Soc*. **1963**, 3945.

[56] M. Wieber, W. Kuenzel, *Z. Anorg. Allg. Chem.* **1974**, 403, 107.

[57] F. Norberto, C. Rosalinda, *J. Chem. Soc. Perkin Tran. 2*, **1987**, 6, 771.

[58] H. Sakurai, N. Iwasawa, K. Narasaka, *Bull. Chem. Soc. Jpn*., **1996**, 69, 2585.

[59] F. Focante, P. Mercandelli, A. Sironi, L. Resconi, *Coord. Chem. Rev.* **2006**, 250-(1-2), 170.

[60] N. Kano, J. Yoshino, T. Kawashima, *Org. Lett.* **2005**, 7, 18, 3909.

[61] P. J. Bailey, D. Lorono-Gonzale, C. McCormack, F. Millican, S. Parsons, R. Pfeifer, P. P. Pinho, F. Rudolphi, A. S. Perucha, *Chem. Eur. J.* **2006,** 12, 5293.

[62] W. P. Griffith, A. J. P. White, D. J. Williams, *Polyhedron*, **1995**, 15, 17, 2835.

[63] J. Meulenhoff, *Rec. traav. Chim*., **1925**, 44, 150.

[64] D. F. Kuemmel, M. G. Mellon, *J. Am. Chem. Soc*. **1956**, 78, 4572.

[65] A. Mitra, L. J. DuPue, J. E. Struss, B. P. Patel, S. Parkin, D. A. Atwood, *Inorg. Chem.* **2006**, 45, 9213.

[66] E. Graf, M. W. Hosseini *et. al*. *Angew. Chem. Int. Ed.* **1995**, 34, 1115.

[67] S. Mohr, G. Heller, U. Timper, K. H. Woller, *Z. Naturforsch*, **1990**, 45, 308.

[68] F. Zettler, H. D. Hausen, H. Hess, Acta Crystallogr., Sect.B: Struct. Crystallogr.Cryst.Chem. **1974,** 30, 1876.

[69] R. Goetz, H. Noeth, H. Pommerening, D. Sedlak, B. Wrackmeyer, *Chem. Ber.* **1981**, 114, 1884.

[70] N. Farfan, R. Contreras, *J. Chem. Soc. Perkin Trans 2*, **1987**, 771.

[71] D. Vagedes, R. Froehlich, G. Erker, *Angew. Chem. Int. Ed.* **1999**, 38, 22, 3362.

[72] W. Clegg, A. J. Scott, F. E. S. Souza, T. B. Marder, *Acta Crystallogr. Sect. C:* **1999**, C55, 11, 885.

[73] H. Sleiman, P. Baxter, J. M. Lehn, *J. Chem. Soc. Chem. Comm*., **1995**, 7, 715.

[74] T. Goslinski, C. Zhong, M. J. Fuchter, C. L. Stern, A. J. P. White, A. G. M. Barrett, B. M. Hoffman, *Inorg. Chem.* **2006**, 45, 9, 3686.

[75] Hoffman, M. Brian, Barrett, G. M. Anthony, U.S. (1999), 37 pp., Cont.-in-part of U.S. 5,675,001. CODEN: USXXAM US 5912341 A 19990615 Application: US 97-928415 19970912. Priority: US 95-403302 19950314. CAN 131:27113 AN 1999:384025.

[76] P. Diehl, E. Fluck, R. Kosfeld, Nuclear Magnetic spectroscopy of boron compounds, Springer-Verlag, Berlin, Heidelberg, New York, **1978**, p. 144.

[77] R. Huetter, W. Keller-Schierlein, F. Knuesel, V. Prelog, G. C. Rodgers, P. Sutter, G. Vogel, W. Voser, H. Zaehner, *Helv. Chim. Acta*. **1967**, 50, 9, 1533.

[78] T. Okazaki, T. Kitahara, Y. Okami, *J. Antibiot*. **1975**, 28, 176; T. J. Stout, J. Clardy, I. C. Pathirana, W. Fenical, *Tetrahedron*, **1991**, 47, 22, 3511.

[79] R. A. Baber, J. P. H. Charmant, J. D. Moore, N. C. Norman, and A. G. Orpen, *Acta. Cryst. Sec. E, Stru. Rept.* **2004**, E60, o1140.

[80] P. S. Pregosin, R. W. Kunz, In ^{31}P and ^{13}C of Transition Metal Phosphine Complexes, Springer-verlag, New York, **1979**, p. 89.

[81] A. P. Gies, D. M. Hercules, A. E. Gerdon, D. E. Cliffel, *J. Am. Chem. Soc.* **2007**, 129, 1095.

[82] P. S. Pregosin, P. G. Anil Kumar, I. Fernandez, *Chem. Rev.* **2005**, 105, 8, 2977.

[83] Dynamic viscosities at 30ºC from *Landolt Boernstein*, Springer, **2002**, 18B; η = 0.506 ($CDCl_3$), 0.743 (DMF-d_7) m Pa.s. The value for DMF-d_7 was interpolated from the available data in the temperature region between 15 and 45ºC.

[84] X. Sun, D. W. Johnson, K. N. Raymond, E. H. Wong. *Inorg. Chem.* **2001**, 40, 4504.

[85] a) B. Kersting, J. R. Relford, M. Meyer, K. N. Raymond, *J. Am. Chem. Soc*. **1996**, 118, 5712. b) M. Meyer, B. Kersting, R. E. Powers, K. N. Raymond, *Inorg. Chem.* **1997**, 36, 5179.

[86] T. B. Karpishin, T. M. Dewey, K. N. Raymond, *J. Am. Chem. Soc.* **1993**, 115, 1842.

[87] R. R. holmes, S. Shafieezad, V. Chandrasekhar, A. C. Sau. J. M. Holmes, R. O. Day, *J. Am. Chem. Soc.* **1988**, 110, 1168.

[88] C. Lamberth, J. C. Machell, D. M. P. Mingos, T. L. Stolberg, *J. Mater. Chem*. **1991**, 1(5), 775.

[89] a) J. K. Stille, *Angew. Chem. Int. ed.* **1986**, 25, 508. b) T. N. Mitchell, *Synthesis* **1992**, 803. c) L. S. Hegedus, *Coord. Chem. Rev*. **1996**, 147, 443.

[90] H. Ishii, M. Ueda, K. Takuechi, M. Asai, *J. Mol. Catal. A: Chem.* **1999**, 138, 311.

[91] A. Rosenheim, I. Baruttschisky, *Ber. Dtsch. Chem. Ges*. **1925**, 58, 891.

[92] A. Rosenheim, *Z. Anorg. Allg. Chem*. **1931**, 200, 173.

[93] G. Smith, A. N. Reddy, K. A. Byriel, C. H. L. Kennard, *Aust. J. Chem.* **1994**, 47, 1413.

[94] H. Suzuki, Y. Matano, Eds. *Organobismuth Chemistry*; Elsevier Science B. V.: Amstredam, **2001**.

[95] C. Silvestru, H. J. Breunig, H. Althaus, *Chem. Rev*. **1999**, 99, 3277.

[96] N. Guilhaume, M. Postel, *Heteroatom. Chem*. **1990**, 1(3), 233.

[97] M. J. Ferreira, A. M. Martins, *Coord. Chem. Rev*. **2006**, 250(1-2), 118.

[98] D. L. Caulder, R. E. Powers, T. N. Parac, K. N. Raymond, *Angew. Chem. Int. Ed.* **1998**, 37, 1840.

[99] D. J. Brauer, P. M. Machnitzki, T. Nickel, O. Stelzer, *Eur. J. Inorg. Chem.* **2000**, 65.

[100] E. Negishi, R. A. John, *J. Org. Chem.* **1983**, 48, 4098.

[101] R. R. Holmes, *ACS Monogr*. **1980**, 175, Chapter 2; R. R. Holmes, J. A. Deiters, *J. Am. Chem. Soc*. **1977**, 99, 3318; R. R. Holmes, R. O. Day, A. C. Sau, J. M. Holmes, *Phosphorus, Sulfur, and Silicon and Related Elements*, **1995**, 98, 423.

[102] E. L. Muetterties, L. J. Guggenberger, *J. Am. Chem. Soc*. **1974**, 96, 1748.

[103] C. N. McMahon, S. J. Obrey, A. Keys, S. G. Bott, A. R. Barron, *J. Chem. Soc. Dalton Tans.* **2000**, 2151.

[104] T. B. Karpishin, T. D. P. Stack, K. N. Raymond, *J. Am. Chem. Soc*. **1993**, 115, 182.

[105] B. A. Borgias, S. J. Barclay, K. N. Raymond, *J. Coord. Chem.* **1986**, 15, 109; M. A. Brown, A. A. El-Hadad, B. R. McGarvey, R. C. W. Sunf, A. K. Trikha, D. G. Tuck, *Inorg. Chim. Acta.* **2000**, 300, 613.

[106] N. R. Bunn, S. Aldridge, C. Jones, *Appl. Organometal. Chem.* **2004**, 18, 425; W. Ziemkowska, P. Stella, R. Anulewicz-Ostrowska, *J. Organomet. Chem.* **2005**, 690, 722.

[107] a) S. Casson, P. Kocienski, *J. Chem. Soc.* , *Perkin Trans. 1* **1994**,1187, b) T. Takeda, Y. Kbasawa, T. Fujiwara, *Tetrahedron*, **1995**, 51, 2515.

[108] G. S. Ferguson, P. T. Wolczanskl, *Organometallics*, **1985**, 4, 1601.

[109] J. S. Kim, A. Sen, I. A. Guzei, L. M. Liable-sands, A. L. Rheingold, *J. Chem. Soc. Dalton Trans.*, **2002**, 4726.

[110] H. A. Bent, *Chem. Rev*. **1961**, 61, 275.

[111] C. Camacho-Camacho, R. Contreras, H. Noth, M. Bechmann, A. Sebald, W. Milius, B. Wrackmeyer, *Mag. Reson. Chem.* **2002**, 40, 31.

[112] M. Colladon, A. Scarso, G. Strukul, *Synlett*., **2006**, 20, 3515; M. V. Baker, D. H. Brown, P. V. Simpson, B. W. Skelton, A. H. White, C. C. Williams, *J. Organomet. Chem.* **2006**, 691, 26, 5845.

[113] W. J. Vickaryous, R. Herges, D. W. Jonson, *Angew. Chem. Int. Ed*. **2004**, 43, 5831.

[114] K. G. Caulton, L. G. Hubert-Pfalzgraf. *Chem. Rev.* **1990**, 90, 969 ; C. N. R. Rao, B. Raveau, *Transition Metal Oxides*, VCH Publishers, New York, **1995**.

[115] D. Villemin, P. A. Jaffres, B. Nechab, F. Courivaud, *Tetra. Lett.* **1997**, 38(37), 6581; M. Xuebing, F. Xiangkai, *J. Mol. Cat. A: Chem.*, **2004**, 208(1-2), 129; G. Potenzo, N. Cosimo-Francesco, M. Giovanni, L. G. Aldo, F. Carla, M. M. Antonietta, P. Pasquale, *J. Mol. Cat.*, **1989**, 53, 349.

[116] T. J. Boyle, L. J. Tribby, T. M. Alam, S. D. Bunge, G. P. Holland, *Polyhedron*, **2005**, 24, 1143.

[117] C. J. Gramer, K. N. Raymond, *Inorg. Chem.* **2004**, 43, 6397.

[118] C. Benelli, D. Gatteschi, *Chem. Rev*. **1998**, 27, 2369; M. Shibasaki, N. Yoshikawa, *Chem. Rev.* **2002**, 102, 2187.

[119] P. W. Roesky, G. Canseco-Melchor, A. Zulys, *Chem. Commun*. **2004**, 738.

[120] P. Miele, J. D. Foulon, N. Hovnanian, L. Cot, *J. Chem. Soc. Chem. Commun*. **1993**, 29-31; B. A. Vaartstra, J. C. Huffman, W. E. Streib, K. G. Caulton, *J. Chem. Soc. Chem. Commun.***1990**, 1750; O. Poncelet, W. J. Sartain, L. G. Hubert-Pfalzgarf, K. Folting, K. G. Caulton, *Inorg. Chem*. **1989**, 28, 263.

[121] W. J. Evans, M. S. Sollberger, *J. Am. Chem. Soc*. **1986**, 108, 6095; M. R. Buergstein, P. W. Roeky, *Angew .Chem. Int. Ed*. **2000**, 39, 549.

[122] S. Braese, A. de Meijere, *Metal-catalyzed Cross-coupling Reactions* (Hrsg. F. Diederich, P. J. Stang), Wiley-VCH, Weinheim, **1998**, p. 99.

[123] C. C Tzschucke, C. Markert, H. Glatz, W. Bannwarth, *Angew. Chem. Int. Ed.* **2002**, 41, 4500.

[124] N. T. Lucas, A. M. McDonagh, I. G. Dance, S. B. Colbran, D. C. Craig, *Dalton Trans*. **2006**, 680.

[125] K. Sonogashira, *Compreh. Org. Synth*. **1991**, 3, 551.

[126] A. Kless, C. Lefeber, A. Spangenberg, R. Kempe, W. Baumann, J. Holz, A. Boerner, *Tetrahedron*, **1996**, 52, 14599.

[127] G. S. Ferguson, P. T. Wolczanski, *J. Am. Chem. Soc*. **1986**, 108, 8293.

[128] L. Friedman, J. G. Miller, *Science*, **1971**, 172, 1044.

[129] T. Nakanishi, N. Yamakawa, T. Asahi, N. Shibata, B. Ohtani, T. Osaka, *Chirality*, **2004**, 16, S36.

[130] N. Takeda, K. Umemoto, K. Yamaguchi, M. Fujita, *Nature*, **1999**, 398, 794.

[131] A. Caneschi, A. Cornia, A. C. Fabretti, S. Foner, D. Gatteschi, R. Grandi, L. Schenetti, *Chem. Eur. J.* **1996**, 2, 1379; B. Hasenknopf, J-M. Lehn, B. O. Kneisel, G. Baum, D. Fenske, *Angew. Chem. Int. Ed.* **1996**, 35, 1838; J. S. Fleming, K. L. V. Mann, C. A. Carraz, E. Psillakis, J. C. Jeffery, J. A. McCleverty, M. D. Ward, *Angew. Chem. Int. Ed.* **1998**, 37, 1279.

[132] D. Fiedler, D. H. Leung, R. G. Bergman, K. N. Raymond, *J. Am. Chem. Soc*. **2004**, 126, 3674.

[133] D. Fiedler, D. H. Leung, R. G. Bergman, K. N. Raymond, *Acc. Chem. Res.* **2005**, 38, 349; T. Kusukawa, M. Fujita, *J. Am. Chem. Soc*. **1999**, 121, 1397.

[134] A. von Zelewsky, *Stereochemistry of Coordination Compounds*, **1996**, Wiley, New York.

[135] G. Seeber, B. E. F. Tiedemann, K. N. Raymond, *Top. Curr. Chem.* **2006**, 265, 147.

[136] D. L. Kepert, *Prog. Inorg. Chem.* **1977**, 23, 1.

[137] A. Rodger, B. F. G. Johnson, *Inorg. Chem.* **1988,** 27, 3061.

[138] H. Jolibois, F. Theobald, R. Mercier, C. Devin, *Inorg. Chim. Acta.* **1985**, 97, 119.

[139] J. Okuda, S. Verch, R. Stuermer, T. P. Spaniol, *J. Organomet. Chem.* **2000**, 605, 55; J. P. Genet, N. Kopola, S. Juge, J. Ruez-Montes, O. A. C. Antunes, S. Tanier, *Tetra. Lett.* **1990**, 31, 22, 3133.

[140] D. D. Perrin, W. L. Armarego, L. F. Willfred, *Purification of Laboratory Chemicals*, Oxford: Pergamon Pr. **1988**.

[141] D. Wittenberg, H. Gilman, *J. Org. Chem.* **1958**, 23, 1063; Diphenyl phosphine was synthesized as reported in the above literature with little modification. Triethyl amine hydrochloride was employed as proton source instead of water.

[142] H. J. Frohn, N. Y. Adonin, V. V. Bardin, V. F. Starichenko, *Z. Anorg. Allg. Chem.* **2002**, 628, 2827.

[143] P. M. Maitlis, *The Organic Chemistry of Palladium Metal Complexes, V.1*, **1971**, Academic Press, New York; and references there in.

[144] J. Chatt, L. M. Vallarino, L. M. Venanzi, *J. Chem. Soc.* **1957**, 2496.

[145] M. Schlosser, Organometallics in Synthesis: A Manual; Wiley, **2002**.

[146] A. Bielecki, A. C. Kolbert, M. H. Levitt, *Chem. Phys. Lett.* **1989**, 155, 341; M. H. Levitt, A. C. Kolbert, A. Bielecki, S. J. Ruben, *Solid State NMR*, **1993**, 2, 151.

[147] N. A. Bondarenko, E. N. Tsvetkov, E. I. Matrosov, M. I. Kabachnik, *Izv. Akad. Nauk. SSSR, Ser. Khim.* **1979**, 432-435; V. I. Evreenov, V. E. Baulin, Z. N. Vostroknutova, N. A. Bondarenko, T. Kh. Syundyukova, E. N. Tsvetkov, *Izv. Akad. Nauk. SSSR, Ser. Khim.* **1989**, 1990.

[148] Computations were performed at the B3LYP/3-21g* level of theory with the Gaussian program suite: Gaussian 98 (Rev. A.7), M. J. Frisch, G. W. Trucks, H. B. Schlegel, G. E. Scuseria, M. A. Robb, J. R. Cheeseman, V.G. Zakrzewski, J. A. Montgomery, R. E. Stratmann, J. C. Burant, S. Dapprich, J. M. Millam, A. D. Daniels, K. N. Kudin, M.C. Strain, O. Farkas, J. Tomasi, V. Barone, M. Cossi, R. Cammi, B. Mennucci, C. Pomelli, C. Adamo, S. Clifford, J.Ochterski, G. A. Petersson, P. Y. Ayala, Q. Cui, K. Morokuma, D. K. Malick, A. D. Rabuck, K. Raghavachari, J. B.Foresman, J. Cioslowski, J. V. Ortiz, B. B. Stefanov, G. Liu, A. Liashenko, P. Piskorz, I. Komaromi, R. Gomperts, R. L.Martin, D. J. Fox, T. Keith, M. A. Al-Laham, C. Y. Peng, A. Nanayakkara, C. Gonzalez, M. Challacombe, P. M. W. Gill, B.G. Johnson, W. Chen, M. W. Wong, J. L.

Andres, M. Head-Gordon, E. S. Replogle and J. A. Pople, Gaussian, Inc., Pittsburgh PA, 1998.

[149] G. S. Ferguson, P. T. Wolczanski, *Organometallics*, **1985**, 4, 1601; G. S. Ferguson, P. T. Wolczanski, *J. Am. Chem. Soc*. **1986**, 108, 8293; G. S. Ferguson, P. T. Wolczanski, L. Parkanyi, M. C. Zonnevylle, *Organometallics*, **1988**, 7, 1967; O. Kühl, S. Blaurock, J. Sieler, E. Hey-Hawkins, *Polyhedron*, **2001**, 20, 2171.

[150] M. Shibasaki, N. Yoshikawa, *Chem. Rev*. **2002**, 102, 2187.

[151] M. Shibasaki, S. Matsunaga, *Chem. Soc. Rev.* **2006**, 35, 269.

[152] O. Kühl, S. Blaurock, J. Sieler, E. Hey-Hawkins, *Polyhedron*, **2001**, 20, 2171.

10. Curriculum Vitae:

Mr. Samir H. Chikkali M.Sc.
Institute of Inorganic Chemistry
University of Stuttgart
Pfaffenwaldring 55
D-70569 Stuttgart
Germany

Phone : +49 711 9719461
Email : chikkali@iac.uni-stuttgart.de

Present status

Working with Prof. Dr. D. Gudat at the University of Stuttgart, Germany. I will be completing my doctoral work by Sep. 2007.

Educational details

University of Stuttgart, Stuttgart, Germany

- Ph.D. (Organometallic Chemistry) – Nov. 2003 onwards
- Research work titled: Complexes of flexible ditopic catechol phosphines: Synthesis, metal assisted self-assembly and catalytic application.
- Supervisor: Prof. Dr. D. Gudat

National Chemical Laboratory, Pune, India

- Summer Fellow of Indian Academy of Science, Banglore: May 2001 to July 2001. Work titled: Syntheses of new bisphenol monomers for the preparation of high performance polymers.
- Supervisor: Dr. S. Sivaram, Director, National Chemical Laboratory.
- Project Assistant under the supervision of Dr. P. K. Saxena: Aug. 2001 to March 2003. Work titled: Synthesis of super high molecular weight polyolefins using Supported Ziegler-Natta catalyst.
- Project Assistant under the supervision of Dr. K. Guruswamy: March 2003 to Oct. 2003. Work titled: Modification of Natural clays and synthesis of polymer nanocomposites

Shivaji University Kolhapur, Maharashtra, India

- M.Sc. (Polymer Chemistry) – June 1999 to Apr 2001 – First class with distinction.
- B. Sc. (General Chemistry)- June 1996 to May 1999 – First class with distinction.

Technical skills

- Spectroscopy – 1D-2D NMR, MS, ESI/MS, FT-IR, UV-vis.
- Polymer characterization – GPC, VPO, DTA, TGA, DSC and Digital viscometry.

Teaching experience

- Teaching assistant for Inorganic chemistry practical courses at University of Stuttgart, Germany: Nov. 2003 onwards.

Publications :

(1) **S. Chikkali**, D. Gudat
Hydrophosphanation of Phenolic Aldehydes as Facile Synthetic Approach to Catechol-Functionalized Phosphane Oxides and Phosphanes
Euro. J. Inorg. Chem. **2006**, *15*, 3005-3009.

(2) **S. Chikkali**, D. Gudat, M. Niemeyer
Template controlled self-assembly of bidentate phosphine complexes with hemilabile coordination behaviour.
Chem. Comm. **2007**, 9, 981-983.

(3) **S. Chikkali**, D. Gudat, M. Nieger, F. Lissner, T. Schleid
Boron templated catechol phosphines as bidentate ligands in silver complexes.
J. Chem. Soc. Dalton Trans. **2007**, *in press*.

(4) **S. Chikkali**, P. K. Saxena.
Titanium phthalocyanine complex, novel catalyst for ethylene polymerization.
J. Polym. Res.. Communicated.

Oral presentations

(1) **S. Chikkali**, D. Gudat, F. Lissner, M. Niemeyer, M. Nieger, T. Schleid.
"Template complexes with Novel ditopic phosphines: Stepwise Aufbau, self-assembly and catalysis"
Presented at: 233rd ACS National meeting, Chicago, USA (March 25 to 27 2007)

(2) **S. Chikkali**, D. Gudat, F. Lissner, M. Niemeyer, M. Nieger, T. Schleid.

"Novel self-assembly of transition metal-bidentate phosphine complexes on main group templates and potential applications in catalysis"
Presented at: 4th Ph.D. workshop on phosphorus chemistry, Center parcs, Zandvoort, Vrije University, Amstredam, Netherland (March 20 & 21 2007)

(3) **S. Chikkali**, D. Gudat, M. Niemeyer.
"*Supramolecular phosphines: stepwise aufbau, self-assembly and catalysis*"
Presented at: German-Austrian Scientific-coworkers workshop on main-group element chemistry, Techinical University of Graz, Austria (April 20 to 22 2006).

(4) **S. Chikkali,** D. Gudat, M. Nieger,
"*Supramolecular Phosphines: New synthetic methodology and Lewis acid-base behaviour*"
Presented at: IX th Regional seminar of Ph. D. Students on organometallic and organophosphorus chemistry, Szklarska Poreba, Poland (April 10 to14, 2005).

Poster presentations

(1) "*Supramolecular phosphines: New synthetic methodology, acid-base behaviour and potential catalysis*" P 023, P-57.
Presented at 13th Woehler-Vereinigung fur Anorganische Chemie, GDCh, (German Chemists society) 18-19 Sep. 2006, RWTH Aachen, Germany.

(2) "*Studies on the stereospecific polymerization of styrene using new titanium catalyst*" P 2.17.
Presented at Frontiers of polymer science and engineering, MACRO-2002, Indian Institute of Techonology, Khargpur, India. (Dec. 2002).

Invited oral presentations

(1) *"Supramolecular phosphines: New synthetic methodology, acid-base behaviour and petential catalysis"* Presented at National Chemical Laboratroy, Pune, Inida (Dec. 2004)
(2) "*Supramolecular phosphines: stepwise aufbau, self-assembly and catalysis"* Presented at National Chemical Laboratory, Pune, India (May 2006)

Academic references

(1) Prof. Dr. D. Gudat
Institute of Inorganic Chemistry
University of Stuttgart
Pfaffenwaldring 55
D-70569 Stuttgart
Germany
E-mail : gudat@iac.uni-stuttgart.de

(2) Dr. K. Guruswamy
Scientist
Department of polymer science and engineering
National Chemical Laboratory
Pune – 411008
Maharashtra
India
E-mail : g.kumaraswamy@ncl.res.in